NASA CONTRACTOR REPORT CR-166536

A MATHEMATICAL MODEL FOR REAL TIME FLIGHT SIMULATION OF A GENERIC TILT-ROTOR AIRCRAFT

S. W. FERGUSON

CONTRACT NAS2- 11317
SEPTEMBER 1988, REV. A

NASA

NASA CONTRACTOR REPORT CR-166536

A MATHEMATICAL MODEL FOR REAL TIME FLIGHT SIMULATION OF A GENERIC TILT-ROTOR AIRCRAFT

S. W. FERGUSON

SYSTEMS TECHNOLOGY, INC.
MOUNTAIN VIEW, CALIFORNIA

PREPARED FOR
AMES RESEARCH CENTER
UNDER CONTRACT NAS2-11317

National Aeronautics and
Space Administration

Ames Research Center
Moffett Field, California 94035

SYSTEMS TECHNOLOGY, INC.

2672 BAYSHORE PARKWAY, SUITE 505 • MOUNTAIN VIEW, CALIFORNIA 94043-1011 • PHONE (415) 961-4674

(817) 473-6820
Mansfield, Tx.

Technical Report No. 1195-2

A MATHEMATICAL MODEL FOR REAL TIME FLIGHT SIMULATION OF A GENERIC TILT ROTOR AIRCRAFT

Samuel W. Ferguson

October 1983
March 1988, Rev. A
September 1988, Rev. A (Final)

National Aeronautics and Space Administration
Ames Research Center
Moffett Field, California 94035

Contract NAS2-11317

ABSTRACT

The objective of this report is to document a mathematical model for the real time flight simulation of a generic tilt-rotor aircraft which can be used in support of aircraft design, pilot training, and flight testing. The mathematical model was originally developed by Bell Helicopter Textron (BHT) under NASA Contract NAS2-6599 for the XV-15 tilt-rotor research aircraft. A real-time version of this model was implemented by Computer Sciences Corporation (CSC) on the NASA Ames Research Center (ARC) Flight Simulator for Advanced Aircraft (FSAA). Systems Technology, Inc., (STI) was given the task under NASA Contract NAS2-11317 to develop, document, and validate a generic tilt-rotor mathematical model version of the BHT mathematical model for XV-15 and generic tilt-rotor simulation on the NASA ARC Vertical Motion Simulator (VMS).

The generic tilt-rotor mathematical model development and documentation effort required that the following specific tasks be completed: (1) restructuring of the original BHT report by (a) updating the list of symbols, (b) rewriting the input/output format, (c) developing a cross reference between the VAX 11/780 and Sigma 8 versions of the generic model, and (d) modifying or adding equations to the mathematical model in several deficient areas; (2) programming, checkout, and validation of the generic tilt-rotor mathematical model; and (3) simulation support.

FOREWORD

STI wishes to acknowledge the help of several groups of people involved in developing and validating the GTRS mathematical model. Mr. Gary Churchill of the NASA ARC XV-15 Project Office was extremely helpful in directing the overall NASA generic tilt-rotor validation effort and in supporting STI from a technical standpoint. Messrs. Steve Belsley and Mike Weinstein of CSC implemented all of the STI-requested modifications to the Sigma 8/VMS version of the GTRS program and helped to check out the modifications. They also provided STI with information for development of the mathematical model/Sigma 8 cross reference (Appendix C) and spent a significant amount of time helping to review documentation in order to help insure accuracy. STI would like to acknowledge the assistance provided by BHT in providing some of the computer source code used in the VAX 11/780 GTRS programming effort and in developing and writing the IFHC80 program (the program from which the GTRS program is derived) and its associated documentation. Without this assistance, it would have been impossible to develop the GTRS program in its present form. Messrs. Roger Marr, Narendra Batra, and Bradford Roberts of BHT were also very helpful in improving and updating the mathematical model for Revision A of this document, and their efforts are greatly appreciated.

TABLE OF CONTENTS

Section		Page
I	INTRODUCTION AND BACKGROUND	1
	A. Restructuring of the Report	1
	B. Implementation of the Generic Tilt-Rotor Mathematical Model on the VAX 11/780 and Sigma 8/VMS Computers	2
	C. Validation of the Generic Tilt-Rotor Mathematical Model	4
	D. Simulation Support	5
II	STRUCTURE OF THE MATHEMATICAL MODEL	7
III	A GENERAL DESCRIPTION OF THE MATHEMATICAL MODEL AND INPUT DATA REQUIREMENTS	11
	A. Subsystem 1: Rotor Aerodynamics	11
	1. Rotor Forces and Moments	11
	2. Rotor-Induced Velocity	13
	3. General Input Data Requirements	15
	B. Subsystem 2: Rotor-Induced Velocities (Also Parts of Subsystems 4, 5, 6, and 14)	18
	1. Model Structure	18
	2. Input Data Requirements	20
	C. Subsystem 3: Fuselage Aerodynamics	24
	1. Model Structure	24
	2. Input Data Requirements	24
	D. Subsystem 4: Wing-Pylon Aerodynamics	24
	1. Model Structure	24
	2. Input Data Requirements	26

TABLE OF CONTENTS (Continued)

Section		Page
E.	Subsystem 5: Horizontal Stabilizer Aerodynamics	27
	1. Model Structure	27
	2. Input Data Requirements	35
F.	Subsystem 6: Vertical Stabilizer Aerodynamics	35
	1. Model Structure	35
	2. Input Data Requirements	38
G.	Subsystem 7: Landing Gear	41
	1. Model Structure	41
	2. Input Data Requirements	41
H.	Subsystem 8: Control System	41
	1. Model Structure	41
	2. Input Data Requirements	42
I.	Subsystem 9: CG and Inertia	42
J.	Subsystems 10 Through 14: Coordinate Transformations and Equations of Motion	43
K.	Subsystem 15: Flight Environment	43
L.	Subsystem 16: Pilot's Instrument Panel	43
M.	Subsystem 17: Rotor Collective Governor	44
	1. Model Structure	44
	2. Input Data Requirements	44
N.	Subsystems 18 and 19: Engines, Fuel, Controls, and Drive System Dynamics	45
	1. Model Structure	45
	2. Input Data Requirements	47

LIST OF FIGURES

Number		Page
1	Generic Tilt-Rotor Mathematical Model Structure and Input/Output Summary	8
2	Side-by-Side Rotor Effect on Induced Velocity	16
3	Sideward Flight Rotor Effects on Induced Velocity	16
4	Effect of Ground Proximity on Hover Power Required	17
5	Rotor Wake on the Horizontal Stabilizer as a Function of Airspeed at a Nacelle Incidence of 90 Degrees	21
6	Representation of In-Ground Effect Rolling Moment	22
7	The Effect of Hover Height on Longitudinal Stick Position	23
8	Wing-Pylon Lift Coefficient Versus Angle of Attack for Flap/Flaperon Settings of 0/0 and 40/25 Degrees	28
9	Wing-Pylon Lift Coefficient Corrections Due to Compressibility	29
10	Wing-Pylon Lift Coefficient at Large Negative Angles of Attack for a Flap/Flaperon Setting of 40/25 Degrees	30
11	Wing-Pylon Drag Coefficient Versus Angle of Attack for Flap/Flaperon Settings of 0/0 and 40/25 Degrees	31
12	Wing-Pylon Drag Coefficient Corrections Due to Compressibility	32
13	Wing-Pylon Drag Coefficient at Large Negative Angles of Attack for a Flap/Flaperon Setting of 40/25 Degrees	33
14	Wing-Pylon Wake Deflection (Downwash) at the Horizontal Stabilizer for Flap/Flaperon Settings of 0/0 and 40/25 Degrees	34
15	Horizontal Stabilizer Lift Coefficient Versus Angle of Attack	36
16	Horizontal Stabilizer Drag Coefficient Versus Angle of Attack	37

LIST OF FIGURES (Concluded)

Number		Page
17	Vertical Stabilizer Side Force Coefficient Versus Sideslip Angle	39
18	Vertical Stabilizer Drag Coefficient Versus Sideslip Angle	40

SECTION I

INTRODUCTION AND BACKGROUND

The objective of this report is to document a mathematical model for the real time flight simulation of a generic tilt-rotor aircraft which can be used in support of aircraft design, pilot training, and flight testing. The mathematical model was originally developed by Bell Helicopter Textron (BHT) under NASA Contract NAS2-6599 for the XV-15 tilt-rotor research aircraft (Ref. 1). A real-time version of this model was implemented by Computer Sciences Corporation (CSC) on the NASA Ames Research Center (ARC) Flight Simulator for Advanced Aircraft (FSAA). Systems Technology, Inc., (STI) was given the task under NASA Contract NAS2-11317 to develop, document, and validate a generic tilt-rotor mathematical model version of the BHT mathematical model for XV-15 and generic tilt-rotor simulation on the NASA ARC Vertical Motion Simulator (VMS). The first release of this development effort was completed in October 1983.

The generic tilt-rotor mathematical model development and documentation effort required that the following specific tasks be completed: (1) restructuring of the original BHT report by (a) updating the list of symbols, (b) rewriting the input/output format, (c) developing a cross reference between the VAX 11/780 and Sigma 8 versions of the generic model, and (d) modifying or adding equations to the mathematical model in several deficient areas; (2) programming, checkout, and validation of the generic tilt-rotor mathematical model; and (3) simulation support.

A. RESTRUCTURING OF THE REPORT

The tilt-rotor mathematical model equations, as originally derived, represented the kinematic, dynamic, and aerodynamic characteristics of the XV-15 rotor, airframe, and flight control system. A description of the development of the mathematical model, in its original form, is presented in Ref. 1. The equations presented in that report are, in many instances,

revised in this report to provide an improved generic model as based on XV-15 flight test data. The equations of this improved generic tilt-rotor mathematical model are provided in Appendix A of this report. The XV-15 input data array taken from Ref. 1 has also been significantly updated and restructured to the generic mathematical model input format and is presented in Appendix B of this report.

All pages from the original BHT mathematical model report (Ref. 1) which remain unchanged are presented in this report with the Bell report number, 301-099-001, located in the lower left-hand corner. New or corrected pages are identified by the STI report number, TR-1195-2. Pages that have been revised for this edition of the STI report are labeled TR-1195-2 (Rev. A).

Appendix C of this report contains a cross reference, developed by STI and CSC, of the mathematical model input data array and the associated computer variable names used in the Sigma 8/VMS version of the program.

B. IMPLEMENTATION OF THE GENERIC TILT-ROTOR MATHEMATICAL MODEL ON THE VAX 11/780 AND SIGMA 8/VMS COMPUTERS

The initial version of what is now the generic tilt-rotor program was developed in the 1970s by BHT for use as an offline XV-15 tilt-rotor analysis tool. A version of this program, IFHC80, was delivered in 1980 to NASA ARC in a non-generic form for use with the XV-15 only. This program is based on the XV-15 tilt-rotor mathematical model of Ref. 1 and was used as a checkout tool prior to BHT XV-15 simulations. A user's guide and programmer's guide, Refs. 2 and 3, were delivered for use with this program.

STI used the IFHC80 program, as requested by the XV-15 Tilt Rotor Project Office, as a basis for development of the generic tilt-rotor simulation program (GTRS) described in this document. The GTRS program has been implemented on the NASA ARC VAX 11/780 computer, and the effort has involved an extensive reformatting and recoding of the IFHC80 program's complete input/output structure and format. In addition, several computer

programming errors were corrected during the creation of the GTRS program. During development of both the original version and Revision A of GTRS, informal discussions were held between STI and BHT in an effort to define areas of similarity which might be maintained between STI's GTRS program and versions of a generic tilt-rotor program that have been developed by BHT for their internal use. As a result of these discussions, STI has adopted some FORTRAN coding supplied by BHT for use with the GTRS program. Almost all of this code is related to the input and internal storage of aerodynamic data so as to maintain commonality between BHT and NASA in the way in which tilt-rotor aerodynamic data is described for use in the program. During the debugging and checkout of the STI GTRS program, BHT was notified of the coding modifications and changes that would be required for any future use of the BHT-supplied FORTRAN code. This was because some of the STI code was developed before some of the BHT code.

A user's guide and a programmer's guide have been written for the VAX 11/780 version of the GTRS program and were originally available as Refs. 4 and 5, respectively. Both of these reports are now superseded by Revision A versions with the same titles (their release date is the same as the release date of this document). Appendices I and J of Ref. 4 provide a cross reference between the input data and computer variable names and the equations in the original version of this document for both the VAX 11/780 and Sigma 8/VMS* computer versions of the generic tilt-rotor mathematical model. The Sigma 8/VMS version has not been released in a Revision A upgrade. All information contained in Refs. 4 and 5, other than that supplied in Appendices I and J, is intended to apply to the STI-developed VAX 11/780 version of the GTRS program only, unless otherwise specified, even though there are many similarities among the STI-, CSC-, and BHT-developed versions of the mathematical models and the associated versions of computer code.

---

*The Sigma 8 version of the GTRS program was developed by CSC under a separate contract and is used presently for real-time simulation of the XV-15. GTRS is also an off-line version developed by STI for use on the VAX 11/780 computer.

C. VALIDATION OF THE GENERIC TILT-ROTOR MATHEMATICAL MODEL

The original XV-15 mathematical model (Ref. 1) was validated by BHT through the use of wind tunnel tests, other computer programs, and limited flight tests. Work accomplished by STI has been directed toward validation of the GTRS program using the earlier XV-15 data base as well as the extensive flight test data base which is presently being developed with the XV-15. Both the VAX 11/780 and Sigma 8/VMS versions of the GTRS program have been used in the validation effort. Output from both of the simulation programs has also been compared for numerous flight conditions in order to ensure that both programs yield the same calculated results. While conducting the validation study with flight test data, the following limitations/deficiencies were identified by STI.

1. The prediction of hover performance was originally found to be clearly overly optimistic (helicopter and airplane forward flight performance was only slightly over predicted).

2. In-ground effect rotor modeling was unacceptable for rotor power calculation.

3. In-ground effect pitching moments were not predicted as observed in flight test.

4. The calculated hover in-ground effect rolling moment instability was excessive and of too high a frequency in comparison with flight data.

5. Spinner drag modeling was discovered to be implemented incorrectly.

6. Pylon drag modeling (including wing-pylon interference drag) was determined to be inadequate.

7. A static B_1 rigging offset term was not included in the control system model so that the rotor controls could be rigged like the XV-15.

8. The XV-15 20-degree flap position (and associated aerodynamic tables) was not available for selection by the pilot with the model (this flap position is one of the three normal XV-15 flap positions)

9. Simulated trimmed sideward flight data did not correlate well with XV-15 flight test data.

10. Short takeoffs and landings were found to require too much distance (possibly due to the lack of a wing in-ground effect model and inaccurate rotor/wing flow field modeling while in ground effect).

11. Questionable input data values were identified for elevator, rudder, and aileron effectiveness as well as the Q-loss value at the respective control surfaces (as observed through correlation of aircraft simulation response to flight test response for the same control input).

12. Values for the XV-15 inertias were demonstrated to be out of date (airframe modifications and flight test instrumentation weights and locations were not included in the calculated inertias).

BHT was notified of each these model limitations/deficiencies. Modifications were made to the GTRS program or input data values which resolved all of the limitations/deficiencies except for the deficiencies involved with short takeoffs and landings. An investigation into the STOL deficiency was beyond the scope of effort STI was tasked to accomplish at that time. Interim results from the mathematical model validation effort are presented in Ref. 6. The final report (Ref. 7) for the contract provides a more detailed discussion of the results from the validation effort.

D. SIMULATION SUPPORT

STI provided engineering support to NASA and CSC for the initial generic tilt-rotor simulation validation effort that was conducted at NASA ARC from January to April 1983. The support to NASA was provided in order to aid in the evaluation of the XV-15 data input configuration (in the generic mathematical model format) and to modify the model as required. Both open- and closed-loop evaluations of the model were conducted using NASA and military XV-15 pilots. CSC support was provided to aid in implementation and checkout of the generic model on the Sigma 8 computer and the VMS. Major off-line simulation efforts were conducted in 1983 and

1984 to investigate improvements to the mathematical model and to correlate results with flight test data taken specifically for simulation validation purposes. Other off-line validation efforts have been conducted using the VAX 11/780 version of the program beginning in 1983 and continuing to the release of this report. Some of these efforts have also involved work with tilt-rotor configurations other than the XV-15.

SECTION II

STRUCTURE OF THE MATHEMATICAL MODEL

The generic tilt-rotor mathematical model structure is presented in the block diagram shown in Fig. 1. The mathematical model differs from that of a conventional fixed-wing aircraft in that there are added requirements to represent the dynamics and aerodynamics of the rotors, the interaction of the rotor wake with the airframe, and the rotor control and drive systems. The rigorousness of the mathematical model of the tilt-rotor aircraft was constrained by two factors. One factor was the requirement to keep the computational loop time to less than 70 ms in order to maintain a real time simulation. In order to achieve this, it was necessary to limit the rotor representation to steady, linearized aerodynamics having a uniform inflow and to approximate the rotor following time. Rotor stall and compressibility effects were used only to define a limit for the maximum rotor thrust coefficient as a function of advance ratio. This rotor mathematical model is satisfactory for most handling qualities studies but may be inadequate to evaluate flight conditions or maneuvers where stall, compressibility, or rotor dynamics are significant.

A second factor constraining the rigorousness of the mathematical model was the lack of sufficient experimental data on rotor wake-airframe aerodynamic interactions, such as the downwash (or upwash) of the rotors at the horizontal tail. The model of the rotor wake-airframe interaction was initially based on a limited amount of data from tests of a powered model of a tilt-rotor aircraft similar to the XV-15. Tests were subsequently completed using a powered model of the XV-15 to obtain detailed information on the rotor wake-airframe aerodynamic interactions. This data was used to update the simulation and refine the model for this important characteristic of a tilt-rotor. Other revisions were made to the mathematical model during the aircraft development in order to reflect design changes in the aircraft, corrections to the mathematical model, and

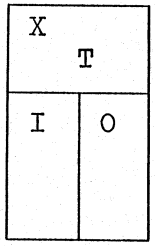

X Module number
T Module title
I Inputs from other modules
O Outputs to other modules

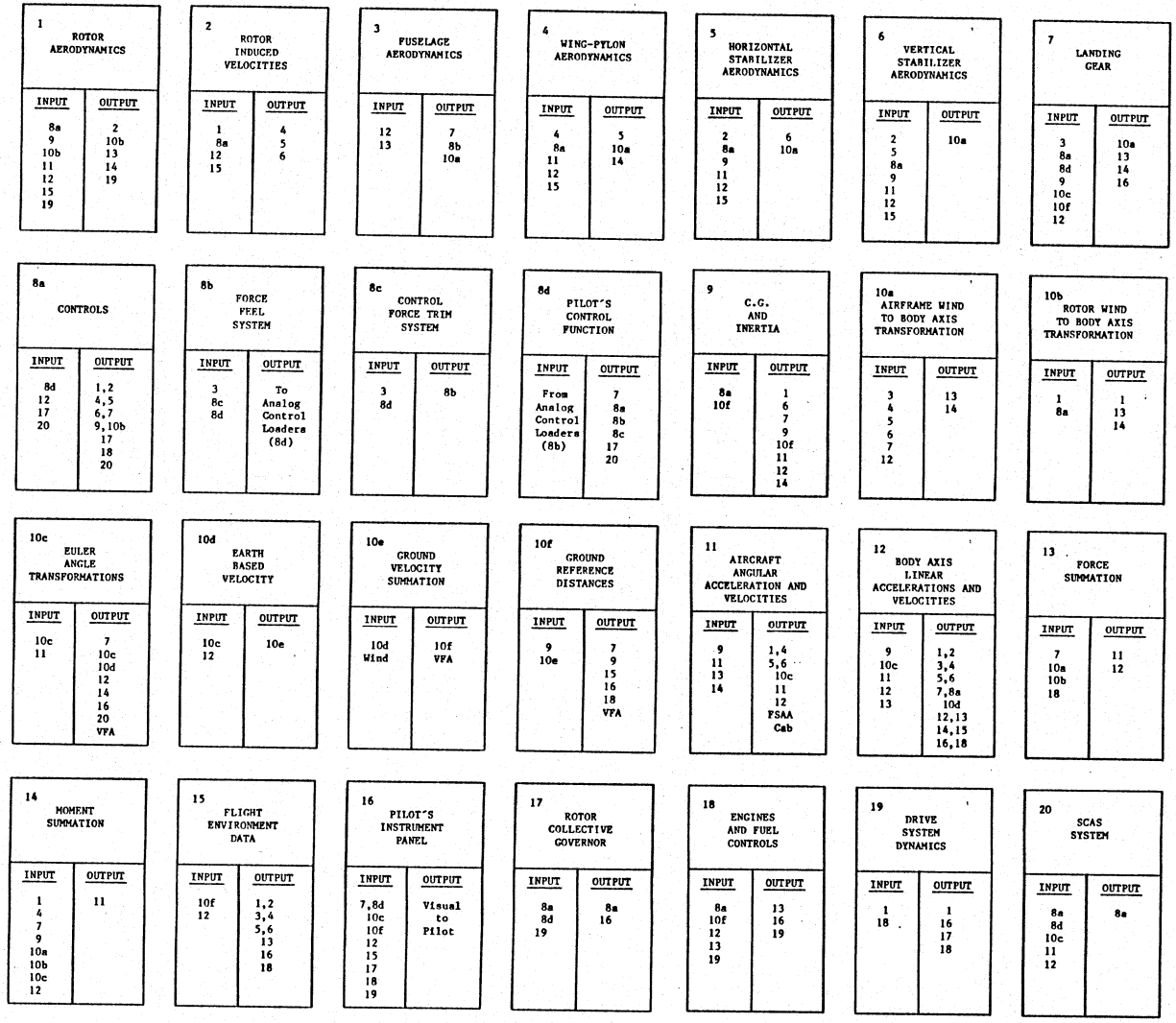

Figure 1. Generic Tilt-Rotor Mathematical Model Structure and Input/Output Summary

additions or improvements to the mathematical model. This latest revision provides the most recently updated documentation of the mathematical model in its generic tilt-rotor form. Many of the changes to the Revision A version of the mathematical model involve improvements that are incorporated as a result of correlation with XV-15 flight test data.

SECTION III

A GENERAL DESCRIPTION OF THE MATHEMATICAL MODEL AND INPUT DATA REQUIREMENTS

This section describes the mathematical models of the generic tilt-rotor aircraft components--the rotors, the airframe, the control system, the engines and drive system, and the automatic flight control systems (Subsystems 1 through 9, and 17 through 20 in Fig. 1)--and the input data requirements for those components. The equations of motion used with the mathematical model (Subsystems 10 through 14 in Fig. 1) are the same as those found in Ref. 8.

Earth-, body-, wind-, and mast-axes systems are used in the generic tilt-rotor mathematical model. The rotor flapping, forces, and moments are calculated in a "wind-mast" axis system, while the airframe aerodynamic forces and moments are calculated in a wind-axis system. Forces and moments from the rotor and airframe are then resolved into the body-axis system for solution of the aircraft equations of motion. The flight path of the tilt-rotor is described with reference to earth-fixed axes with the orientation given by the Euler angles Ψ, Θ, and Φ, in that order of rotation. Details on individual subsystem sign conventions are provided in the following sections.

A. SUBSYSTEM 1: ROTOR AERODYNAMICS

1. Rotor Forces and Moments

The mathematical model of the rotor is similar to that described in Refs. 9 and 10, except that it is derived in a mast-axis system (the theory in Ref. 9 is based on an axis system perpendicular to the axis of no flapping, i.e., the tip-path-plane, and that of Ref. 10 is based on the

axis of no feathering) and contains provisions for prop-rotor characteristics such as nonlinear twist, flapping restraint, and pitch-flap coupling. The mast-axis system and sign convention used for the rotor are shown in Fig. A1-1 (in Appendix A). The rotor flapping, forces, and moments are calculated in the "wind-mast" axis system ($\overline{a_1}$, $\overline{b_1}$, $\overline{T}$, $\overline{H}$, and $\overline{Y}$) and are then transformed into the mast-axis system (a_1, b_1, T, H, and Y).

Major assumptions that are made in the rotor mathematical model include:

1. Average values for the lift-curve slope and profile-drag coefficient are used over the entire span of the blade. These are adjusted to approximate the rotor thrust- and power-required characteristics.

2. The blade angle of attack, α_r, is approximated by sin α_r. Substitution of sin α_r for α_r in the blade element equations makes it possible to develop equations for rotor forces without restricting blade pitch, θ, and inflow angle, ϕ, to small angles.

3. Blade flapping with respect to the mast is considered to be small so that the small angle assumption can be made, and harmonics of flapping greater than one-per-revolution are ignored.

4. The blade flapping due to cyclic inputs is assumed to occur instantaneously, i.e., the flapping equations assume that the rotor is in an equilibrium condition. This assumption was made because of limits imposed by the computation time of the simulation computer. Differential equations for blade flapping that would properly account for the rotor following time were determined to require a solution time in excess of that allowable for real time simulation. Furthermore, there is a transport lag, between the time that a control input is made at the simulator cab and the time that an aircraft response is updated at the cab (by the motion and visual systems), of from one to two frame times. By neglecting the rotor following time in the equation of motion, this transport lag is approximated by the cab-control input to computer time lag; for example, in hover, the rotor following time is 0.08 sec compared to an average computational lag time of at least as much as 0.075 sec using the Sigma 8 computer with the VMS located at NASA ARC.

5. Blade stall and compressibility effects are approximated by limiting the maximum rotor thrust coefficient as a function of advance ratio and by arbitrarily modifying coefficients in the rotor power required equation (i.e., rotor profile drag is increased as a function of the cubes of the rotor inflow and advance ratios multiplied by empirically adjusted coefficients).

2. Rotor-Induced Velocity

The rotor-induced velocity is computed by calculating the induced velocity of an isolated, out-of-ground effect rotor and then modifying the induced velocity to account for the side-by-side rotor effect, the tandem rotor effect (in sideward flight), and for operation in ground effect.

The mean value of the isolated, out-of-ground effect rotor-induced velocity is approximated using a modified expression from Ref. 11.

$$v_i = \frac{(\Omega R)C}{\sqrt{0.866\lambda^2 + \mu^2} + \dfrac{0.6|C_T|^{1.5}\left(|C_T| - 8/3\lambda|\lambda|\right)}{\left(|C| + 8\mu^2\right)\left(|C| + 8\lambda^2\right)}}$$

where $C = C_T/2B^2$ (the 0.866 factor on λ^2 has been added to improve power correlation in hover).

The major assumption made with regard to induced velocity is that it is uniform over the rotor disk. The main effect of this assumption is that lateral flapping is underpredicted in the low-speed helicopter regime (μ = 0.05 to 0.2). However, lateral flapping has only a second-order effect on stability and control characteristics in the helicopter mode, so this is not a serious limitation.

The side-by-side rotor effect on the rotor-induced velocity is approximated using an expression derived in Ref. 12.

$$\Delta v_{i_{SS}} = X_{SS} \frac{(\Omega R) C_T}{2B^2 \mu}$$

The factor X_{SS} is called the mutual induction coefficient, and it is obtained from Fig. 3.7 of Ref. 12. In the determination of X_{SS}, the increased mass flow of the side-by-side configuration is taken into account, and the rotor wakes are assumed to remain separate if the distance between the rotor centers is greater than the rotor diameter. The value of X_{SS} depends on the direction of rotation, the distance between the rotors, the advance ratio, and the rotor angle of attack. The value of X_{SS} given in Ref. 12 is valid for μ greater than 0.15. In this analysis, the value of X_{SS} for μ less than 0.15 has been approximated by providing a smooth transition between a value of X_{SS} equal to zero at $\mu = 0.06$ and the value at $\mu = 0.15$. The term $\Delta v_{i_{SS}}$ is added to the induced velocity for the isolated rotor during the induced-velocity solution process.

The added induced-velocity component at the trailing rotor of the tilt rotor in sideward flight (the tandem rotor effect) is approximated as a function of the normalized sideward flight velocity ($\overline{V}$). This component, $\Delta V_{i_{SF}}$, is then added to the induced velocity for the isolated trailing rotor, along with the value for $\Delta V_{i_{SS}}$ during the induced-velocity solution process.

The reduction in induced velocity caused by ground effect is computed using an exponential expression

$$\Delta v_{i_{IGE}} = v_{i_{OGE}} \left[1 + (G-1)(e^W)\right]$$

where $G = 1\text{-GECON1}(e^{\text{GECON2}(h_H/2R)})$ and $W = \text{GEWASH}(u^2 + v^2)^{1/2}$. If $e^W \leq 0.001$ or $G > 1$, then G is set equal to one. This form of ground effect equation is a variation of an equation derived by Hayden in Ref. 13 and shown in Ref. 6 to provide excellent correlation of the mathematical model with XV-15 flight test data. The factor e^W washes out exponentially the effect of ground proximity with forward speed. At 30 ft/sec and greater, the effect is completely washed out.

3. General Input Data Requirements

The input data requirements for the rotor are described in an organized format on Pages A-5 through A-12 of Appendix A. The majority of the required rotor input data values are geometric constants which are self-explanatory or are rotor- or blade-specific parameters which are configuration dependent [e.g., δ_3, blade inertia (I_b), flapping spring rate (K_H)]. The values for average rotor blade lift-curve slope and drag coefficient, $a_{0,1,2}$ and $\delta_{0,1,2}$ respectively, should be iteratively determined using rotor test stand data or other rotor performance programs via correlation with the generic tilt-rotor program output. If this type of approach is not possible, or if data does not exist, then input data values for these parameters should not be input without careful consideration, because it is highly unlikely that any prop-rotor configuration will have average rotor blade aerodynamic characteristics similar to the low twist and usually single airfoil section characteristics of untapered helicopter rotor blades.

Input data requirements for determining side-by-side (X_{SS}), tandem rotor (X_{SF}), and ground effects are obtained using sources such as those discussed in the previous section. In most cases it would be expected that the input data used for the XV-15 would be appropriate for most tilt-rotor investigations. The values for X_{SS} and X_{SF} are obtained from data tables in the simulation computer program (plotted in Figs. 2 and 3); whereas, the coefficients for the ground effect equation (GECON1 and GECON2) were iteratively determined by curve fitting data (originally presented in Ref. 14) and then correlating with XV-15 flight test data (Fig. 4 from Ref. 6).

Input data values for Mach number effects and induced-velocity coefficients have been determined from experience and correlation with XV-15 wind-tunnel and flight-test data. Unless specific knowledge about rotor characteristics unquestionably indicates that a change is needed in one of these parameters, it is recommended that XV-15 values be used.

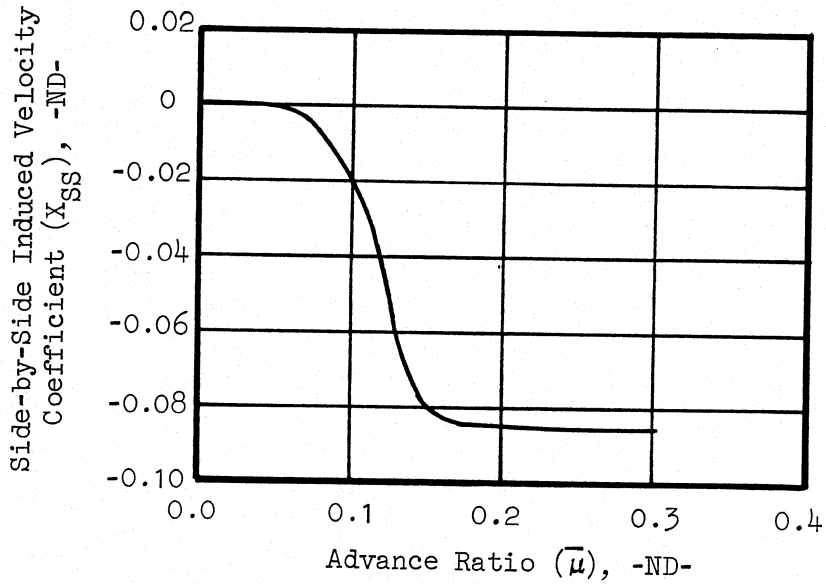

Figure 2. Side-by-Side Rotor Effect on Induced Velocity

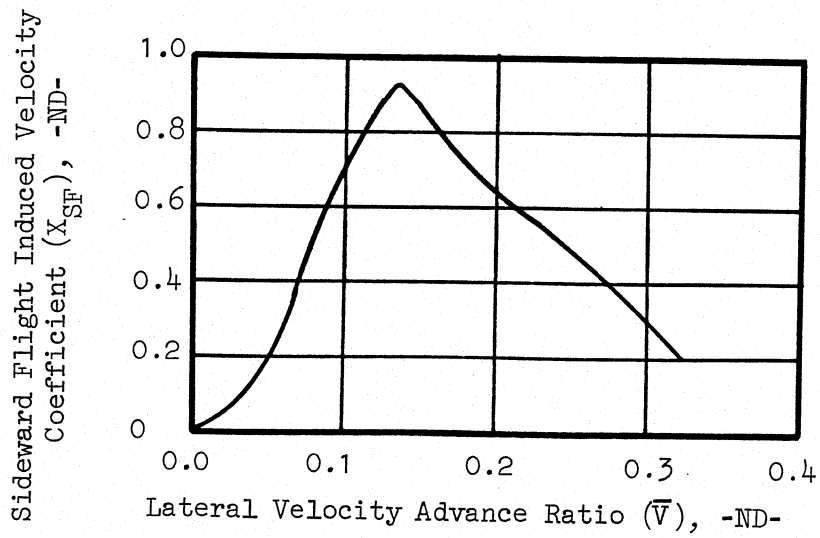

Figure 3. Sideward Flight Rotor Effects on Induced Velocity

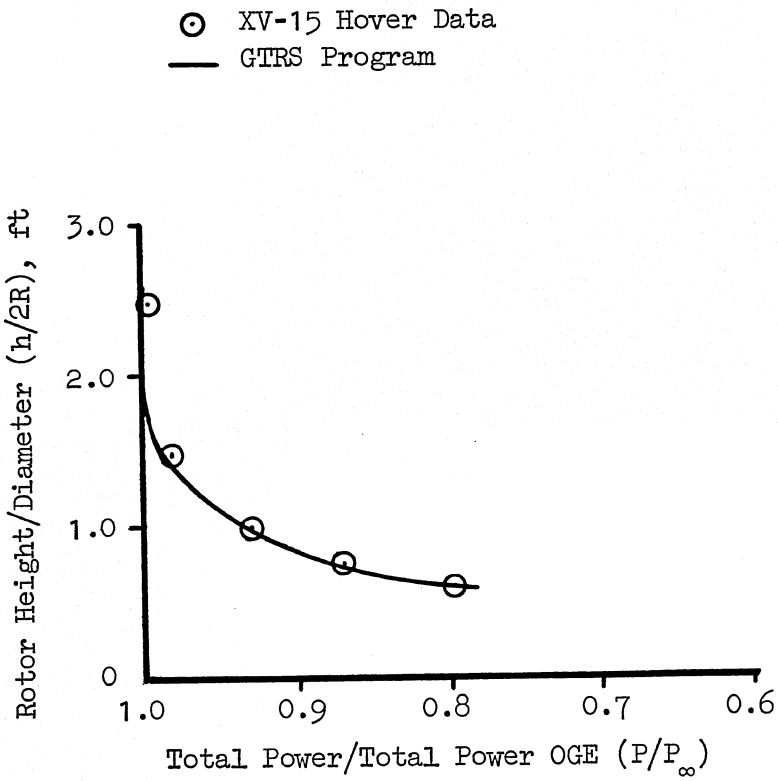

Figure 4. Effect of Ground Proximity on Hover Power Required

The tables provided for setting an upper bound limit on usable rotor thrust coefficient $\overline{C}_T$ are defined as a function of μ and β_m. These tables can be modified from the XV-15 values based upon either analytical or rotor test data from the rotor which is to be simulated. For simulated flight conditions not requiring high thrust, e.g., high-g maneuvers, these tables have no effect on the calculated results and would not be in need of modification.

B. SUBSYSTEM 2: ROTOR-INDUCED VELOCITIES (ALSO PARTS OF SUBSYSTEMS 4, 5, 6, AND 14)

The rotor wake-airframe aerodynamic interferences (or rotor-induced velocities) represented in the generic tilt-rotor mathematical model consist of three parts:

1. The effect of the rotor wakes on the wing lift and drag.
2. The effect of the rotor wakes on the horizontal stabilizer and vertical fin lift and drag.
3. The effect of the rotor wake-airframe-ground interaction in producing net rolling moment and pitching moment effects when hovering near the ground.

1. Model Structure

The calculation of the wing aerodynamic forces and moments due to rotor wake effects is made separately from the forces and moments generated by the freestream flow. The calculation of the rotor wake effect involves calculating the area, angle of attack, and dynamic pressure of the portion of the wing immersed in the wake. Figure A4-1 (in Appendix A) illustrates the representation of this effect.

The area of the wing immersed in the rotor wake, S_{iW} (shown in Fig. A4-1) is computed as a function of wake radius, conversion angle, wake angle of attack, and sideslip angle of the fuselage. The expression used to compute the wake radius of a hovering rotor as a function of vertical distance from the rotor disk is derived in Ref. 15. Experimental

data also show that the contracted wake remains stable as it reaches the wing and horizontal stabilizer surfaces. Therefore, the equation for the wake radius (Eq. 3 of Ref. 15) has been simplified, since the wing and stabilizer surfaces are located at approximately 0.4 R below the rotor disk.

$$R_W = R\{0.78 + 0.22 \text{ Exp } [-(0.3 + 2Z \sqrt{C_{RF}} + 60 \ C_{RF})]\}$$

The rotor-induced velocity at the wing varies with speed and mast tilt and is given by the following expression:

$$W_i\Big|_{R/W} = (K_0 + K_1\mu + K_2\mu^2 + K_3\lambda + K_4\lambda^2)(W_i)$$

where the constants K_{0-4} are determined from powered rotor test data. Wing loads at high negative incidences caused by the rotor wake at low speeds are determined using lift and drag coefficient data tables that are defined up to angles of attack of ± 90 deg. Asymmetric flight at low speeds, which causes unequal portions of the left and right wing to be affected by the left and right rotor wakes and which generates roll and yaw moments, is also taken into account.

The induced velocity at the horizontal stabilizer and the vertical fins (a function of airspeed and mast angle) is determined by first calculating the rotor-induced velocity for trimmed flight and then correcting it for angle of attack and sideslip from data tables based upon wind-tunnel data. The values calculated are assumed to be constant across the empennage for the analysis.

When hovering in ground effect (h/D < 2.0), both an unstable rolling moment and a pitching moment are generated by aerodynamic interaction between the rotor wake, fuselage, wing, horizontal stabilizer, and the ground. The rolling moment effect is represented in the mathematical model by a polynomial equation for the rolling moment as a function of h/d

and then applied at the aircraft center of gravity. The in-ground effect pitching moment is modeled as an exponential function of rotor thrust, rotor hub height above the ground, and airspeed; and the pitching moment is applied at the aircraft center of gravity. The decision to model this effect was made following an evaluation of pilot comments and flight test data first presented in Ref. 6 and later in Ref. 16.

2. Input Data Requirements

The details of the input data requirements are listed on Pages A-34 through A-37 of Appendix A. The coefficients $K_{0,1,2,3,4}$ are determined from powered-model wind-tunnel data. The rotor-induced velocity at the horizontal stabilizer and vertical fins is also based on powered-model wind-tunnel data. The velocity induced at the tail by the rotors was derived for the XV-15 by analysis of pitching moment data with the tail ON and OFF as well as with and without the rotors (Refs. 17 and 18). Data generated by this method should look similar to the XV-15 data for $\beta_m = 0$ deg presented in Fig. 5, which is plotted from Appendix B, Table 2-Ia on Page B-22. (Data for β_m values other than 0 deg are not plotted but are contained in the tables.) Further corrections to data from these tables (which are corrections for angle of attack) are made for sideslip from Table 2-II.

The data used to fit the polynomial equation for the rolling moment data was measured using a 0.2 scale powered XV-15 wind-tunnel model (Ref. 17). This data is shown plotted in Fig. 6. The data used to fit the in-ground effect pitching moment equation is based on flight test data from Refs. 14 and 16, which is presented in Fig. 7, and compared with the simulation results using the GTRS program.

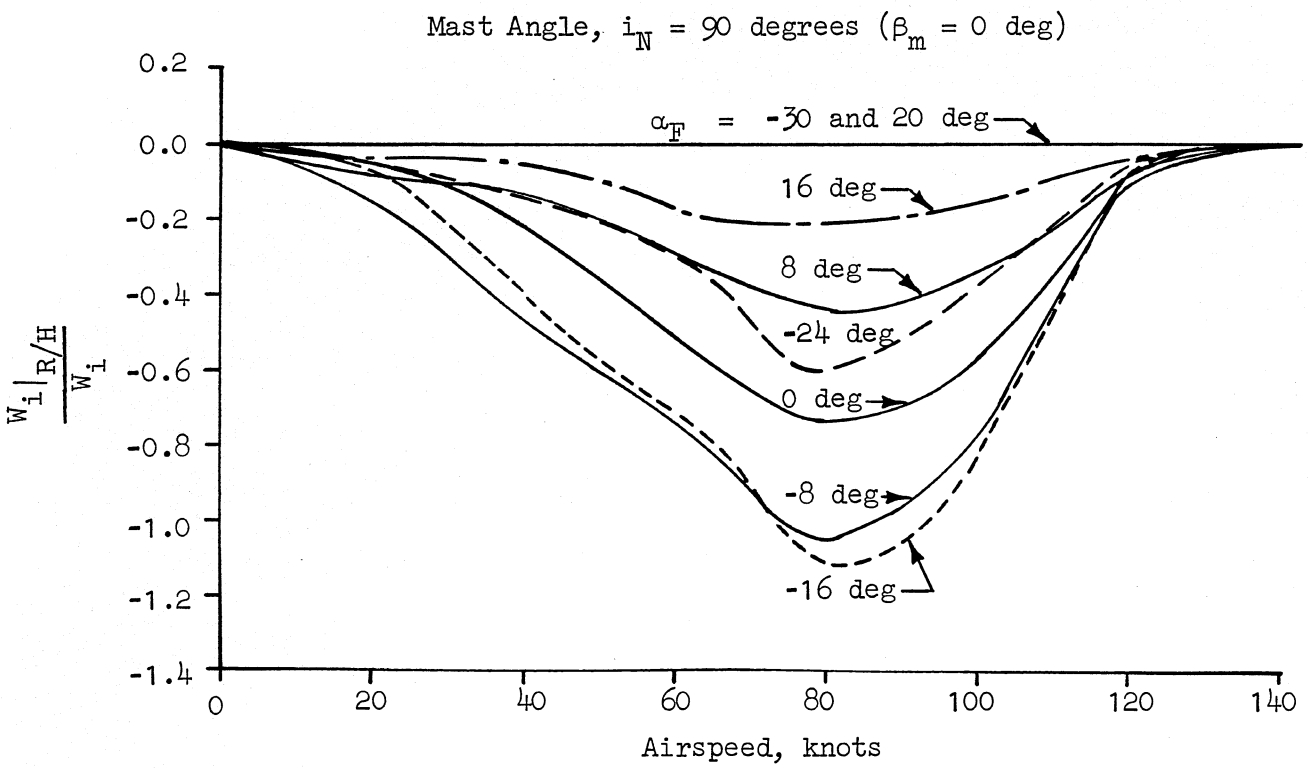

Figure 5. Rotor Wake On the Horizontal Stabilizer as a Function of Airspeed at a Nacelle Incidence of 90 Degrees

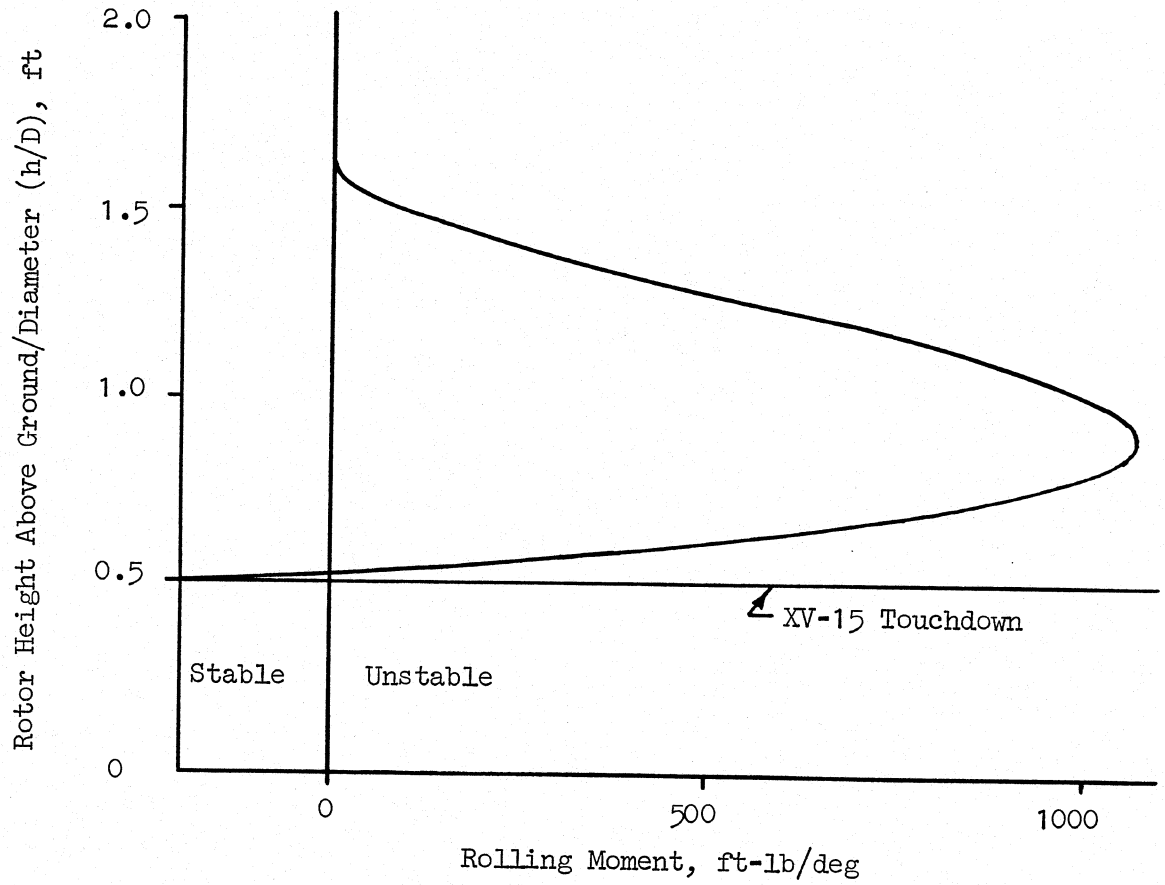

Figure 6. Representation of In-Ground Effect Rolling Moment

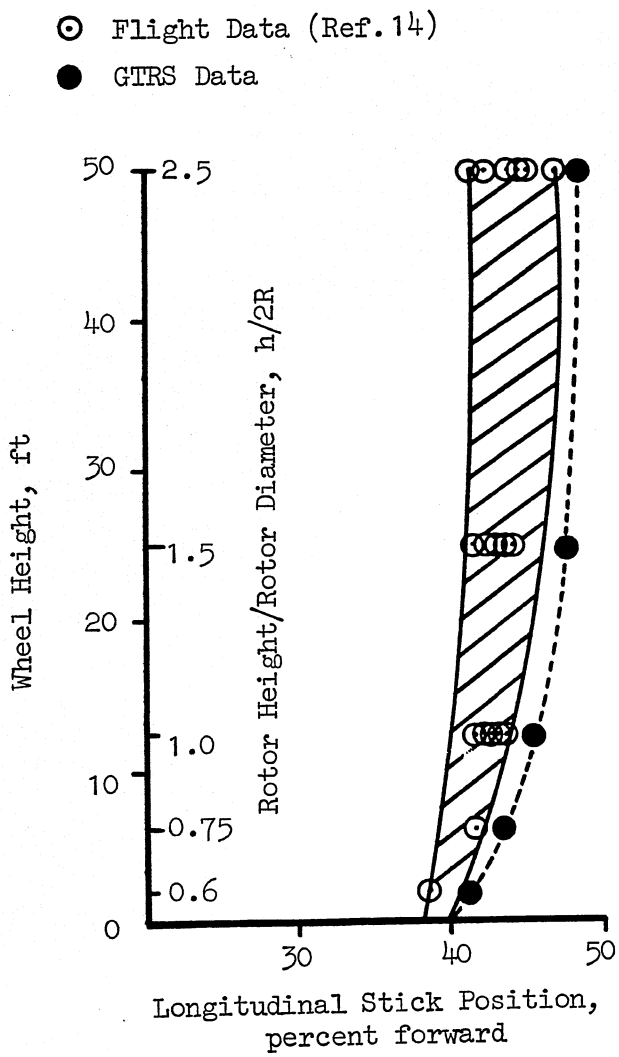

Figure 7. The Effect of Hover Height on Longitudinal Stick Position

C. SUBSYSTEM 3: FUSELAGE AERODYNAMICS

1. Model Structure

The fuselage, wing-pylon assembly, horizontal tail, and vertical fins are modeled separately in order to facilitate accounting for the influence of the rotor wake on the airframe aerodynamics. Equations for the fuselage lift, drag, side force, pitching moment, yawing moment, and rolling moment are referenced to the wind-axis system and defined at the input fuselage center of pressure. Aircraft angular rates as well as the rotor wakes are neglected in calculating the fuselage aerodynamic forces and moments.

2. Input Data Requirements

In general, the wind-axis airframe aerodynamics are extracted from wind tunnel test data. For the XV-15, this data is tabulated in Appendix B on Pages B-26 through B-30. Where wind tunnel data was not available for the XV-15, characteristics were estimated using Refs. 19, 20, and 21. [For the XV-15, the coefficients in the equations for angles of attack and sideslip less than or equal to 20 deg are based on wind-tunnel data. For angles of attack greater than 20 deg, the coefficients have been approximated.] The values for the constants LBFO, DBFO, and MBFO are the same values as those in the data tables at $\alpha_F = \beta_F = 0$ and must be subtracted out. Otherwise, the equations would add the respective numbers together twice (once from each of the α_F and B_F tables), thereby resulting in double the actual value being used in calculations.

D. SUBSYSTEM 4: WING-PYLON AERODYNAMICS

1. Model Structure

The wing-pylon aerodynamic forces and moments are defined in the local wind-axis system. Wing-body interference effects are included in the aerodynamic data.

Calculation of the wing aerodynamic forces and moments is made up of two parts: the first part is composed of the part of the wing which is influenced by the rotor wakes, and the second part, that which is influenced by only the free stream flow. The mathematical model and all sign conventions are described and flow charted in Appendix A or in the previous section of text (Subsystem 2).

The wing-pylon lift and drag generated by the free stream flow are functions of angle of attack, conversion angle, flap setting, and Mach number. The pitching moment is a function of flap setting.

The wing lateral-directional aerodynamic forces and moments are calculated using equations for stability derivatives from Ref. 19. Compressibility effects and the wing loading are included in the lateral-directional characteristics.

Wing-pylon lift and drag coefficients are provided for mast angles of 0 deg and 90 deg and for four flap settings. Coefficients for intermediate mast angles and flap settings are obtained by interpolation. Mach number corrections are made only for the flaps-up airplane mode configuration.

The angle of attack of the wing is also modified in order to reflect the induction effect of the thrusting rotors. The expression for the wing angle of attack is:

$$\alpha_W = \alpha_F - KXRW\,(x_{R/W})\left[\frac{C_{RFR} + C_{RFL}}{MAX^2(\mu,\ 0.15)}\right](57.3)$$

where $x_{R/W}$, the induction coefficient, is a function of the distance between the rotor and the wing and of mast angle; and $C_{RFR,L}$ are the non-dimensionalized rotor force coefficients for the right and left rotors.

2. Input Data Requirements

The wing subsystem requires more data input than any other section of the GTRS model. A detailed listing of the input data requirements is provided on Pages A-45 through A-56 in Appendix A. Constants and many of the coefficients listed on Pages A-45 and A-46 are either wing geometric values or can be calculated using Ref. 19. (Other sources for calculation of wing lateral-directional stability derivatives should also be acceptable). Values for calculation of the constants in the equation for the rotor flow field effects on angle of attack are for the XV-15 and, in general, should be applicable for other tilt-rotor configurations similar to the XV-15. The constants in the rotor downwash/wing equations for flap effects are based on wind-tunnel or flight-test data and are used to adjust wing download as a function of flap setting. The spinner drag coefficients were determined for the XV-15 from wind-tunnel test data of the full scale XV-15 rotor and pylon (shown in Ref. 20). Values for the pylon interference drag were determined for the XV-15 from flight-test data and were a correction or addition to the model in order to account for extra drag due to wing-pylon interference. Significant differences exist between the "smooth and clean" skin surfaces of the wing tip and the inside surface of the pylon for the XV-15 wind tunnel model and the surfaces around the XV-15 wing-pylon interface. (These differences can easily be seen in a photograph of the XV-15 in helicopter flight.) This input variable will probably not be obtainable from wind-tunnel data, since the pylon drag will normally be included with the wing drag and input into the wing-pylon tables described in this model. However, in evaluating a tilt-rotor configuration using this program, it would nevertheless be advisable to use XV-15 input data as a minimum if flight-test data cannot be obtained. The effect of this parameter can be significant in the deceleration of the tilt rotor during reconversion to helicopter mode and is noticeable by pilots in a manned simulation environment.

Coefficients for wing lift, drag, and pitching moment should be obtained whenever possible through use of wind-tunnel testing. The XV-15 aerodynamic coefficients which are supplied in Appendix B (Pages B-31

through B-55) are based on wind-tunnel data for angles of attack up to stall. At angles of attack above stall, the coefficients are approximated based on the test data presented in Ref. 21. Examples of how data should look for wing lift and drag for the flap/flaperon settings of 0/0 and 40/25 deg are presented in Figs. 8 through 13. The dihedral effect of the wing-pylon is based on wind-tunnel test data and is a function of angle of attack and flap setting as well as sideslip. The aileron effectiveness and yawing moment coefficients are also based on wind-tunnel data (or in some cases may have to be calculated) and are a function of angle of attack, mast angle, and flaperon deflection.

The wake deflection or downwash at the empennage due to the wing-pylon for the XV-15 is determined from wind-tunnel data for angles of attack up to stall. Above wing stall, the downwash is approximated using data for the high wing-low tail configuration given in Ref. 22. Figure 14 presents example data for the XV-15 for two flap/flaperon positions at two mast angles (helicopter and airplane). The downwash at the empennage due to the rotor wake is discussed in a previous section.

E. SUBSYSTEM 5: HORIZONTAL STABILIZER AERODYNAMICS

1. Model Structure

Detailed input data requirements for the horizontal stabilizer model are described on Pages A-78 through A-82 in Appendix A. The dynamic pressure and angle of attack calculations for the horizontal stabilizer model, as shown in Fig. A5-1, take into account wing-body blockage, mast angle, the wing-pylon wake, the rotor wake, and the fuselage attitude and angular velocities.

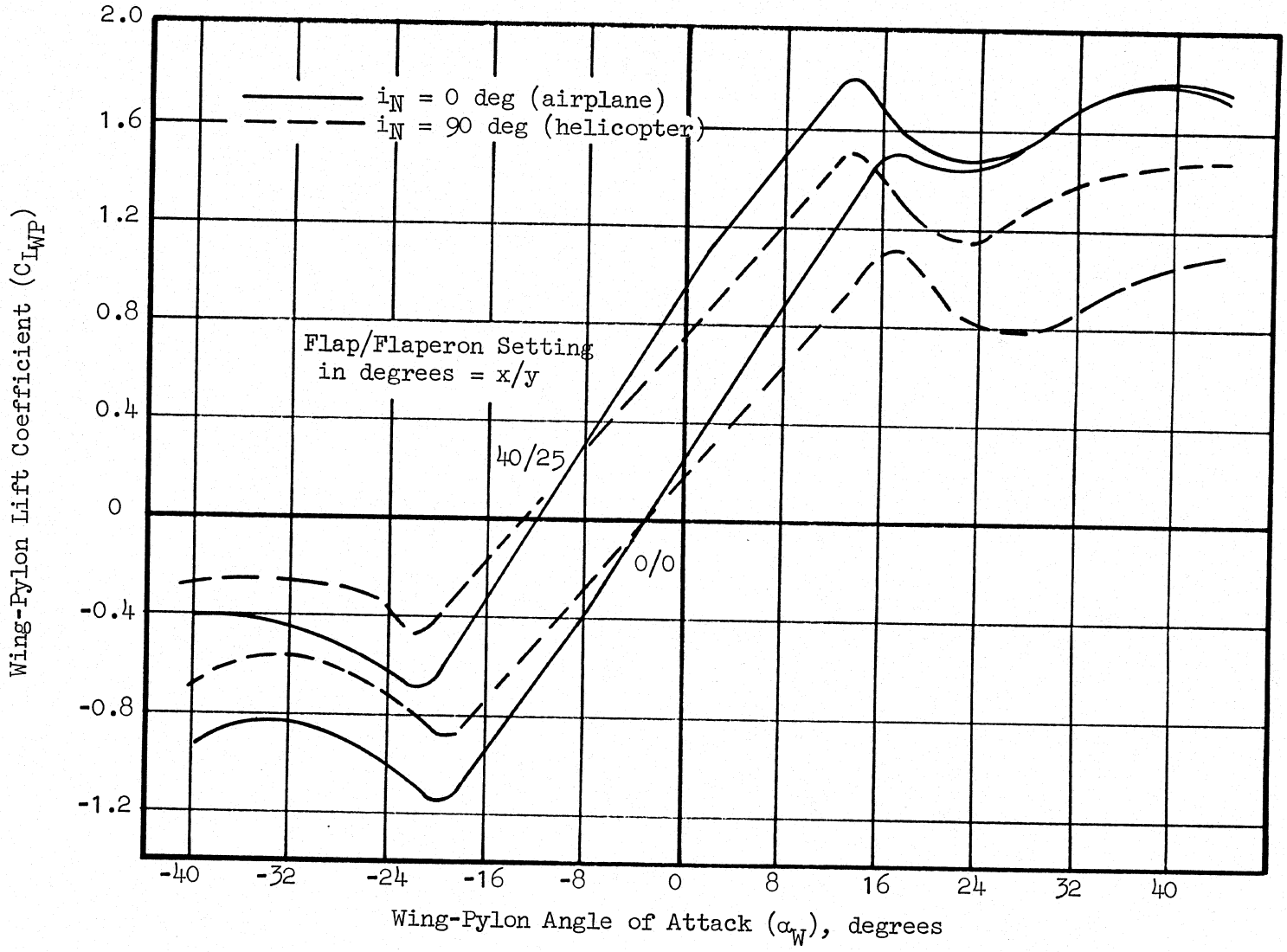

Figure 8. Wing-Pylon Lift Coefficient Versus Angle of Attack for Flap/Flaperon Settings of 0/0 and 40/25 Degrees

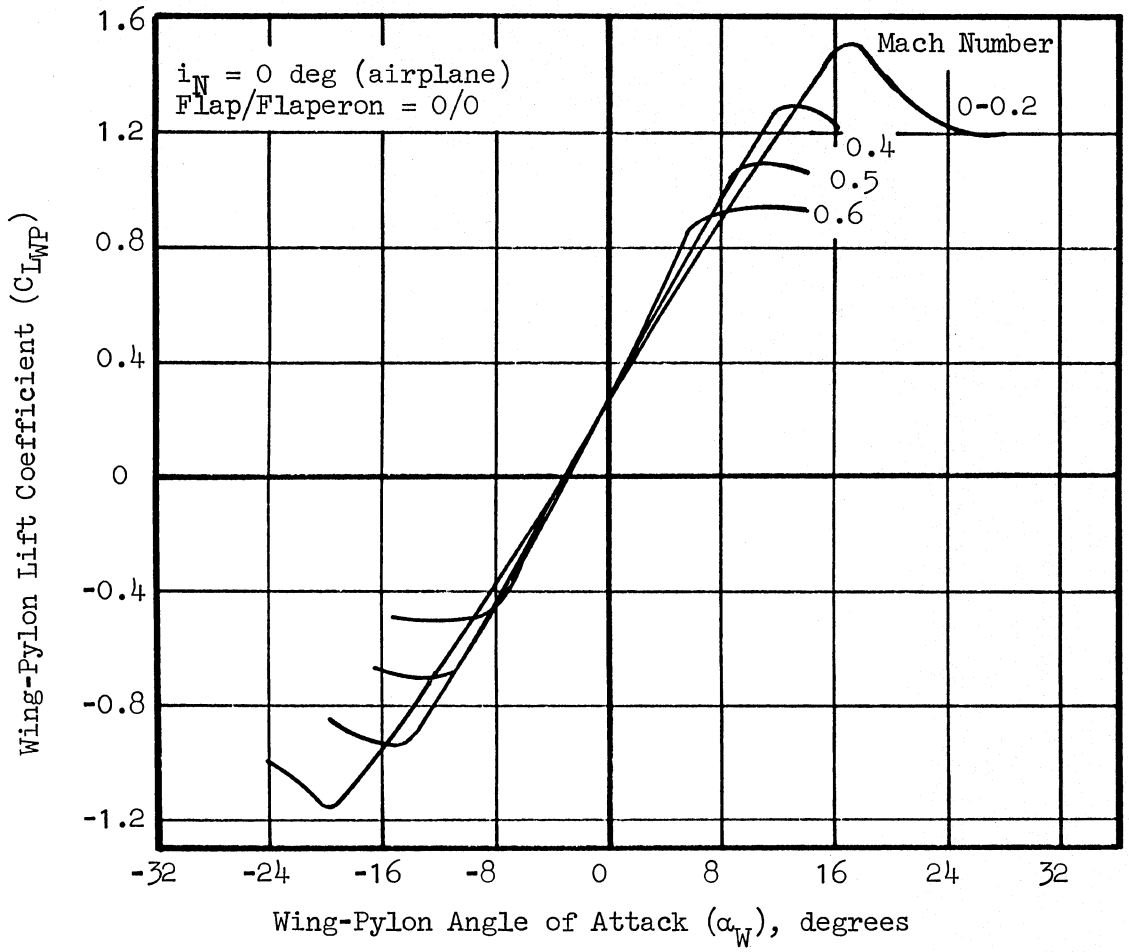

Figure 9 . Wing-Pylon Lift Coefficient Corrections Due to Compresibility

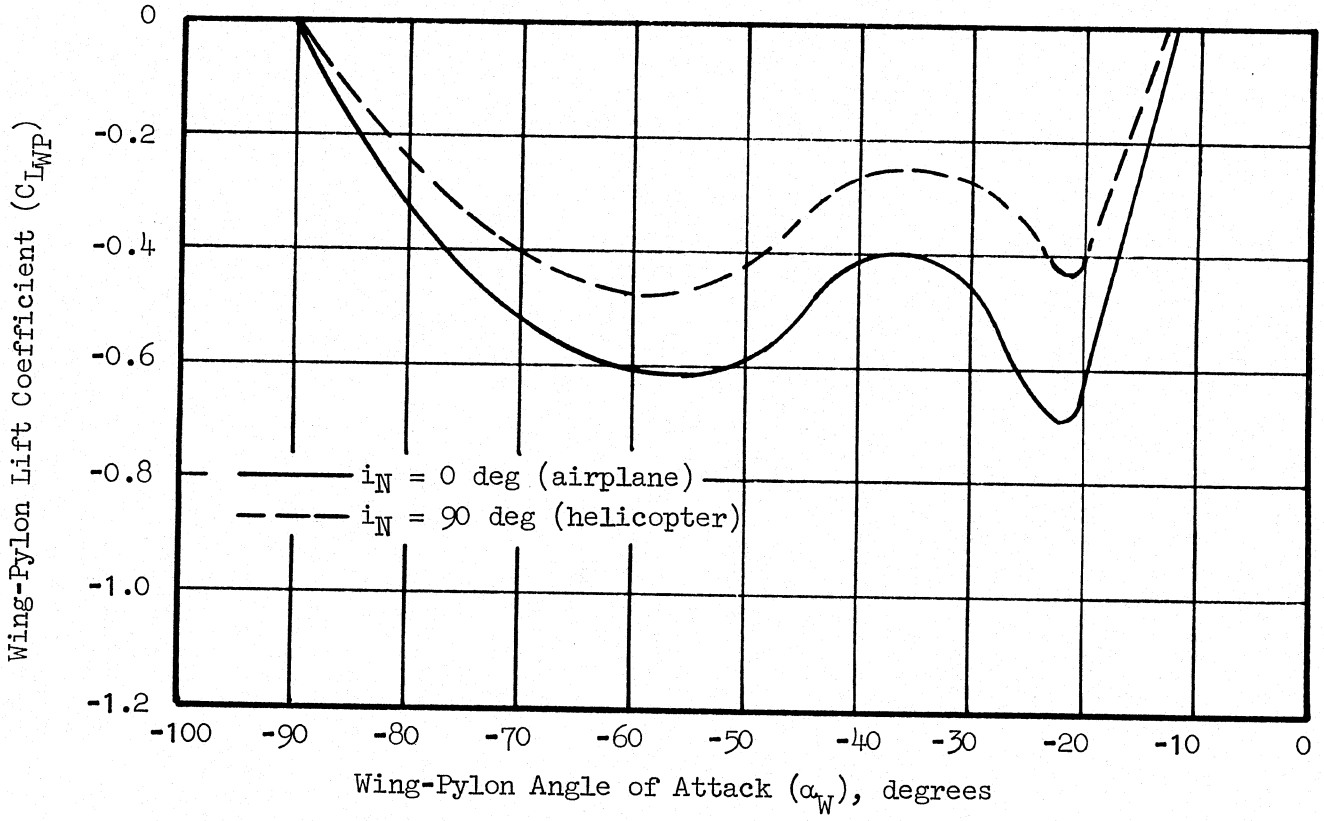

Figure 10. Wing-Pylon Lift Coefficient at Large Negative Angles of Attack for a Flap/Flaperon Setting of 40/25 Degrees

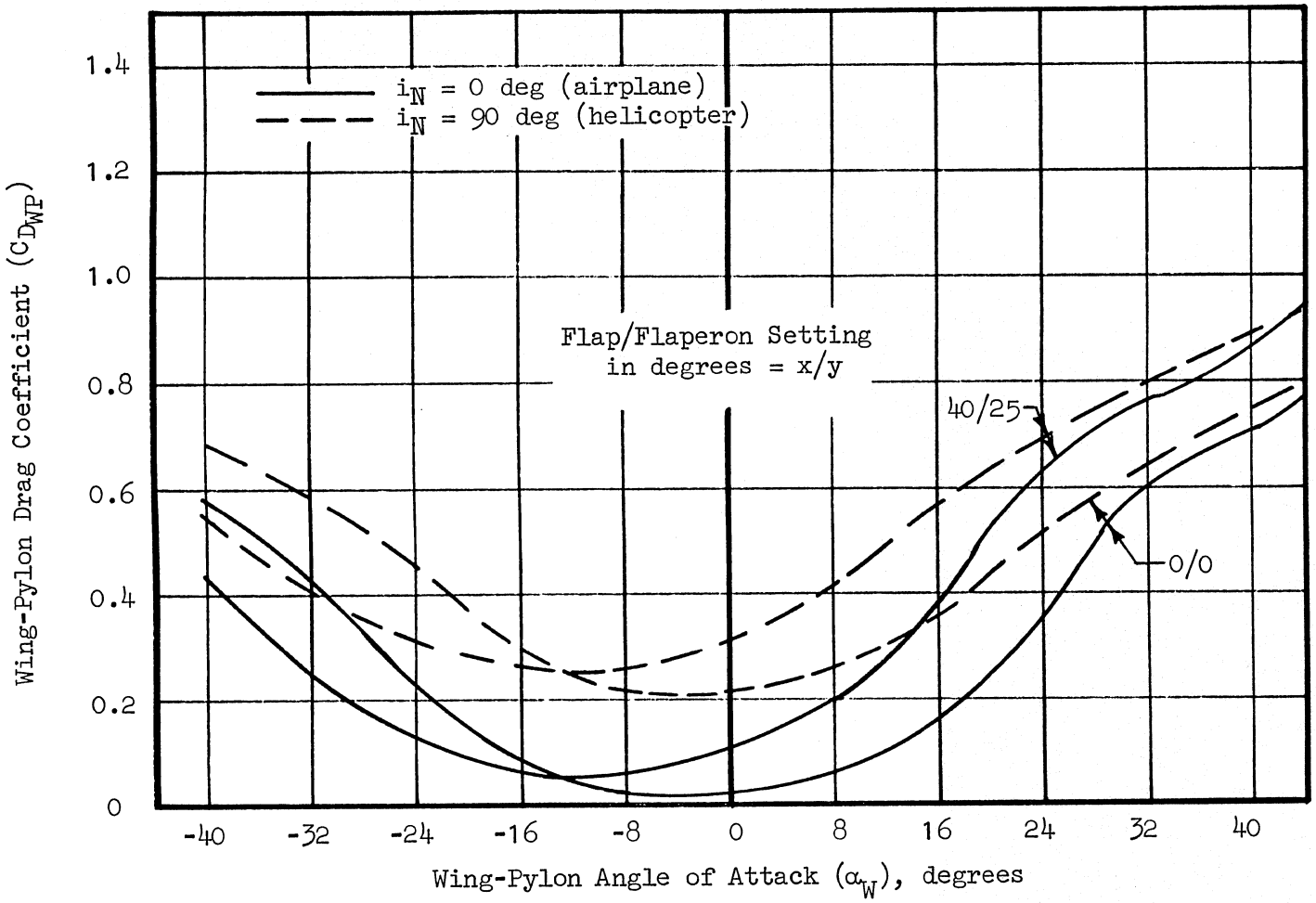

Figure 11. Wing-Pylon Drag Coefficient Versus Angle of Attack for Flap/Flaperon Settings of 0/0 and 40/25 Degrees

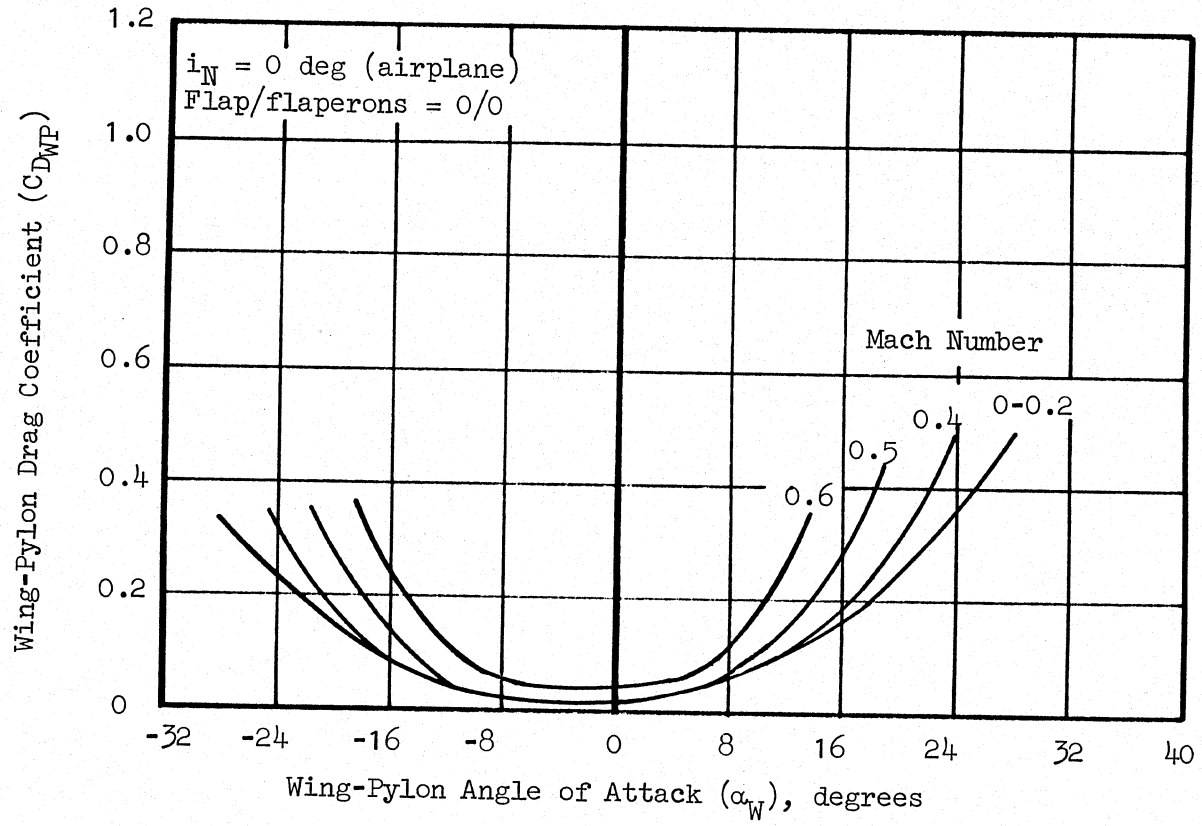

Figure 12. Wing-Pylon Drag Coefficient Corrections Due to Compressibility

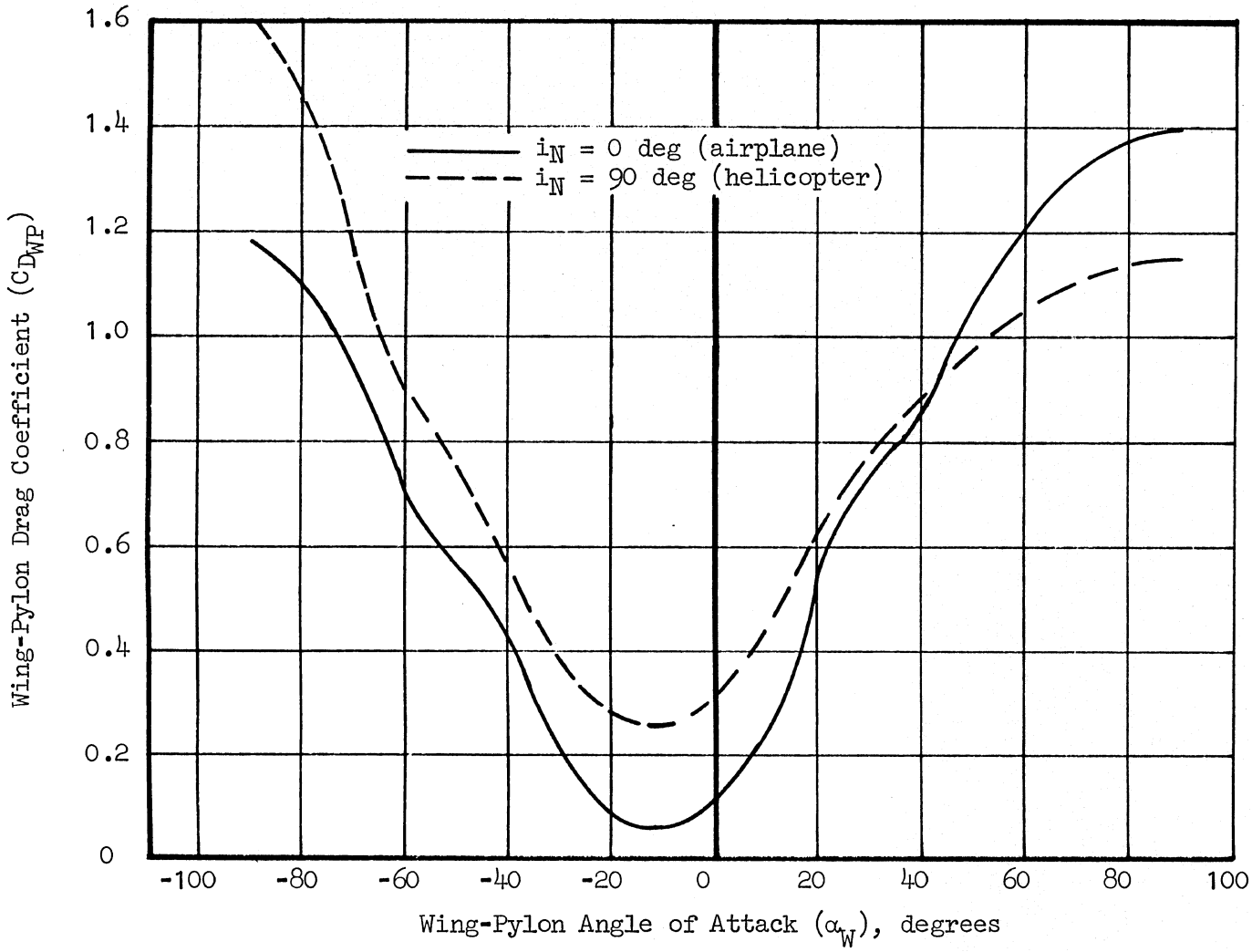

Figure 13. Wing-Pylon Drag Coefficient at Large Negative Angles of Attack for a Flap/Flaperon Setting of 40/25 Degrees

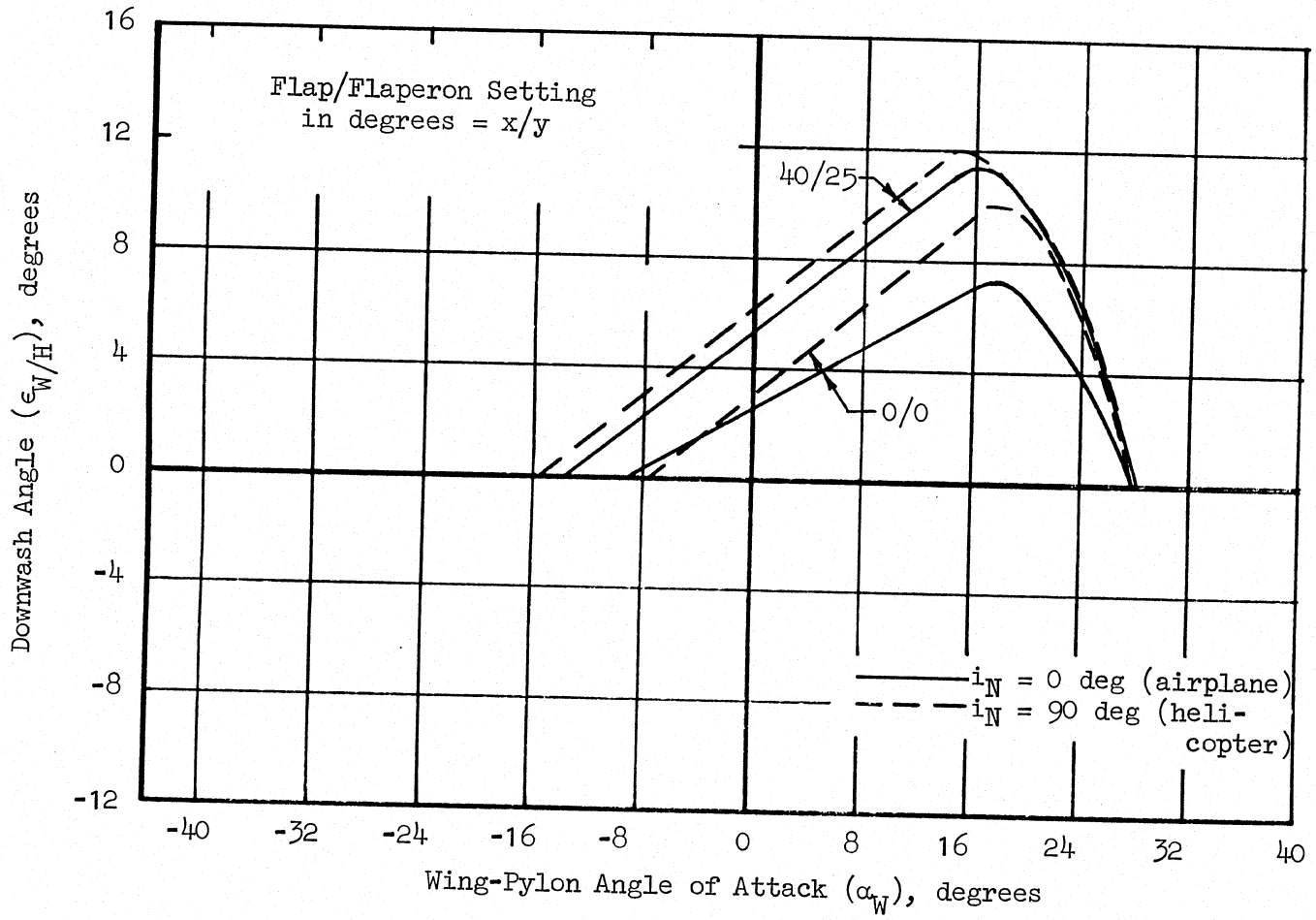

Figure 14. Wing-Pylon Wake Deflection (Downwash) at the Horizontal Stabilizer For Flap/Flaperon Settings of 0/0 and 40/25 Degrees

2. Input Data Requirements

The constants required for the horizontal stabilizer model on Page A-79 are geometric in nature and are a function of the empennage configuration of interest. The value(s) for elevator effectiveness (τ_e) can be measured both from a wind-tunnel model (Ref. 23) or from sources such as Ref. 19. Data table input allows for further correction due to Mach number effects. The values for change in horizontal stabilizer lift coefficient $C_{L_{H_\beta}}$ with sideslip and pitching moment are best determined from sources such as Ref. 19. The horizontal stabilizer dynamic pressure loss multiplier (KHNU) is included in the model for the purpose of providing a simple term to provide the capability to account for the dynamic pressure loss if detailed wind-tunnel data is not available for mapping empennage dynamic pressure losses as a function of angle of attack, sideslip, and airspeed. If this type of data is available, it can be entered as data tables as described on Page A-79 and tabulated on Pages B-65 through B-68.

The lift and drag coefficients for the horizontal stabilizer should be determined from wind-tunnel test data for angles of attack up to stall whenever possible. Examples of the data requirement, as measured for the XV-15 are presented in Figs. 15 and 16. Otherwise, sources such as Ref. 19 can be used to compute these coefficients. Above stall, the coefficients can be approximated using data from Ref. 21.

F. SUBSYSTEM 6: VERTICAL STABILIZER AERODYNAMICS

1. Model Structure

The GTRS model assumes an H-tail vertical fin configuration like the XV-15, and the forces and moments on the left and right fins are computed separately in order to account for the variation in rotor wake effects with sideslip. The dynamic pressure and angle of attack at the fins, as shown in Fig. A6-1, take into account the wing-body blockage, mast angle,

Figure From Ref. 1

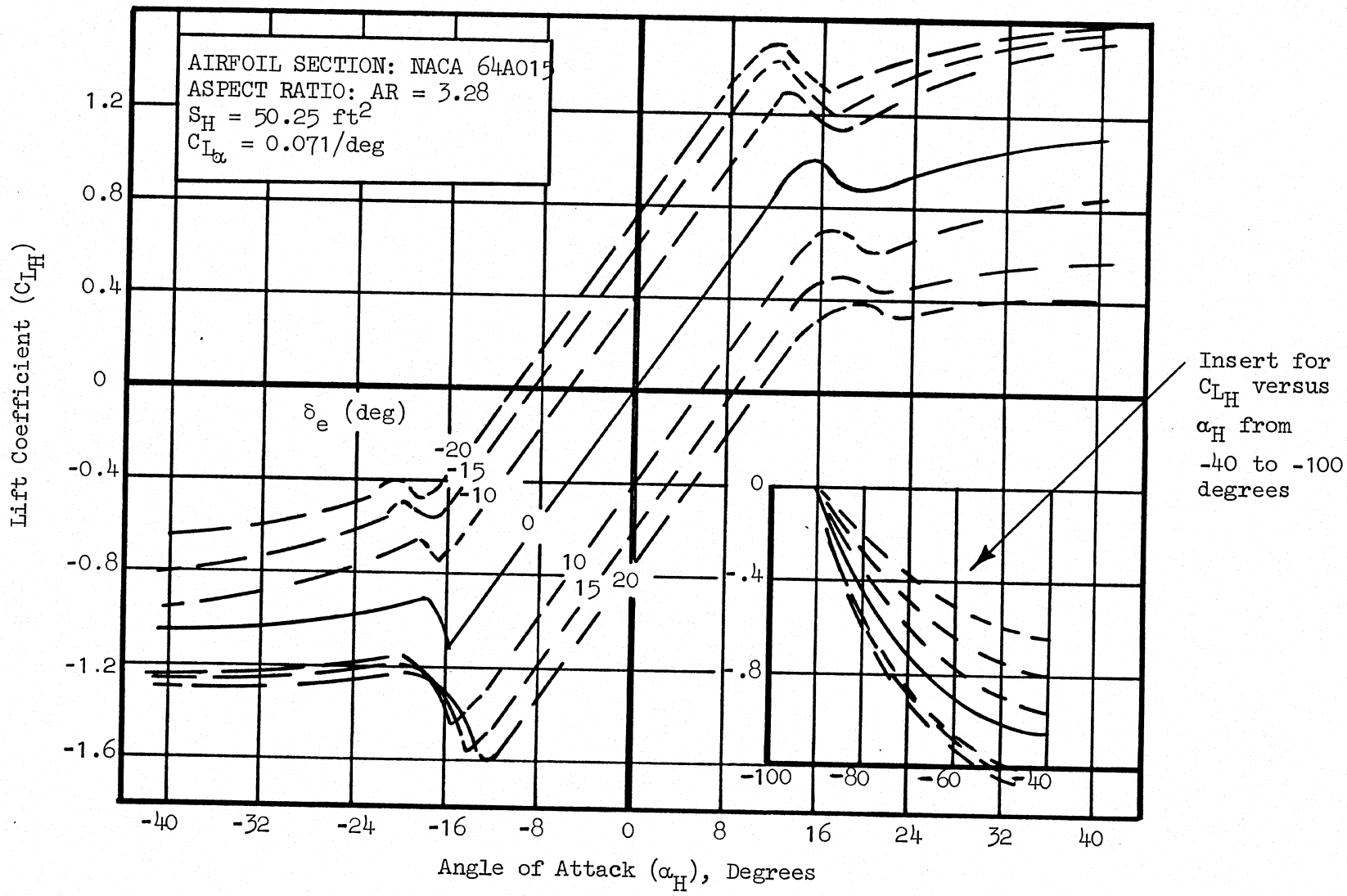

Figure 15. Horizontal Stabilizer Lift Coefficient Versus Angle of Attack

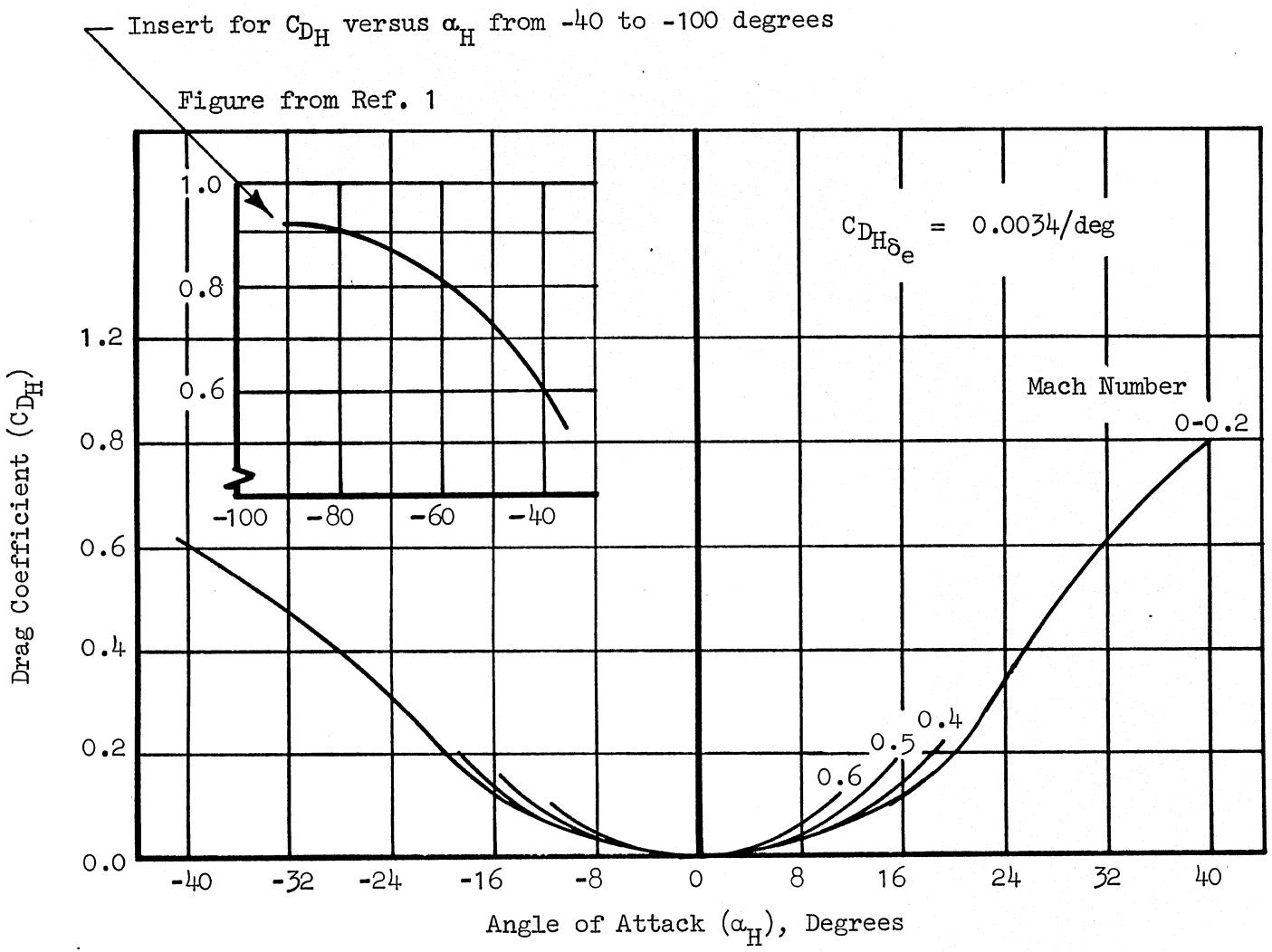

Figure 16. Horizontal Stabilizer Drag Coefficient Versus Angle of Attack

wing-pylon wake, rotor wake, and fuselage attitude and angular velocities. Detailed input data requirements for the vertical stabilizers are described on Pages A-89 through A-94 in Appendix A.

2. Input Data Requirements

The constants required are generally geometric in nature and are a function of the empennage configuration of interest. The rudder effectiveness factors (τ_r and K_r) can be measured both from a wind-tunnel model (i.e., Ref. 23) or from sources such as Ref. 19. The roll and yaw rate correction coefficients which are a function of sideslip angle are determined from sources such as Ref. 19. The vertical fin dynamic pressure loss multiplier (KUNU) is included for the same general reason as was the horizontal stabilizer coefficient (KHNU).

The lift and drag coefficients of the fins should be determined from wind-tunnel data for angles of attack up to stall whenever possible. Examples of the data requirements, as measured for the XV-15, are presented in Figs. 17 and 18. Otherwise, sources such as Ref. 19 can be used to compute these coefficients. Above stall, the coefficients are approximated using data from Ref. 21. The fuselage sidewash factor ($1-\partial\sigma/\partial\beta$) at the fins is a function of flap setting, mast angle, fuselage angle of attack, and sideslip angle. The rotor sidewash factor ($K_{\beta R}$) is a function of the sideslip angle of the fin and the forward airspeed. Both of these groups of tables are best determined from powered model wind-tunnel data. If wind-tunnel data are not available, careful attention should be given to calculation of these parameters, or the XV-15 data values should be used.

Figure From Ref. 1

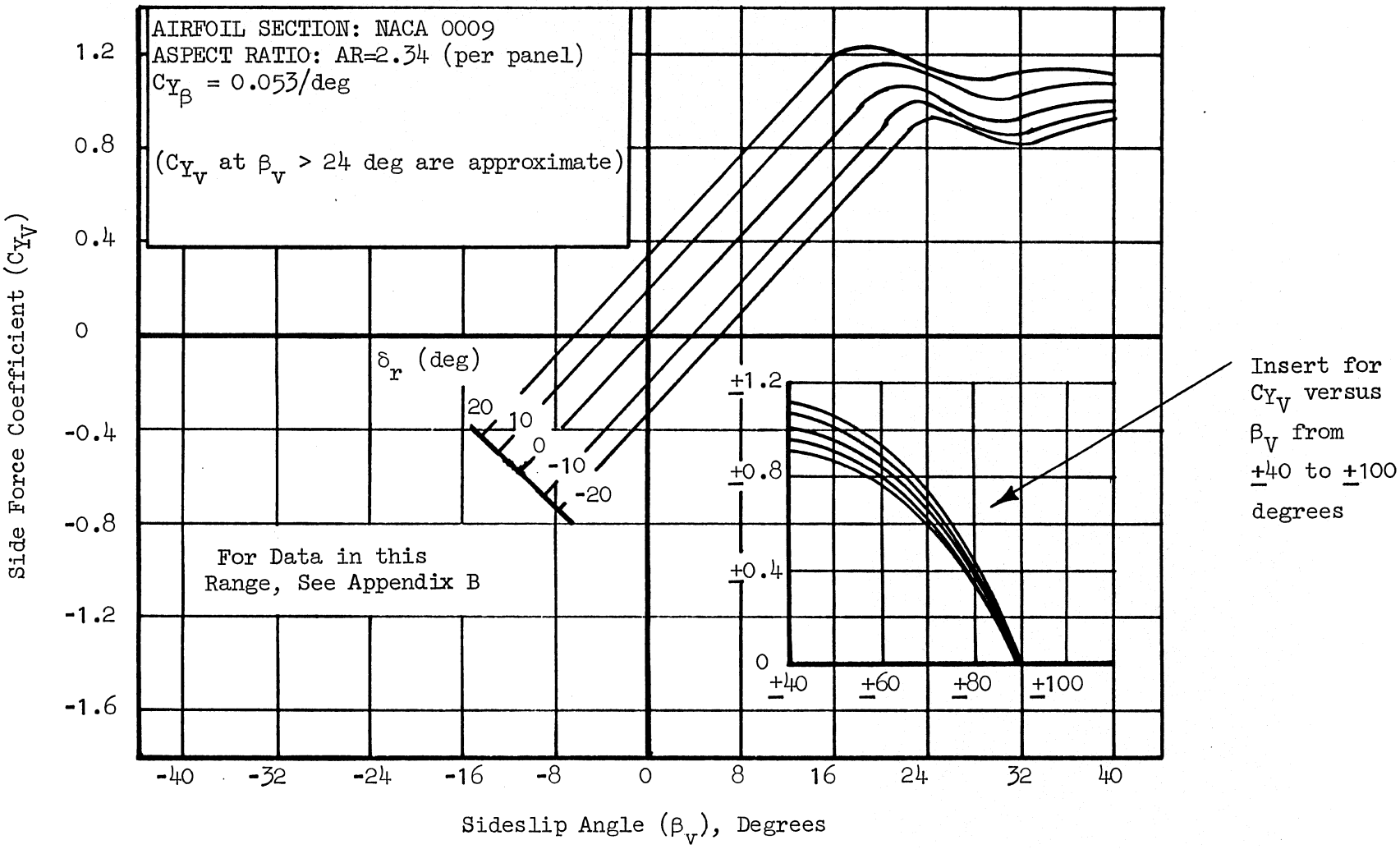

Figure 17. Vertical Stabilizer Side Force Coefficient Versus Sideslip Angle

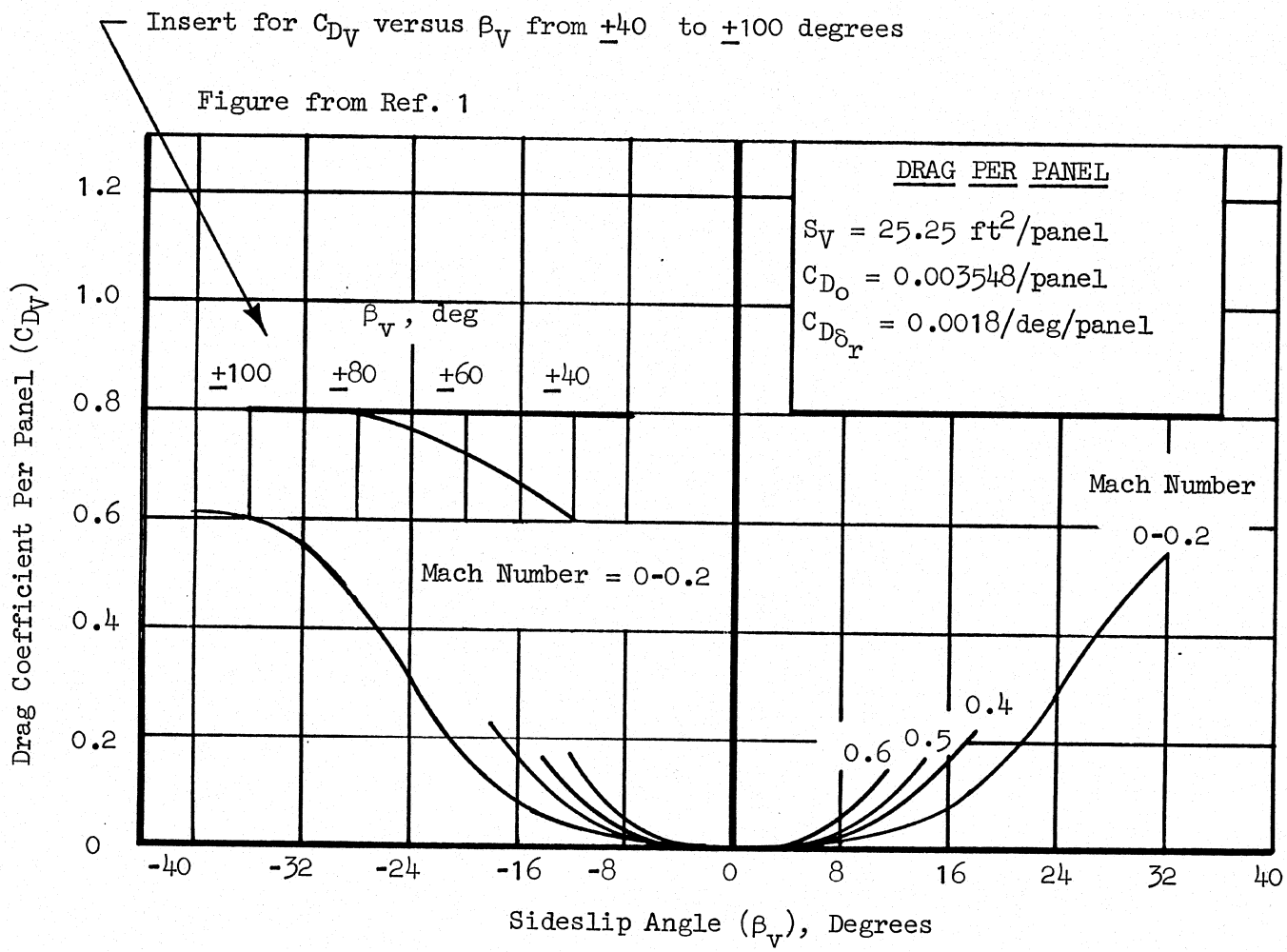

Figure 18. Vertical Stabilizer Drag Coefficient Versus Sideslip Angle

G. SUBSYSTEM 7: LANDING GEAR

1. Model Structure

Two landing gear model structures are presented in Pages A-103 through A-122 of Appendix A; however, only the Subsystem 7A structure has been used for real-time simulation purposes due to computer cycle time limitations which have resulted in landing gear modeling instabilities (the model is derived from Ref. 24). Use of the Subsystem 7A model structure requires careful tuning at NASA ARC; therefore, the input data provided for the XV-15 is for reference only, since it "works" for the XV-15. Any modeling of another tilt rotor would probably require modification to these coefficients. Therefore, a detailed discussion on most of the actual landing gear coefficients is not really useful.

2. Input Data Requirements

Most of the constants, as described on pages A-103 and A-104 of Appendix A, are geometric in nature and are primarily of value (especially in the batch version of the GTRS program) for computation of the location of landing gear drag. Both landing gear drag and landing gear pod drag are best determined from wind-tunnel data; however, numerous references exist (e.g., Ref. 25) which do provide guidance on landing gear drag for extended landing gear. Data for drag is input as a function of the percent of gear extension or retraction which, in turn, is a function of the "time" required for the landing gear to cycle up or down following the pilot's command to cycle the landing gear.

H. SUBSYSTEM 8: CONTROL SYSTEM

1. Model Structure

The control system mathematical model consists of a controls mixing model and a force gradient model. Details of the XV-15 control system are presented on Pages A-123 through A-164 of Appendix A. The flight control

system is illustrated schematically, and sign conventions are presented in Figs. A8a-1 and A8a-2, respectively. The mathematical model of the control system contains mixing for the pilot and automatic flight control system inputs, washout of the rotor controls as a function of mast angle and airspeed, and conversion, landing gear, and flap controls. The mathematical model does not include friction or free play, and the time constants of the control actuators are assumed zero, since, in practice, they are less than the computer frame time. This assumption was tested in a simulation of the XV-15, and results presented in Ref. 6 confirmed the assumption.

The pedal and cyclic stick longitudinal and lateral gradients are specified as a function of airspeed. The location of the gradient detent (zero force position) may be moved by the pilot in order to trim out steady stick forces.

2. Input Data Requirements

Input data requirements, such as the control system gearing and control system limits, are generally self-explanatory as described and discussed in Appendix A. The force feel system, the control force trim system, and the pilot's control functions, as described in Subsystems 8b, 8c, and 8d, respectively, are only applicable to the NASA ARC VMS simulation version of the mathematical model. Therefore, further discussion on the control system is thought to be unwarranted, since most researchers will either use the XV-15 control system and the input values as described herein or will design their own control systems for replacement of the XV-15 control system.

I. SUBSYSTEM 9: CG AND INERTIA

The center of gravity and inertia subsystem, described on Pages A-165 through A-171 of Appendix A, provides modeling for the dynamic effects due to pylon acceleration. The changes in center-of-gravity location and inertia due to pylon tilt are also computed. Input data values for the

subsystem are either geometric or are values of inertia which can be calculated or determined from several sources (i.e., Ref. 26).

J. SUBSYSTEMS 10 THROUGH 14: COORDINATE TRANSFORMATIONS AND EQUATIONS OF MOTION

The equations of motion used to solve for the six-degrees-of-freedom flight path are identical to the ones provided in Ref. 8. The pylon degrees of freedom are neglected, since the wing-pylon natural frequencies are well above the frequency capability of the simulation software and hardware.

Transformation of forces and moments from wind to body axes and from mast to body axes is required for a number of subsystems. These transformations are provided in Subsystems 10a through 10f. Tilt-rotor accelerations, velocities, force and moment calculations, and summations are provided by Subsystems 11, 12, 13, and 14, respectively. Except for Subsystem 14, only tilt-rotor geometric data is required for input. Input data values required for the empirical calculation of the unstable rolling moment and the pitching moment in ground effect were discussed previously in Section B on the rotor-induced velocities.

K. SUBSYSTEM 15: FLIGHT ENVIRONMENT

The atmospheric model described on Pages A-235 through A-238 of Appendix A is the ICAO standard atmospheric model as described in Ref. 27.

L. SUBSYSTEM 16: PILOT'S INSTRUMENT PANEL

The pilot's instrument panel, as described in Pages A-239 through A-246 in Appendix A, is the instrument panel which is available at NASA ARC for use in the VMS cab. This instrument panel configuration provides important flight information and, in general, is a functional replica of the instruments of importance on the actual XV-15 instrument panel. Instruments such as radios, navigation aids, flight test instrumentation,

etc., which are not directly related to flying the XV-15, are either simulated by a cardboard replica or are omitted.

M. SUBSYSTEM 17: ROTOR COLLECTIVE GOVERNOR

1. Model Structure

The rotor rpm governor representation, described on Pages A-247 through A-255, consists of a single channel model of the actual flight rpm governor feedback network (Fig. A17-1). In the XV-15, the rotor blade collective pitch is changed so as to maintain constant rpm; the blade pitch is proportional to the integral of the error in rpm (e.g., the difference between the actual and the pilot-selected rpm) so that any steady error is completely washed out. The gain of the integral feedback is very low so that the governor will not destabilize structural modes.

A position gain is used in parallel with the integral gain in order to provide damping to the rotor rotational mode under conditions of low inflow, such as low power descents in the helicopter mode. The position gain is phased out as the pylons are converted to airplane mode in order to prevent destabilizing structural modes.

Control of the rpm governor consists of a thumb-operated, three-position switch spring loaded to center, which is located on the power lever head. Pushing the switch forward increases the reference rpm by 20 rpm for each second that the switch is depressed; pulling aft decreases the reference rpm by 20 rpm/sec. A pointer on the rotor tachometer indicates the selected rpm. This system is modeled in the VMS cab.

2. Input Data Requirements

The input data required by the subsystem and provided in Appendix B is for the XV-15, but it can be changed as desired by the researcher according to the block diagram in Fig. A17-1. At present, this model has been fully incorporated (with failure modes, etc.) and checked out only in the real-time simulation version of the GTRS program and not in the VAX

version. The VAX version contains only a simplified governor for realistically maintaining control of rotor RPM.

N. SUBSYSTEMS 18 AND 19: ENGINES, FUEL CONTROLS, AND DRIVE SYSTEM DYNAMICS

1. Model Structure

The engine, fuel control, and drive system model is described on Pages A-256 through A-271 of Appendix A. The drive system is represented by the zero frequency symmetric mode, e.g., the rotors speed up or slow down in response to the imbalance between aerodynamic torque and engine torque. The frequencies of the flexible modes of the drive system (3.67 cps and 11.8 cps for the first antisymmetric and second symmetric modes, respectively) are too high to significantly influence the simulation.

The engine and power turbine (NII) governor models are composed of equations to calculate engine horsepower during transient and steady-state operation. The equations are based on the operating characteristics of the combined engine-fuel control system. This approach was taken rather than one involving time constants, inertias, and derivation of engine components to minimize the computational requirements.

The engine equations are derived in terms of the optimum power turbine speed and the horsepower developed at that speed. For a given throttle setting (or fuel flow rate), the engine will develop the maximum horsepower if the turbine is operating at the optimum speed. The commanded optimum power--referred to sea level, standard, static conditions--is given by equations presented in Fig. A18-1 where K_8 through K_{14} are constants derived to fit the engine power versus throttle (X_{TH}) setting characteristics given in the engine installation manual (Ref. 28).

The referenced optimum power, HP_{RO}, at any time, t, after a power lever change is given by the equation

$$HP_{RO} = (HP_{RO})_0 + \int_{t_o}^{t} \frac{dHP_{ROP}}{dt}\, dt$$

where $(HP_{RO})_0$ is the power before the change in the power lever position and $(dHP_{ROP})/dt$ is the engine power acceleration schedule given as:

$$\frac{dHP_{ROP}}{dt} = \text{sign}\ (HP_{ROC}-HP_{RO})*\min\ \{1, \frac{(100)[1-(HP_{RO})/(HP_{ROC})]}{pctmxp}\}*f(HP_{RO},h)$$

where $f(HP_{RO},h)$ is the engine power acceleration schedule, derived to correlate with measured engine acceleration characteristics.

The actual horsepower, HP, is then computed by correcting the referred optimum horsepower, HP_{RO}, for nonstandard conditions using the following equation

$$HP = [HP_{RO}\ \delta\ \sqrt{\theta}\ ]\ [K_1\ (\frac{9.55\ \Omega_{RPT}}{\sqrt{\theta}\ RPM_{RO}})^2 + K_2(\frac{9.55\ \Omega_{RPT}}{\sqrt{\theta}\ RPM_{RO}}) + K_3]$$

where K_1, K_2, and K_3 are constants used to curve fit the power to the engine characteristics given in the installation manual, Ω_R is the actual power turbine speed, RPM_{RO} is the referred optimum power turbine speed, and δ and θ are terms used to correct for nonstandard pressure and temperature, respectively.

The equations used for the power turbine governor (N_{II}) are similar to those for the engine except that the optimum power is referred to the N_{II} speed commanded by the pilot rather than the throttle setting. It should be noted that in the XV-15, the N_{II} governing speed is set at that corresponding to the rotor limit speed so that the N_{II} governor is used only to prevent overspeeding.

2. Input Data Requirements

Input data values provided for use of the engine, fuel control, and drive system are specifically for the T-53-L-11 engine and the XV-15. While some modifications to the input data for the model can be made in order to simulate a "larger" or "smaller" version of the T-53-L-11 engine, any need to simulate a significantly different engine should be accomplished by modifying the model to whatever extent necessary to accurately simulate the new engine instead of trying to change input data values for the model described herein.

O. SUBSYSTEM 20: STABILITY AND CONTROL AUGMENTATION SYSTEM (SCAS)

The SCAS mathematical model consists of a single channel representation of the electronic feedback network. The main feature of the SCAS mathematical model is the representation of the system gains. All gains are functions of pylon angle. The attitude-hold circuit is turned OFF or ON by a switch on the SCAS panel. SCAS actuator characteristics are not modeled; however, total system authorities are used. Simple failures can also be evaluated for the SCAS, even in the VAX version of the program. The decision not to model the actuator characteristics is discussed in more detail in Ref. 6. This evaluation verified that, when these characteristics are modeled, they are more than compensated for by the lag or reduction in bandwidth introduced into the system by the simulation computer cycle time delay.

Two different SCAS models are provided for use with the simulation version of the GTRS mathematical model. These models, the Bell developed S/N 702 model and the NASA ARC developed S/N 703 model (Ref. 29), are described in the block diagrams on Pages A-277 through A-282 of Appendix A. Gains and time constants shown on these block diagrams can be varied as desired by the researcher from those values used with the XV-15 (as tabulated in Appendix B). Presently, only the NASA ARC-developed SCAS is available for use in the VAX version of the GTRS model.

SECTION IV

VALIDATION OF THE MATHEMATICAL MODEL

The accuracy of the GTRS mathematical model has been investigated with regard to rotor performance and force characteristics, airframe aerodynamics, rotor wake-airframe aerodynamic interaction, static and dynamic stability characteristics, and control power and damping. The majority of the data used in making this investigation has come from powered model wind-tunnel data, and Ref. 1 describes much of the early work conducted by BHT. Rotor test data has also been used for comparison, where available. Flight test data has been used more recently for correlation and validation efforts, and Refs. 6, 7, 30, and 31 provide correlation results between this version of GTRS and the XV-15. The most complete summary of correlation work accomplished in conjunction with this contract effort is presented in Ref. 7.

REFERENCES

1. Harendra, P. B., M. M. Joglekar, T. M. Gaffey, and R. L. Marr, V/STOL Tilt Rotor Study-Volume 5: A Mathematical Model for Real Time Flight Simulation of the Bell Model 301 Tilt Rotor Research Aircraft, NASA CR-114614, April 1973.

2. Schramm, M., and L. M. Landry, Jr., IFHC80 XV-15 Tilt Rotor Simulation Users' Manual, Bell Helicopter Company (Draft) Report prepared under Contract NAS2-10349.

3. Schramm, M., and L. M. Landry, Jr., IFHC80 XV-15 Tilt Rotor Simulation Programmer's Manual, Bell Helicopter Company (Draft) Report prepared under Contract NAS2-10349.

4. Hanson, Gregory D., and Samuel W. Ferguson, Generic Tilt-Rotor Simulation (GTRSIM) User's and Programmer's Guide. Volume 1: User's Guide, NASA CR-166535, October 1983.

5. Hanson, Gregory D., and Samuel W. Ferguson, Generic Tilt-Rotor Simulation (GTRSIM) User's and Programmer's Guide. Volume II: Programmer's Guide, NASA CR-166535, October 1983.

6. Ferguson, S. W., G. D. Hanson, and G. B. Churchill, "Simulation Validation of the XV-15 Tilt-Rotor Research Aircraft," Preprint No. A-84-40-09-4000 presented at the 40th Annual Forum of the American Helicopter Society, Arlington, Virginia, May 16-18, 1984.

7. Ferguson, Samuel W., Development and Validation of the Generic Tilt-Rotor Simulation (GTRSIM) Program, NASA CR-166537, March 1988.

8. Etkin, B., Dynamics of Flight, John Wiley and Sons, 1959.

9. Gessow, A., and A. Crim, An Extension of Lifting Rotor Theory to Cover Operation at Large Angles of Attack and High Inflow Conditions, NACA TN 2665, April 1952.

10. Castles, W., Jr., and N. New, A Blade Element Analysis for Lifting Rotors That is Applicable for Large Inflow and Blade Angles and Any Reasonable Blade Geometry, NACA TN 2656, 1952.

11. Drees, J. M., "A Theory of Airflow Through Rotors and Its Application to Some Helicopter Problems," The Journal of the Helicopter Association of Great Britain, Vol. 3, No. 2, September 1949.

12. Mil, M. L., et al., Helicopter Calculation and Design. Volume 1: Aerodynamics, NASA TTF-494, September 1967.

13. Hayden, James, "The Effect of the Ground on Helicopter Hovering Power Required," Preprint No. 1000 presented at the 32nd Annual Forum of the American Helicopter Society, Washington, D. C., May 1976.

14. Maisel, M., and D. Harris, "Hover Tests of the XV-15 Tilt Rotor Research Aircraft," AIAA Paper No. 81-2501, presented at the 1st AIAA Flight Testing Conference, November 11-13, 1981.

15. Landgrebe, A., An Analytical and Experimental Investigation of Helicopter Rotor Hover Performance and Wake Geometric Characteristics, USAAMRDL TR-71-024, (needs date).

16. Ball, LCDR J.C., and D. A. DuFresne, Shipboard Evaluation of the XV-15 Tilt Rotor Research Aircraft, Naval Air Test Center Technical Report RW-54R-82, April 18, 1983.

17. Marr, R. L., K. W. Sambell, and G. T. Neal, V/STOL Tilt Rotor Study. Volume VI: Hover, Low Speed, and Conversion Tests of a Tilt Rotor Aeroelastic Model, NASA CR-114615, May 1973.

18. Wilson, J., R. Mineck, and C. Freeman, Aerodynamic Characteristics of a Powered Tilt Prop Rotor Wind Tunnel Model, NASA TM X-72818, March 1976.

19. Anon., USAF Stability and Control Datcom, Air Firce Flight Dynamics Laboratory, Wright-Patterson Air Force Base, Ohio, October 1960 (Revised September 1970).

20. Marr, R. L., Wind Tunnel Test Results of 25 ft Tilt Rotor Druing Autorotation, Bell Helicopter Report 301-099-005, NASA CR-137824, February 1, 1976.

21. Knight, Montgomery, and Wenzinger, Carl J., Wind Tunnel Tests on a Series of Wing Models Through a Large Angle of Attack Range. Part I-Force Tests, NACA Report No. 317,

22. Byrnes, A. L., et al., "Effect of Horizontal Stabilizer Vertical Location on the Design of Large Transport Aircraft," Journal of Aircraft, April 1966.

23. Anon., V/STOL Tilt Rotor Research Aircraft. Volume 2: Stability and Control and Handling Qualities Analyses, Bell Helicopter Report 301-199-002, 1973.

24. Stapleford, R. L., W. F. Clement, R. K. Heffley, et al., Flight Control/Flying Qualities Investigation for Lift/Cruise Fan V/STOL. Volume III: Simulation Model, NADC-77143-30, August 1979.

25. Hoerner, Dr.-Ing. S.F., Fluid-Dynamic Drag, published by author, 1958.

26. Lanham, Charles, Inertia Calculation Procedure for Preliminary Design, Aeronautical Systems Division Report, ASD-TR-79-5004, April 1979.

27. Anon., U. S. Standard Atmosphere, 1962, NASA, U. S. Government Printing Office, 1962.

28. Anon., T-53-L-11 Gas Turbine Engine Installation Instructions, Lycoming Report No. 13611.1, August 1966.

29. Churchill, Gary B., and Ronald M. Gerdes, "Advanced AFCS Developments on the XV-15 Tilt Rotor Research Aircraft," Preprint No. A-84-40-10-4000 presented at the 40th Annual Forum of the American Helicopter Society, Arlington, Virginia, May 16-19, 1984.

30. Churchill, Gary B., and Daniel C. Dugan, "Simulation of the XV-15 Tilt Rotor Research Aircraft," NASA TM-84222, USAAVRADCOM TR-82-A-4, March 1982.

31. Tischler, Mark B., Joseph G. M. Leung, and Daniel C. Dugan, "Frequency-Domain Identification of XV-15 Tilt-Rotor Aircraft Dynamics," Paper presented at the AIAA/AHS/IES/SETP/SFTE/DGLR 2nd Flight Testing Conference, Las Vegas, NE, November 16-18, 1983.

APPENDIX A

GENERIC TILT-ROTOR SIMULATION MATHEMATICAL MODEL

TABLE OF CONTENTS

Subsystem Number	Subsystem Description	Page
1	Rotor Aerodynamics	A-5
2	Rotor Induced Velocities	A-34
3	Fuselage Aerodynamics	A-41
4	Wing-Pylon Aerodynamics	A-45
5	Horizontal Stabilizer Aerodynamics	A-78
6	Vertical Stabilizer Aerodynamics	A-89
7a	Landing Gear (Present Sigma 8 Model)	A-103
7b	Landing Gear (Unused Bell Model)	A-117
8a	Controls	A-123
8b	Force Feel System	A-134
8c	Control Force Trim System	A-140
8d	Pilot's Control Function	A-144
9	CG and Inertia	A-165
10a	Axes Transformation (Airframe Aerodynamic Forces and Moments from Wind to Body Axis)	A-172
10b	Axes Transformation (Rotor Forces and Moments from Wind to Body Axis)	A-185
10c	Axes Transformation (Euler Angles)	A-189
10d	Axes Transformation (Earth Based Velocity)	A-192
10e	Axes Transformation (Ground Velocity Summation)	A-195
10f	Axes Transformation (Ground Reference Distances)	A-198
11	Aircraft Angular Accelerations and Velocities	A-202

LIST OF SUBSYSTEMS (Concluded)

Subsystem Number	Subsystem Description	Page
12	Body Axis Linear Accelerations and Velocities	A-210
13	Force Summation	A-217
14	Moment Summation	A-222
15	Flight Environment	A-235
16	Pilot's Instrument Panel	A-239
17	Rotor Collective Governor	A-247
18	Engines and Fuel Controls	A-256
19	Drive System Dynamics	A-265
20	Stability and Control Augmentation System	A-272

LIST OF FIGURES

Figure Number	Figure Description	Page
A1-1	Rotor Axes Systems and Sign Conventions	A-13
A1-2	Block Diagram of Ground Effect, Side-by-Side, and Tandem Rotor Calculations	A-23
A1-3	Block Diagram of Induced Velocity and Thrust Calculations	A-24
A4-1	Sign Convention and Notation for Mathematical Model of Rotor Wake-Wing Interaction	A-57

LIST OF FIGURES

Figure Number	Figure Description	Page
A4-2	Flow Chart of Tilt Rotor Wing Aerodynamics Affected by the Rotor Wake	A-61
A5-1	Sign Conventions and Notation for Horizontal Stabilizer Aerodynamics	A-84
A6-1	Sign Conventions and Notation for Vertical Stabilizer Aerodynamics	A-96
A8a-1	Control System Block Diagram	A-129
A8a-2	Control Position/Force-Force and Moment Sign Convention	A-130
A8d-1	XV-15 Collective Head Switches	A-147
A8d-2	XV-15 Cyclic Grip Switches	A-148
A8d-3	XV-15 Flap Switch Selector Control	A-149
A8d-4	XV-15 SCAS Control Panel	A-150
A8d-5	XV-15 Governor Control Panel	A-151
A16-1	XV-15 Pilot's Control Panel	A-246
A17-1	XV-15 Rotor RPM Governor Failure Logic Block Diagram	A-254
A18-1	Engine Model Block Diagram	A-262
A20-1	Modified XV-15 Pitch SCAS Block Diagram (S/N 703)	A-277
A20-2	Modified XV-15 Roll SCAS Block Diagram (S/N 703)	A-278
A20-3	Modified XV-15 Yaw SCAS Block Diagram (S/N 703)	A-279
A20-4	Bell XV-15 Pitch Axis SCAS Block Diagram (S/N 702)	A-280
A20-5	Bell XV-15 Roll Axis SCAS Block Diagram (S/N 702)	A-281
A20-6	Bell XV-15 Yaw Axis SCAS Block Diagram (S/N 702)	A-282

1	ROTOR AERODYNAMICS

Inputs: Variables		Outputs:	
From Subsystem	Symbol	To Subsystem	Symbol
12	U V W V_T	2,10b	T_R H_R Y_R T_L H_L Y_L
11	p q r	1,2	W_{iR} W_{iL}
		2,4	μ_R μ_L
15	ρ M_N	2	λ_R λ_L
19	Ω_R Ω_L		Ω_R' Ω_L'
9	h_H SL_{CG} WL_{CG}	10b	$M_{a_{1R}}$ $l_{b_{1R}}$ $M_{a_{1L}}$ $l_{b_{1L}}$
8a	β_m θ_{oR} B_{1R} A_{1R} θ_{oL} B_{1L} A_{1L}	10b,19	Q_R Q_L
		14	T_R T_L
10b	X_R X_L		

Inputs: Constants, Coefficients, and Data Tables

Constants: n_b, m, X_m, θ_m, R, δ_3, c_b, I_b, l_m, ϕ_m, BL_{CG}, SL_{SP}, BL_{SP}, WL_{SP}, K_H, K_{HUB}, $\bar{a}_o$

(continued on next page)

1	**ROTOR AERODYNAMICS** (CONCLUDED)

Inputs: Constants, Coefficients, and Data Tables (Concluded)

Coefficients: a_0, a_1, a_2, δ_0, δ_1, δ_2, B, α_{OL}, CDMACH, CDMAX, CDALPH, CDLIM, CDFACT, CTMAXM, GECON1, GECON2, GEWASH, SFWASH, MUL0, MUH1, KMU1, KMU2, KMUSF

Data Tables:		
	$C_{\bar{T}}/\sigma = f(\mu, \beta_m)$	Table 1-I
	$X_{SF} = f(\lvert\bar{V}\rvert)$	Table 1-II
	$X_{SS} = f(\bar{u})$	Table 1-III

SUBSYSTEM NO. 1: ROTOR AERODYNAMICS

Inputs: Variables

Symbol	Description	Units
U	x-velocity (longitudinal) of the aircraft c.g. in body axis with respect to the air	ft/sec
V	y-velocity (lateral) of the aircraft c.g. in body axis with respect to the air	ft/sec
W	z-velocity (vertical) of the aircraft c.g. in body axis with respect to the air	ft/sec
V_T	Total linear velocity of the aircraft c.g. with respect to the air	ft/sec
p	Body axis roll rate	rad/sec
q	Body axis pitch rate	rad/sec
r	Body axis yaw rate	rad/sec
ρ	Air density	slug/ft^3
M_N	Mach number	ND
Ω_R	Instantaneous right rotor speed	rad/sec
Ω_L	Instantaneous left rotor speed	rad/sec
h_H	Rotor hub height above ground	ft
SL_{CG}	Station line of c.g.	in
WL_{CG}	Water line of c.g.	in
β_m	Mast conversion angle (+ fwd, 0 deg = vertical or helicopter, 90 deg = horizontal or airplane)	rad
θ_{oR}	Right rotor root collective pitch	rad
B_{1R}	Right rotor forward cyclic input	rad
A_{1R}	Right rotor lateral cyclic input	rad
θ_{oL}	Left rotor root collective pitch	rad

SUBSYSTEM NO. 1--ROTOR DYNAMICS (Continued)

Inputs: Constants, Coefficients, and Data Tables

Symbol	Description	Units
B_{1L}	Left rotor forward cyclic input	rad
A_{1L}	Left rotor lateral cyclic input	rad
X_R	Right rotor x-force (body axis)	lb
X_L	Left rotor x-force (body axis)	lb
n_b	Number of rotor blades	ND
m	Number of rotor segments	ND
X_m	Blade station/R	ND
θ_m	Blade twist	deg
R	Rotor radius	ft
δ_3	Pitch flap coupling	deg
c_b	Blade chord	in
I_b	Blade flapping inertia	slug-ft
l_m	Mast length	ft
ϕ_m	Lateral mast tilt	deg
BL_{CG}	Butt line of c.g.	in
SL_{SP}	Station line of engine nacelle shaft pivot point	in
BL_{SP}	Butt line of engine nacelle shaft pivot point	in
WL_{SP}	Water line of engine nacelle shaft pivot point	in
K_H	Flapping spring rate	ft-lb/deg
K_{HUB}	Coning hubspring	ft-lb/deg

SUBSYSTEM NO. 1: ROTOR AERODYNAMICS (Continued)

Inputs: Constants, Coefficients, and Data Tables (Continued)

Symbol	Description	Units
$\bar{a}_o$	Precone angle	deg
a_0	Blade lift coefficient	1/rad
a_1	Blade lift coefficient	$1/\mu$
a_2	Blade lift coefficient	$1/\mu^2$
δ_0	Blade drag coefficient	ND
δ_1	Blade drag coefficient	1/rad
δ_2	Blade drag coefficient	$1/rad^2$
B	Blade tip loss factor	ND
α_{OL}	Blade zero lift coefficient	deg
CDMACH	Coefficient for lower limit of rotor mach effects	ND
CDMAX	Maximum rotor drag coefficient	ND
CDALPH	Rotor drag equation coefficient (slope with alpha)	ND
CDLIM	Onset of profile drag rise	ND
CDFACT	Rotor drag equation coefficient	ND
CTMAXM	Rotor CT max multiplier coefficient	ND
GECON1	Constant in the rotor ground effect equation	ft/sec
GECON2	Constant in the rotor ground effect equation	ft/sec
GEWASH	Airspeed washout for rotor ground effects	ft/sec
SFWASH	Airspeed washout for side-by-side rotor effects	ft/sec

Inputs: Constants, Coefficients, and Data Tables (Concluded)

Symbol	Description	Units
MUH0	Induced velocity distribution equation coefficient	ND
MUH1	Induced velocity distribution equation coefficient	ND
KMU1	Induced velocity distribution equation coefficient	ND
KMU2	Induced velocity distribution equation coefficient	ND
KMUSF	Induced velocity distribution equation coefficient for sideward flight	ND
$\overline{C}_T/\sigma$	Maximum available rotor thrust coefficient, $= f(\mu,\beta_m)$	ND
X_{SF}	Sideward flight rotor correction factor, $= f(\lvert\overline{V}\rvert)$	ND
X_{SS}	Side-by-side rotor effect correction factor, $= f(\overline{u})$	ND
Outputs:		
T_R	Mast axis right rotor thrust (+ up for helicopter)	lb
H_R	Mast axis H-force right rotor thrust (+ aft for helicopter)	lb
Y_R	Mast axis Y-force right rotor thrust (+ right for helicopter)	lb
T_L	Mast axis left rotor thrust (+ up for helicopter)	lb
H_L	Mast axis H-force left rotor thrust (+ aft for helicopter)	lb
Y_L	Mast axis Y-force left rotor thrust (+ right for helicopter)	lb

SUBSYSTEM NO. 1—ROTOR AERODYNAMICS (Continued)

Outputs: Continued

Symbol	Description	Units
W_{iR}	Mast axis uniform component of induced velocity at right rotor (+ downward for helicopter)	ft/sec
W_{iL}	Mast axis uniform component of induced velocity at left rotor (+ downward for helicopter)	ft/sec
μ_R	Tip speed (advance) ratio, right rotor	ND
μ_L	Tip speed (advance) ratio, left rotor	ND
λ_R	Inflow ratio, right rotor	ND
λ_L	Inflow ratio, left rotor	ND
Ω'_R	Total right rotor speed (corrected for aircraft angular rate)	rad/sec
Ω'_L	Total left rotor speed (corrected for aircraft angular rate)	rad/sec
$M_{a_{1R}}$	Mast axis longitudinal flapping restraint exerted by right rotor on airframe (+ nose up for helicopter)	ft-lb
$l_{b_{1R}}$	Mast axis lateral flapping restraint exerted by right rotor on airframe (+ outboard for helicopter)	ft-lb
$M_{a_{1L}}$	Mast axis longitudinal flapping restraint exerted by left rotor on airframe (+ nose up for helicopter)	ft-lb
$l_{b_{1L}}$	Mast axis lateral flapping restraint exerted by left rotor on airframe (+ outboard for helicopter)	ft-lb

SUBSYSTEM NO. 1—ROTOR AERODYNAMICS (Concluded)

Outputs: Concluded

Symbol	Description	Units
Q_R	Mast axis right rotor torque (+ trying to slow rotor down)	ft-lb
Q_L	Mast axis left rotor torque (+ trying to slow rotor down)	ft-lb

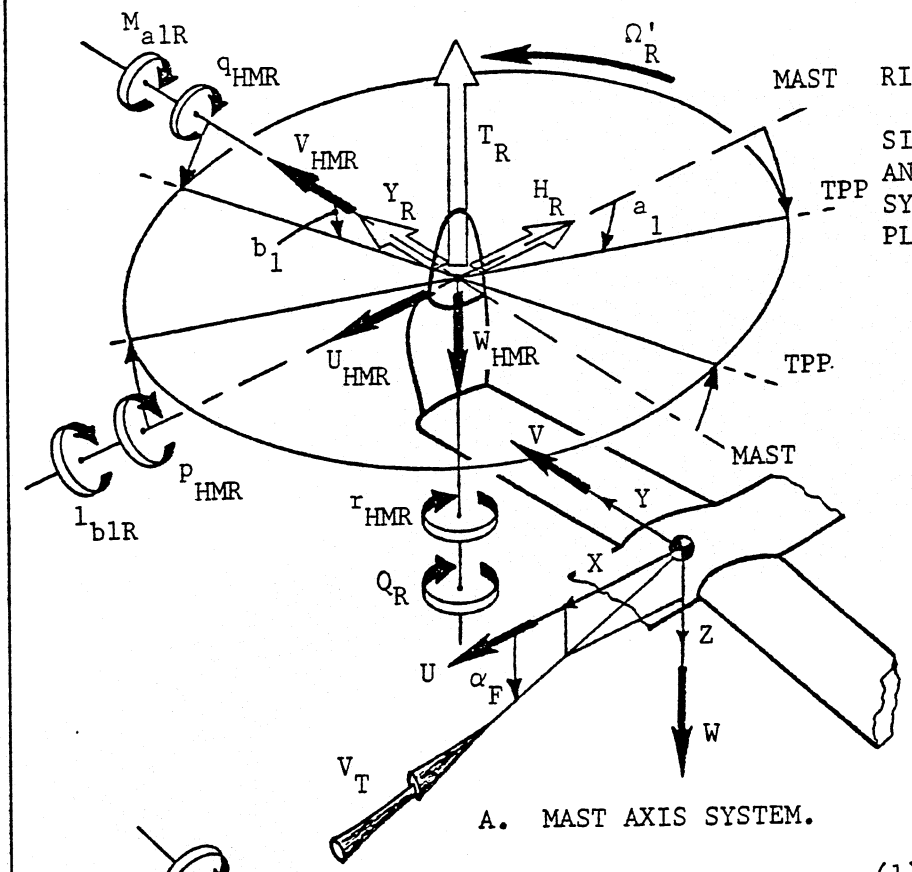

SIGN CONVENTIONS ON RIGHT AND LEFT SIDE ARE COMPLETELY SYMMETRICAL ABOUT AIRCRAFT PLANE-OF-SYMMETRY

A. MAST AXIS SYSTEM.

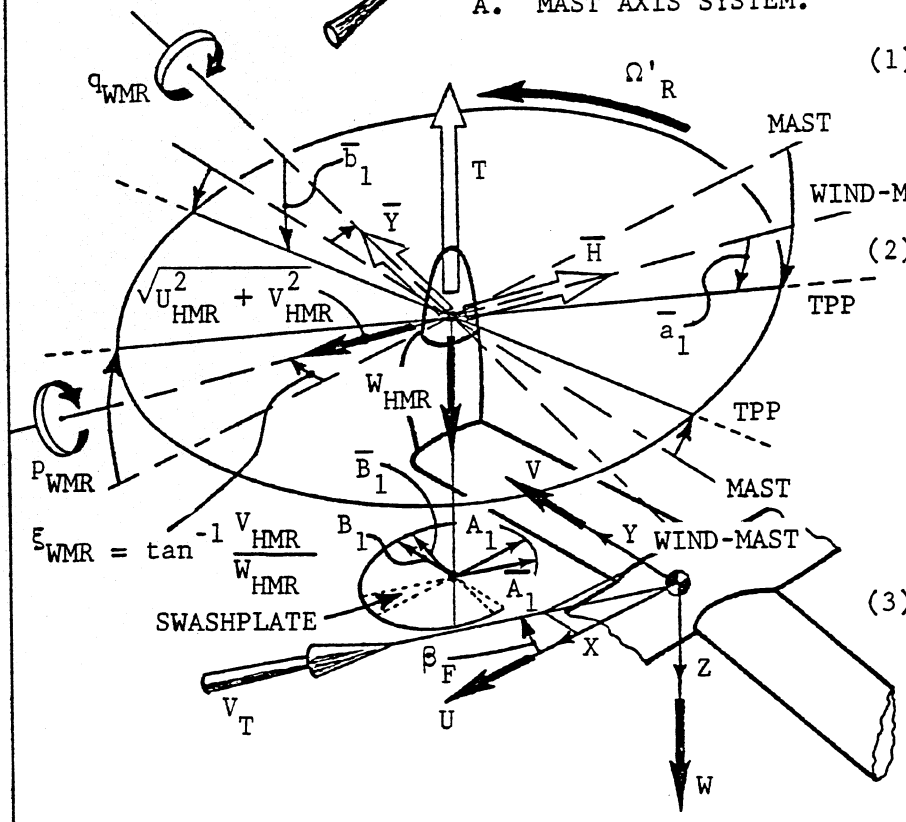

(1) U, V, W_{HMR} ARE TRANSFORMED FROM BODY (FUSELAGE) AXIS SYSTEM -

(2) FLAPPING AND PERFORMANCE CALCULATIONS ARE MADE IN WIND-MAST SYSTEM OBTAINED BY RESOLVING U_{HMR} AND V_{HMR} INTO A SINGLE WIND VECTOR AS SHOWN IN (B) BELOW

(3) T, $\bar{H}$, $\bar{Y}$, $\bar{a}_1$ AND $\bar{b}_1$ ARE CALCULATED IN WIND-MAST AXIS SYSTEM - THEN TRANSFORMED TO MAST AXIS SYSTEM TO OBTAIN T, H, Y, a_1 AND b_1.

B. "WIND-MAST" AXIS SYSTEM.

Figure A1-1. Rotor Axes Systems and Sign Conventions

A. Blade Twist Constants
(One Time Per Rotor)

$$K_{so,m} = \frac{1}{\theta_1^m}\left[\cos\left(\theta_1^m X_m\right) - \cos\left(\theta_1^m X_{m-1}\right)\right]$$

$$K_{co,m} = \frac{1}{\theta_1^m}\left[\sin\left(\theta_1^m X_{m-1}\right) - \sin\left(\theta_1^m X_m\right)\right]$$

$$K_{s1,m} = \frac{1}{\theta_1^m}\left\{\left(K_{co,m}\right) - \left[X_{m-1}\cos\left(\theta_1^m X_{m-1}\right) - X_m \cos\left(\theta_1^m X_m\right)\right]\right\}$$

$$K_{c1,m} = \frac{-1}{\theta_1^m}\left\{\left(K_{so,m}\right) - \left[X_{m-1}\sin\left(\theta_1^m X_{m-1}\right) - X_m \sin\left(\theta_1^m X_m\right)\right]\right\}$$

$$K_{s2,m} = \frac{2}{\theta_1^m}\left(K_{c1,m}\right) - \frac{1}{\theta_1^m}\left[\left(X_m - 1\right)^2\cos\left(\theta_1^m X_{m-1}\right) - \left(X_m\right)^2\cos\left(\theta_1^m X_m\right)\right]$$

$$K_{c2,m} = \frac{-2}{\theta_1^m}\left(K_{s1,m}\right) + \frac{1}{\theta_1^m}\left[\left(X_m - 1\right)^2\sin\left(\theta_1^m X_{m-1}\right) - \left(X_m\right)^2\sin\left(\theta_1^m X_m\right)\right]$$

$$K_{s3,m} = \frac{3}{\theta_1^m}\left(K_{c2,m}\right) - \frac{1}{\theta_1^m}\left[\left(X_{m-1}\right)^3\cos\left(\theta_1^m X_{m-1}\right) - \left(X_m\right)^3\cos\left(\theta_1^m X_m\right)\right]$$

$$K_{c3,m} = \frac{-3}{\theta_1^m}\left(K_{s2,m}\right) + \frac{1}{\theta_1^m}\left[\left(X_{m-1}\right)^3\sin\left(\theta_1^m X_{m-1}\right) - \left(X_m\right)^3\sin\left(\theta_1^m X_m\right)\right]$$

where θ_1^m = twist rate of mth segment $= \left(\dfrac{\theta_m - \left(\theta_{m-1}\right)}{X_m - \left(X_{m-1}\right)}\right)$

X_m = Radial station of mth segment

θ_m = Blade pitch angle at m^{th} segment

A. Blade Twist Constants (Concluded)

$K_{Cn,m}$ = Blade twist constants (n = 0, 1, 2, 3)

m = number of geometric segments, starting from tip (r/R = 1.0) to root (r/R = 0.0)

$$\theta_R' = \theta_R + \alpha_{OL}$$

Define blade pitch constant components as:

$$TW1_n = \sum_{m=1}^{l} K_{Cn,m} \cos \Delta\theta_{0m}$$

$$TW2_n = \sum_{m=1}^{l} K_{Cn,m} \sin \Delta\theta_{0m}$$

$$TW3_n = \sum_{m=1}^{l} K_{Sn,m} \sin \Delta\theta_{0m}$$

$$TW4_n = \sum_{m=1}^{l} K_{Sn,m} \cos \Delta\theta_{0m}$$

Where, $\Delta\theta_{0m} = \left(\theta_m - \theta_R'\right) - X_m \theta_1^m$

θ_R = Blade pitch at the rotor center

l = Number of m aerodynamic segments to account for blade root cutout.

B. Initial Transformation Equations (One Time Per Rotor)

$$A = \pi R^2$$

$$DN' = AR^2 = \pi R^4$$

B. Initial Transformation Equations (Concluded) (One Time Per Rotor)

$$TD3 = TAN(\delta_3)$$

$$\sigma = \frac{n_b c_b}{\pi R}$$

$$\gamma' = \frac{c_b R^4}{I_b}$$

$$\gamma_m = \rho \gamma'$$

C. Long Term Transformations

1. Rotor Angular Velocity in Space

$$\Omega_R' = \Omega_R + p \sin\beta_m \cos\phi_m + q \cos\beta_m \sin\phi_m - r \cos\beta_m \cos\phi_m$$

$$\Omega_L' = \Omega_L - p \sin\beta_m \cos\phi_m + q \cos\beta_m \sin\phi_m + r \cos\beta_m \cos\phi_m$$

2. "Wind-Mast" Axis Angular Rates

Right Rotor

$$p_{WMR} = p_{HMR} \cos\xi_{WMR} + q_{HMR} \sin\xi_{WMR}$$

$$q_{WMR} = -p_{HMR} \sin\xi_{WMR} + q_{HMR} \cos\xi_{WMR}$$

where

$$p_{HMR} = p \cos\beta_m - q \sin\beta_m \sin\phi_m + r \sin\beta_m \cos\phi_m$$

$$q_{HMR} = \qquad q \cos\phi_m \qquad + r \sin\phi_m$$

2. "Wind-Mast" Axis Angular Rates: Right Rotor (Concluded)

ξ_{WMR} = wind azimuth angle defined to be equal to $\tan^{-1}\frac{V_{HMR}}{U_{HMR}}$

$$\hat{p}_{WMR} = \frac{p_{WMR}}{\Omega_R'}$$

$$\hat{q}_{WMR} = \frac{q_{WMR}}{\Omega_R'}$$

Left Rotor

$$p_{WML} = p_{HML}\cos\xi_{WML} + q_{HML}\sin\xi_{WML}$$

$$q_{WML} = -p_{HML}\sin\xi_{WML} + q_{HML}\cos\xi_{WML}$$

where

$$p_{HML} = -p\cos\beta_m - q\sin\beta_m\sin\phi_m - r\sin\beta_m\cos\phi_m$$

$$q_{HML} = \qquad q\cos\phi_m \qquad -r\sin\phi_m$$

ξ_{WML} = wind azimuth angle defined to be equal to $\tan^{-1}\frac{V_{HML}}{U_{HML}}$

$$\hat{p}_{WML} = \frac{p_{WML}}{\Omega_L'}$$

$$\hat{q}_{WML} = \frac{q_{WML}}{\Omega_L'}$$

3. Rotor Hub Velocity--Mast Axes

Right Rotor

$$U_{HMR} = U_{HBR}\cos\beta_m - V_{HBR}\sin\beta_m\sin\phi_m + W_{HBR}\sin\beta_m\cos\phi_m$$

$$V_{HMR} = V_{HBR}\cos\phi_m + W_{HBR}\sin\phi_m$$

$$W_{HMR} = -U_{HBR}\sin\beta_m - V_{HBR}\cos\beta_m\sin\phi_m + W_{HBR}\cos\beta_m\cos\phi_m$$

Where,

$$U_{HBR} = U - q(L_{ZH}) - r(L_{YH})$$

$$V_{HBR} = V + p(L_{ZH}) + r(L_{XH})$$

$$W_{HBR} = W + p(L_{YH}) - q(L_{XH})$$

$$L_{XH} = \frac{(SL_{CG} - SL_{SP})}{12} + l_m\sin\beta_m\cos\phi_m$$

$$L_{YH} = \frac{(BL_{SP} - BL_{CG})}{12} + l_m\sin\phi_m$$

$$L_{ZH} = \frac{(WL_{SP} - WL_{CG})}{12} + l_m\cos\beta_m\cos\phi_m$$

3. Rotor Hub Velocity--Mast Axes; Right Rotor (Concluded)

Left Rotor

$$U_{HML} = U_{HBL}\cos\beta_m + V_{HBL}\sin\beta_m\sin\phi_m + W_{HBL}\sin\beta_m\cos\phi_m$$

$$V_{HML} = -V_{HBL}\cos\phi_m + W_{HBL}\sin\phi_m$$

$$W_{HML} = -U_{HBL}\sin\beta_m + V_{HBL}\cos\beta_m\sin\phi_m + W_{HBL}\cos\beta_m\cos\phi_m$$

Where,

$$U_{HBL} = U - q(L_{ZH}) + r(L_{YH})$$

$$V_{HBL} = V + p(L_{ZH}) + r(L_{XH})$$

$$W_{HBL} = W - p(L_{YH}) - q(L_{XH})$$

4. Aerodynamic Coefficients

Right Rotor

$$DN_R = \rho \Omega_R'^2 DN'$$

$$DNQ_R = DN_R\left(\Omega_R' R/550\right)$$

$$\mu_R = \frac{\left(U_{HMR}^2 + V_{HMR}^2\right)^{1/2}}{\Omega_R' R}$$

$$\lambda_{OR} = -\frac{W_{HMR}}{\Omega_R' R}$$

$$\xi_{WMR} = \tan^{-1}\left(\frac{V_{HMR}}{U_{HMR}}\right)$$

$$a_R = \left[a_0 + \mu_R\left(a_1 - a_2 \mu_R\right)\right]\left(\frac{1}{\left[1 - (0.75 M_{TIP})^2 \sin\beta_m\right]^{1/2}}\right)$$

Where a_0, a_1, a_2 = blade lift coefficients

$$C_{KFAR} = \frac{(2/3)K_H}{I_b \Omega_R'^2}$$

$$C_{KLTR} = \frac{(2/3)K_H}{I_b \Omega_R'^2}$$

$$\gamma_R = \frac{\rho a_R c_b R^4}{I_b}\left(1 + \frac{\mu_R}{2}\right) = \gamma_{MR}\left(1 + \frac{\mu_R}{2}\right)$$

$$\gamma_{MR} = \gamma_m a_R$$

4. Aerodynamic Coefficients; Right Rotor (Concluded)

Define,

$$Q_{6R} = 0.5\sigma a_R (DN_R)$$

(For left rotor, replace subscript R with L)

D. Short Term Transformations (Every Update Cycle)

1. "Wind-Mast" Axis Cyclic Inputs

Right Rotor

$$\overline{A}_{1R} = A_{1R}\cos\xi_{WMR} - B_{1R}\sin\xi_{WMR}$$

$$\overline{B}_{1R} = A_{1R}\sin\xi_{WMR} + B_{1R}\cos\xi_{WMR}$$

(For left rotor, replace subscript R with L)

2. Blade Pitch Constants

Right Rotor

$$C_{SnR} = (TW1_n - TW3_n)\sin\theta_{OR} + (TW2_n + TW4_n)\cos\theta_{OR}$$

$$C_{CnR} = -(TW2_n + TW4_n)\sin\theta_{OR} + (TW1_n - TW3_n)\cos\theta_{OR}$$

(For left rotor, replace subscript R with L)

3. Performance Parameters

Right Rotor

$$\alpha_{rR} = \frac{7C_{TR}}{\sigma a_R}$$

$$M_{TIP} = \frac{1}{V_{sound}}\left[V_T^2 + (\Omega_R' R)^2 + 2V_T\Omega_R' R\cos\beta_m\right]^{1/2}$$

3. Performance Parameters; Right Rotor (Concluded)

$$C_d = \min\{CDMAX, \delta_0 + \alpha_{rR}(\delta_1 + \alpha_{rR}\delta_2) + \max\{0, CDALPH(\alpha_{rR}) + CDFACT[CDLIM + \max(M_{TIP}, CDMACH)]\}\}$$

$$C_{d_{fR}} = C_d / n_b a_R$$

(For left rotor, replace subscript R with L)

4. Ground Effect, Side-by-Side and Tandem Rotor Factors

(See Fig. A1-2)

5. Thrust and Induced Velocity

(See Fig. A1-3)

6. Rotor Flapping (Wind-Mast Axis System)

Right Rotor

$$a_{0_R} = \frac{0.75R(T_R/n_b) + K_{HUB}\bar{a}_o}{I_b \Omega_R'^2 + K_{HUB}}$$

TW34 = twist at 3/4 radius (starting at root)

(For the XV-15, TW34 = 34.525 degrees)

The first-order flapping equations used are described in matrix form as follows:

$$\begin{bmatrix} C_{11} & C_{12} \\ C_{21} & C_{22} \end{bmatrix} \begin{Bmatrix} \dot{\bar{a}}_1 \\ \dot{\bar{b}}_1 \end{Bmatrix} + \begin{bmatrix} A_{11} & A_{12} \\ A_{21} & A_{22} \end{bmatrix} \begin{Bmatrix} \bar{a}_1 \\ \bar{b}_1 \end{Bmatrix} = \begin{Bmatrix} B_1 \\ B_2 \end{Bmatrix}$$

Figure A1-2. Block Diagram of Ground Effect, Side-by-Side, and Tandem Rotor Calculations

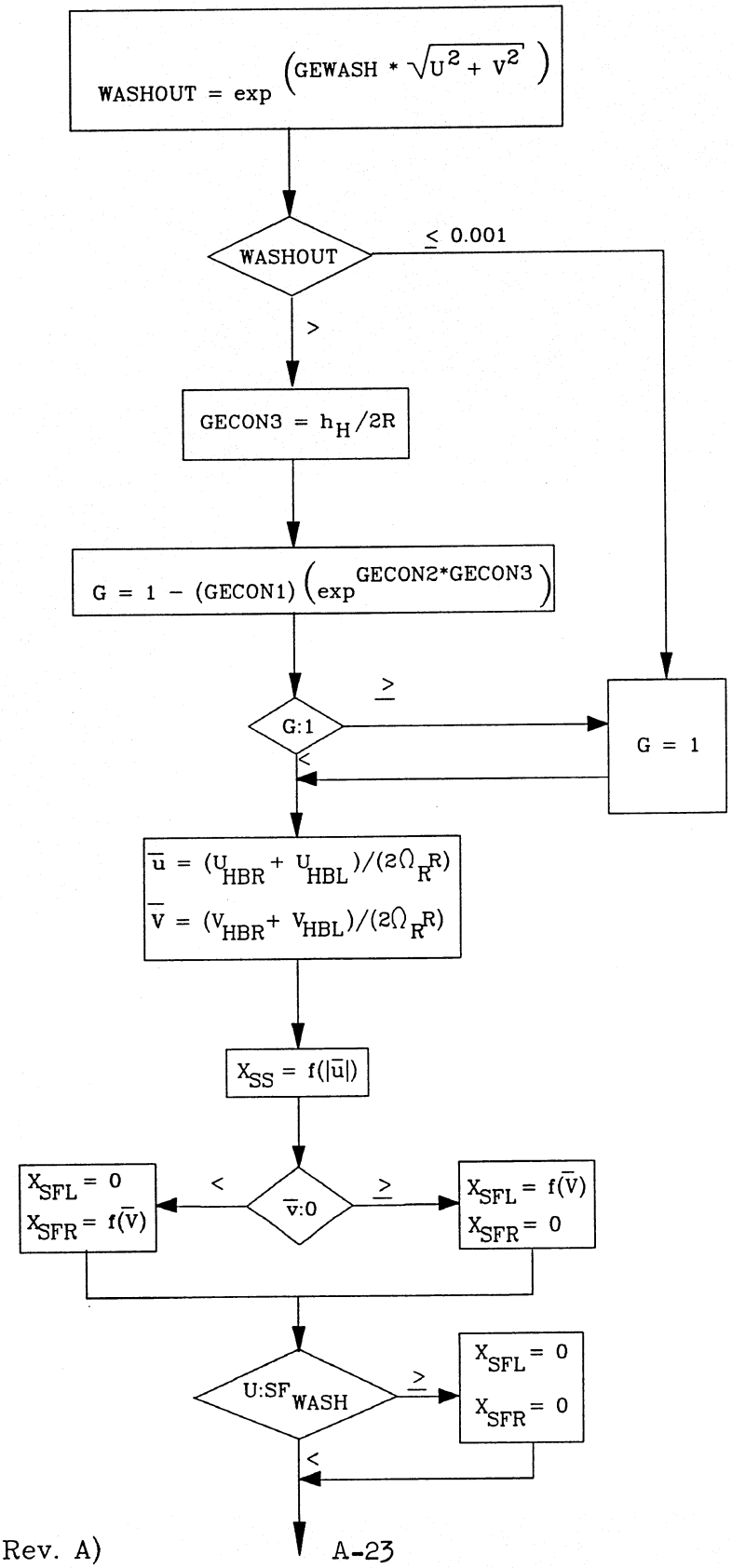

Figure A1-3. Block Diagram of Induced Velocity and Thrust Calculations

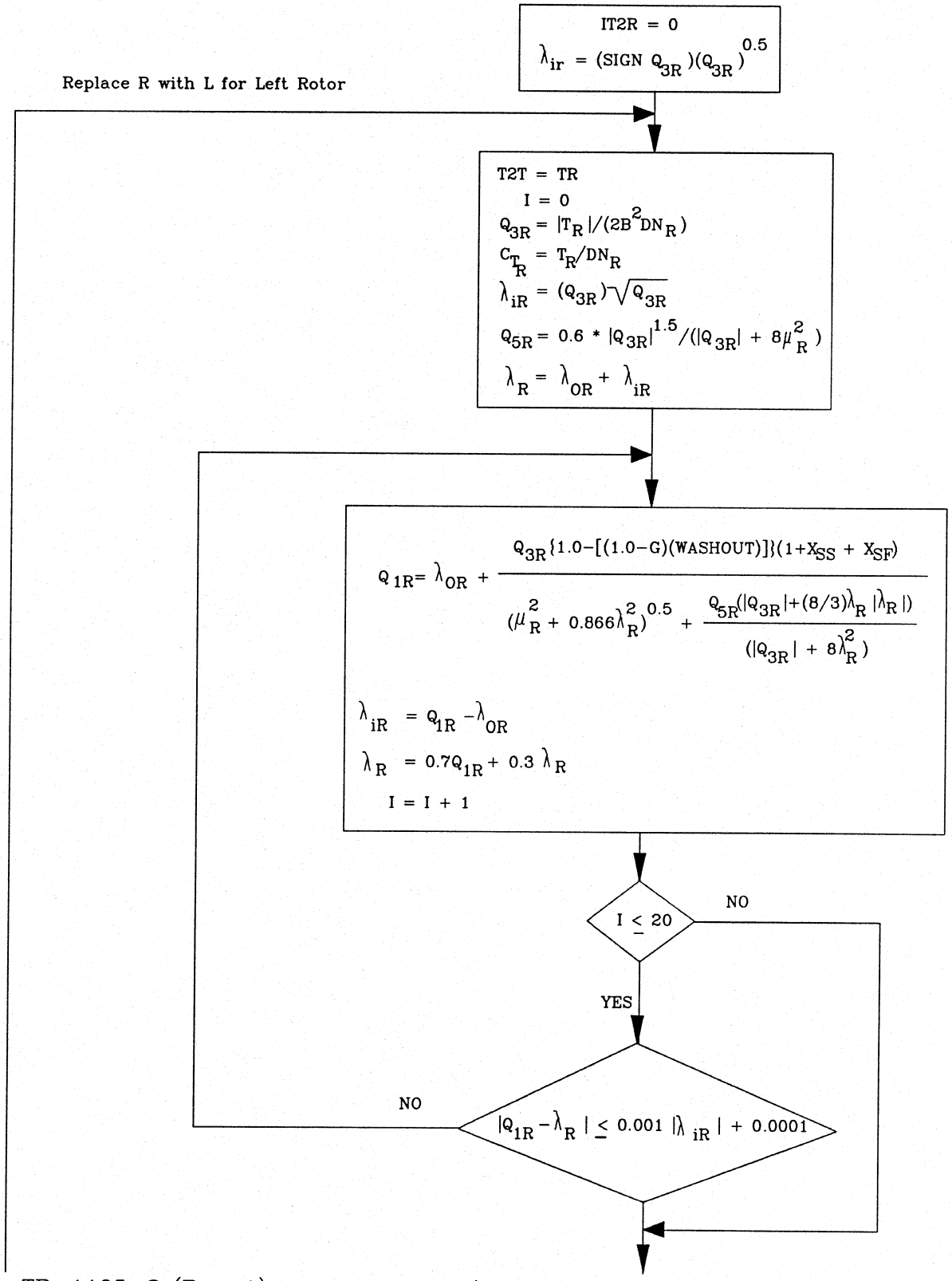

Figure A1-3 (Concluded)

$$T_{2R} = Q_{6R}\{C_{S2R} + C_{S0R}\mu_R^2/2 - C_{S1R}\mu_R\hat{q}_{WMR} - C_{C1R}[\lambda_R - (\mu_R/2)\hat{p}_{WMR}]$$
$$- \bar{B}_{1R}[C_{C1R}\mu_R + C_{S2R}(\bar{a}_{1R}/2 - \hat{p}_{WMR}/2)]$$
$$+ \bar{A}_{1R}[(1/2)C_{S2R}(\bar{b}_{1R} - (4/3)K_R\lambda_{iR} + \hat{q}_{WMR})]$$
$$+ \tan\delta_3[C_{C1R}\mu_R\bar{b}_{1R}]\}$$
$$- Q_{6R}C_{d_{f_R}}(1 + (16/9)\lambda_R^2)^{1/2}[(4/3)\lambda_R - (2/3)\mu_R\hat{p}_{WMR}]$$

IT2R = IT2R + 1

IT2R $\leq$ 5 — NO / YES

$|T_{2R} - T_R| \leq 0.001\,|T_{2R}| + 0.0001$

$T_R = T_{2R}$

$C_{T_R} = T_R/DN_R$

$T_R = \text{MIN}\,|T_R, \bar{T}_R|$

$W_{iR} = \lambda_{iR}(\Omega_R')(R)$

Where

$\bar{T}_R = (\bar{C}_T/\sigma)(DN_R)(\sigma_R)$

$\bar{C}_T/\sigma = f(\mu, \beta_m)$

NOTE: Cycle through rotor four times to insure flapping convergence (update on λ with better λ_{iR})

6. Rotor Flapping (Wind-Mast Axis System) Right Rotor (Continued)

A simplified zero-order (algebraic) flapping equation is used at the user's option (switch incorporated) by solving the following:

$$\begin{bmatrix} A_{11} & A_{12} \\ A_{21} & A_{22} \end{bmatrix} \begin{Bmatrix} \bar{a}_1 \\ \bar{b}_1 \end{Bmatrix} = \begin{Bmatrix} B_1 \\ B_2 \end{Bmatrix}$$

The above coefficients are as follows:

$$A_{11} = \left[\frac{\lambda_R}{6} \sin\left(\theta_{0_R} - TW34\right) + \left(\frac{1}{8} + \frac{\mu_R^2}{18}\right) \cos\left(\theta_{0_R} - TW34\right) \right] RQ_{6R} \tan\delta_3 + K_H$$

$$A_{12} = \left(\frac{1}{8} + \frac{\mu_R^2}{18}\right) RQ_{6R} \cos\left(\theta_{0_R} - TW34\right)$$

$$+ \left[\frac{\mu_R}{18} \left(a_{0_R} \mu_R + K_R \lambda_{iR}\right) \sin\left(\theta_{0_R} - TW34\right) \right] RQ_{6R} \tan\delta_3$$

$$A_{21} = \left(-\frac{1}{8} + \frac{\mu_R^2}{18}\right) RQ_{6R} \cos\left(\theta_{0_R} - TW34\right)$$

$$+ \left[\frac{\mu_R}{18} \left(a_{0_R} \mu_R + K_R \lambda_{iR}\right) \sin\left(\theta_{0_R} - TW34\right) \right] RQ_{6R} \tan\delta_3$$

$$A_{22} = [\frac{\lambda_R}{6} \sin\left(\theta_{0_R} - TW34\right)$$

$$+ \left(\frac{1}{8} + \frac{\mu_R^2}{6}\right) \cos\left(\theta_{0_R} - TW34\right)] RQ_{6R} \tan\delta_3 + K_H$$

6. Rotor Flapping (Wind-Mast Axis System) Right Rotor (Continued)

$$C_{11} = \left[\left(\frac{RQ_{6R}}{8\Omega_R'}\right)\cos\left(\theta_{0_R} - TW34\right)\right]$$

$$C_{12} = [\left(\frac{RQ_{6R}}{4\Omega_R'}\right)a_{0_R}\sin\left(\theta_{o_R} - TW34\right) - \left(\frac{RQ_{6R}}{6\Omega_R'}\right)a_{0_R}\lambda_R\cos\left(\theta_{0_R} - TW34\right)$$

$$+ n_b I_b \Omega_R']$$

$$C_{21} = -C_{12}$$

$$C_{22} = \left[\left(\frac{RQ_{6R}}{8\Omega_R'}\right)\cos\left(\theta_{0_R} - TW34\right)\right]$$

$$B_1 = \frac{RQ_{6R}}{6}\left(a_{0_R}\mu_R + K_R\lambda_{i_R}\right)\cos\left(\theta_{0_R} - TW34\right)$$

$$-[\left(\frac{RQ_{6R}}{4}\right)a_{0_R}\sin\left(\theta_{0_R} - TW34\right) - \left(\frac{RQ_{6R}}{6}\right)a_{0_R}\lambda_R\cos\left(\theta_{0_R} - TW34\right)$$

$$+ n_b I_b \Omega_R'^2]\hat{p}_{WMR} - \left[\left(\frac{RQ_{6R}}{8}\right)\cos\left(\theta_{0_R} - TW34\right)\right]\hat{q}_{WMR}$$

$$+ \overline{B}_{1R}\left[\left(\frac{RQ_{6R}}{18}\right)\mu_R\left(a_{0_R}\mu_R + K_R\lambda_{i_R}\right)\sin\left(\theta_{0_R} - TW34\right)\right]$$

$$+ \overline{A}_{1R}[\left(\frac{RQ_{6R}}{6}\right)\lambda_R\sin\left(\theta_{0_R} - TW34\right)$$

$$+ RQ_{6R}\left(\frac{1}{8} + \frac{\mu_R^2}{18}\right)\cos\left(\theta_{0_R} - TW34\right)]$$

6. Rotor Flapping (Wind-Mast Axis System) Right Rotor (Concluded)

$$B_2 = \frac{RQ_{6R}}{6}\left[\frac{4}{3}\mu_R\lambda_R - 2\mu_R\tan\left(\theta_{0_R} - TW34\right)\right]\cos\left(\theta_{0_R} - TW34\right)$$

$$+\left[\left(\frac{RQ_{6R}}{4}\right)a_{0_R}\sin\left(\theta_{0_R} - TW34\right) - \left(\frac{RQ_{6R}}{6}\right)a_{0_R}\lambda_R\cos\left(\theta_{0_R} - TW34\right)\right.$$

$$\left. + n_b I_b \Omega_R'^2\right]\hat{q}_{WMR} - \left[\left(\frac{RQ_{6R}}{8}\right)\cos\left(\theta_{0_R} - TW34\right)\right]\hat{p}_{WMR}$$

$$+\bar{B}_{1R}\left[\left(\frac{RQ_{6R}}{6}\right)\lambda_R\sin\left(\theta_{0_R} - TW34\right) + RQ_{6R}\left(\frac{1}{8} + \frac{\mu_R^2}{6}\right)\cos\left(\theta_{0_R} - TW34\right)\right]$$

$$+\bar{A}_{1R}\left[\left(\frac{RQ_{6R}}{18}\right)\mu_R\left(a_{0_R}\mu_R + K_R\lambda_{i_R}\right)\sin\left(\theta_{0_R} - TW34\right)\right]$$

$$\dot{\bar{a}}_{1R} = \frac{C_{22}B_1 - C_{12}B_2 + \left(C_{12}A_{21} - C_{22}A_{11}\right)\bar{a}_{1R} + \left(C_{12}A_{22} - C_{22}A_{12}\right)\bar{b}_{1R}}{C_{11}C_{22} - C_{12}C_{21}}$$

$$\dot{\bar{b}}_{1R} = \frac{C_{11}B_2 - C_{21}B_1 + \left(C_{21}A_{11} - C_{11}A_{21}\right)\bar{a}_{1R} + \left(C_{21}A_{12} - C_{11}A_{22}\right)\bar{b}_{1R}}{C_{11}C_{22} - C_{12}C_{21}}$$

$$\bar{a}_{1R} = \int \dot{\bar{a}}_{1R}$$

$$\bar{b}_{1R} = \int \dot{\bar{b}}_{1R}$$

7. Inflow Distribution Factor K_R

Right Rotor

(For left rotor, replace subscript R with L)

At low airspeeds $K_R = f(\mu, \beta_F)$ where:

$$KR1 = KMUSF + (KMU1 - KMUSF)\left(\left|\cos^3 \beta_F\right|\right)$$

At higher airspeeds, $K_R = f(\mu)$ where the following table summarizes the options for the calculation of K_R

μ_R	K_R
$0 < \mu_R < MUL0$	$KR1\ (\mu_R)$
$MUL0 < \mu_R < MUH1$	$KR1(MUL0) + KMU2(\mu_R - MUL0)$
$\mu_R > MUH1$	$KR1(MUL0) + KMU2(MUH1 - MUL0)$

8. Rotor Flapping in Mast Axis System

Right Rotor

(For left rotor, replace subscript R with L)

$$a_{1R} = \bar{a}_{1R} \cos \xi_{WMR} + \bar{b}_{1R} \sin \xi_{WMR}$$

$$b_{1R} = -\bar{a}_{1R} \sin \xi_{WMR} + \bar{b}_{1R} \cos \xi_{WMR}$$

9. Rotor Inplane Forces in Wind-Mast Axis System

Right Rotor

(For left rotor, replace subscript R with L)

$$\bar{H}_R = Q_{6R}\{C_{SOR}\left(\frac{\mu_R \lambda_R}{2}\right) + C_{S2R}\left(\bar{a}_{1R} - \frac{\hat{p}_{WMR}}{2}\right)$$

$$-C_{1R}\lambda_R\left(\frac{3}{2}\bar{a}_{1R} - \hat{p}_{WMR}\right) - C_{C2R}\left(\frac{a_{0R}}{2}\right)\left[\left(\bar{b}_{1R} - \frac{4}{3}K_R\lambda_{i_R}\right) + \hat{q}_{WMR}\right]\}$$

$$-\bar{B}_{1R}\left[\frac{1}{2}C_{C1R}\lambda_R + \frac{1}{2}C_{SOR}\lambda_R^2\right]$$

$$+\bar{A}_{1R}\left[\frac{1}{2}C_{C2R}a_{0R} + \frac{1}{2}C_{S1R}a_{0R}\lambda_R\right]$$

$$-\tan\delta_3[\frac{1}{2}C_{C2R}a_{0R}\bar{a}_{1R} - \frac{1}{2}C_{C1R}\lambda_R\bar{b}_{1R}$$

$$-\frac{8}{9}C_{S2R}\lambda_R^2\bar{b}_{1R}]\}$$

$$+Q_{6R}C_{d_{f_R}}\left(1 + \frac{16}{9}\lambda_R^2\right)^{1/2}\left(\frac{4}{3}\mu_R - a_{0R}\hat{q}_{WMR}\right)$$

9. Rotor Inplane Forces in Wind-Mast Axis System Right Rotor (Concluded)

$$\overline{Y}_R = Q_{6R}\{C_{SOR}\left(\frac{\mu_R^2}{2}\right)\overline{b}_{1R} + C_{S2R}\left[\left(\overline{b}_{1R} - \frac{2}{3}K_R\lambda_{i_R}\right) + \left(\frac{\hat{q}_{WMR}}{2}\right)\right]$$

$$-C_{C1R}\lambda_R\left[\frac{3}{2}\left(\overline{b}_{1R} - \frac{8}{9}K_R\lambda_{i_R}\right) + \hat{q}_{WMR}\right] + C_{C2R}\left(\frac{a_{0R}}{2}\right)\left(\overline{a}_{1R} - \hat{p}_{WMR}\right)$$

$$-\frac{3}{2}C_{S1R}\mu_R a_{0_R}$$

$$+\overline{B}_{1R}\left[\frac{1}{2}C_{C2R}a_{0_R} + \frac{1}{2}C_{S1R}a_{0_R}\lambda_R\right]$$

$$+\overline{A}_{1R}\left[\frac{1}{2}C_{C1R}\lambda_R + \frac{1}{2}C_{SOR}\lambda_R^2\right]$$

$$-\tan\delta_3[\frac{1}{2}C_{C2R}a_{0_R}\overline{b}_{1R} + \frac{1}{2}C_{C1R}\lambda_R\overline{a}_{1R}$$

$$+\frac{8}{9}C_{S2R}\lambda_R^2\overline{a}_{1R}]\}$$

$$+Q_{6R}C_{d_{f_R}}\left(1 + \frac{16}{9}\lambda_R^2\right)^{1/2}\left(a_{0_R}\hat{p}_{WMR}\right)$$

10. Rotor Inplane Forces in Mast Axis System Right Rotor

(For left rotor, replace subscript R with L)

$$H_R = \overline{H}_R\cos\xi_{WMR} + \overline{Y}_R\sin\xi_{WMR}$$

$$Y_R = -\overline{H}_R\sin\xi_{WMR} + \overline{Y}_R\cos\xi_{WMR}$$

11. Rotor Power and Torque Required

Right Rotor

(For left rotor, replace subscript R with L)

$$HP_{REQ_R} = (DNQ_R)\frac{\sigma a_R}{2}\{C_{S2R}\left(\lambda_R - \frac{1}{2}\mu_R \hat{p}_{WMR}\right)$$

$$-C_{C1R}\left(\lambda_R^2 - \mu_R \lambda_R \bar{a}_{1R}\right) - \frac{1}{2}C_{C3R}\{\bar{a}_{1R}^2 + \left(\bar{b}_{1R} - \frac{4}{3}K_R \lambda_{iR}\right)^2$$

$$-2\hat{p}_{WMR}\left(\bar{a}_{1R} - \frac{\hat{p}_{WMR}}{2}\right) + 2\hat{q}_{WMR}\left[\left(\bar{b}_{1R} - \frac{4}{3}K_R \lambda_{iR}\right) + \frac{\hat{q}_{WMR}}{2}\right]\}$$

$$-\bar{B}_{1R}[\frac{1}{2}C_{C3R}\left(\bar{a}_{1R} - \hat{p}_{WMR}\right) + \frac{1}{2}C_{C1R}\lambda_R \mu_R$$

$$+C_{S2R}\lambda_R\left(\bar{a}_{1R} - \hat{p}_{WMR}\right)]$$

$$+\bar{A}_{1R}\{\frac{1}{2}C_{C3R}\left[\left(\bar{b}_{1R} - \frac{4}{3}K_R \lambda_{iR}\right) + \hat{q}_{WMR}\right]$$

$$+C_{S2R}\left[\lambda_R\left(\left\{\bar{b}_{1R} - \frac{4}{3}K_R \lambda_{iR}\right\} + \hat{q}_{WMR}\right)\right]\}$$

$$-\tan\delta_3\left[\frac{1}{2}C_{C3R}\left(\bar{b}_{1R}\hat{p}_{WMR} + \bar{a}_{1R}\hat{q}_{WMR}\right)\right]\}$$

$$+(DNQ_R)\frac{\sigma a_R}{2}C_{d_{f_R}}\left(1 + \frac{16}{9}\lambda_R^2\right)^{1/2}\left(\frac{3}{4} + \frac{2}{3}\mu_R^2 - a_{0_R}\mu_R \hat{q}_{WMR}\right)$$

$$Q_R = \frac{550\, HP_{REQ_R}}{\Omega_R'}$$

12. Rotor Moments in Mast Axis System

Right Rotor

(For left rotor, replace subscript R with L)

$$M_{a_{1R}} = K_H a_{1R}$$

$$l_{b_{1R}} = K_H b_{1R}$$

13. Propeller Efficiency

$$\eta_{PROP_R} = \frac{X_R(V_T)}{550(HP_{REQ_R})}$$

$$\eta_{PROP_L} = \frac{X_L(V_T)}{550(HP_{REQ_L})}$$

2	ROTOR INDUCED VELOCITIES

Inputs: Variables		Outputs:	
From Subsystem	**Symbol**	**To Subsystem**	**Symbol**
1	T_R	4	$U_i \vert^{B}_{R/WL}$
	H_R		$W_i \vert^{B}_{R/WL}$
	Y_R		R_{WL}
	T_L		$U_i \vert^{B}_{R/WR}$
	H_L		$W_i \vert^{B}_{R/WR}$
	Y_L		R_{WR}
	W_{iR}		C_{RFL}
	W_{iL}		C_{RFR}
	μ_R		$W_i \vert_{R/WL}$
	μ_L		$W_i \vert_{R/WR}$
	λ_R	5	$U_i \vert^{B}_{R/H}$
	λ_L		$W_i \vert^{B}_{R/H}$
	Ω'_R	6	$U_i \vert^{B}_{R/V}$
	Ω'_L		$W_i \vert^{B}_{R/V}$
8a	β_m		
12	α_F		
	β_F		
15	V_T		
	ρ		
	M_N		

Inputs: Constants, Coefficients, and Data Tables

Constants: R, l_m, SL_H, SL_{SP}

Coefficients: K_0, K_1, K_2, K_3, K_4

Data Tables: $\dfrac{W_i \vert_{R/H}}{W_i} = f(\alpha_F, \beta_m, V_T)$ Table 2-I

$K_{H_\beta} = f(\beta_F, \beta_m)$ Table 2-II

SUBSYSTEM NO. 2—ROTOR INDUCED VELOCITIES

Inputs: Variables

Symbol	Description	Units
T_R	Mast axis right rotor thrust (+ up for helicopter)	lb
H_R	Mast axis H-force right rotor (+ aft for helicopter)	lb
Y_R	Mast axis Y-force right rotor (+ right for helicopter)	lb
T_L	Mast axis left rotor thrust (+ up for helicopter)	lb
H_L	Mast axis H-force left rotor (+ aft for helicopter)	lb
Y_L	Mast axis Y-force left rotor (+ right for helicopter)	lb
W_{iR}	Mast axis uniform component of induced velocity at right rotor (+ downward for helicopter)	ft/sec
W_{iL}	Mast axis uniform component of induced velocity at left rotor (+ downward for helicopter)	ft/sec
μ_R	Tip speed (advance) ratio, right rotor	ND
μ_L	Tip speed (advance) ratio, left rotor	ND
λ_R	Inflow ratio, right rotor	ND
λ_L	Inflow ratio, left rotor	ND
Ω'_R	Total right rotor speed (corrected for aircraft angular rate)	rad/sec
Ω'_L	Total left rotor speed (corrected for aircraft angular rate)	rad/sec

Inputs: Variables (Concluded)

Symbol	Description	Units
β_m	Mast conversion angle (+ fwd, 0 deg = vertical or helicopter, 90 deg = horizontal or airplane	rad
α_F	Fuselage angle of attack	rad
β_F	Fuselage sideslip angle	rad
V_T	Total linear velocity of the aircraft c.g. with respect to the air	ft/sec
ρ	Air density	slug/ft^3
M_N	Mach number	ND

Inputs: Constants, Coefficients, and Data Tables

R	Rotor radius	ft
l_m	Mast length	ft
SL_H	Station line of the horizontal stabilizer center of pressure	in
SL_{SP}	Station line of the engine nacelle shaft pivot point	in
$K_0 \ldots K_4$	Constants in the rotor/wing wake equation	ND
$\frac{W_i \vert R/H}{W_i}$	Ratio of the induced z-axis rotor wake velocity on the horizontal stabilizer to the mean induced velocity at the rotor (for both right and left rotor) $= f(\alpha_F, \beta_m, V_T)$	ND

SUBSYSTEM NO. 2—ROTOR INDUCED VELOCITIES (Concluded)

Outputs:

Symbol	Description	Units
K_{H_β}	Rotor wake on the horizontal stabilizer (constant) $= f(\beta_m, \beta_F)$	ND
$U_i \Big\vert^{B}_{R/WL}$	Induced x-velocity at the left wing in body axis due to the rotor	ft/sec
$W_i \Big\vert^{B}_{R/WL}$	Induced z-velocity at the left wing in body axis due to the rotor	ft/sec
R_{WL}	Left rotor wake contraction ratio	ND
$U_i \Big\vert^{B}_{R/WR}$	Induced x-velocity at the right wing in body axis due to the rotor	ft/sec
$W_i \Big\vert^{B}_{R/WR}$	Induced z-velocity at the right wing in body axis due to the rotor	ft/sec
R_{WR}	Right rotor wake contraction ratio	ND
C_{RFL}	Left rotor force coefficient	ND
C_{RFR}	Right rotor force coefficient	ND
$W_i \Big\vert_{R/WL}$	Induced velocity at the left wing in mast axis due to the rotor	ft/sec
$W_i \Big\vert_{R/WR}$	Induced velocity at the right wing in mast axis due to the rotor	ft/sec
$U_i \Big\vert^{B}_{R/H}$	Induced x-velocity at the horizontal stabilizer in body axis due to the rotor	ft/sec
$W_i \Big\vert^{B}_{R/H}$	Induced z-velocity at the horizontal stabilizer in body axis due to the rotor	ft/sec
$U_i \Big\vert^{B}_{R/V}$	Induced x-velocity at the vertical fin in body axis due to the rotor	ft/sec
$W_i \Big\vert^{B}_{R/V}$	Induced z-velocity at the vertical fin in body axis due to the rotor	ft/sec

EQUATIONS

SUBSYSTEM 2--ROTOR-INDUCED VELOCITIES

A. Rotor Wake

Right Rotor

$$R_{WR} = R\left\{0.78 + 0.22\left[\exp^{-\left(0.3+2Z\sqrt{C_{RFR}}+60C_{RFR}\right)}\right]\right\}$$

Where,

$$Z = \frac{\left(WR_{HUB} - WR_{W}\right)_{\beta_m = 0}}{12R} = \frac{l_m}{R}$$

$$C_{RFR} = \frac{\left(T_R^2 + H_R^2 + Y_R^2\right)^{1/2}}{\rho \pi \Omega_R'^{\,2} R^4}$$

(For left rotor, replace subscript R with L)

B. Rotor Wake at Wing, Horizontal Stabilizer and Vertical Stabilizer in Mast Axes

Note: For rotor wake effects on the horizontal stabilizer and on the vertical stabilizer, the values of the average induced velocity will be used.

1. Wing

$$W_i\,|_{R/WR} = \left(K_0 + K_1\mu_R + K_2\mu_R^2 + K_3\lambda_R + K_4\lambda_R^2\right)\left(W_{iR}\right)$$

$$W_i\,|_{R/WL} = \left(K_0 + K_1\mu_L + K_2\mu_L^2 + K_3\lambda_L + K_4\lambda_L^2\right)\left(W_{iL}\right)$$

2. Horizontal Stabilizer

$$W_i|_{R/H} = \left(\frac{W_i|_{R/H}}{W_{iL}}\right)\left(K_{H_\beta}\right)\left[\left(W_{iL} + W_{iR}\right)/2\right]\left(\frac{1}{\tau S + 1}\right)$$

Where,

$$\frac{W_i|_{R/H}}{W_{iL}} = f\left(\alpha_F, \beta_m, V_T\right)$$

$$\tau = \frac{l_{X_{RH}}}{U}$$

$$K_{H_\beta} = f\left(\beta_F, \beta_m\right)$$

$$l_{X_{RH}} = \left[SL_H - \left(SL_{SP} - l_m \sin\beta_m\right)\right]\left(\frac{1}{12}\right)$$

3. Vertical Stabilizer

$$W_i|_{R/V} = \left(\frac{W_i|_{R/H}}{W_{iL}}\right)\left[\left(W_{iL} + W_{iR}\right)/2\right]\left(\frac{1}{\tau S + 1}\right)$$

C. Components of Rotor Wake in Body Axes

1. Wing--Right Rotor

$$U_i|^B_{R/WR} = \left(W_i|_{R/WR}\right)\left(\sin\beta_m\right)$$

$$W_i|^B_{R/WR} = \left(-W_i|_{R/WR}\right)\left(\cos\beta_m\right)$$

(For left rotor, replace subscript R with L)

SUBSYSTEM 2--ROTOR-INDUCED VELOCITIES

2. Horizontal Stabilizer

$$U_i|^B_{R/H} = \left(W_i|_{R/H}\right)\left(\sin\beta_m\right)$$

$$W_i|^B_{R/H} = \left(-W_i|_{R/H}\right)\left(\cos\beta_m\right)$$

3. Vertical Stabilizer

$$U_i|^B_{R/V} = \left(W_i|_{R/V}\right)\left(\sin\beta_m\right)$$

$$W_i|^B_{R/V} = \left(-W_i|_{R/V}\right)\left(\cos\beta_m\right)$$

3	FUSELAGE AERODYNAMICS

Inputs: Variables		Outputs:	
From Subsystem	Symbol	To Subsystem	Symbol
12	V_T	10a	L_F
	α_F		D_F
	β_F		Y_F'
15	ρ		M_F'
	M_N		l_F'
			N_F'
		7, 8b, 8c	q_F

Inputs: Constants, Coefficients, and Data Tables

Constants: LLANG, DLANG, LBFO, DBFO, MBFO

Coefficients:

Data Tables:		
	$L_\alpha = f(\alpha_F)$	Table 3-I
	$L_\beta = f(\beta_F)$	Table 3-II
	$D_\alpha = f(\alpha_F)$	Table 3-III
	$D_\beta = f(\beta_F)$	Table 3-IV
	$M_\alpha = f(\alpha_F)$	Table 3-V
	$M_\beta = f(\beta_F)$	Table 3-VI
	$Y_\beta = f(\beta_F)$	Table 3-VII
	$l_\beta = f(\beta_F)$	Table 3-VIII
	$N_\beta = f(\beta_F)$	Table 3-IX

SUBSYSTEM NO. 3: FUSELAGE AERODYNAMICS

Inputs: Variables

Symbol	Description	Units
V_T	Total linear velocity of the rotorcraft c.g. with respect to the air	ft/sec
α_F	Fuselage angle of attack	rad
β_F	Fuselage sideslip angle	rad
ρ	Air density	$slug/ft^3$
M_N	Mach number	ND

Inputs: Constants, Coefficients, and Data Tables

LLANG	Extra fuselage lift	ft^2
DLANG	Extra fuselage drag	ft^2
LBFO	Fuselage lift at $\alpha = 0$ deg, $\beta = 0$ deg	ft^2
DBFO	Fuselage drag at $\alpha = 0$ deg, $\beta = 0$ deg	ft^2
MBFO	Fuselage pitching moment at $\alpha = 0$ deg, $\beta = 0$ deg	ft^3
L_α	Fuselage lift variation with angle of attack, $= f(\alpha)$	ft^2
L_β	Fuselage lift variation with sideslip angle, $= f(\beta)$	ft^2
D_α	Fuselage drag variation with angle of attack, $= f(\alpha)$	ft^2
D_β	Fuselage drag variation with sideslip angle, $= f(\beta)$	ft^2

SUBSYSTEM NO. 3—FUSELAGE AERODYNAMICS (Concluded)

Inputs: Constants, Coefficients, and Data Tables (Concluded)

Symbol	Description	Units
M_α	Fuselage pitching moment variation with angle of attack, = f(α)	ft^3
M_β	Fuselage pitching moment variation with sideslip angle, = f(β)	ft^3
Y_β	Fuselage side force variation with sideslip angle, = f(β)	ft^2
l_β	Fuselage rolling moment variation with sideslip angle, = f(β)	ft^3
N_β	Fuselage yawing moment variation with sideslip angle, = f(β)	ft^3

Outputs:

L_F	Aerodynamic lift on fuselage (wind axis)	lb
D_F	Aerodynamic drag on fuselage (wind axis)	lb
Y'_F	Aerodynamic side force on fuselage (wind axis)	lb
M'_F	Aerodynamic pitching moment on fuselage (wind axis)	ft-lb
l'_F	Aerodynamic rolling moment on fuselage (wind axis)	ft-lb
N'_F	Aerodynamic yawing moment on fuselage (wind axis)	ft-lb
q_F	Fuselage dynamic pressure	lb/ft^2

EQUATIONS

SUBSYSTEM 3--FUSELAGE AERODYNAMICS

A. Fuselage Dynamic Pressure

$$q_F = \frac{1}{2}\rho V_T^2$$

B. Fuselage Forces

$$L_F = q_F\left[\left(L_\alpha \mid_{\beta_F = 0\,deg}\right)\cos^2\beta_F + L_\beta + LBFO + LLANG\right]$$

$$D_F = q_F\left[\left(D_\alpha \mid_{\beta_F = 0\,deg}\right)\cos^2\beta_F + D_\beta + DBFO + DLANG\right)$$

$$Y_F' = q_F\left(Y_\beta\right)$$

C. Fuselage Moments

$$M_F' = q_F\left[\left(M_\alpha \mid_{\beta_F = 0}\right)\cos^2\beta_F + M_\beta + MBFO\right]$$

$$l_F' = q_F\left(l_\beta\right)$$

$$N_F' = q_F\left(N_\beta\right)$$

Note: for landing gear pod drag, see Subsystem 7

4	WING-PYLON AERODYNAMICS

Inputs: Variables		Outputs:	
From Subsystem	Symbol	To Subsystem	Symbol
1	W_{iL}	5	$\epsilon_{W/H}$
	W_{iR}	10a	α_{iWL}
2	$U_i \vert^{B}_{R/WL}$		α_{iWR}
			β_{iWL}
	$W_i \vert^{B}_{R/WL}$		β_{iWR}
			L_{iWPL}
	R_{WL}		L_{iWPR}
	$U_i \vert^{B}_{R/WR}$		D_{iWPL}
	$W_i \vert^{B}_{R/WR}$		D_{iWPR}
	R_{WR}		α_{WFS}
	C_{RFL}		L_{WP}
	C_{RFR}		D_{WP}
	$W_i \vert_{R/WL}$		M'_{WP}
	$W_i \vert_{R/WR}$		Y'_{WP}
			l'_{WP}
1	μ_L		N'_{WP}
	μ_R		SD
8a	β_m		D_{PYLN}
	δ_F		D_{PLAT}
	δ_a		α_{PLAT}
12	V_T		β_{PLAT}
	α_F		α_{SP}
	β_F		β_{SP}

(Continued on next page)

SUBSYSTEM NO. 4--WING-PYLON AERODYNAMICS (Continued)

Inputs: Variables		Outputs:	
From Subsystem	Symbol	To Subsystem	Symbol
12 (concl)	U		
	V	14	$(X_{iW}, Y_{iW})_R$
	W		
15	ρ		$(X_{iW}, Y_{iW})_L$
	M_N		
11	p		
	q		
	r		

Inputs: Constants, Coefficients, and Data Tables

Constants: l_m, SL_{WP}, SL_{SP}, BL_{SP}, BL_{CG}, SL_{WTE}, S_W, c_W, b_W, Λ_W, S_{PYL}, ϕ_m

Coefficients:

$$C_{Y_\beta}|_{M_N=0}, \quad \frac{C_{Y_p}}{C_{L_{WP}}}|_{M_N=0}, \quad C_{Y_r}|_{M_N=0}$$

$$C_{l_p}|_{C_{L_{Wp}}=M_N=0}, \quad \frac{C_{l_r}}{C_{L_{WP}}}|_{M_N=0}$$

$$\frac{\Delta C_{l_r}}{(\partial\alpha_{WFS}/\partial\delta_F)(\delta_F)}, \quad C_{l_{\delta_a}}|^{\delta_F=0\text{ deg}}_{\alpha_{WFS}<8\text{ deg}}$$

$$C_{n_\beta}|_{C_{L_{WP}}=M_N=0}, \quad \frac{C_{n_\beta}}{C^2_{L_{WPFS}}}|_{M_N=0}, \quad \frac{C_{n_r}}{C^2_{L_{WP}}}, \quad \frac{C_{n_r}}{C_{D_{oWP}}}$$

$$\frac{C_{n_p}}{C_{L_{WP}}}|_{M_N=0}, \quad (\partial\alpha_{WFS}/\partial\delta_F), \quad K_{np}, \quad K_{RW}, \quad K_{XRW},$$

$$X_{RWO}, X_{RW1}, X_{RW2}, K_{FWO}, K_{FWDF}, (SD/q)_{\beta_m=90}, (SD/q)$$

(Continued on next page)

SUBSYSTEM NO. 4--WING-PYLON AERODYNAMICS (Continued)		
Inputs: Constants, Coefficients, and Data Tables (Continued)		
Data Tables:	$C_{L_{WP}} = f(\alpha_W, \beta_m, \delta_F, M_N)$	Tables 4-I, 4-II
	$C_{D_{WP}} = f(\alpha_W, \beta_m, \delta_F, M_N)$	Tables 4-III, 4-IV
	$\epsilon_{W/HOGE} = f(\alpha_{WFS}, \beta_m, \delta_F)$	Table 4-V
	$C_{l_\beta} \mid_{C_{L_{WP}} = M_N = 0} = f(\delta_F, \beta_F, \beta_m)$	Table 4-VI
	$\frac{C_{l_\beta}}{C_{L_{WP}}} \mid_{M_N = 0} = f(\delta_F, \beta_F, \beta_m)$	Table 4-VII
	$C_{m_{WP}} = f(\delta_F, \beta_m)$	Table 4-VIII
	$\frac{\partial C_{L_{WPFS}}}{\partial \alpha_{WFS}} \mid_{C_{L_{WP}} = 0} = f(M_N, \beta_m, \delta_F)$	Table 4-IX
	$C_{D_{oWP}} \mid_{C_{L_{WP}} = 0} = f(M_N, \beta_m, \delta_F)$	Table 4-X
	$K_{l_{\delta_a}} = f(\alpha_{WFS}, \beta_m, \delta_F)$	Table 4-XI
	$C_{L_{\delta_a}} = f(\delta_F)$	Table 4-XII

(Concluded on next page)

Inputs: Constants, Coefficients, and Data Tables (Concluded)

Data Tables: (Concluded)	$K_{no_{\delta_a}} = f(\delta_F, \beta_m)$	Table 4-XIII
	$K_{n_{\delta_a}} = f(\delta_F, \beta_m)$	Table 4-XIV
	$D_{PYINT} = f(\beta_m)$	Table 4-XV
	$K_{PLAT} = f(\bar{\alpha}_{PYL})$	Table 4-XVI

SUBSYSTEM NO. 4--WING-PYLON AERODYNAMICS

Inputs: Variables

Symbol	Description	Units
W_{iL}	Mast axis uniform component of induced velocity at left rotor (+ downward in helicopter mode)	ft/sec
W_{iR}	Mast axis uniform component of induced velocity at right rotor (+ downward in helicopter mode)	ft/sec
$U_i \Big\vert^{B}_{R/WL}$	Induced x-velocity at the left wing in body axis due to the rotor	ft/sec
$W_i \Big\vert^{B}_{R/WL}$	Induced z-velocity at the left wing in body axis due to the rotor	ft/sec
R_{WL}	Left rotor wake contraction ratio	ND
$U_i \Big\vert^{B}_{R/WR}$	Induced x-velocity at the right wing in body axis due to the rotor	ft/sec
$W_i \Big\vert^{B}_{R/WR}$	Induced z-velocity at the right wing in body axis due to the rotor	ft/sec
R_{WR}	Right rotor wake contraction ratio	ND
C_{RFL}	Left rotor force coefficient	ND
C_{RFR}	Right rotor force cofficient	ND
$W_i \Big\vert_{R/WL}$	Induced velocity at the left wing in mast axis due to the rotor	ft/sec
$W_i \Big\vert_{R/WR}$	Induced velocity at the right wing in mast axis due to the rotor	ft/sec
μ_L	Left rotor tip speed (advance) ratio	ND
μ_R	Right rotor tip speed (advance) ratio	ND

Inputs: Variables (Concluded)

Symbol	Description	Units
β_m	Mast conversion angle (+ fwd, 0 deg = vertical or helicopter, 90 deg = horizontal or airplane)	deg
δ_F	Flap position indicator	ND
δ_a	Aileron mean deflection angle (+ right aileron up)	deg
V_T	Total linear velocity of the aircraft c.g. with respect to the air	ft/sec
α_F	Fuselage freestream angle of attack	deg
β_F	Fuselage freestream sideslip angle	deg
U	x-velocity (longitudinal) of the aircraft c.g. in body axis with respect to the air	ft/sec
V	y-velocity (lateral) of the aircraft c.g. in body axis with respect to the air	ft/sec
W	z-velocity (vertical) of the aircraft c.g. in body axis with respect to the air	ft/sec
ρ	Air density	$slug/ft^3$
M_N	Mach number	ND
p	Body axis roll rate	rad/sec
q	Body axis pitch rate	rad/sec
r	Body axis yaw rate	rad/sec
l_m	Mast length	ft
SL_{WP}	Station line of the wing-pylon center of pressure	inch

Inputs: Constants, Coefficients, and Data Tables

Symbol	Description	Units
SL_{SP}	Station line of engine nacelle shaft pivot point	inch
BL_{SP}	Butt line of engine nacelle shaft pivot point	inch
BL_{CG}	Butt line of c.g.	inch
SL_{WTE}	Station line of wing trailing edge	inch
S_W	Wing area	ft^2
c_W	Wing chord	ft
b_W	Wing span	ft
Λ_w	Wing quarter chord sweep angle	deg
S_{PYL}	Projected lateral pylon area	ft^2
ϕ_m	Lateral mast tilt	deg
$C_{Y_\beta}\|_{M_N=0}$	Aerodynamic coefficient in the wing side force equation	1/rad
$\frac{C_{Y_p}}{C_{L_{WP}}}\|_{M_N=0}$	Aerodynamic coefficient in the wing side force equation	1/rad
$C_{Y_r}\|_{M_N=0}$	Aerodynamic coefficient in the wing side force equation	1/rad
$C_{l_p}\|_{C_{L_{WP}}=M_N=0}$	Aerodynamic coefficient in the wing rolling moment equation	1/rad
$\frac{C_{l_r}}{C_{L_{WP}}}\|_{M_N=0}$	Aerodynamic coefficient in the wing rolling moment equation	1/rad
$\frac{\Delta C_{l_r}}{(\partial \alpha_{WFS}/\partial \delta_F)(\delta_F)}$	Aerodynamic coefficient in the wing rolling moment equation	1/deg

Inputs: Constants, Coefficients, and Data Tables (Continued)

Symbol	Description	Units
$C_{l_{\delta_a}} \Big\vert_{\alpha_{WFS}<8\ deg}^{\delta_F=0\ deg}$	Aerodynamic coefficient in the wing rolling moment equation	1/deg
$C_{n_\beta} \vert_{C_{L_{WP}}=M_N=0}$	Aerodynamic coefficient in the wing yawing moment equation	1/rad
$\frac{C_{n_\beta}}{C_{L_{WPFS}}^2} \vert_{M_N=0}$	Aerodynamic coefficient in the wing yawing moment equation	1/rad
$\frac{C_{n_r}}{C_{L_{WP}}^2}$	Aerodynamic coefficient in the wing yawing moment equation	1/rad
$\frac{C_{n_r}}{C_{D_{oWP}}}$	Aerodynamic coefficient in the wing yawing moment equation	1/rad
$\frac{C_{n_p}}{C_{L_{WP}}} \vert_{M_N=0}$	Aerodynamic coefficient in the wing yawing moment equation	1/rad
$\frac{\partial \alpha_{WFS}}{\partial \delta_F}$	Partial of wing angle of attack with respect to partial of flap deflection	ND
K_{np}	Wing yawing moment equation constant	ND
K_{RW}	Rotor skew angle velocity distribution factor	ND
K_{XRW}	Constant in the rotor downwash/wing equation	ND
X_{RWO}	Constant in the rotor downwash/wing equation	ND
X_{RW1}	Constant in the rotor downwash/wing equation	1/deg
X_{RW2}	Constant in the rotor downwash/wing equation	$1/deg^2$

Inputs: Constants, Coefficients, and Data Tables (Continued)

Symbol	Description	Units
K_{FWO}	Constant in the rotor downwash/ wing equation for flap effects	ND
K_{FWDF}	Slope in the rotor downwash/wing equation for flap effects	1/deg
$(SD/q)_{\beta_{m-90}}$	Constant for drag of the spinner at 90 degrees of mast conversion angle	ft^2
(SD/q)	Constant in the variable drag portion of the spinner drag equation (function of mast angle)	ft^2
$C_{L_{WP}}$	Wing-pylon lift coefficient, $= f(\alpha_W, \beta_m, \delta_F, M_N)$	ND
$C_{D_{WP}}$	Wing-pylon drag coefficient, $= f(\alpha_W, \beta_m, \delta_F, M_N)$	ND
$\epsilon_{W/H}$	Wing wake deflection at the horizontal stabilizer, $f(\alpha_{WFS}, \beta_m, \delta_F, M_N)$	ND
$C_{l_\beta} \mid_{C_{L_{WP}}=M_N=0}$	Aerodynamic coefficient in the wing rolling moment equation, $= f(\delta_F, \beta_F, \beta_m)$	1/rad
$\frac{C_{l_\beta}}{C_{L_{WP}}} \mid_{M_N=0}$	Aerodynamic coefficient in the wing rolling moment equation, $= f(\delta_F, \beta_F, \beta_m)$	1/rad
$C_{m_{WP}}$	Wing-pylon pitching moment coefficient, $= f(\delta_F, \beta_m)$	ND
$\frac{\partial C_{L_{WP}}}{\partial \alpha_W} \mid_{C_{L_{WP}}=0}$	Partial of wing coefficient of lift with respect to angle of attack, $= f(M_N, \beta_m, \delta_F)$	ND

Inputs: Constants, Coefficients, and Data Tables (Concluded)

Symbol	Description	Units
$C_{D_{oWP}}\|_{C_{L_{WP}}=0}$	Wing coefficient of drag at wing coefficient of lift equal to zero, $=f(M_N, \beta_m, \delta_F)$	ND
$K_{l_{\delta_a}}$	Aileron effectiveness correction factor, $=f(\alpha_{WFS}, \beta_m, \delta_F)$	ND
$C_{L_{\delta_a}}$	Aerodynamic coefficient for the wing lift coefficient reduction due to aileron deflection, $=f(\delta_F)$	1/deg
$K_{n_{o\delta_a}}$	Yawing moment (aileron) coefficient, $=f(\delta_F, \beta_m)$	1/deg
$K_{n_{\delta_a}}$	Yawing moment (aileron) coefficient, $=f(\delta_F, \beta_m)$	ND
D_{PYINT}	Pylon interference drag, $=f(\beta_m)$	ft^2
K_{PLAT}	Pylon lateral drag coefficient, $=f(\bar{\alpha}_{PYL})$	ND

Outputs:

$\epsilon_{W/H}$	Wing wake deflection at the horizontal stabilizer, $=f(\alpha_{WFS}, \beta_m, \delta_F, M_N)$	ND
α_{iWL}	Angle of attack of the wing portion immersed in the left rotor wake	deg
α_{iWR}	Angle of attack of the wing portion immersed in the right rotor wake	deg
β_{iWL}	Sideslip angle of the wing portion immersed in the left rotor wake	deg

Outputs: (Continued)

Symbol	Description	Units
β_{iWR}	Sideslip angle of the wing portion immersed in the right rotor wake	deg
L_{iWPL}	Aerodynamic lift of the left wing portion immersed in the rotor wake	lb
L_{iWPR}	Aerodynamic lift of the right wing portion immersed in the rotor wake	lb
D_{iWPL}	Aerodynamic drag of the left wing portion immersed in the rotor wake	lb
D_{iWPR}	Aerodynamic drag of the right wing portion immersed in the rotor wake	lb
α_{WFS}	Angle of attack of the wing portion outside the rotor wake (freestream)	rad
L_{WP}	Aerodynamic lift on the wing portion outside the rotor wake (freestream)	lb
D_{WP}	Aerodynamic drag on the wing portion outside the rotor wake (freestream)	lb
M'_{WP}	Pitching moment of the wing-pylon in wind axis	ft-lb
Y'_{WP}	Side force of the wing-pylon in wind axis	lb
l'_{WP}	Rolling moment of the wing-pylon in wind axis	ft-lb
N'_{WP}	Yawing moment of the wing-pylon in wind axis	ft-lb
SD	Spinner drag	lb
D_{PYLN}	Pylon interference drag	lb
D_{PLAT}	Pylon drag due to sideslip	lb

Outputs: (Concluded)

Symbol	Description	Units
α_{PLAT}	Pylon angle of attack used for transformation from wind to body axis	rad
β_{PLAT}	Pylon sideslip angle used for transformation from wind to body axis	rad
α_{SP}	Spinner angle of attack used for transformation from wind to body axis	rad
β_{SP}	Spinner sideslip angle used for transformation from wind to body axis	rad
$(X_{iW}, Y_{iW})_R$	Moment arms for right wing-pylon z-force due to rotor wake	inch
$(X_{iW}, Y_{iW})_L$	Moment arms for left wing-pylon z-force due to rotor wake	inch

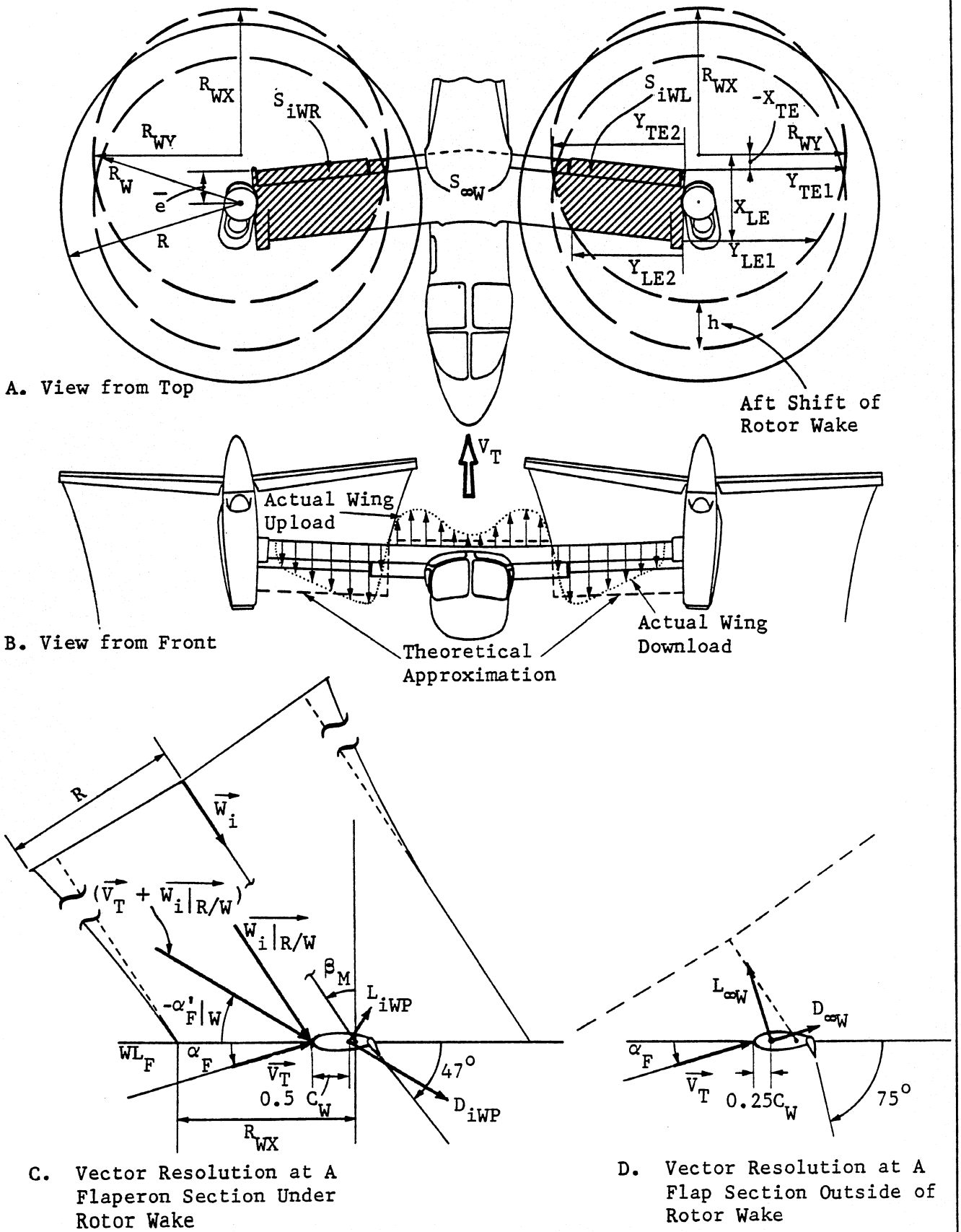

Figure A4-1. Sign Convention and Notation for Mathematical Model of Rotor Wake - Wing Interaction

EQUATIONS

SUBSYSTEM NO. 4--WING-PYLON AERODYNAMICS

A. Wing Aerodynamics Affected by the Rotor Wake

Note: In this subsystem, K is used frequently as a dummy subscript when describing the equations utilized in calculating the portion of a tilt rotor wing that is affected by the rotor wake. The subscript is replaced by R and L when computing the right and left portions of the affected wing area (S_{iWR} and S_{iWL}).

1. Initialization of values for the calculation of the portion of the wing being affected by the rotor induced velocity.

If

$$\cos\beta_m = 0,$$

$$G = 1.5708 = \pi/2$$

Otherwise,

$$G = \tan^{-1}\left[\left(\cos\phi_m\right)\left(\sin\beta_m/\cos\beta_m\right)\right]$$

$$SG = \sin(G)$$

$$CG = \cos(G)$$

$$ZL = \left(l_m\right)\left(\cos\phi_m\right)(CG)$$

2. Velocities at the Wing

$$U_{WK} = -\left(U + W_i|_{R/WK}\right)(SG)$$

$$W_{WK} = -W + \left(W_i|_{R/WK}\right)\left(\cos\phi_m\right)(CG)$$

If $W_{WK} < 0.0001$, then $W_{WK} = 0.0001$

$$V_{WR} = V + \left(W_i|_{R/WR}\right)\left(\sin\phi_m\right)(CG)$$

2. Velocities at the Wing (Concluded)

$$V_{WL} = -V + \left(W_i|_{R/WL}\right)\left(\sin\phi_m\right)(CG)$$

if

$$\max\left(\left|\frac{U_{WK}}{W_{WK}}\right|, \left|\frac{V_{WK}}{W_{WK}}\right|\right) > 100.0, \text{ then}$$

$$\frac{U_{WK}}{W_{WK}} = \left(\frac{U_{WK}}{W_{WK}}\right)\left(\frac{110.0}{\max\left(\left|\frac{U_{WK}}{W_{WK}}\right|, \left|\frac{V_{WK}}{W_{WK}}\right|\right)}\right)$$

$$\frac{V_{WK}}{W_{WK}} = \left(\frac{V_{WK}}{W_{WK}}\right)\left(\frac{100.0}{\max\left(\left|\frac{U_{WK}}{W_{WK}}\right|, \left|\frac{V_{WK}}{W_{WK}}\right|\right)}\right)$$

3. Wing Geometry Information

$$\bar{\epsilon} = \left(\frac{SL_{WTE} - SL_{SP}}{12}\right)$$

$$X_{TEK} = -\bar{\epsilon} - \left[\left(l_m\right)(SG)\right] - \left(\frac{U_{WK}}{W_{WK}}\right)\left[(ZL)\left(K_{RW}\right)\right]$$

$$X_{LEK} = c_W + X_{TEK}$$

$$Y_{TIPK} = ZL\left\{\sin\phi_m / \cos\phi_m - \left[V_{WK} / \left[\left(U_{WK}^2 + W_{WK}^2\right)^{1/2}(sign)\left(W_{WK}\right)\right]\right]\right\}$$

$$R_{WXK} = R_{WK}\left\{\left[\left(\frac{U_{WK}}{W_{WK}}\right)\left(\sin\phi_m\right)\right]^2 + \left[CG - \left(\frac{U_{WK}}{W_{WK}}\right)\left[(SG)\left(\cos\phi_m\right)\right]\right]^2\right\}^{1/2}$$

3. Wing Geometry Information (Concluded)

$$R_{WYK} = R_{WK} \left\{ \left[\left(\frac{V_{WK}}{W_{WK}} \right) \left(SG * \cos\phi_m \right) - \left(SG * \sin\phi_m \right) \right]^2 + \left[\cos\phi_m + \frac{V_{WK} \sin\phi_m}{\left(U_{WK}^2 + W_{WK}^2 \right)^{1/2} * sign\left(W_{WK} \right)} \right]^2 \right\}^{1/2}$$

$$\delta_k = \tan^{-1} \left[\frac{\left(\frac{U_{WK}}{W_{WK}} \right) * \sin\phi_m}{CG - \left(\frac{U_{WK}}{W_{WK}} \right) \left(\cos\phi_m * SG \right)} \right] + \tan^{-1} \left[\frac{V_{WK} * \sin\phi_m}{\left(U_{WK}^2 + W_{WK}^2 \right)^{1/2} * sign\left(W_{WK} \right)} \right]$$

$$F_{RWK} = \frac{R_{WYK}}{R_{WXK}}$$

$$SDEL_K = \sin\delta_K$$

$$CDEL_K = |\cos\delta_K|$$

4. Procedure for Calculating the Wing Areas S_{iWR} and S_{iWL} Under the Two Rotor Wakes

a. If $\beta_m > 30.0$, then the procedure is bypassed and the affected areas are set to zero.

$$S_{iWL} = S_{iWR} = 0.0$$

b. If $\beta_m \leq 30.0$, then the procedure outlined in the flow chart of Fig. A4-2 is followed to determine the affected wing area and the location of application of forces and moments for the affected wing area (X_{iWK}, Y_{iWK}).

c. F1(C1K,C2K) and F2(C1K,C2K) are procedures called in the flow chart of Fig. A4-2 which carry out most of the actual calculations of the affected wing area and the associated point of application of forces and moments. The equations used in these procedures are detailed in the next section.

Figure A4-2. Flow Chart of Tilt Rotor Wing Aerodynamics Affected by the Rotor Wake

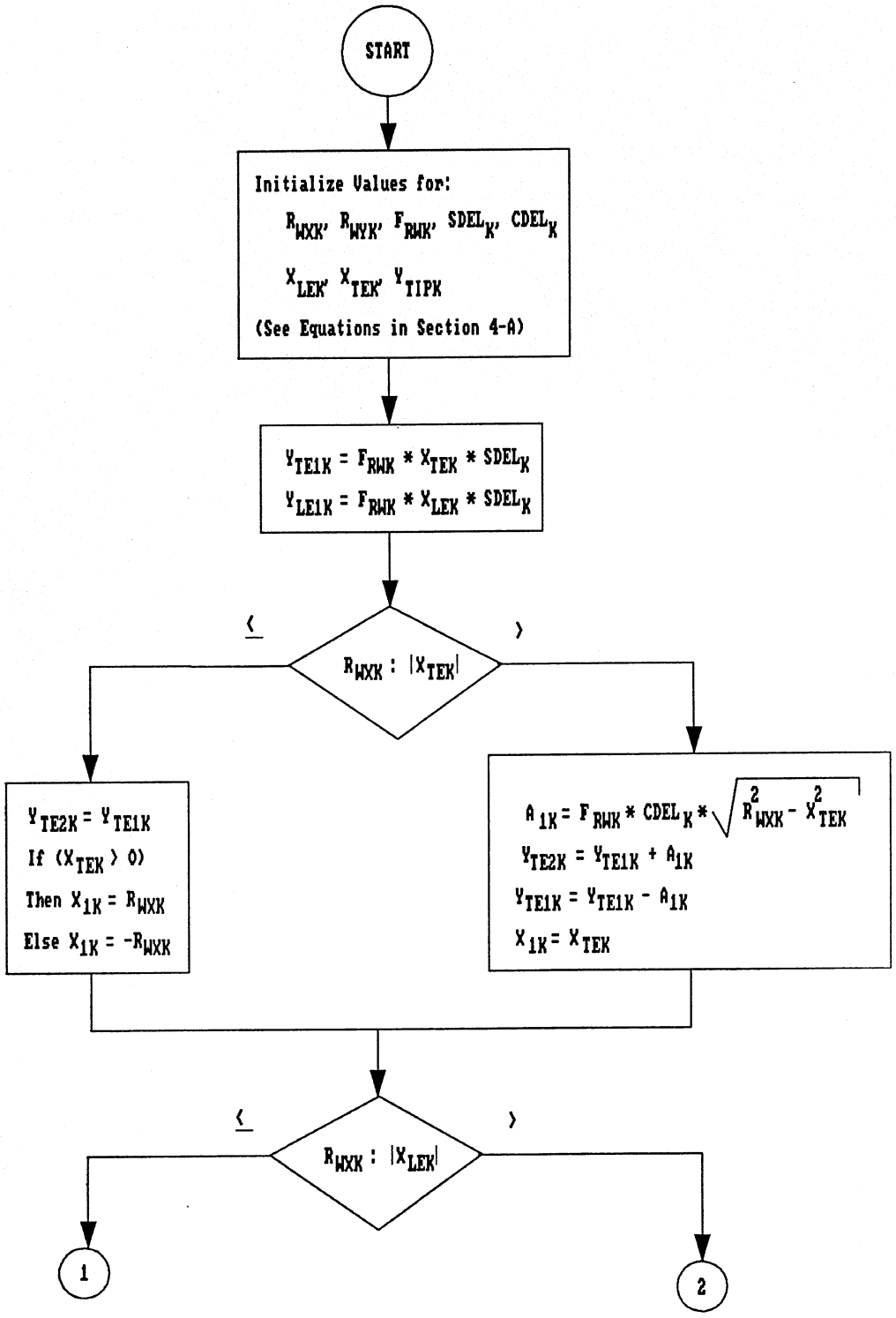

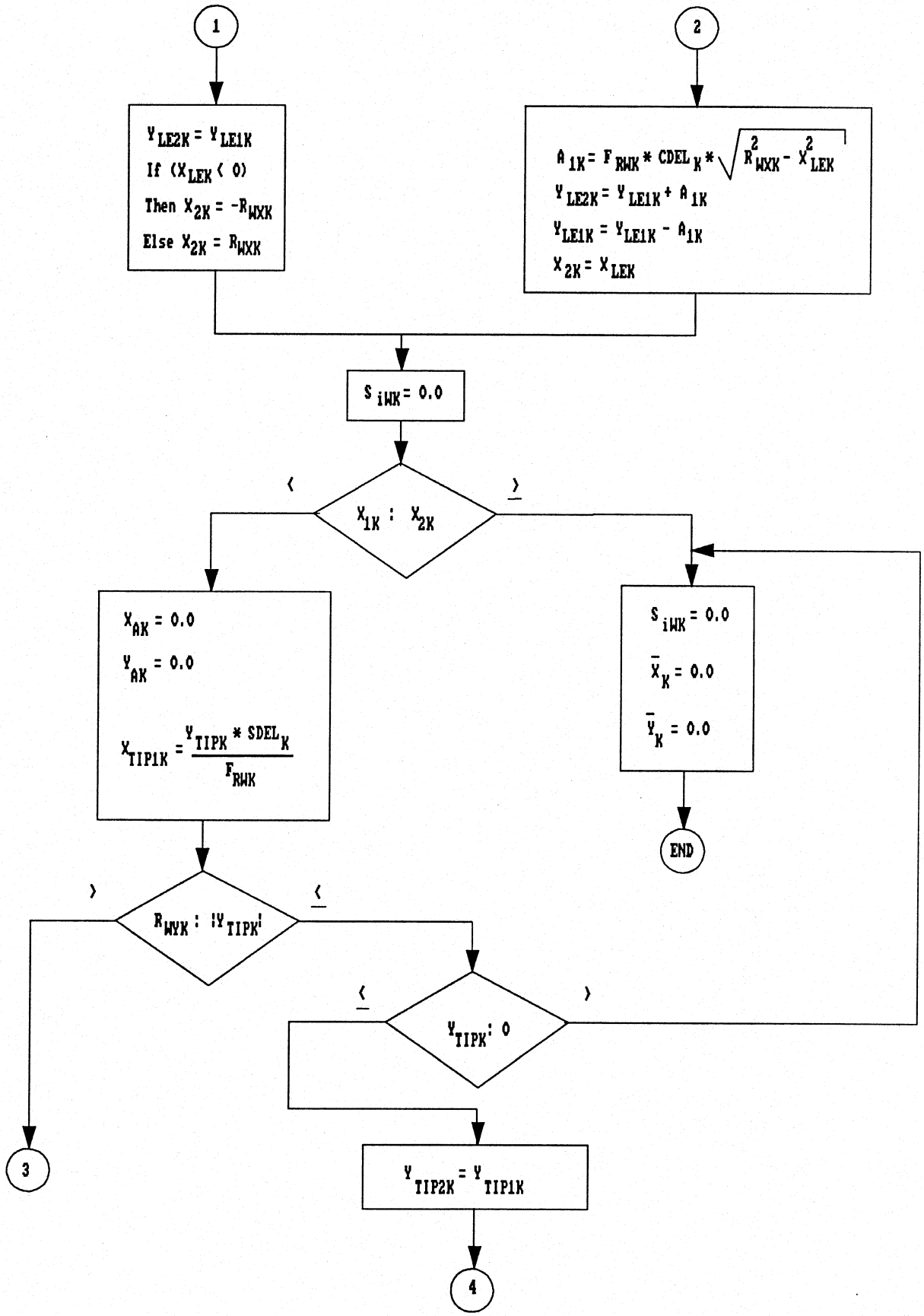
1
2
$Y_{LE2K} = Y_{LE1K}$
If $(X_{LEK} < 0)$
Then $X_{2K} = -R_{WXK}$
Else $X_{2K} = R_{WXK}$
$A_{1K} = F_{RWK} * CDEL_K * \sqrt{R^2_{WXK} - X^2_{LEK}}$
$Y_{LE2K} = Y_{LE1K} + A_{1K}$
$Y_{LE1K} = Y_{LE1K} - A_{1K}$
$X_{2K} = X_{LEK}$
$S_{iWK} = 0.0$
$X_{1K} : X_{2K}$
<
≥
$X_{AK} = 0.0$
$Y_{AK} = 0.0$
$X_{TIP1K} = \frac{Y_{TIPK} * SDEL_K}{F_{RWK}}$
$S_{iWK} = 0.0$
$\bar{X}_K = 0.0$
$\bar{Y}_K = 0.0$
END
>
$R_{WYK} : |Y_{TIPK}|$
≤
≤
>
$Y_{TIPK} : 0$
3
$Y_{TIP2K} = Y_{TIP1K}$
4

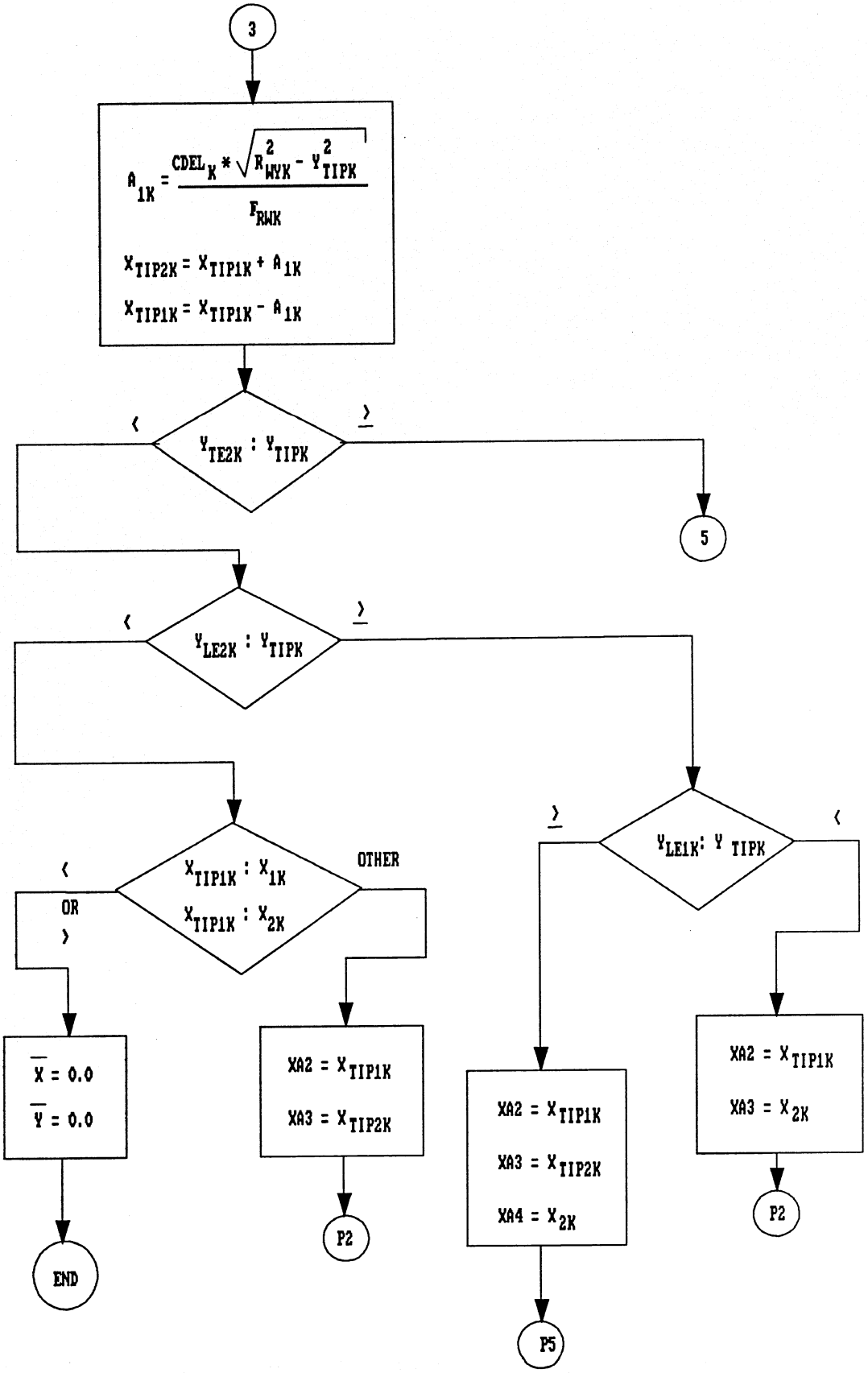
3
$A_{1K} = \frac{CDEL_K * \sqrt{R^2_{WYK} - Y^2_{TIPK}}}{F_{RWK}}$
$X_{TIP2K} = X_{TIP1K} + A_{1K}$
$X_{TIP1K} = X_{TIP1K} - A_{1K}$
$Y_{TE2K} : Y_{TIPK}$
<
≥
5
$Y_{LE2K} : Y_{TIPK}$
<
≥
$X_{TIP1K} : X_{1K}$
$X_{TIP1K} : X_{2K}$
<
OR
>
OTHER
$Y_{LE1K} : Y_{TIPK}$
≥
<
$\bar{X} = 0.0$
$\bar{Y} = 0.0$
END
$XA2 = X_{TIP1K}$
$XA3 = X_{TIP2K}$
P2
$XA2 = X_{TIP1K}$
$XA3 = X_{TIP2K}$
$XA4 = X_{2K}$
P5
$XA2 = X_{TIP1K}$
$XA3 = X_{2K}$
P2

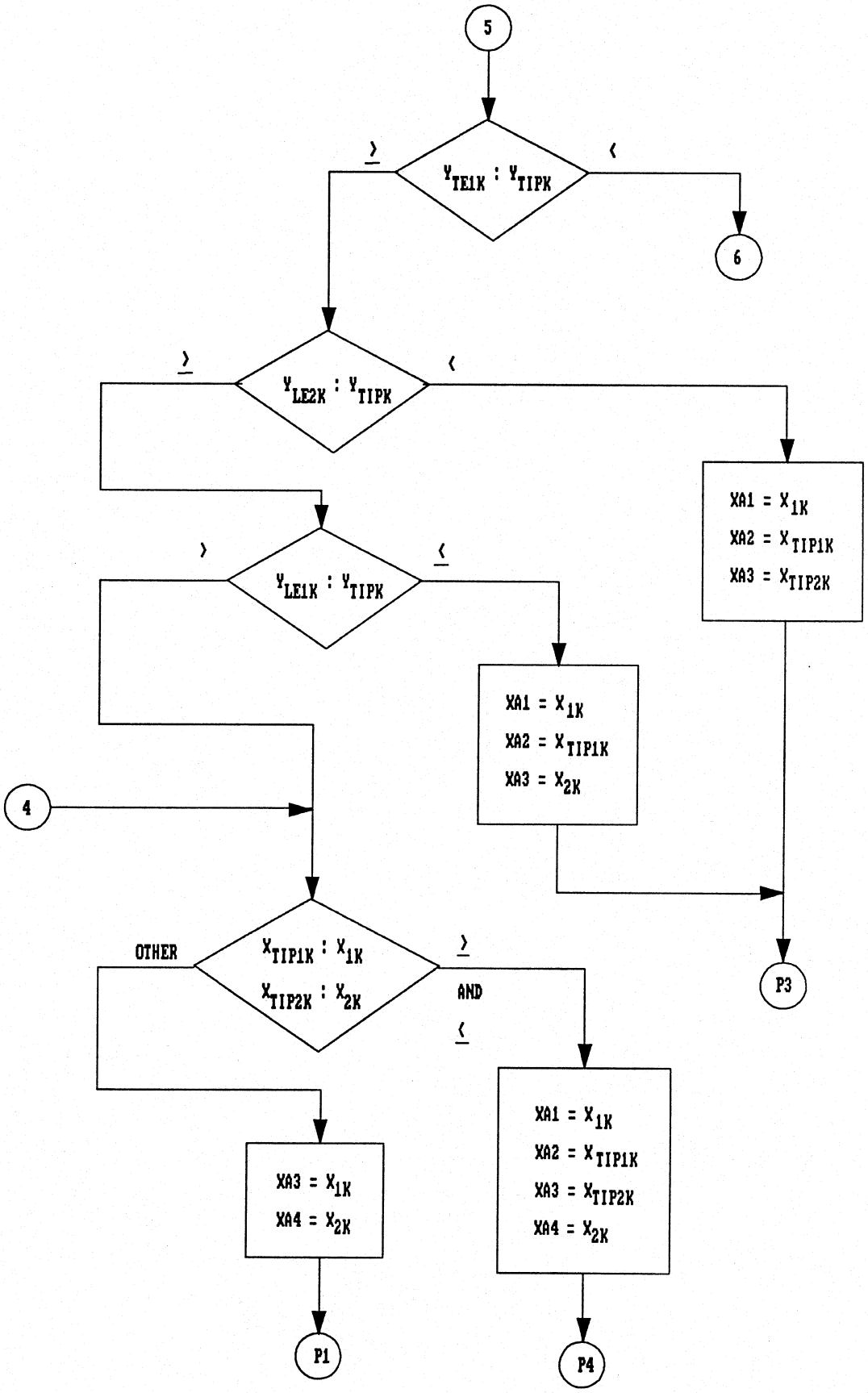
5
$Y_{TE1K} : Y_{TIPK}$
≥
<
6
$Y_{LE2K} : Y_{TIPK}$
≥
<
$XA1 = X_{1K}$
$XA2 = X_{TIP1K}$
$XA3 = X_{TIP2K}$
$Y_{LE1K} : Y_{TIPK}$
≥
<
$XA1 = X_{1K}$
$XA2 = X_{TIP1K}$
$XA3 = X_{2K}$
4
$X_{TIP1K} : X_{1K}$
$X_{TIP2K} : X_{2K}$
OTHER
≥
AND
<
P3
$XA3 = X_{1K}$
$XA4 = X_{2K}$
$XA1 = X_{1K}$
$XA2 = X_{TIP1K}$
$XA3 = X_{TIP2K}$
$XA4 = X_{2K}$
P1
P4

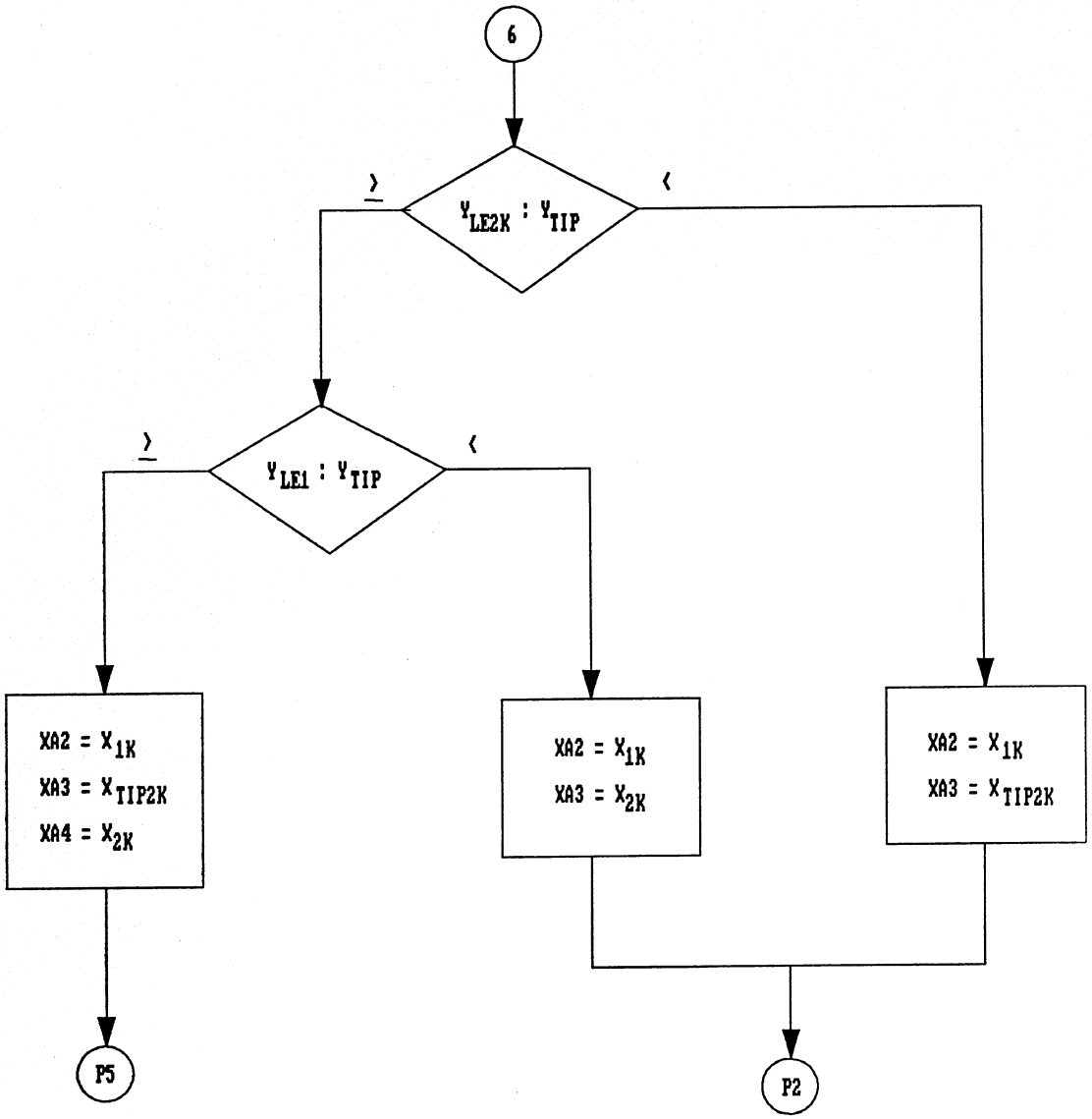
6
$Y_{LE2K} : Y_{TIP}$
≥
<
$Y_{LE1} : Y_{TIP}$
≥
<
XA2 = X_{1K}
XA3 = X_{TIP2K}
XA4 = X_{2K}
XA2 = X_{1K}
XA3 = X_{2K}
XA2 = X_{1K}
XA3 = X_{TIP2K}
P5
P2

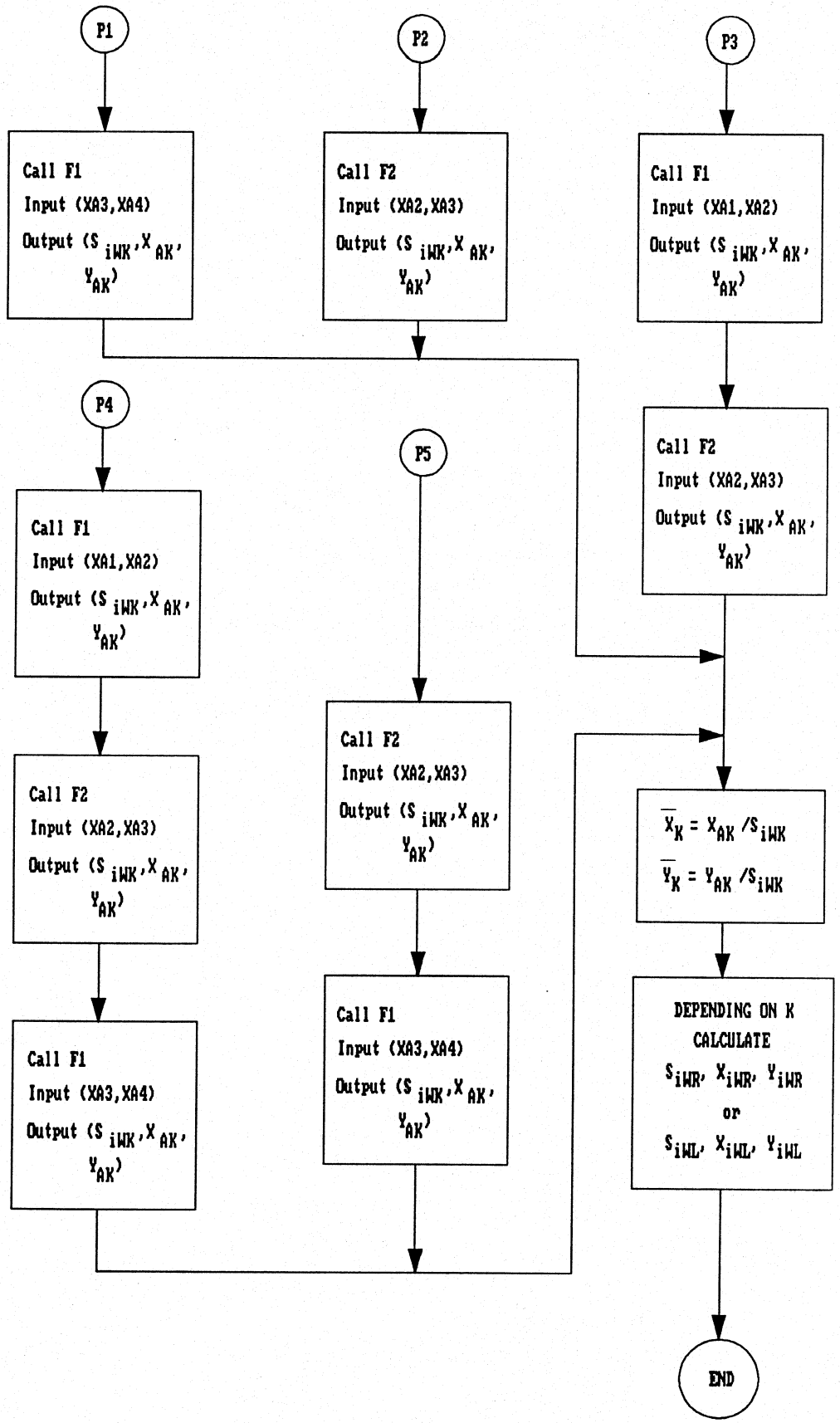
P1
Call F1
Input (XA3,XA4)
Output (S_{iWK},X_{AK}, Y_{AK})
P2
Call F2
Input (XA2,XA3)
Output (S_{iWK},X_{AK}, Y_{AK})
P3
Call F1
Input (XA1,XA2)
Output (S_{iWK},X_{AK}, Y_{AK})
P4
Call F1
Input (XA1,XA2)
Output (S_{iWK},X_{AK}, Y_{AK})
Call F2
Input (XA2,XA3)
Output (S_{iWK},X_{AK}, Y_{AK})
Call F1
Input (XA3,XA4)
Output (S_{iWK},X_{AK}, Y_{AK})
P5
Call F2
Input (XA2,XA3)
Output (S_{iWK},X_{AK}, Y_{AK})
Call F1
Input (XA3,XA4)
Output (S_{iWK},X_{AK}, Y_{AK})
Call F2
Input (XA2,XA3)
Output (S_{iWK},X_{AK}, Y_{AK})
$\overline{X}_K = X_{AK} / S_{iWK}$
$\overline{Y}_K = Y_{AK} / S_{iWK}$
DEPENDING ON K
CALCULATE
S_{iWR}, X_{iWR}, Y_{iWR}
or
S_{iWL}, X_{iWL}, Y_{iWL}
END

5. Procedures F1(C1K,C2K) and F2(C1K,C2K)

(See Fig. A4-2 to determine values for C1K and C2K)

a. Procedure F1(C1K,C2K)

$$S_{iWK} = S_{iWK} + A_{1K}$$

$$X_{AK} = X_{AK} + XA_{1K}$$

$$Y_{AK} = Y_{AK} + (XA_{1K})(SDEL_K)(F_{RWK})$$

b. Procedure F2(C1K,C2K)

$$S_{iWK} = S_{iWK} + \frac{1}{2}\left(A_{1K} + (F_{RWK})(SDEL_K)(C2K^2 - C1K^2)\right)$$

$$-(Y_{TIPK})(C2K - C1K)$$

$$X_{AK} = X_{AK} + \frac{1}{2}(XA_{1K}) + \frac{1}{3}(F_{RWK})(SDEL_K)(C2K^3 - C1K^3)$$

$$-\frac{1}{2}(Y_{TIPK})(C2K^2 - C1K^2)$$

$$Y_{AK} = Y_{AK} + F_{RWK}\left(\frac{1}{2}(XA_{1K})(SDEL_K) + \frac{1}{6}(F_{RWK})(SDEL_K^2 - CDEL_K^2)\right.$$

$$\left.(C2K^3 - C1K^3) + \frac{1}{2}\left((R_{WYK} * CDEL_K)^2 - Y_{TIPK}^2\right)(C2K - C1K)\right)$$

c. Component Equations of Above Two Procedures

$$\theta_{C1K} = \sin^{-1}\left(\frac{C1K}{R_{WXK}}\right)$$

$$\theta_{C2K} = \sin^{-1}\left(\frac{C2K}{R_{WXK}}\right)$$

$$A_{1K} = (R_{WXK})(R_{WYK})(CDEL_K)(\sin\theta_{C2K}\cos\theta_{C2K}$$

$$-\sin\theta_{C1K}\cos\theta_{C1K} + \theta_{C2K} - \theta_{C1K})$$

$$XA_{1K} = -\frac{2}{3}(F_{RWK})(CDEL_K)\left((R_{WXK}^2 - C2K^2)^{3/2} - (R_{WXK}^2 - C1K^2)^{3/2}\right)$$

6. Calculate Values for S_{iWK}, X_{iWK}, and Y_{iWK}

a. $\bar{X}_K = X_{AK}/S_{iWK}$

$\bar{Y}_K = Y_{AK}/S_{iWK}$

b. If K = R (Right Wing)

$S_{iWR} = S_{iWK}$

$X_{iWR} = \bar{X}_K + SL_{CG} - SL_{WTE} - X_{TER}$

$Y_{iWR} = -\bar{Y}_K - BL_{CG} + BL_{SP} + Y_{TIPR}$

c. If K = L (Left Wing)

$S_{iWL} = S_{iWK}$

c. If K = L (Left Wing) (Concluded)

$$X_{iWL} = \bar{X}_K + SL_{CC} - SL_{WTE} - X_{TEL}$$

$$Y_{iWL} = \bar{Y}_K + BL_{CC} - BL_{SP} - Y_{TIPL}$$

7. Total Velocity, Angle of Attack, and Sideslip Angle

$$V_{T_{iWK}} = \left((U + U_i|^B_{R/WK})^2 + (W + W_i|^B_{R/WK})^2\right)^{1/2}$$

$$\alpha_{iWK} = \tan^{-1}\left(\frac{W + W_i|^B_{R/WK}}{U + U_i|^B_{R/WK}}\right)(57.3)$$

$$\beta_{iWK} = \tan^{-1}\left[\frac{V}{((U + U_i|^B_{R/WK})^2 + (W + W_i|^B_{R/WK})^2)^{1/2}}\right](57.3)$$

8. Dynamic Pressure

$$q_{iWK} = \frac{1}{2}\rho V_{T_{iWK}}^2$$

9. Lift and Drag in Local Wind Axis System

$$L_{iWPK} = q_{iWK} S_{iWK} C_{L_{WPK}} K_{FW}$$

$$D_{iWPK} = q_{iWK} S_{iWK} C_{D_{WPK}} K_{FW}$$

Where

$$C_{L_{WPK}} = (C_{L_{WP}} = f(\alpha_{iWK}, \beta_m, \delta_F, M_N))$$

$$C_{D_{WPK}} = (C_{D_{WP}} = f(\alpha_{iWK}, \beta_m, \delta_F, M_N))$$

$$K_{FW} = K_{FWO} - K_{FWDF}(\delta_F)$$

B. Wing Aerodynamics in Freestream Flow

1. Area of Wing in Freestream Flow

$$S_{WFS} = S_W - (S_{iWL} + S_{iWR})$$

2. Wing Freestream Dynamic Pressure

$$q_{WFS} = \frac{1}{2}\rho(U^2 + W^2)$$

3. Rotor Flowfield Effects on Freestream Angle of Attack

$$\alpha_{WFS} = \alpha_F - K_{XRW}(X_{RW})\left[\frac{C_{RFR} + C_{RFL}}{\left(\max\left(0.15, \frac{\mu_R + \mu_L}{2}\right)\right)^2}\right](57.3)$$

where

$$X_{RW} = X_{RWO} + \beta_m(X_{RW1} + \beta_m(X_{RW2}))$$

4. Lift, Drag, and Pitching Moment in Local Wind Axis System

$$L_{WP} = q_{WFS} S_{WFS} C_{L_{WPFS}} - q_{WFS} S_W C_{L_{\delta_a}} |\delta_a|$$

$$D_{WP} = q_{WFS} S_{WFS} C_{D_{WPFS}}$$

$$M'_{WP} = q_{WFS} S_W c_W C_{m_{WP}}$$

where

$$C_{L_{WPFS}} = (C_{L_{WP}} = f(\alpha_{WFS}, \beta_m, \delta_F, M_N))$$

$$C_{L_{\delta_a}} = f(\delta_F)$$

$$C_{D_{WPFS}} = (C_{D_{WP}} = f(\alpha_{WFS}, \beta_m, \delta_F, M_N))$$

4. Lift, Drag, and Pitching Moment in Local Wind Axis System (Concluded)

$$C_{m_{WP}} = f\left(\beta_m, \delta_F\right)$$

Note: $C_{m_{WP}}$ is chosen at $C_{L_{WP}} \cong 0$

C. Lateral/Directional Equations (Based totally on freestream flow at all airspeeds where U > 15 ft/sec)

1. Prandtl-Glauert Compressibility Factor

$$B_c = \left[1 - M_N^2 \cos^2\left(\Lambda_W\right)\right]^{1/2}$$

$$AR_W = b_W^2 / S_W$$

$$C_\beta = \frac{AR_W + 4\cos\left(\Lambda_W\right)}{AR_W B_c + 4\cos\left(\Lambda_W\right)}$$

2. Side Force, Rolling Moment, and Yawing Moment Equations

$$Y'_{WP} = q_{WFS} S_W \left[C_{Y_\beta} \beta_F + \frac{b_W}{2U}\left(C_{Y_p} p_W + C_{Y_r} r_W\right)\right]$$

$$l'_{WP} = q_{WFS} S_W b_W \left[C_{l_\beta} \beta_F + \frac{b_W}{2U}\left(C_{l_p} p_W + C_{l_r} r_W\right)\right]$$

$$+ S_W b_W \left[\left(\frac{q_{iWL} + q_{iWR}}{2}\right)\left(C_{l_{\delta_a}} \delta_a\right)\right]$$

$$N'_{WP} = q_{WFS} S_W b_W \left[C_{n_\beta} \beta_F + \frac{b_W}{2U}\left(C_{n_p} p_W + C_{n_r} r_W\right)\right]$$

$$+ \; S_W b_W \left[\left(\frac{q_{iWL} + q_{iWR}}{2}\right)\left(C_{n_{\delta_a}} \delta_a\right)\right]$$

2. Side Force, Rolling Moment, and Yawing Moment Equations (Continued)

where

$$p_W = p\cos\alpha_{WFS}\cos\beta_F + q\sin\beta_F + r\sin\alpha_{WFS}\cos\beta_F$$

$$r_W = -p\sin\alpha_{WFS} \qquad\qquad + r\cos\alpha_{WFS}$$

and the lateral-directional stability derivatives are:

a. $C_{Y_\beta} = (C_\beta)\left(C_{Y_\beta}|_{M_N=0}\right)$

b. $C_{Y_p} = (C_\beta)\left(C_{L_{WPFS}}\right)\left(\frac{C_{Y_p}}{C_{L_{WP}}}|_{M_N=0}\right)\left(\frac{AR_W B_c + \cos(\Lambda_W)}{AR_W + \cos(\Lambda_W)}\right)$

c. $C_{Y_r} = (C_\beta)\left(C_{Y_r}|_{M_N=0}\right)$

d. $C_{l_\beta} = (C_\beta)\left(C_{l_\beta}|_{C_{L_{WP}}=M_N=0}\right) + \left(C_{L_{WPFS}}\right)\left(\frac{C_{l_\beta}}{C_{L_{WP}}}|_{M_N=0}\right)$

for

$0 \text{ deg} < |\beta_F| \le 15 \text{ deg},$

$C_{l_\beta}\beta_F = \left(C_{l_\beta}\right)(\beta_F/57.3)$

$15 \text{ deg} < |\beta_F| < 165 \text{ deg},$

$C_{l_\beta}\beta_F = \left(C_{l_\beta}\right)\left(sign(\beta_F)(15.0/57.3)\right)$

$165 \text{ deg} \le |\beta_F| < 180 \text{ deg},$

$C_{l_\beta}\beta_F = \left(C_{l_\beta} * 15.0 - C_{l_\beta}\left(|\beta_F| - 165.0\right)\right)\left(sign(\beta_F)/57.3\right)$

2. Side Force, Rolling Moment, and Yawing Moment Equations (Continued)

where

$$C_{l_\beta}\big|_{C_{L_{WP}}=M_N=0} = f\left(\delta_F, \beta_F, \beta_m\right)$$

$$\frac{C_{l_\beta}}{C_{L_{WP}}}\Big|_{M_N=0} = f\left(\delta_F, \beta_F, \beta_m\right)$$

e.

$$C_{l_p} = \left(C_\beta\right)\left(C_{l_p}\big|_{C_{L_{WP}}=M_N=0}\right)\left[\frac{\partial C_{L_{WPFS}}/\partial \alpha_{WFS}}{\left(\partial C_{L_{WPFS}}/\partial \alpha_{WFS}\right)\big|_{C_{L_{WP}}=0}}\right] - \left(\frac{1}{8}\right)\left(C_{D_{WPFS}} - \frac{C_{L_{WPFS}}^2}{\pi AR_W}\right)$$

where

$$\left(\frac{\partial C_{L_{WPFS}}}{\partial \alpha_{WFS}}\right)\Big|_{C_{L_{WFS}}=0} = f\left(M_N, \beta_m, \delta_F\right)$$

f.

$$C_{l_r} = \left(C_{L_{WPFS}}\right)\left(\frac{C_{l_r}}{C_{L_{WP}}}\Big|_{M_N=0}\right)\left(1 + \frac{AR_W\left(1-B_c\right)^2}{2B_c\left(AR_W B_c + 2\right)}\right) + \left(\frac{\Delta C_{l_r}}{\left(\partial \alpha_{WFS}/\partial \delta_F\right)\left(\delta_F\right)}\right)\left(\frac{\partial \alpha_{WFS}}{\partial \delta_F}\right)\left(\delta_F\right)$$

g.

$$C_{l_{\delta_a}} = \left(K_{l_{\delta_a}}\right)\left(C_{l_{\delta_a}}\Big|_{\substack{\delta_F=0\ \mathrm{deg} \\ \alpha_{WFS}<\ 8\ \mathrm{deg}}}\right)$$

where

$$K_{l_{\delta_a}} = f\left(\delta_F, \beta_m, \alpha_{WFS}\right)$$

2. Side Force, Rolling Moment, and Yawing Moment Equations (Concluded)

h.
$$C_{n_\beta} = \left(C_\beta\right)\left(C_{n_\beta}\,|_{C_{L_{WP}}=M_N=0}\right) + \left(C_{L_{WPFS}}\right)^2\left(\frac{C_{n_\beta}}{C_{L_{WPFS}}^2}\,|_{M_N=0}\right)$$

i.
$$C_{n_p} = \left(C_{l_p}\right)\left(\alpha_{WFS}\right)\left(K_{n_p} - 1.0\right) + \left(K_{n_p}\right)\left(C_\beta\right)\left(B_c\right)\left(C_{L_{WPFS}}\right)\left(\frac{C_{n_p}}{C_{L_{WP}}}\,|_{M_N=0}\right)$$

j.
$$C_{n_r} = \left(\frac{C_{n_r}}{C_{L_{WP}}^2}\right)\left(C_{L_{WPFS}}^2\right) + \left(\frac{C_{n_r}}{C_{D_{oWP}}}\right)\left(C_{D_{oWP}}\,|_{C_{L_{WP}}=0}\right)$$

where

$$C_{D_{oWP}}\,|_{C_{L_{WP}}=0} = f\left(M_N, \beta_m, \delta_F\right)$$

k.
$$C_{n_{\delta_a}} = K_{no_{\delta_a}} + \left(K_{n_{\delta_a}}\right)\left(C_{l_{\delta_a}}\right)\left(C_{L_{WPFS}}\right)$$

where

$$K_{no_{\delta_a}} = f\left(\delta_F, \beta_m\right)$$

$$K_{n_{\delta_a}} = f\left(\delta_F, \beta_m\right)$$

D. <u>Wing Wake Deflection at the Horizontal Tail</u>

$$\epsilon_{W/H} = \epsilon_{W/HOGE}\left[\frac{1}{\left(1 - M_N^2\right)^{1/2}}\right]$$

where,

$$\epsilon_{W/HOGE} = f\left(\alpha_{WFS}, \beta_m, \delta_F\right)$$

E. Wing/Pylon Interference Drag (resulting from the intersection of the tilt rotor pylon and wing)

$$D_{PYLN} = D_{PYINT}\left(\frac{q_{iWL} + q_{iWR}}{2}\right)$$

where

$$D_{PYINT} = f(\beta_m)$$

F. Spinner and Pylon Velocities and Angle of Attack

1. Average Induced Velocity in Body Axis

$$U_{iSP} = \left(\frac{W_{iL} + W_{iR}}{2}\right)(\sin\beta_m)$$

$$W_{iSP} = -\left(\frac{W_{iL} + W_{iR}}{2}\right)(\cos\beta_m)$$

2. Total Velocity in Mast Axis System

$$U_{MSP} = (U)\cos\beta_m + (W)\sin\beta_m$$

$$W_{MSP} = -\left(\frac{W_{iL} + W_{iR}}{2}\right) - (U)\sin\beta_m + (W)\cos\beta_m$$

$$V_{TSP} = \left(U_{MSP}^2 + V^2 + W_{MSP}^2\right)^{1/2}$$

$$q_{sp} = \frac{1}{2}\rho V_{TSP}^2$$

3. Spinner/Pylon Angle of Attack in Mast Axis

$$\bar{\alpha}_{SPN} = \tan^{-1}\left(\frac{\left(U_{MSP}^2 + V^2\right)^{1/2}}{\left|W_{MSP}\right|}\right)(57.3)$$

G. Spinner Drag

1. Spinner Drag for Two Spinners

$$SD = 2.0\left(q_{SP}\right)\left[(SD/q)_{\beta_m = 90} + (SD/q)\sin^3\left(\bar{\alpha}_{SPN}\right)\right]$$

2. Angle of Attack and Sideslip Angle for Transformation to Body Axis

The angle of attack and sideslip angle for transformation to body axis are:

$$\alpha_{SP} = \tan^{-1}\left(\frac{W + W_{iSP}}{U + U_{iSP}}\right)$$

$$\beta_{SP} = \tan^{-1}\left\{\frac{V}{\left[\left(U + U_{iSP}\right)^2 + \left(W + W_{iSP}\right)^2\right]^{1/2}}\right\}$$

where

$$\left(U + U_{iSP}\right) = \max\left(0.01, U + U_{iSP}\right)$$

H. Wing/Pylon Drag During Sideslip

The following equations allow for additional drag on tilt rotor pylons during sideslip. Pylon drag due to forward flight is included in the wing/pylon drag tables.

1. Projected Lateral Flat Plate Area of One Nacelle as a Function of Mast Axis Sideslip

$$S_{PLAT} = \left(S_{PYL}\right)\left|\frac{V}{\left(U_{MSP}^2 + V^2\right)^{1/2}}\right|$$

2. Increased Pylon Drag Area (two pylons)

$$D_{PLAT} = 2.0\left(q_{PLAT}\right)\left(S_{PLAT}\right)\left(K_{PLAT}\right)$$

where

$$q_{PLAT} = q_{SP}$$

$$K_{PLAT} = f\left(\bar{\alpha}_{PYL}\right)$$

$$\bar{\alpha}_{PYL} = \bar{\alpha}_{SPN}$$

3. Angles of Attack and Sideslip For Transformation to Body Axis

$$\alpha_{PLAT} = \alpha_{SP}$$

$$\beta_{PLAT} = \beta_{SP}$$

5	HORIZONTAL STABILIZER AERODYNAMICS

Inputs: Variables		Outputs:	
From Subsystem	Symbol	To Subsystem	Symbol
4	$\epsilon_{W/H}$	10a	α_H
9	SL_{CG}		L_H
	WL_{CG}		D_H
11	p		M'_H
	q		
	r	6	α_H
2	$U_i \Big\vert^{B}_{R/H}$		
	$W_i \Big\vert^{B}_{R/H}$		
8a	β_m		
	δ_e		
12	U		
	V		
	W		
	$\dot{W}$		
	α_F		
	β_F		
	V_T		
15	ρ		
	M_N		

(Concluded on next page)

5	HORIZONTAL STABILIZER AERODYNAMICS (Concluded)

Inputs: Constants, Coefficients, and Data Tables

Constants: SL_H, WL_H, S_H, c_H, i_H

Coefficients: $\tau_e, C_{LH\beta}, K_{HNU}, D_{WB}, C_{MHO}, C_{MHA}, D_{Ke}$

Data Tables:	$C_{LH} = f(\alpha_{HL}, \delta_e, M_N)$	Tables 5-I, 5-II
	$C_{DH} = f(\alpha_{HD}, M_N)$	Table 5-III
	$X_{Ke} = f(M_N)$	Table 5-IV
	$\eta_H = f(\alpha_F, \beta_m, V_T)$	Table 5-V
	$K_{\beta HS} = f(\beta_F)$	Table 5-VI
	$PCPM = f(M_N)$	Table 5-VII

SUBSYSTEM NO. 5: HORIZONTAL STABILIZER AERODYNAMICS

Inputs: Variables

Symbol	Description	Units
$\epsilon_{W/H}$	Wing wake deflection at the horizontal stabilizer, $= f(\alpha_W, \beta_m, \delta_F, M_N)$	deg
SL_{CG}	Station line of c.g.	inch
WL_{CG}	Water line of c.g.	inch
p	Body axis roll rate	rad/sec
q	Body axis pitch rate	rad/sec
r	Body axis yaw rate	rad/sec
$U_i \Big\vert^{B}_{R/H}$	Induced x-velocity at horizontal stabilizer in body axis due to the rotor	ft/sec
$W_i \Big\vert^{B}_{R/H}$	Induced z-velocity at horizontal stabilizer in body axis due to the rotor	ft/sec
β_m	Mast conversion angle (+ fwd, 0 deg = vertical or helicopter, 90 deg = horizontal or airplane)	deg
δ_e	Elevator mean deflection angle (+ trailing edge down)	deg
U	x-velocity (longitudinal) of the rotorcraft c.g. in body axis with respect to the air	ft/sec
V	y-velocity (lateral) of the rotorcraft c.g. in body axis with respect to the air	ft/sec

Inputs: Variables (Concluded)

Symbol	Description	Units
W	z-velocity (vertical) of the rotorcraft c.g. in body axis with respect to the air	ft/sec
$\dot{W}$	Rate of change of z-velocity (vertical) of the rotorcraft c.g. in body axis with respect to the air	ft/sec^2
α_F	Fuselage angle of attack	deg
β_F	Fuselage sideslip angle	deg
V_T	Total linear velocity of the rotorcraft c.g. with respect to the air	ft/sec
ρ	Air density	$slug/ft^3$
M_N	Mach number	ND

Inputs: Constants, Coefficients, and Data Tables

SL_H	Station line of the horizontal stabilizer center of pressure	inch
WL_H	Water line of the horizontal stabilizer center of pressure	inch
S_H	Horizontal stabilizer area	ft^2
c_H	Horizontal stabilizer chord	ft
i_H	Horizontal stabilizer incidence	deg
τ_e	Elevator effectiveness $\left(\partial\alpha_H/\partial\delta_e\right)$	ND

Inputs: Constants, Coefficients, and Data Tables (Concluded)

Symbol	Description	Units
$C_{LH\beta}$	Horizontal stabilizer lift coefficient as a function of sideslip angle	1/deg
K_{HNU}	Horizontal stabilizer dynamic pressure loss multiplier	ND
D_{WB}	Coefficient in the wing/body damping equation	ND
C_{MHO}	Horizontal stabilizer pitching moment coefficient at zero angle of attack	ND
C_{MHA}	Horizontal stabilizer pitching moment coefficient variation with angle of attack	1/deg
D_{Ke}	Elevator effectiveness reduction factor for large elevator angles	ND
C_{LH}	Horizontal stabilizer lift coefficient, $= f(\alpha_H, \delta_e, M_N)$	ND
C_{DH}	Horizontal stabilizer drag coefficient, $= f(\alpha_H, M_N)$	ND
X_{Ke}	Elevator effectiveness factor, $= f(M_N)$	ND
η_H	Dynamic pressure ratio at the horizontal stabilizer, $= f(\alpha_F, \beta_m, V_T)$	ND
$K_{\beta HS}$	Sideslip factor on dynamic pressure ratio at the horizontal stabilizer, $= f(\beta_F)$	ND
PCPM	Mach number effect on the $(\partial\epsilon_{W/H}/\partial\alpha_W)$, $= f(M_N)$	ND

Outputs:

Symbol	Description	Units
α_H	Horizontal stabilizer angle of attack	deg
L_H	Aerodynamic lift on the horizontal stabilizer	lb
D_H	Aerodynamic drag on the horizontal stabilizer	lb
M_H'	Aerodynamic pitching moment on the horizontal stabilizer	ft-lb

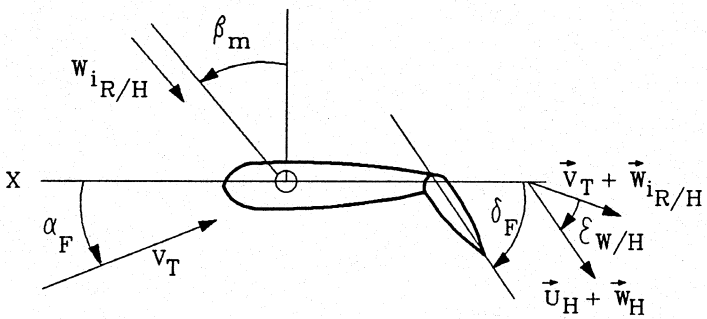

Wing Fuselage
Vector Diagram

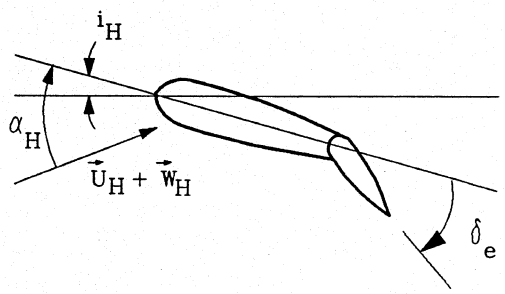

Horizontal Stabilizer
Vector Diagram

Note: Angles shown are positive values in mathematical model sign convention.

Figure A5-1. Sign Conventions and Notation for Horizontal Stabilizer Aerodynamics

EQUATIONS

SUBSYSTEM NO. 5--HORIZONTAL STABILIZER AERODYNAMICS

A. Geometric Distances From C.G. to Horizontal Stabilizer 25% Chord

$$l_{XH} = \left(SL_H - SL_{CG}\right)/12$$

$$l_{ZH} = \left(WL_H - WL_{CG}\right)/12$$

B. Velocities

$$U_H = U + U_i\,|^{B}_{R/H} - q\left(l_{ZH}\right)$$

$$V_H = V - r\left(l_{XH}\right) + p\left(l_{ZH}\right)$$

$$W_H = W + W_i\,|^{B}_{R/H} + q\left(l_{XH}\right)$$

Where if $\left|U_H\right| < 0.01$ ft/sec then $U_H = 0.01$ ft/sec

C. Total Velocity

$$V_{HT} = \left(U_H^2 + W_H^2\right)^{1/2}$$

D. Angle of Attack For Lift Equation

If $M_N < 0.2$

$$\alpha_{HL} = i_H + \left[\tan^{-1}\left(\frac{W_H}{U_H}\right)(57.3)\right] - \epsilon_{W/H}$$

If $M_N \geq 0.2$

$$\alpha_{HL} = i_H + \left[\tan^{-1}\left(\frac{W_H}{U_H}\right)(57.3)\right] - \epsilon_{W/H} + K_e \tau_e \delta_e$$

D. Angle of Attack for Lift Equation (Concluded)

where

$$\epsilon_{W/H} = f\left(\alpha_W, \beta_m, \delta_F, M_N\right)$$

$$X_{Ke} = f\left(M_N\right)$$

and if

$$\left|\delta_e\right| < 15 \quad \text{deg}$$

$$K_e = X_{Ke}$$

Otherwise, if

$$\left|\delta_e\right| > 15 \quad \text{deg}$$

$$K_e = X_{Ke} - \left[D_{Ke}\left(\frac{\left|\delta_e\right| - 15}{15}\right)\right]$$

E. Angle of Attack for Drag Equation

For all M_N

$$\alpha_{HD} = \alpha_{HL}\,|_{M_N > 0.2}$$

F. Sideslip Angle

$$\beta_H = \tan^{-1}\left[\frac{V_H}{\left(U_H^2 + W_H^2\right)^{1/2}}\right](57.3)$$

G. Dynamic Pressure Loss Function

$U \geq 0$ and $|\beta_H| < 90.0$

$$\eta_{HS} = 1.0 - (1.0 - \eta_H)(K_{\beta HS})$$

Otherwise

$$\eta_{HS} = 1.0$$

Where

$$\eta_H = f(\alpha_F, \beta_m, V_T)$$

$$K_{\beta HS} = f(\beta_F)$$

Note: At the present time, the η_H and β_{HS} function tables are the same ones used for the vertical stabilizer.

H. Dynamic Pressure at Horizontal Stabilizer

$$q_H = \frac{1}{2}\rho K_{HNU}\left[\left(U * \sqrt{\eta_{HS}} - q * l_{ZH}\right)^2 + \left(W * \sqrt{\eta_{HS}} + q * l_{XH}\right)^2\right]$$

I. Lift Coefficient Due to Vertical Acceleration and Wing/Body Damping

$$U_H = \max(U_H, 35)$$

$$C_{L_{\dot{W}}} = D_{WB}\left(\frac{\partial C_{LH}}{\partial \alpha_{HL}}\right)\left(\frac{\partial \epsilon_{W/H}}{\partial \alpha_W}\right)\left(\frac{PCPM|_{M_N}}{PCPM|_{M_N=0}}\right)\left(\frac{l_{XH}}{U_H^2}\right) \quad (57.3)$$

Where

$$PCPM = f(M_N)$$

SUBSYSTEM NO. 5--HORIZONTAL STABILIZER AERODYNAMICS

J. Total Lift of the Horizontal Stabilizer in Wind Axis

$$L_H = q_H S_H \left\{ C_{LH} + C_{L_{\dot{W}}} \dot{W} + C_{LH\beta}\left[\min\left(15, |\beta_H|\right)\right]\left(\cos\beta_m\right) \right\}$$

Where

$$C_{LH} = \left(\alpha_{HL}, M_N, \delta_e\right)$$

K. Drag of the Horizontal Stabilizer in Wind Axis

$$D_H = q_H S_H C_{DH}$$

Where

$$C_{DH} = f\left(\alpha_{HD}, M_N\right)$$

L. Pitching Moment of the Horizontal Stabilizor in Wind Axis

$$M_H' = q_H S_H c_H\left[C_{MHO} + C_{MHA}\left(\alpha_{HL}\right)\right]$$

M. Local Angle of Attack (For Resolving Forces)

$$\alpha_H = \tan^{-1}\left(\frac{W_H}{U_H}\right)(57.3) - \epsilon_{W/H}$$

6	VERTICAL STABILIZER AERODYNAMICS

Inputs: Variables		Outputs:	
From Subsystem	Symbol	To Subsystem	Symbol
12	U	10a	$\beta_V(i)$
	V		$Y'_V(i)$
	W		$D_V(i)$
	$\dot{U}$	14	$l_{XV}(i)$
	$\dot{V}$		$l_{YV}(i)$
	$\dot{W}$		$l_{ZV}(i)$
	α_F		
	β_F		
	V_T		
5	α_H		
11	p		
	q		
	r		
2	$U_i \Big\vert^{B}_{R/V}$		
	$W_i \Big\vert^{B}_{R/V}$		
15	ρ		
	M_N		
8a	β_m		
	δ_r		
	δ_F		
9	SL_{CG}		
	WL_{CG}		

(Concluded on next page)

6	VERTICAL STABILIZER AERODYNAMICS (Concluded)

Inputs: Constants, Coefficients, and Data Tables

Constants: NVSTAB, $SL_V(i)$, $WL_V(i)$, $BL_V(i)$, $S_V(i)$, $i_V(i)$, BL_{CG}, SL_{SP}, BL_{SP}, l_m, R, b_W

Coefficients: $\tau_r, \partial\sigma/\partial\hat{p}, \partial\sigma/\partial\hat{r}, K_{VNU}, a_V, D_{Kr}$

Data Tables:		
	$C_{YV} = f(\beta_V, \delta_r, M_N)$	Tables 6-I, 6-II
	$C_{DV} = f(\beta_V, \delta_r, M_N)$	Table 6-III
	$(1 - \partial\sigma/\partial\beta_F) = f(\beta_F, \beta_m, \delta_F, \alpha_F)$	Tables 6-IV, 6-V 6-VI, 6-VII
	$K_{\beta R} = f(\beta_F, V_T)$	Table 6-VIII
	$X_{Kr} = f(M_N)$	Table 5-IV
	$\eta_V = f(\alpha_F, \beta_m, V_T)$	Table 5-V
	$K_{\beta VS} = f(\beta_F)$	Table 5-VI

SUBSYSTEM NO. 6: VERTICAL STABILIZER AERODYNAMICS

Inputs: Variables

Symbol	Description	Units
U	x-velocity (longitudinal) of rotorcraft c.g. in body axis with respect to the air	ft/sec
V	y-velocity (lateral) of the rotorcraft c.g. in body axis with respect to the air	ft/sec
W	z-velocity (vertical) of the rotorcraft c.g. in body axis with respect to the air	ft/sec
$\dot{U}$	Rate of change of x-velocity (longitudinal) of the rotorcraft c.g. in body axis with respect to the air	ft/sec^2
$\dot{V}$	Rate of change of y-velocity (lateral) of the rotorcraft c.g. in body axis with respect to the air	ft/sec^2
$\dot{W}$	Rate of change of z-velocity (vertical) of the rotorcraft c.g. in body axis with respect to the air	ft/sec^2
α_F	Fuselage angle of attack	deg
β_F	Fuselage sideslip angle	deg
V_T	Total linear velocity of the rotorcraft c.g. with respect to the air	ft/sec
α_H	Horizontal stabilizer angle of attack	deg
p	Body axis roll rate	rad/sec
q	Body axis pitch rate	rad/sec

Inputs: Variables (Concluded)

Symbol	Description	Units
r	Body axis yaw rate	rad/sec
$U_i \Big\vert^{B}_{R/V}$	Induced x-velocity at the vertical fin in body axis due to the rotor	ft/sec
$W_i \Big\vert^{B}_{R/V}$	Induced z-velocity at the vertical fin in body axis due to the rotor	ft/sec
ρ	Air density	slug/ft^3
M_N	Mach number	ND
β_m	Mast conversion angle (+ fwd, 0 deg = vertical or helicopter, 90 deg = horizontal or airplane)	deg
δ_r	Rudder mean deflection angle (+ trailing edge right)	deg
δ_F	Flap position	deg
SL_{CG}	Station line of c.g.	inch
WL_{CG}	Water line of c.g.	inch

Inputs: Constants, Coefficients, and Data Tables

NVSTAB	Number of vertical stabilizers	ND
SL_V	Station line of the vertical stabilizer center of pressure	inch

Inputs: Constants, Coefficients, and Data Tables (Continued)

Symbol	Description	Units
WL_V	Water line of the vertical stabilizer center of pressure	inch
BL_V	Butt line of the vertical stabilizer center of pressure	inch
S_V	Vertical stabilizer total area	ft^2
i_V	Incidence of vertical stabilizer	deg
BL_{CG}	Butt line of c.g.	inch
SL_{SP}	Station line of engine nacelle shaft pivot point	inch
BL_{SP}	Butt line of engine nacelle shaft pivot point	inch
l_m	Mast length	ft
R	Rotor radius	ft
b_W	Wing span	ft
τ_r	Rudder effectiveness $(\partial\beta_V/\partial\delta_r)$	ND
$\partial\sigma/\partial\hat{p}$	Roll rate correction coefficient to fin sideslip angle	ND
$\partial\sigma/\partial\hat{r}$	Yaw rate correction coefficient to fin sideslip angle	ND
K_{VNU}	Vertical stabilizer dynamic pressure loss multiplier	ND

Inputs: Constants, Coefficients, and Data Tables (Concluded)

Symbol	Description	Units
a_V	Lift curve slope of the vertical tail	1/rad
D_{Kr}	Rudder effectiveness reduction factor for large rudder angles	ND
C_{YV}	Vertical fin side force (lift) coefficient, $= f(\beta_V, \delta_r, M_N)$	ND
C_{DV}	Vertical fin drag coefficient, $= f(\beta_V, \delta_r, M_N)$	ND
$\left(1 - \frac{\partial \sigma}{\partial \beta_F}\right)$	Vertical stabilizer sidewash factor, $= f(\beta_F, \beta_m, \delta_F, \alpha_F)$	ND
$K_{\beta R}$	Rotor sidewash factor on dynamic pressure, $= f(\beta_F, V_T)$	ND
X_{Kr}	Rudder effectiveness factor, $= f(M_N)$	ND
η_V	Dynamic pressure ratio at the vertical stabilizer, $= f(\alpha_F, \beta_m, V_T)$	ND
$K_{\beta VS}$	Sideslip factor on dynamic pressure ratio at the vertical stabilizer, $= f(\beta_F)$	ND

Outputs:

Symbol	Description	Units
β_V	Vertical stabilizer sideslip angle	deg
Y'_v	Aerodynamic side force (lift) on the vertical stabilizer (wind axis)	lb
D_V	Aerodynamic drag on the vertical stabilizer (wind axis)	lb
l_{XV}	Station line distance from the c.g. to the vertical stabilizer center of pressure	ft
l_{YV}	Butt line distance from the c.g. to the vertical stabilizer center of pressure	ft
l_{ZV}	Water line distance from the c.g. to the vertical stabilizer center of pressure	ft

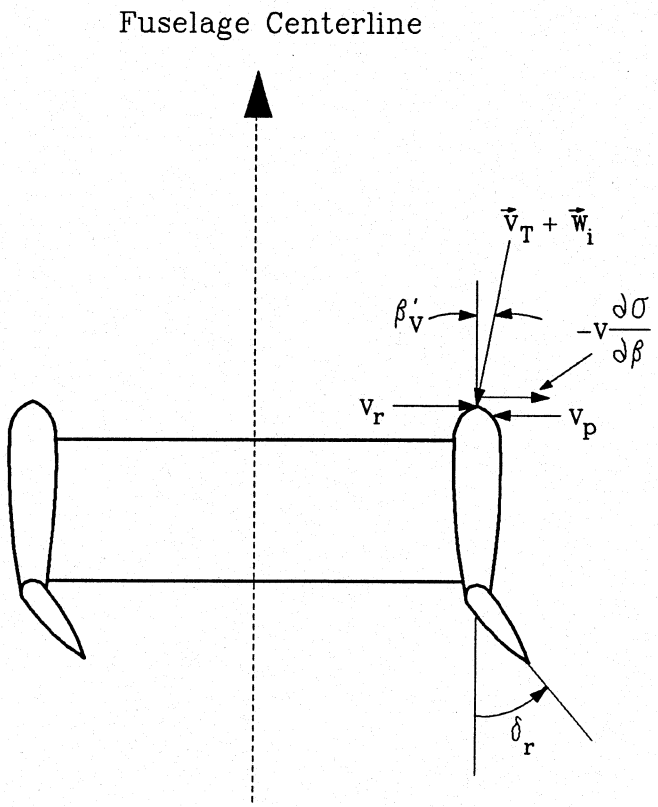

Left Hand Side Right Hand Side

Vertical Stabilizer
Vector Diagram
(top view)

Note: Angles shown are positive values in mathematical model sign convention.

Figure A6-1. Sign Conventions and Notation for Vertical Stabilizer Aerodynamics

EQUATIONS
SUBSYSTEM NO. 6--VERTICAL STABILIZER AERODYNAMICS

The maximum number of vertical stabilizers is four. The aerodynamics of each fin are computed and transferred separately to the equations that sum the fuselage forces and moments.

A. Geometric Distances from c.g. to Vertical Stabilizer(s) Aerodynamic Center

i = 1, NVSTAB

$$l_{XV}(i) = \left[SL_V(i) - SL_{CG}\right]/12$$

$$l_{YV}(i) = \left[BL_V(i) - BL_{CG}\right]/12$$

$$l_{ZV}(i) = \left[WL_V(i) - WL_{CG}\right]/12$$

B. Definition of Interference Velocities Induced at the Fin

1. Definition of Rotor Wake Boundaries on Each Fin

a. Left Rotor

$$BL_{RTIP}(1) = \left(-BL_{SP} - R\right)/12$$

$$BL_{RTIP}(2) = \left(-BL_{SP} + R\right)/12$$

b. Right Rotor

$$BL_{RTIP}(3) = \left(BL_{SP} - R\right)/12$$

$$BL_{RTIP}(4) = \left(BL_{SP} + R\right)/12$$

1. Definition of Rotor Wake Boundaries on Each Fin (Concluded)

$$l_{YRV}(i,j) = \left[BL_{TIP}(j) - BL_V(i)\right]$$

$$l_{XRV}(i) = SL_V(i) - SL_{SP} + (12)(l_m)(\sin\beta_m)$$

$$\gamma_{RV}(i,j) = \tan^{-1}\left(\frac{l_{YRV}(i,j)}{l_{XRV}(j)}\right)(57.3)$$

for i = 1, NVSTAB
    j = 1, 4

2. Definition of Rotor Induced Velocity (Body Axis) on Each Fin

$$\left.\begin{matrix} U_i|^B_{R/V} \\ \\ W_i|^B_{R/V} \end{matrix}\right\} = 0 \quad \text{when} \quad \left\{\begin{matrix} & \beta_F < \gamma_{RV}(1,j) \\ \gamma_{RV}(2,j) < & \beta_F \le \gamma_{RV}(3,j) \\ & \beta_F > \gamma_{RV}(4,j) \end{matrix}\right.$$

C. <u>Velocity on Each Fin</u>

$$U_V(i) = U + U_i|^B_{R/V} - q\left[l_{ZV}(i)\right] - r\left[l_{YV}(i)\right]$$

$$V_V(i) = V - r\left[l_{XV}(i)\right] + p\left[l_{ZV}(i)\right]$$

$$W_V(i) = W + W_i|^B_{R/V} + q\left[l_{XV}(i)\right] + p\left[l_{YV}(i)\right]$$

$$V_{VT}(i) = \left[U_V^2(i) + V_V^2(i) + W_V^2(i)\right]^{1/2}$$

D. Angle of Attack for Fin Lift Calculations at Zero Rudder

If

$|U_V(i)| < 35$ ft/sec, then $U_V(i) = (35\,\text{ft/sec})\,\text{sign}[U_V(i)]$

If in a maneuver,

$$\dot{\beta} = \left[\frac{(U^2+W^2)^{1/2}}{(U^2+V^2+W^2)^{1/2}}\right]\left[\left(\dot{V} - \frac{V\left(U\dot{U}+W\dot{W}\right)}{(U^2+W^2)}\right)\right]$$

Otherwise

$$\dot{\beta} = 0$$

$$\beta_V(i) = -i_V(i) + \left\{\tan^{-1}\left[\frac{V_V(i)}{[U_V(i)^2+W_V(i)^2]^{1/2}}\right]\right.$$

$$\left. -\frac{0.5b_W}{U_V(i)}\left(\frac{\partial\sigma}{\partial\hat{p}}p + \frac{\partial\sigma}{\partial\hat{r}}r\right) + \frac{l_{XV}(i)}{U_V(i)}\left(\frac{\partial\sigma}{\partial\beta_F}\right)\dot{\beta}\right\} \quad (57.3)$$

Where

$$\left(1 - \frac{\partial\sigma}{\partial\beta_F}\right) = f(\beta_F, \beta_m, \delta_F, \alpha_F)$$

NOTE: To obtain term $(\partial\sigma/\partial\beta_F)$, the values in the tables in Appendix B must be subtracted from "1.0" in a computer program.

E. Angle of Attack for Drag Calculations

$$\beta_{VD}(i) = \beta_V(i) + K_r\tau_r\delta_r$$

E. Angle of Attack for Drag Calculations (Concluded)

Where

$$X_{Kr} = f(M_N)$$

And if

$$|\delta_r| < 15\,\text{deg}$$

$$K_r = X_{Kr}$$

$$|\delta_r| > 15\,\text{deg}$$

$$K_r = X_{Kr} - \left[D_{Kr}\left(\frac{|\delta_r| - 15}{15} \right) \right]$$

F. Dynamic Pressure Loss Function

For $U \geq 0$ and $|\beta_V| < 90.0$

$$\eta_{VS} = 1.0 - (1.0 - \eta_{VS})(K_{\beta VS})$$

Otherwise

$$\eta_{VS} = 1.0$$

Where

$$\eta_V = f(\alpha_F, \beta_m, V_T)$$

$$K_{\beta VS} = f(\beta_F)$$

NOTE: At present, the η_{VS} and $K_{\beta VS}$ function tables are the same ones used for the horizontal stabilizer.

G. Dynamic Pressure at Each Fin Position

$$q_V = \frac{1}{2}\rho K_{VNU}[(U*\sqrt{\eta_{VS}} - q*l_{ZV} - R*l_{YV})^2$$

$$+(V*\sqrt{\eta_{VS}} + p*l_{ZV} - R*l_{XV})^2$$

$$+(W*\sqrt{\eta_{VS}} + q*l_{XV} + p*l_{YV})^2]$$

H. Fin Lift Coefficient

For $M_N \leq 0.2$

$$C_{YV}(i) = (C_{YV}|_{\delta_r=0})\left[K_{\beta R}\left(1 - \frac{\partial\sigma}{\partial\beta_F}\right)\right] + (C_{YV}|_{\delta_r} - C_{YV}|_{\delta_r=0})$$

For $M_N > 0.2$

$$C_{YV}(i) = (C_{YV}|_{\delta_r=0})\left[K_{\beta R}\left(1 - \frac{\partial\sigma}{\partial\beta_F}\right)\right] + a_V(i)K_r\tau_r\delta_r$$

Where

$$C_{YV} = f(\beta_V, \delta_r, M_N)$$

$$K_{\beta R} = f(\beta_F, V_T)$$

$$\left(1 - \frac{\partial\sigma}{\partial\beta_F}\right) = f(\beta_F, \beta_m, \delta_F, \alpha_F)$$

$$X_{Kr} = f(M_N)$$

H. Fin Lift Coefficient (Concluded)

And if

$$|\delta_r| < 15\text{deg}$$

$$K_r = X_{Kr}$$

$$|\delta_r| > 15\text{deg}$$

$$K_r = X_{Kr} - \left[D_{Kr} \left(\frac{|\delta_r| - 15}{15} \right) \right]$$

I. Fin Drag Coefficient

$$C_{DV}(i) = (C_{DV}|_{\delta_r}) \left[K_{\beta R} \left(1 - \frac{\partial \sigma}{\partial \beta_F} \right) \right]$$

Where

$$C_{DV} = f(\beta_{VD}(i), M_N)$$

$$K_{\beta R} = f(\beta_F, V_T)$$

$$\left(1 - \frac{\partial \sigma}{\partial \beta_F} \right) = f(\beta_F, \beta_m, \delta_F, \alpha_F)$$

J. Fin Lift and Drag in Wind Axis

$$Y'_V(i) = -[C_{YV}(i)][q_V(i)][S_V(i)]$$

$$D_V(i) = -[C_{DV}(i)][q_V(i)][S_V(i)]$$

7A	LANDING GEAR* (Present Sigma 8 Model)

Inputs: Variables		Outputs:	
From Subsystem	Symbol	To Subsystem	Symbol
3	q_F	10a	D_{MG}
8a	L_{LG}		D_{NG}
10f	h_{CG} $\dot{h}_{CG}$	13	$(\Delta X, \Delta Y, \Delta Z)_{LG}$
12	V_T U	14	$(\Delta l, \Delta M, \Delta N)_{LG}$
8d	δ_{B_n} δ_{NW}	16	LG_{TLT}
10c	θ ϕ ψ $\dot{\psi}$		
9	SL_{CG} WL_{CG}		

Inputs: Constants, Coefficients, and Data Tables

Constants: (Where n = 1, 2, or 3 depending on which wheel is of interest)

BL_{CG}, SL_{Gn}, WL_{Gn}, BL_{Gn}, $\delta_{B_{n_{MIN}}}$, K_{B_W}, A_{MAX}, g, T_{DN}, T_{UP}

Coefficients: DPOD, G_{A_n}, G_{B_n}, G_{C_n}, μ_{S_n}, μ_{G_n}, μ_{RF}

Data Tables: (Aerodynamic)

VAX Model (Rev. A)

$D_{o_{MG}} = f(LG_{PCT})$ Table 7A-I

$D_{o_{NG}} = f(LG_{PCT})$ Table 7A-I

*Reference 24

(Concluded on next page)

7A	**LANDING GEAR* (Present Sigma 8 Model) (Concluded)**

Inputs: Constants, Coefficients, and Data Tables (Concluded)

Data Tables: (Aerodynamic)

Sigma 8 Model	$D_{o_{MGU}} = f(t)$	Table 7A-II
	$D_{o_{MGD}} = f(t)$	Table 7A-II
	$D_{o_{NGU}} = f(t)$	Table 7A-III
	$D_{o_{NGD}} = f(t)$	Table 7A-III

SUBSYSTEM NO. 7A: LANDING GEAR

Inputs: Variables

Symbol	Description	Units
q_F	Fuselage dynamic pressure	lb/ft^2
L_{LG}	Landing gear position indicator	ND
h_{CG}	Altitude of aircraft	ft
$\dot{h}_{CG}$	Climb rate	ft/sec
V_T	Total linear velocity of the aircraft c.g. with respect to the air	ft/sec
U	x-velocity (longitudinal) of the aircraft c.g. in body axis with respect to the air	ft/sec
δ_{B_n}	Brake pedal deflection	deg
δ_{NW}	Nose wheel steering angle	rad
θ	Euler pitch angle	rad
ϕ	Euler roll angle	rad
ψ	Euler yaw angle	rad
$\dot{\psi}$	Rate of change of Euler yaw angle	rad/sec
SL_{CG}	Station line of c.g.	in
WL_{CG}	Water line of c.g.	in

Inputs: Constants, Coefficients, and Data Tables

BL_{CG}	Butt line of c.g.	in
SL_{Gn}	Station line of landing gear [where n = 1 (nose), 2 (right), 3 (left) landing gear]	in

Inputs: Constants, Coefficients, and Data Tables (Continued)

Symbol	Description	Units
WL_{Gn}	Water line of landing gear [where n = 1 (nose), 2 (right), 3 (left) landing gear]	in
BL_{Gn}	Butt line of landing gear [where n = 1 (nose), 2 (right), 3 (left) landing gear]	in
$\delta_{B_{n_{MIN}}}$	Brake threshold deflection	deg
K_{B_n}	Brake sensitivity	ft/sec^2-deg
A_{MAX}	Maximum braking deceleration	ft/sec^2
g	Gravitational constant	ft/sec^2
T_{DN}	Time for landing gear to extend (VAX version)	sec
T_{UP}	Time for landing gear to retract (VAX version)	sec
DPOD	Fuselage landing gear pod drag	ft^2
G_{A_n}	Landing gear linear damping term	lb-sec/ft
G_{B_n}	Landing gear nonlinear damping term	$lb\text{-}sec/ft^3$
G_{C_n}	Landing gear nonlinear stiffness term	lb/ft^4
μ_{S_n}	Landing gear side force slope	ND
μ_{G_n}	Landing gear maximum side force coefficient	ND
μ_{RF}	Coefficient of rolling friction	ND
$D_{o_{MG}}$	Drag of the main landing gear (VAX version), = $f(LG_{PCT})$	ft^2
$D_{o_{NG}}$	Drag of the nose landing gear (VAX version), = $f(LG_{PCT})$	ft^2

SUBSYSTEM NO. 7A: LANDING GEAR (Concluded)

Inputs: Constants, Coefficients, and Data Tables (Concluded)

Symbol	Description	Units
$D_{o_{MGU}}$	Drag of the main landing gear during retraction (Sigma 8 version), = f(t)	ft^2
$D_{o_{NGU}}$	Drag of the nose landing gear during retraction (Sigma 8 version), = f(t)	ft^2
$D_{o_{MGD}}$	Drag of the main landing gear during extension (Sigma 8 version), = f(t)	ft^2
$D_{o_{NGD}}$	Drag of the nose landing gear during extension (Sigma 8 version), = f(t)	ft^2

Outputs:

D_{MG}	Aerodynamic drag on the main landing gear	lb
D_{NG}	Aerodynamic drag on the nose landing gear	lb
$(\Delta X, \Delta Y, \Delta Z)_{LG}$	Total landing gear forces in body axis	lb
$(\Delta l, \Delta M, \Delta N)_{LG}$	Total landing gear rolling, pitching, and yawing moments in body axis	ft-lb
LG_{TLT}	Landing gear touchdown light	ND

EQUATIONS

SUBSYSTEM NO. 7A—LANDING GEAR
(Present Sigma 8 Model)

A. LANDING GEAR LOCATIONS

$$X_n = SL_{CG} - SL_{Gn}$$

$$Y_n = BL_{CG} - BL_{Gn}$$

$$Z_n = WL_{CG} - WL_{Gn}$$

Buttlines positive to right. Waterlines defined with zero loads in landing gears.

Where: n = 1, nose gear
= 2, right gear
= 3, left gear

B. AERODYNAMIC EQUATIONS

1. VAX Version

$$D_{MG} = q_F \left(D_{o_{MG}} + DPOD\right)$$

$$D_{NG} = q_F \left(D_{o_{NG}}\right)$$

where

$$D_{o_{MG}} = f(LG_{PCT})$$

$$D_{o_{NG}} = f(LG_{PCT})$$

and the percentage main and nose gear extension are a function of the present computer frame time (t), computer cycle time (Δt), and total time for the landing gear to extend (T_{DN}) or retract (T_{UP}). Limits are 0% (retracted) and 100% (extended).

a. Gear Extend (limit 100%):

$$LG_{PCT} = \left(LG_{PCT}\right)_{t-\Delta t} + \left[\frac{(100.0)(\Delta t)}{\left(T_{DN}\right)}\right]$$

b. Gear Retract (limit 0%):

$$LG_{PCT} = \left(LG_{PCT}\right)_{t-\Delta t} - \left[\frac{(100.0)(\Delta t)}{\left(T_{UP}\right)}\right]$$

2. Sigma 8 Version

a. Gear Extension

$$D_{MG} = q_F \left[D_{o_{MGD}}(t) + DPOD\right]$$

$$D_{NG} = q_F \, D_{o_{NGD}}(t)$$

b. Gear Retraction

$$D_{MG} = q_F \left[D_{o_{MGU}}(t) + DPOD\right]$$

$$D_{NG} = q_F \, D_{o_{NGU}}(t)$$

C. GROUND DYNAMIC EQUATIONS

1. Gear Height

$$h_{G_n} = \frac{h_{CG} + \sin\theta \, X_n - \sin\phi \cos\theta \, Y_n - \cos\phi \cos\theta \, Z_n}{\cos\phi \cos\theta}$$

if $h_{G_n} > 0 \quad F_{N_{G_n}} = F_{S_n} = F_{D_n} = 0$

2. Gear Normal Force

$$F_{N_{G_n}} = \begin{cases} F_{N_n} \text{ for } F_{N_n} \leq 0 \\ 0 \text{ for } F_{N_n} > 0 \end{cases}$$

$$F_{N_n} = \left[G_{A_n} + G_{B_n}\left(\Delta S_{t_n}\right)^2\right]\left(\Delta \dot{S}_{t_n}\right) - G_{C_n}\left(\Delta S_{t_n}\right)^4$$

Where: F_{N_n} = gear normal force (lbs), positive sign down

ΔS_{t_n} = oleo stroke (ft), negative for compression

$\Delta \dot{S}_{t_n}$ = oleo stroke rate (ft/sec), negative for compression

SUBSYSTEM NO. 7A—LANDING GEAR
(Present Sigma 8 Model)

3. Gear Side Force

$$F_{S_n} = \begin{cases} S_n & \text{for } |S_n| < S_{MAX_n} \\ S_{MAX_n} \text{ sign } (S_n) & \text{for } |S_n| > S_{MAX_n} \end{cases}$$

$$S_n = -57.3\ \mu_{S_n}\ F_{N_{G_n}}\ \Delta G_n$$

$$S_{MAX_n} = -\mu_{G_n} F_{N_{G_n}}$$

$$\Delta G_n = \begin{cases} \delta_{NW} - \left[\dfrac{\dot{\psi} X_n + \dot{Y}_{REL}}{|V_T|} \right] & \text{for } n = 1 \\ - \left[\dfrac{\dot{\psi} X_n + \dot{Y}_{REL}}{|V_T|} \right] & \text{for } n = 2,3 \end{cases}$$

Where: F_{S_n} = gear side force in the plane of the landing surface (lbs), positive to the right

δ_{NW} = nose wheel steering angle (rad), positive turning right

$\dot{\psi}$ = aircraft Euler yaw rate (rad/sec)

V_T = Ground speed component of the aircraft velocity relative to the landing surface (ft/sec)

$\dot{Y}_{REL} = V_T \sin\left(\gamma_H - \psi\right)$ (ft/sec)

4. Gear Drag Force

$$F_{D_n} = \begin{cases} -\mu_{RF}\ F_{N_n} \text{ sign } (U) + F_{S_n} \text{ sign } (\delta_{NW}) & \text{for } n = 1 \\ -\mu_{RF}\ F_{N_n} \text{ sign } (U) + F_{B_n} & \text{for } n = 2,3 \end{cases}$$

Where: F_{D_n} = Gear drag force in the plane of the landing surface due to friction (lbs), positive aft

F_{B_n} = Brake force (lbs),

$$F_{B_n} = \begin{cases} K_{B_n} \delta_{B_n} F_{N_n}/g & \text{for } F_{B_n} < F_{B_{n_{MAX}}} \\ F_{B_{n_{MAX}}} & \text{for } F_{B_n} > F_{B_{n_{MAX}}} \end{cases}$$

$$F_{B_{n_{MAX}}} = A_{MAX} F_{N_n}/g$$

$$\delta_{B_n} = \begin{cases} 0 & \text{for } \delta_{B_n} < \delta_{B_{n_{MIN}}} \\ \delta_{B_n} & \text{for } \delta_{B_n} \geq \delta_{B_{n_{MIN}}} \end{cases}$$

Where: δ_{B_n} = brake pedal deflection (deg)

5. Gear Force and Moment Summation

$$F_{G_{X_n}} = F_{D_n} - F_{N_{G_n}} \theta$$

$$F_{G_{Y_n}} = F_{S_n} + F_{N_{G_n}} \phi$$

$$F_{G_{Z_n}} = F_{D_n} \sin \theta - F_{S_n} \sin \phi + F_{N_{G_n}}$$

$$\ell_{G_n} = +F_{N_{G_n}} Y_n - F_{G_{Y_n}} (Z_n + h_{G_n})$$

$$M_{G_n} = -F_{N_{G_n}} X_n + F_{G_{X_n}} (Z_n + h_{G_n})$$

$$N_{G_n} = -F_{G_{X_n}} Y_n + F_{G_{Y_n}} X_n$$

EQUATIONS (CONCLUDED)

SUBSYSTEM NO. 7A—LANDING GEAR
(Present Sigma 8 Model)

$$\Delta X_{LG} = \sum_{1}^{3} F_{G_{X_n}}$$

$$\Delta Y_{LG} = \sum_{1}^{3} F_{G_{Y_n}}$$

$$\Delta Z_{LG} = \sum_{1}^{3} F_{G_{Z_n}}$$

$$\Delta \ell_{LG} = \sum_{1}^{3} \ell_{G_n}$$

$$\Delta M_{LG} = \sum_{1}^{3} M_{G_n}$$

$$\Delta N_{LG} = \sum_{1}^{3} N_{G_n}$$

ADDITIONAL NOTES REGARDING THE LANDING GEAR MODEL
(Provided by CSC)

A. Computation of Landing Gear Kinematics

Gear location (body frame, origin at c.g.) is given by X_G, Y_G, and Z_G

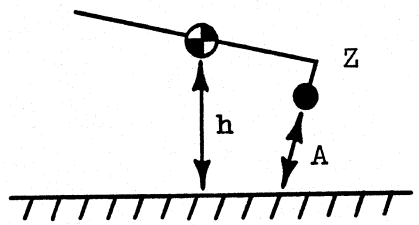

Compute A = distance from gear to ground <u>above extension of gear strut</u>

Contribution due to h:

$$A_n = \frac{h}{\cos\theta \cos\phi} \text{ since h is a projection of } A_n$$

Contribution due to roll and pitch of airplane:

Body axis location relative to c.g. = X_G, Y_G, Z_G = $\overline{V}_G$

Location in inertial frame = $T_{L2B}^{-1}\,\overline{V}_G$

$$= \begin{bmatrix} \text{———} \\ \text{———} \\ -\sin\theta & \sin\phi\cos\theta & \cos\phi\cos\theta \end{bmatrix} \begin{bmatrix} X_G \\ Y_G \\ Z_G \end{bmatrix}$$

So the Z-component in the inertial frame is

$$h_{\theta\phi} = -\sin\theta\, X_G + \sin\phi\cos\theta\, Y_G + \cos\phi\cos\theta\, Z_G$$

This is the projection of $A_{\theta\phi}$ into the Z inertial axis

So $A_{\theta\phi} = h_{\theta\phi}/\cos\theta\cos\phi$

[Since Z is positive down]

The total distance $A = A_h - A_{\theta\psi} = (1/\cos\theta\cos\psi)$

$(h + \sin\theta X_G - \sin\phi\cos\theta Y_G - \cos\theta\cos\psi Z_G)$

B. Distance from gear to ground along extension of gear strut

$$A_W = \frac{1}{\cos\theta\cos\psi}\left(h + \sin\theta X_G - \sin\phi\cos\theta Y_G - \cos\theta\cos\phi Z_G\right)$$

$$A_W = \text{"Stroke"} = \frac{1}{T_{33}}\left(h - T_{13}X_G - T_{23}Y_G - T_{33}Z_G\right)$$

C. Computation of Landing Gear Stroke

Define an inertial coordinate system having its origin at the aircraft c.g. Gear locations are given as X_G, Y_G, and Z_G in the body frame. The inertial position of the gear is given by

$$\begin{bmatrix} G_X \\ G_Y \\ G_Z \end{bmatrix} = \begin{bmatrix} & T^T_{L2B} & \\ \underbrace{T_{13} \quad T_{23} \quad T_{33}}_{\text{Basic}} \end{bmatrix} \begin{bmatrix} X_G \\ Y_G \\ Z_G \end{bmatrix} = \begin{bmatrix} G_X \\ G_Y \\ T_{13}X_G + T_{23}Y_G + T_{33}Z_G \end{bmatrix}$$

$G_Z = -\sin\theta X_G + \sin\phi\cos\theta Y_G + \cos\phi\cos\theta Z_G$ (Z measured positive down)

Relative to the ground, the Z location of the gear is

$$Z_{G_g} = -h + G_Z = -h - \sin\theta\, X_G + \sin\phi \cos\theta\, Y_G + \cos\phi \cos\theta\, Z_G$$

Measured positive up

$$H_{G_g} = -Z_{G_g} = h + \sin\theta\, X_G - \sin\phi \cos\theta\, Y_G - \cos\phi \cos\theta\, Z_G$$

Divide by $\cos\phi \cos\theta$ to put into strut axis

$$A_g = \frac{h}{\cos\phi \cos\theta} + \frac{\sin\theta}{\cos\phi \cos\theta} X_G - \frac{\sin\phi \cos\theta}{\cos\phi \cos\theta} Y_G - Z_G$$

D. Calculation of Landing Gear Stroke Rate

In inertial frame:

$$\dot{Z}_{GEAR} = \dot{Z}_{cg} + \underbrace{[\,T_{B2I}\,]}_{\text{Body to Inertial}}\ \underbrace{[\Omega]}_{\text{P, Q, R}} \times \underbrace{\begin{bmatrix} X_G \\ Y_G \\ Z_G + A_W \end{bmatrix}}_{Z'_g}$$

Gear Position to c.g.

Stroke

$$[\Omega] \times \begin{bmatrix} X_G \\ Y_G \\ Z'_G \end{bmatrix} = \begin{bmatrix} qZ'_g - rY_G \\ rX_G - pZ'_g \\ pY_G - qX_G \end{bmatrix}$$

$$[\ T_{B2I}\ ][\Omega] \times \begin{bmatrix} \\ \\ \\ \end{bmatrix} = \begin{bmatrix} \text{———} \\ \text{———} \\ T_{13} \quad T_{23} \quad T_{33} \end{bmatrix} \begin{bmatrix} qZ_G' - rY_G \\ rX_G - pZ_G' \\ pY_G - qX_G \end{bmatrix}$$

$$= X_G\,(T_{23}r - T_{33}q) + Y_G\,(T_{33}p - T_{13}r) + Z_g'\,(T_{13}q - T_{23}p)$$

Which is positive down, which causes increase in gear stroke as does $\dot{h}$

In aircraft body frame, stroke rate $\dot{A}_W$

$$\dot{A}_W = \frac{1}{T_{33}}\,[\dot{h} + X_G\,(T_{33}q - T_{23}r) + Y_G(T_{13}r - T_{33}p)$$

$$+ Z_g'\,(T_{23}p - T_{13}q)]$$

7B	LANDING GEAR (Unused Bell Model)

Inputs: Variables		Outputs:	
From Subsystem	Symbol	To Subsystem	Symbol
3	q_F	10a	D_{MG}
8a	L_{LG}		D_{NG}
10f	h_{CG} $\dot{h}_{CG}$	13	$(\Delta X, \Delta Y, \Delta Z)_{LG}$
		14	$(\Delta l, \Delta M, \Delta N)_{LG}$
12	V_T U	16	LG_{TLT}
10c	θ ϕ ψ		
9	SL_{CG} WL_{CG}		

Inputs: Constants, Coefficients, and Data Tables

Constants: (Where n = 1, 2, or 3 depending on which wheel is of interest)

BL_{CG}, SL_{Gn}, WL_{Gn}, BL_{Gn}, Z_{TIRE_n}

Coefficients: G_{1_n}, G_{2_n}, G_{3_n}, G_{4_n}, μ_0, μ_1, μ_{s_n}, DPOD

Data Tables: (Aerodynamic)

$D_{o_{MGU}} = f(t)$	Table 7A-II
$D_{o_{MGD}} = f(t)$	Table 7A-II
$D_{o_{NGU}} = f(t)$	Table 7A-III
$D_{o_{NGD}} = f(t)$	Table 7A-III

SUBSYSTEM NO. 7B—LANDING GEAR

Inputs: Variables

Symbol	Description	Units
q_F	Fuselage dynamic pressure	lb/ft^2
L_{LG}	Landing gear position indicator	ND
h_{CG}	Altitude of aircraft	ft
$\dot{h}_{CG}$	Climb rate	ft/sec
V_T	Total linear velocity of the aircraft c.g. with respect to the air	ft/sec
U	x-velocity (longitudinal) of the aircraft c.g. in body axis with respect to the air	ft/sec
θ	Euler pitch angle	rad
ϕ	Euler roll angle	rad
ψ	Euler yaw angle	rad
SL_{CG}	Station line of c.g.	in
WL_{CG}	Water line of c.g.	in

Inputs: Constants, Coefficients, and Data Tables

BL_{CG}	Butt line of c.g.	in
SL_{Gn}	Station line of landing gear [where n = 1 (nose), 2 (right), 3 (left) landing gear]	in
WL_{Gn}	Water line of landing gear [where n = 1 (nose), 2 (right), 3 (left) landing gear]	in
BL_{Gn}	Butt line of landing gear [where n = 1 (nose), 2 (right), 3 (left) landing gear]	in

SUBSYSTEM NO. 7B—LANDING GEAR (Concluded)

Inputs: Constants, Coefficients, and Data Tables (Concluded)

Symbol	Description	Units
Z_{TIRE_n}	Maximum tire deflection	ft
$G_{1_n-4_n}$	Landing gear ground dynamic coefficients (gear oleo force)	ND
$(\mu_{o,1,s_n})$	Landing gear ground dynamic coefficients (gear rolling friction and side force)	ND
DPOD	Fuselage landing gear pod drag	ft^2
$D_{o_{MGU}}$	Drag of the main landing gear during retraction, = f(t)	ft^2
$D_{o_{NGU}}$	Drag of the nose landing gear during retraction, = f(t)	ft^2
$D_{o_{MGD}}$	Drag of the main landing gear during extension, = f(t)	ft^2
$D_{o_{NGD}}$	Drag of the nose landing gear during extension, = f(t)	ft^2

Outputs:

D_{MG}	Aerodynamic drag on the main landing gear	lb
D_{NG}	Aerodynamic drag on the nose landing gear	lb
$(\Delta X,\Delta Y,\Delta Z)_{LG}$	Total landing gear forces in body axis	lb
$(\Delta l,\Delta M,\Delta N)_{LG}$	Total landing gear rolling, pitching, and yawing moments in body axis	ft-lb
LG_{TLT}	Landing gear touchdown light	ND

Landing Gear Locations

$$X_n = SL_{CG} - SL_{Gn}$$

$$Y_n = BL_{CG} - BL_{Gn}$$

$$Z_n = WL_{CG} - WL_{Gn}$$

Buttlines positive to right. Waterlines defined with zero loads in landing gears.

Where; n =1, nose gear
=2, right gear
=3, left gear

Aerodynamic Equations

A. Gear Extension

$$D_{MG} = q_F\left(D_{o_{MGD}}(t) + DPOD\right)$$

$$D_{NG} = q_F\, D_{o_{NGD}}(t)$$

II

B. Gear Retraction

$$D_{MG} = q_F\left(D_{o_{MGU}}(t) + DPOD\right)$$

$$D_{NG} = q_F\, D_{o_{NGU}}(t)$$

II

Ground Dynamic Equations

A. Gear Height

$$h_{G_n} = \frac{h_{CG} + \sin\theta\, X_n - \sin\phi\cos\theta\, Y_n - \cos\phi\cos\theta\, Z_n}{\cos\phi\cos\theta}$$

if $h_{G_n} > 0$ $\qquad F_{G_{X_n}} = F_{G_{Y_n}} = F_{G_{Z_n}} = 0$

B. Gear Oleo Force

$$F_{G_{o_n}} = F_{G_{n\ STATIC}} + F_{G_{n\ DYNAMIC}}$$

$$F_{G_{n\ STATIC}} = F_{1_{n\ STAT}} + F_{2_{n\ STAT}} + F_{3_{n\ STAT}}$$

B. Gear Oleo Force (Contd)

$$F_{G_{n\ DYNAMIC}} = F_{1_{n\ DYN}} + F_{2_{n\ DYN}}$$

$$F_{1_{n\ STAT}} = 0 \qquad IGSTOL = 1.0$$

$$F_{2_{n\ STAT}} = G_{1_n} \Big/ (G_{2_n} - Z_n') \qquad Z' < Z\ switch$$

$$Z\ switch = 20.$$

$$F_{3_{n\ STAT}} = G_{3_n} \Big/ (G_{4_n} - Z_n') \qquad Z' > Z\ switch$$

$$F_{1_{n\ DYN}} = \left[\frac{.5\ m\ Z_n\ \dot{Z}_n\ |\dot{Z}_n|}{Z_{TIRE_n}(G_{2_n} - Z_{TIRE_n})} \right] C_{R_n}$$

$$F_{2_{n\ DYN}} = \left[\frac{.5\ m\ \dot{Z}_n\ |\dot{Z}_n|}{(G_{2_n} - Z_{TIRE_n})} \right] C_{R_n}$$

Where; C_{R_n} = DCOMP or DEXT depending or stroke sign, DCOMP = 12, DEXT for n = 1 is 0.0, for n = 2,3 is 0.12.

Z_n = Stroke, ft

Z_n' = Oleo stroke, ft

Z_{TIRE_n} = Max. tire deflection, ft

$\dot{Z}_n$ = Stroke rate, ft/sec

m = Mass, slugs

C. Gear Rolling Friction

$$F_{G_{\mu_n}} = -(\mu_o + \mu_1 U_{ROLLING}) F_{G_{O_n}} \frac{U}{|U|}$$

$$U_{ROLLING} = 1.0 - 0.1\ U_G$$

if $U_{ROLLING} < 0.0$ $\qquad U_{ROLLING} = 0.0$

if $U < 1.0$ $\qquad F_{G_{\mu_n}} = 0.0$

D. Gear Side Force

$$F_{G_{S_n}} = -\mu_S F_{G_{o_n}} \frac{V}{|V|}$$

if $V < 1.0$ $\qquad F_{G_{S_n}} = 0.0$

E. Gear Force and Moment Summation

$$F_{G_{X_n}} = F_{G_{\mu_n}} - F_{G_{o_n}} \theta$$

$$F_{G_{Y_n}} = F_{G_{S_n}} + F_{G_{o_n}} \phi$$

$$F_{G_{Z_n}} = F_{G_{\mu_n}} \sin\theta - F_{G_{S_n}} \sin\phi + F_{G_{o_n}}$$

$$\ell_{G_n} = + F_{G_{o_n}} Y_n - F_{G_{Y_n}} (Z_n + h_{G_n})$$

$$M_{G_n} = - F_{G_{o_n}} X_n + F_{G_{X_n}} (Z_n + h_{G_n})$$

$$N_{G_n} = - F_{G_{X_n}} Y_n + F_{G_{Y_n}} X_n$$

$$\Delta X_{LG} = \sum_1^3 F_{G_{X_n}} \qquad \Delta \ell_{LG} = \sum_1^3 \ell_{G_n}$$

$$\Delta Y_{LG} = \sum_1^3 F_{G_{Y_n}} \qquad \Delta M_{LG} = \sum_1^3 M_{G_n}$$

$$\Delta Z_{LG} = \sum_1^3 F_{G_{Z_n}} \qquad \Delta N_{LG} = \sum_1^3 N_{G_n}$$

8a	CONTROLS

Inputs: Variables		Outputs:	
From Subsystem	Symbol	To Subsystem	Symbol
17	$\theta_{oL/G}$ $\theta_{oR/G}$	1	θ_{oR} θ_{oL} A_{1L} B_{1L} A_{1R} B_{1R}
8d	X_{LN} X_{LT} X_{PD} X_{COL} X_{FL} X_{LG} IDIFF INACB	5	δ_e
		6	δ_r δ_F
		4	δ_a δ_F
20	PSCAS RSCAS YSCAS	7	L_{LG}
12	U	1, 2, 4	β_m
		5, 6, 9	
		10b, 14, 17, 18	
		20	
		9	$\dot{\beta}_m$
		18	X_{THR} X_{THL}

Inputs: Contants, Coefficients, and Data Tables

Constants: COLRATE, $\Delta\theta_{oLIM}$, PBMMAX, PBMMIN, δ_{B1}, X_{LNN}, X_{LTN}, X_{PDN}

Coefficients: $\partial\delta_e/\partial X_{LN}$, $\partial\delta_r/\partial X_{PD}$, $\partial\delta_a/\partial X_{LT}$, $\partial\delta_F/\delta t$, ω_n, ζ_D

(Continued on next page)

8a	CONTROLS (CONCLUDED)

Inputs: Constants, Coefficients, and Data Tables (Concluded)

Data Tables:	$\partial B_1/\partial X_{LN} = f(\beta_m)$	Table 8a-1
	$\partial B_1/\partial X_{PD} = f(\beta_m, U)$	Table 8a-II
	$\partial \theta_o/\partial X_{LT} = f(\beta_m)$	Table 8a-III
	$\partial \theta_o/\partial X_{COL} = f(\beta_m)$	Table 8a-IV
	$\theta_{oLL} = f(\beta_m)$	Table 8a-IV
	$\dot{\beta}_{mC} = f(\beta_m)$	Table 8a-V
	$X_{THR,L} = f(X_{COL})$	Table 8a-VI
	$A_{1_{B_m}} = f(\beta_m)$	Table 8a-VII
	$A_{1_{V_T}} = f(U)$	Table 8a-VIII

SUBSYSTEM NO. 8a: CONTROLS

Variables:

Symbol	Description	Units
$\theta_{oL/G}$	Left rotor collective pitch input from the left rotor collective governor	deg
$\theta_{oR/G}$	Right rotor collective pitch input from the right rotor collective governor	deg
X_{LN}	Longitudinal stick position, inches from full aft	in
X_{LT}	Lateral stick position, inches from full left	in
X_{PD}	Pedal position, inches from full left	in
X_{COL}	Collective stick position, inches from full down	in
X_{FL}	Position of flap indicator	ND
X_{LG}	Position of landing gear indicator	ND
IDIFF	Differential collective switch position	ND
INACB	Nacelle beep switch position	ND
PSCAS	Pitch (elevator) SCAS input	in
RSCAS	Roll (Aileron) SCAS input	in
YSCAS	Yaw (rudder) SCAS input	in
U	x-velocity (longitudinal) of rotorcraft c.g. in body axis with respect to the air	ft/sec

Inputs: Constants, Coefficients, and Data Tables

Symbol	Description	Units
COLRATE	Differential collective trim rate constant	deg/sec
$\Delta\theta_{oLIM}$	Differential collective trim limit	deg
PBMMAX	Maximum forward pylon position	deg
PBMMIN	Maximum aft pylon position	deg
δ_{B1}	B1 offset rigging constant	deg
X_{LNN}	Longitudinal stick neutral position	in
X_{LTN}	Lateral stick neutral position	in
X_{PDN}	Pedal neutral position	in
$\partial\delta_e/\partial X_{LN}$	Elevator to longitudinal stick position gearing ratio	deg/in
$\partial\delta_r/\partial X_{PD}$	Rudder to pedal position gearing ratio	deg/in
$\partial\delta_a/\partial X_{LT}$	Aileron to lateral stick position gearing ratio	deg/in
$\partial\delta_F/\partial t$	Rate of change of flaps with time	deg/sec
ω_n	Lateral flapping controller natural frequency	rad/sec
ζ_d	Lateral flapping controller damping parameter	ND
$\partial B_1/\partial X_{LN}$	Longitudinal cyclic pitch control gearing ratio, = $f(\beta_m)$	deg/in
$\partial B_1/\partial X_{PD}$	Differential cyclic pitch control gearing ratio, = $f(\beta_m, U)$	deg/in
$\partial\theta_o/\partial X_{LT}$	Differential collective pitch control gearing ratio, = $f(\beta_m)$	deg/in

Inputs: Constants, Coefficients, and Data Tables (Concluded)

Symbol	Description	Units
$\partial\theta_o/\partial X_{COL}$	Collective pitch control gearing ratio, = $f(\beta_m)$	deg/in
θ_{oLL}	Root collective pitch lower limit, = $f(\beta_m)$	deg
$\dot{\beta}_{mC}$	Commanded mast conversion rate, = $f(\beta_m)$	deg/sec
X_{THR}	Right engine throttle position at the fuel control	deg
$A_{1_{B_m}}$	Lateral flapping controller coefficient, = $f(\beta_m)$	ND
$A_{1_{V_T}}$	Lateral flapping controller coefficient, = $f(U)$	deg

Outputs:

θ_{oR}	Right rotor root collective pitch	rad
θ_{oL}	Left rotor root collective pitch	rad
A_{1L}	Left rotor lateral cyclic input	rad
B_{1L}	Left rotor forward cyclic input	rad
A_{1R}	Right rotor lateral cyclic input	rad
B_{1R}	Right rotor forward cyclic input	rad
δ_e	Elevator mean deflection angle (+ trailing edge down)	deg
δ_r	Rudder mean deflection angle (+ trailing edge right)	deg
δ_F	Flap position	deg

SUBSYSTEM NO. 8a: CONTROLS (Concluded)

Outputs: (Concluded)

Symbol	Description	Units
δ_a	Aileron mean deflection angle (+ right aileron up)	deg
L_{LG}	Landing gear position indicator	ND
β_m	Mast conversion angle (+ fwd, 0 deg = vertical or helicopter, 90 deg = horizontal or airplane)	deg
$\dot{\beta}_m$	Mast conversion rate	deg/sec
X_{THR}	Right engine throttle position at the fuel control	deg
X_{THL}	Left engine throttle position at the fuel control	deg

Figure A8a-1.

CONTROL SYSTEM BLOCK DIAGRAM

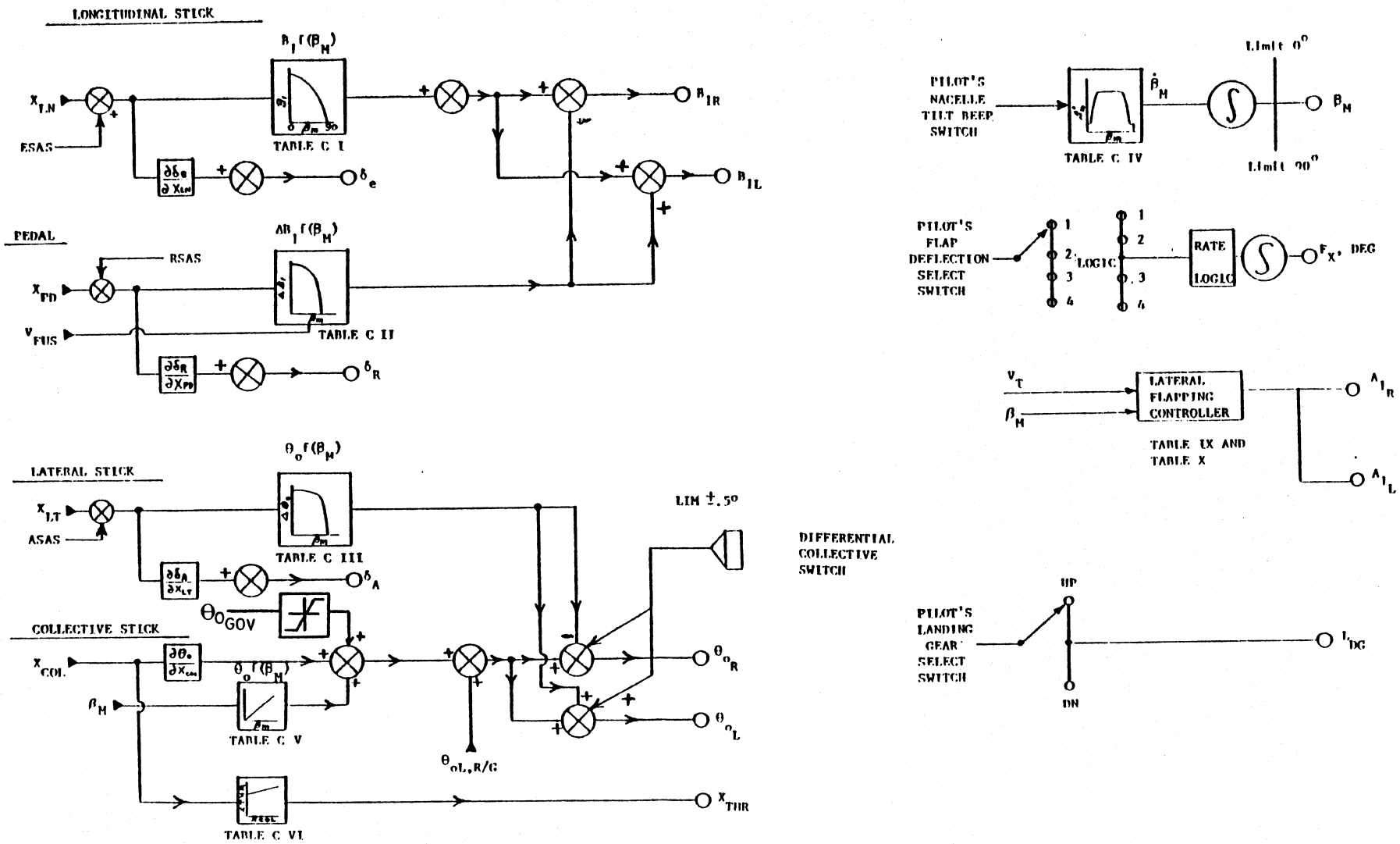

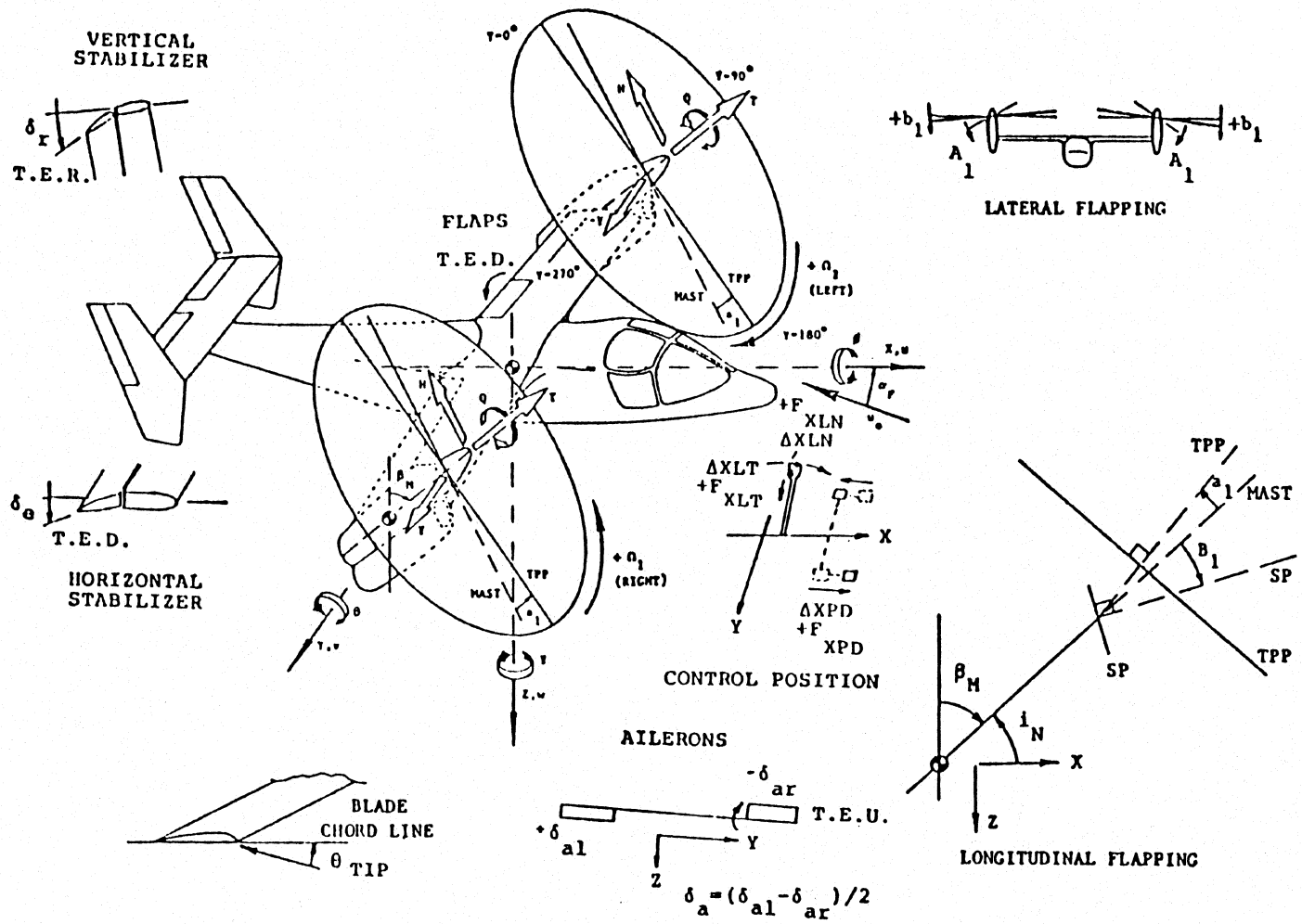

Figure A8a-2. Control Position/Force-Force and Moment Sign Convention

EQUATIONS

SUBSYSTEM NO. 8a--CONTROLS

A. Collective Pitch

$$\theta_{oR} = \left(\partial\theta_o / \partial X_{COL}\right)\left(X_{COL}\right) + \theta_{oLL} + \theta_{oR/G}$$

$$-\left(\frac{\partial\theta_o}{\partial X_{LT}}\right)\left(X_{LT} - X_{LTN} + RSCAS\right) + \Delta\theta_o$$

$$\theta_{oL} = \left(\partial\theta_o / \partial X_{COL}\right)\left(X_{COL}\right) + \theta_{oLL} + \theta_{oL/G}$$

$$+\left(\frac{\partial\theta_o}{\partial X_{LT}}\right)\left(X_{LT} - X_{LTN} + RSCAS\right) + \Delta\theta_o$$

B. Differential Collective Trim

$$\Delta\theta_o = \Delta\theta_o + (COLRATE)(\Delta t)(IDIFF)$$

where

$\Delta\theta_o$ is limited to $\Delta\theta_{oLIM}$

Δt is the simulation cycle time

IDIFF is the pilot actuated differential collective trim switch that is a (left, off, right) setting corresponding to (-1, 0, 1) in value

C. Longitudinal Cyclic

$$B_{1R} = \left(\frac{\partial B_1}{\partial X_{LN}}\right)\left(X_{LN} - X_{LNN} + PSCAS\right)$$

$$-\left(\frac{\partial B_1}{\partial X_{PD}}\right)\left(X_{PD} - X_{PDN} + YSCAS\right) + \delta_{B1}\left(1 - \cos\beta_m\right)$$

C. Longitudinal Cyclic (Concluded)

$$B_{1L} = \left(\frac{\partial B_1}{\partial X_{LN}}\right)\left(X_{LN} - X_{LNN} + PSCAS\right)$$

$$+\left(\frac{\partial B_1}{\partial X_{PD}}\right)\left(X_{PD} - X_{PDN} + YSCAS\right) + \delta_{B1}\left(1 - \cos\beta_m\right)$$

D. Lateral Cyclic

$$A_{1R} = A_{1L} = 0$$

Note: This function could be added if the control law is desired. Lateral cyclic is not used in the basic XV-15 control system.

E. Elevator, Rudder, Aileron

$$\delta_e = \left(\frac{\partial \delta_e}{\partial X_{LN}}\right)\left(X_{LN} - X_{LNN} + PSCAS\right)$$

$$\delta_r = \left(\frac{\partial \delta_r}{\partial X_{PD}}\right)\left(X_{PD} - X_{PDN} + YSCAS\right)$$

$$\delta_a = \left(\frac{\partial \delta_a}{\partial X_{LT}}\right)\left(X_{LT} - X_{LTN} + RSCAS\right)$$

F. Nacelle Tilt

$$\dot{\beta}_m = \left(\dot{\beta}_{mC}\right)(INACB)$$

where

INACB equals (1, 0, -1) = (fwd, neutral, aft) on the pilot's nacelle tilt keep siwtch

$$\dot{\beta}_{mC} = f\left(\beta_m\right)$$

F. Nacelle Tilt (Concluded)

$$\beta_m = \int_0^t \beta_m \, dt$$

where

β_m is limited such that PBMMIN $\leq \beta_m \leq$ PBMMAX

G. Flap Selector

The discreet flap/flaperon settings are:

0/0 deg $= X_{FL1}$

20/12.5 deg $= X_{FL2}$

40/25 deg $= X_{FL3}$

75/47 deg $= X_{FL4}$

where

X_{FLn} is the pilot's flap selector (a four position switch)

H. Landing Gear Selector

$L_{LG} = (0, 1) = (\text{up, down})$

where

X_{LG} is the pilot's gear selector in a discrete up or down position

I. Lateral Cyclic (Lateral Flapping Controller)

$$A_{1_R} = \left(A_{1_{B_m}}\right)\left(A_{1_{V_T}}\right)\left[\frac{1}{\left(\frac{1}{\omega_n^2}\right)s^2 + \left(\frac{\zeta}{\omega_n}\right)s + 1}\right]$$

$$A_{1_L} = A_{1_R}$$

If $U < 0.0$, $\quad A_{1_R} = 0.0$

8b	FORCE FEEL SYSTEM

Inputs: Variables		Outputs:	
From Subsystem	Symbol	To Subsystem	Symbol
3	q_F	To analog control loaders (8d)	G_{XLN}
8c	X_{LNT}		G_{XLT}
	X_{LTT}		G_{XPD}
	X_{PDT}		ζ_{XLN}
			ζ_{XLT}
			ζ_{XPD}
8d	IMB		H_{XLN}
	IFFON		H_{XPD}
	IFFENG		H_{XLT}
	IAN		

Inputs: Constants, Coefficients, and Data Tables

Constants: None

Coefficients: Longitudinal Axis

G_{LN0}, G_{LN1}, K_{LN}, ζ_{LN}, H_{LN}

Lateral Axis

G_{LT0}, G_{LT1}, K_{LT}, ζ_{LT}, H_{LT}

Directional Axis

G_{PD0}, G_{PD1}, ζ_{PD}, H_{PD}, H_{RUD}, $F_{ACT_{RUD_{LIM}}}$

FFS ON

$\dot{X}_{LNT0}$, $\dot{X}_{LNT1}$, $\dot{X}_{LTT0}$, $\dot{X}_{LTT1}$, $\dot{X}_{PDT0}$, $\dot{X}_{PDT1}$

FFS OFF

$\dot{X}_{LNT0}$

Data Tables: None

SUBSYSTEM NO. 8b—FORCE FEEL SYSTEM

Inputs: Variables

Symbol	Description	Units
q_F	Fuselage dynamic pressure	lb/ft^2
X_{LNT}	Longitudinal stick force feel trim position	in
X_{LTT}	Lateral stick force feel trim position	in
X_{PDT}	Pedal force feel trim position	in
IMB	Force feel system release switch	ND
IFFON	Force feel system ON/OFF switch	ND
IFFENG	Force feel system engage switch	ND
IAN	Yaw trim switch	ND

Inputs: Constants, Coefficients, and Data Tables

G_{LN0}	Longitudinal force feel system gradient	lb/in
G_{LN1}	Longitudinal force feel system gradient	lb/in/PSF
K_{LN}	Longitudinal force feel system constant (system off)	lb/in
ζ_{LN}	Longitudinal force feel system viscous damping coefficient	ND
H_{LN}	Longitudinal force feel system hysteresis force	lb
G_{LT0}	Lateral force feel system gradient	lb/in
G_{LT1}	Lateral force feel system gradient	lb/in/PSF

Inputs: Constants, Coefficients, and Data Tables (Concluded)

Symbol	Description	Units
K_{LT}	Lateral force feel system constant (system off)	lb/in
ζ_{LT}	Lateral force feel system viscous damping coefficient	ND
H_{LT}	Lateral force feel system hysteresis force	lb
G_{PD0}	Pedal force feel system gradient	lb/in
G_{PD1}	Pedal force feel system hysteresis	lb/in/PSF
ζ_{PD}	Pedal force feel system viscous damping coefficient	ND
H_{PD}	Pedal force feel system hyseresis force	lb
H_{RUD}	Rudder force feel constant	ft^2/in
$F_{ACT_{RUD_{LIM}}}$	Rudder force feel actuator limit	lb
$\dot{X}_{LNT0}$	Longitudinal trim rate force feel system constant	in/sec
$\dot{X}_{LNT1}$	Longitudinal trim rate force feel system constant	in/sec/PSF
$\dot{X}_{LTT0}$	Lateral trim rate force feel system constant	in/sec
$\dot{X}_{LTT1}$	Lateral trim rate force feel system constant	in/sec/PSF
$\dot{X}_{PDT0}$	Pedal trim rate force feel system constant	in/sec
$\dot{X}_{PDT1}$	Pedal trim rate force feel system constant	in/sec/PSF

SUBSYSTEM NO. 8b—FORCE FEEL SYSTEM (Concluded)

Outputs:

Symbol	Description	Units
G_{XLN}	Longitudinal force feel system gradient (system on)	lb/in
G_{XLT}	Lateral force feel system gradient (system on)	lb/in
G_{XPD}	Pedal force feel system gradient (system on)	lb/in
ζ_{XLN}	Longitudinal force feel viscous damping coefficient	ND
ζ_{XLT}	Lateral force feel viscous damping coefficient	ND
ζ_{XPD}	Pedal force feel viscous damping coefficient	ND
H_{XLN}	Longitudinal force feel system hysteresis force	lb
H_{XLT}	Lateral force feel system hysteresis force	lb
H_{XPD}	Pedal force feel system hysteresis force	lb

EQUATIONS:

A. Force feel system ON gradients:

$$G_{XLN} = G_{LNO} + G_{LN1}\ q_F$$

$$G_{XLT} = G_{LTO} + G_{LT1}\ q_F$$

$$G_{XPD} = G_{PDO} + G_{PD1}\ q_F$$

Viscous Damping:

$$\zeta_{XLN} = \zeta_{XLT} = \zeta_{XPD} = \zeta_{FFS}$$

Hysteresis

$$H_{XLN} = H_{XLT} = H_{XPD} = 0$$

Note: Adjust McFadden loader such that stick mass at the reference point on the grip is effectively 0.172 slugs and the pedal mass is effectively 0.183 slugs (for two pedals).

B. Force Feel System OFF

$$G_{XLN} = K_{LN}$$

$$G_{XLT} = K_{LT}$$

$$G_{XPD} = F_{RUD}/(X_{PD} - X_{PDT})$$

$$F_{RUD} = \left| H_{RUD}\ q_F\ (X_{PD} - X_{PDT}) \right| - F_{ACT_{RUD_{LIM}}}$$

If $F_{RUD} \leq 0$, set $F_{RUD} = 0$

If $F_{RUD} > 0$, set $F_{RUD} = F_{RUD}$

$$\zeta_{XLN} = \zeta_{XLT} = \zeta_{XPD} = 0$$

Hysteresis:

$H_{XLN} = H_{LN}$

$H_{XLT} = H_{LT}$

$H_{XPD} = H_{PD}$

C. Trim Rate and Position

$\dot{X}_{LNT} = \dot{X}_{LNTO} + \dot{X}_{LNT1}\, q_F$

$\dot{X}_{LTT} = \dot{X}_{LTTO} + \dot{X}_{LTT1}\, q_F$

$\dot{X}_{PDT} = \dot{X}_{PDTO} + \dot{X}_{PDT1}\, q_F$

$X_{LNT} = \frac{1}{S}\dot{X}_{LNT}$

$X_{LTT} = \frac{1}{S}\dot{X}_{LTT}$

$X_{PDT} = \frac{1}{S}\dot{X}_{PDT}$

D. Relief Value (force limiter)

If $X_{LNT} \geqslant \frac{15.75}{|G_{XLN}-K_{LN}|}$ then $G_{XLN} = K_{LN}$; $G_{XLN}X_{LNT} \leqslant 25.$

If $X_{LTT} \geqslant \frac{4.8}{|G_{XLT}-K_{LT}|}$ then $G_{XLT} = K_{LT}$; $G_{XLT}X_{LTT} \leqslant 25.$

$G_{XPD}X_{PDT} \leqslant 25.$

8c	CONTROL FORCE TRIM SYSTEM

Inputs: Variables		Outputs:	
From Subsystem	Symbol	To Subsystem	Symbol
3	q_F	8b	X_{LNT}
8d	X_{LN}		X_{LTT}
	X_{LT}		X_{PDT}
	X_{PD}		
	$B_{FT_{XLN}}$		
	$B_{FT_{XLT}}$		
	$B_{FT_{XPD}}$		

Inputs: Constants, Coefficients, and Data Tables

Constants: None

Coefficients: $\dot{X}_{LNTO}$, $\dot{X}_{LNT1}$, $\dot{X}_{LTTO}$, $\dot{X}_{LTT1}$, $\dot{X}_{PDTO}$, $\dot{X}_{PDT1}$

Data Tables: None

SUBSYSTEM NO. 8c—CONTROL FORCE TRIM SYSTEM

Inputs: Variables

Symbol	Description	Units
q_F	Fuselage dynamic pressure	lb/ft^2
X_{LN}	Longitudinal stick position, inches from full aft	in
X_{LT}	Lateral stick position, inches from full left	in
X_{PD}	Pedal position, inches from full left	in
$B_{FT_{XLN}}$	Longitudinal control force trim switch constant	ND
$B_{FT_{XLT}}$	Lateral control force trim switch constant	ND
$B_{FT_{XPD}}$	Pedal control force trim switch constant	ND

Inputs: Constants, Coefficients, and Data Tables

$\dot{X}_{LNT0}$	Longitudinal trim rate force feel system constant	in/sec
$\dot{X}_{LNT1}$	Longitudinal trim rate force feel system constant	in/sec/PSF
$\dot{X}_{LTT0}$	Lateral trim rate force feel system constant	in/sec
$\dot{X}_{LTT1}$	Lateral trim rate force feel system constant	in/sec/PSF
$\dot{X}_{PDT0}$	Pedal trim rate force feel system constant	in/sec
$\dot{X}_{PDT1}$	Pedal trim rate force feel system constant	in/sec/PSF

SUBSYSTEM NO. 8c—CONTROL FORCE TRIM SYSTEM (Concluded)

Outputs:

Symbol	Description	Units
X_{LNT}	Longitudinal stick force feel trim position	in
X_{LTT}	Lateral stick force feel trim position	in
X_{PDT}	Pedal stick force feel trim position	in

EQUATIONS:

$$X_{LNT} = X_{LNT_0} + \left(\text{SIGN } \beta_{FT_{XLN}}\right) * \int_0^t \dot{X}_{LNT}$$

where: $\dot{X}_{LNT} = \dot{X}_{LNT0} + \dot{X}_{LNT1} * q_F$

$$X_{LTT} = X_{LTT_0} + \left(\text{SIGN } \beta_{FT_{XLT}}\right) * \int_0^t \dot{X}_{LTT}$$

where: $\dot{X}_{LTT} = \dot{X}_{LTT0} + \dot{X}_{LTT1} * q_F$

$$X_{PDT} = X_{PDT_0} + \left(\text{SIGN } \beta_{FT_{XPD}}\right) * \int_0^t \dot{X}_{PDT}$$

where: $\dot{X}_{PDT} = \dot{X}_{PDT0} + \dot{X}_{PDT1} * q_F$

Note: Perform indicated integration only when $\beta_{FT_i} \neq 0$.
(i.e., trim switch on)

8d	PILOT'S CONTROL FUNCTION

Inputs: Variables		Outputs:	
From Subsystem	**Symbol**	**To Subsystem**	**Symbol**
From analog control loaders	F_{LN} F_{LT} F_{PD}	8a, 8c, 20	X_{LN} X_{LT} X_{PD}
		8a	X_{COL}
		7A	δ_{B_n} δ_{NW}
		8a	X_{FL} X_{LG} IDIFF INACB
		8c	$B_{FT_{XLN}}$ $B_{FT_{XLT}}$ $B_{FT_{XPD}}$
		8b	IMB IFFON IFFENG IAN
		17	IRPM MENB IGB IGOVENG
		17, 19	RPM_{SEL}
		20	ISCRLS IQDAMP IPDAMP IRDAMP IPCH IRCH IFAH ISCENG

Inputs: Constants, Coefficients, and Data Tables

Pilot in the Loop

SUBSYSTEM NO. 8d: PILOT'S CONTROL FUNCTION

Inputs: Variables

Symbol	Description	Units
F_{LN}	Longitudinal stick force from the pilot (+ fwd)	lb
F_{LT}	Lateral stick force from the pilot (+ right)	lb
F_{PD}	Pedal force from the pilot (+ right)	lb
Outputs:		
X_{LN}	Longitudinal stick position, inches from full aft	in
X_{LT}	Lateral stick position, inches from full left	in
X_{PD}	Pedal position, inches from full left	in
X_{COL}	Collective stick position, inches from full down	in
δ_{B_n}	Brake pedal deflection	deg
δ_{NW}	Nose wheel steering angle	rad
X_{FL}	Position of flap indicator	ND
X_{LG}	Position of landing gear indicator	ND
IDIFF	Differential collective switch position	ND
INACB	Nacelle beep switch position	ND
$B_{FT_{XLN}}$	Longitudinal control force trim switch constant	ND
$B_{FT_{XLT}}$	Lateral control force trim switch constant	ND
$B_{FT_{XPD}}$	Pedal control force trim switch constant	ND

SUBSYSTEM NO. 8d: PILOT'S CONTROL FUNCTION (Concluded)

Outputs: (Concluded)

Symbol	Description	Units
IMB	Force feel system trim release switch	ND
IFFON	Force feel system ON/OFF switch	ND
EFFENG	Force feel system engage switch	ND
IAN	Yaw trim switch	ND
IRPM	RPM adjustment wheel (increase/decrease)	ND
MENB	Pylon lock switch	ND
IGB	RPM governor disengage switch	ND
IGOVENG	RPM governor engage switch	ND
RPM_{SEL}	Pilot's selected operating rotor speed	RPM
ISCRLS	SCAS release switch	ND
IQDAMP	Pitch SCAS ON/OFF switch	ND
IPDAMP	Roll SCAS ON/OFF switch	ND
IRDAMP	Yaw SCAS ON/OFF switch	ND
IPCH	Pitch channel switch (Channel 1, 2, both)	ND
IRCH	Roll channel switch (Channel 1, 2, both)	ND
IFAH	Attitude retention ON/OFF switch	ND
ISCENG	SCAS engage switch	ND

Figure A8d-1. XV-15
Collective Head Switches

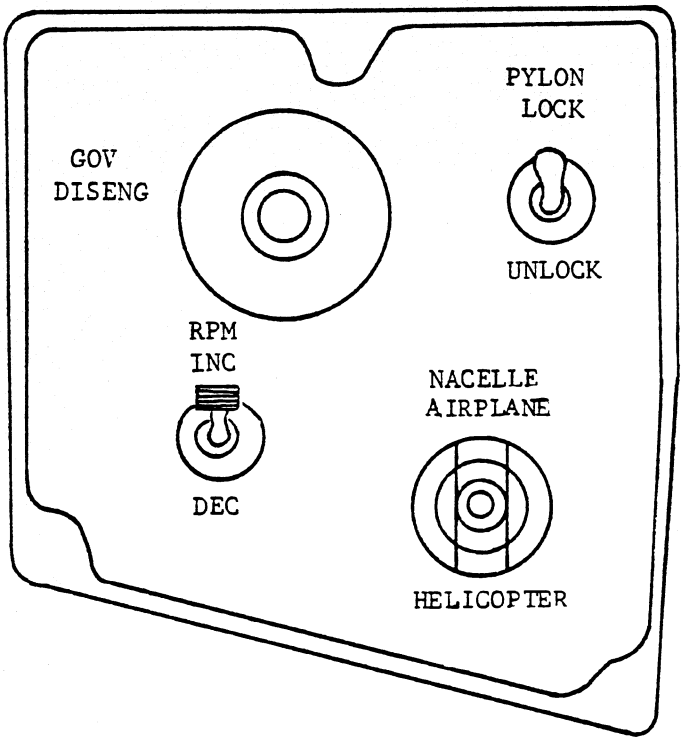

Figure A8d-2. XV-15

CYCLIC
GRIP
SWITCHES

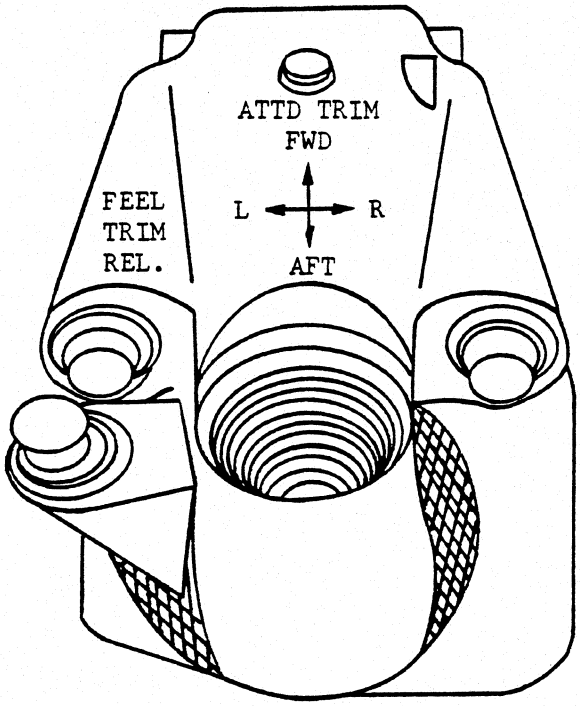

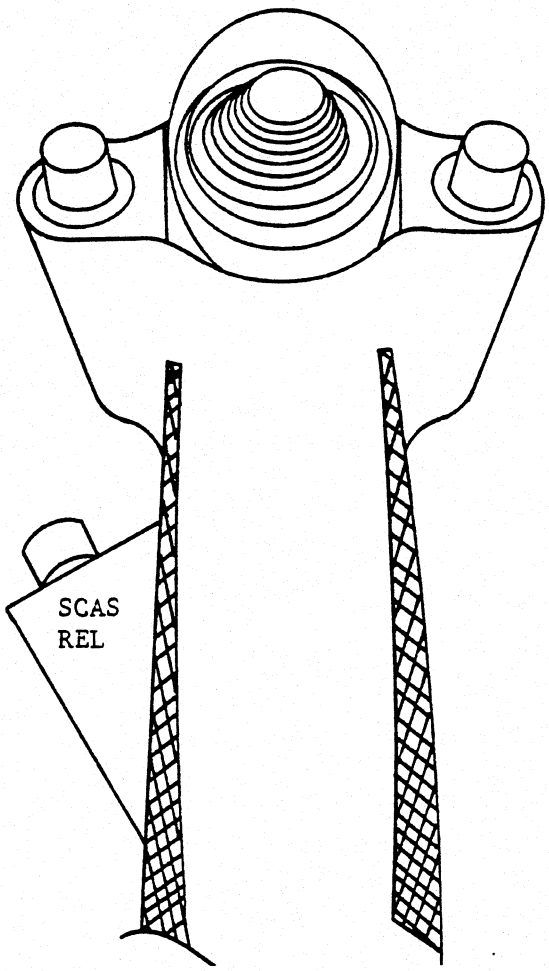

Figure A8d-3. XV-15 Flap Switch Selector Control

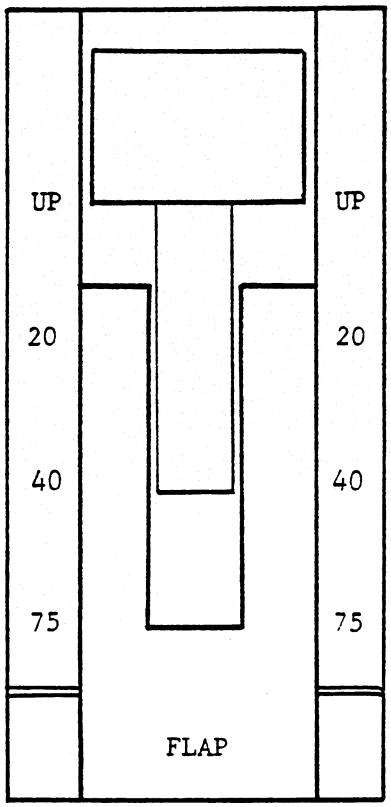

SELECTOR SWITCH
FLAP CONTROL

Similar to
Avionic Products Engineering Corp.
758001-1 (Drwg. D758)

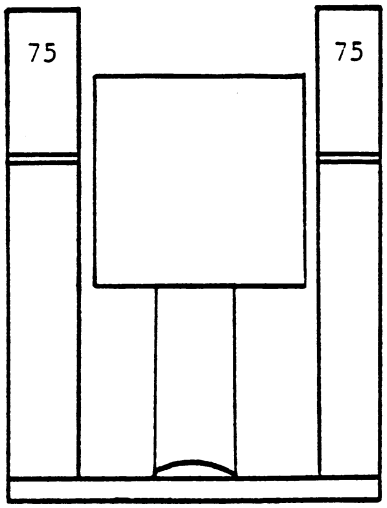

Figure A8d-4. XV-15 SCAS Control Panel

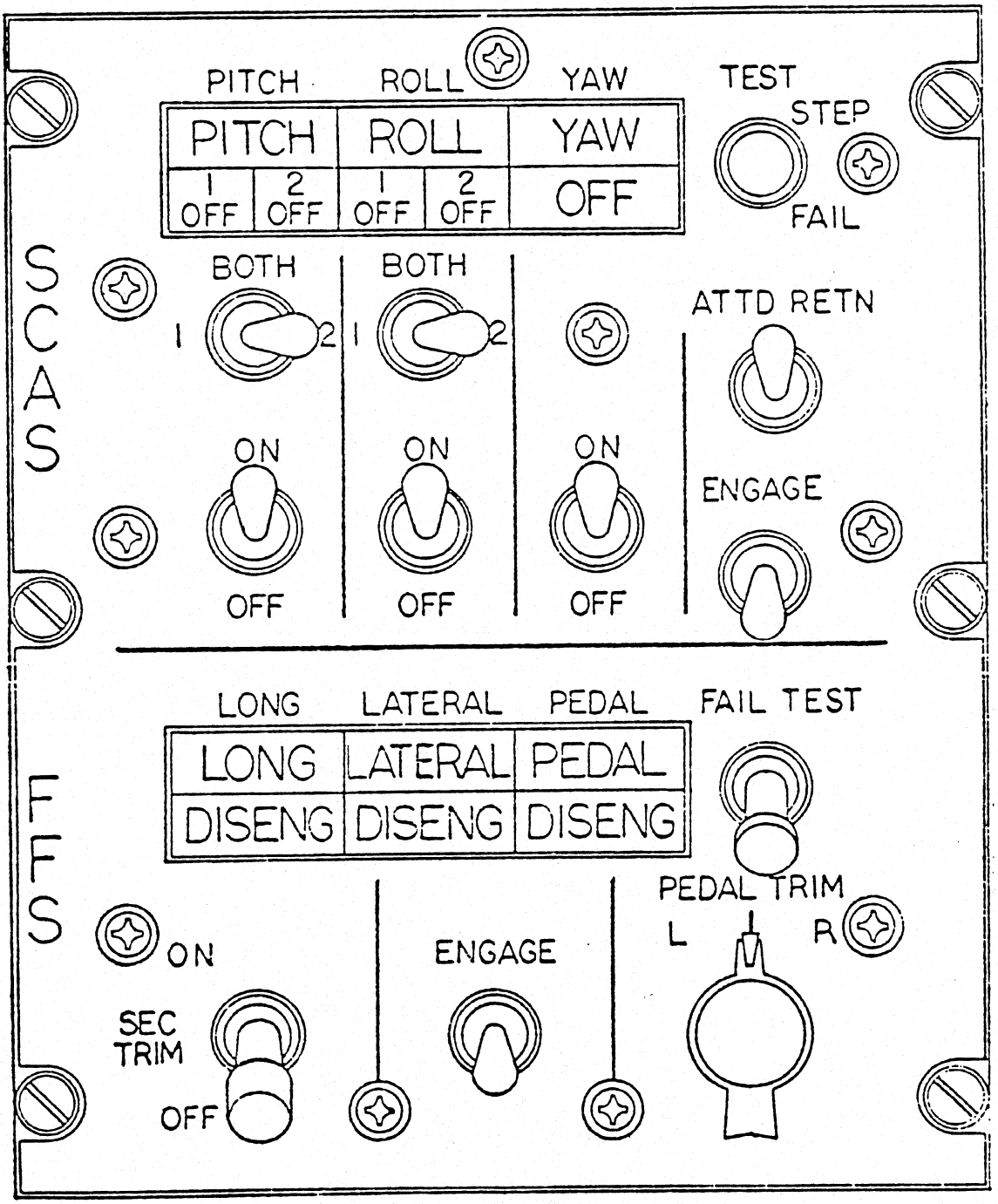

Figure A8d-5. XV-15 Governor Control Panel

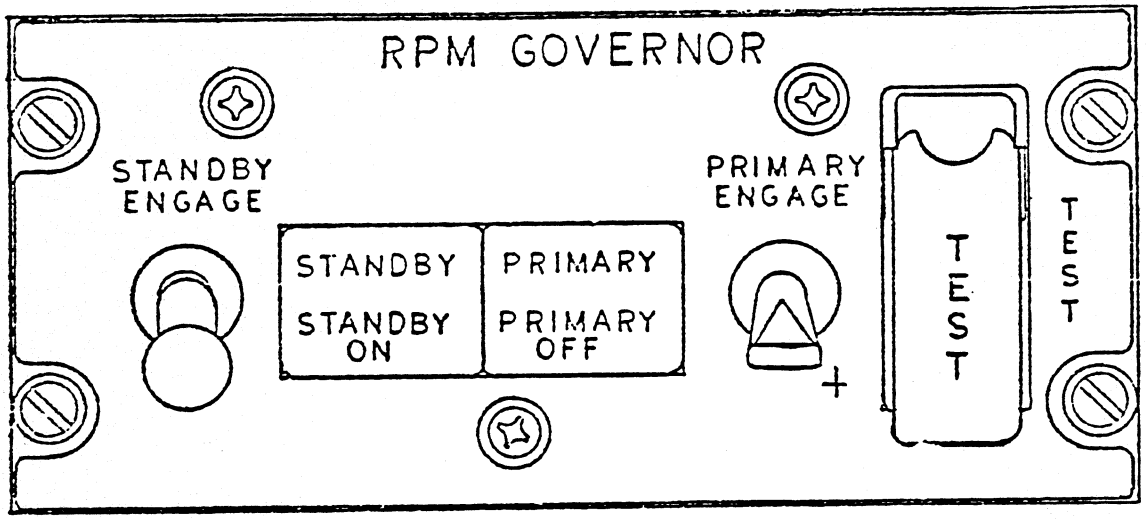

SUBSYSTEM CONTROLS AND FAILURE LOGIC

I. SCAS Control Panel

Lights:

PITCH - ROLL - YAW

OFF	- lights out during normal operation (system engaged)
ON (RED)	- illuminates to indicate when the respective axis fails

1 OFF - 2 OFF - OFF

OFF	- lights out during normal operation (system engaged) and master power switch OFF.
ON (AMBER)	- illuminates when pilot selects channel (1 or 2) for pitch or roll axis, or turns yaw axis off; - all five lights on when system is disengaged by pilot from the SCAS disengage on cyclic stick, SCAS power switches and Master Power ON; - all five lights on when SCAS power switches are set to off with master power ON - master caution "on" when any "OFF" light is "on"

Switches:

ON/OFF	- Two position, used to apply power to the system. ON switch engages SCAS gyros but does not actuate system.
1/BOTH/2	- Three position, used to select channel number 1, BOTH, or number 2.
ENGAGE	- Momentary on, used to activate the SCAS system to the configuration preset by the ON/OFF and 1/BOTH/2 switches.

I. SCAS Control Panel (Continued)

Switches:

ATTITUDE RETENTION	- Solenoid held, used to turn attitude retention ON/OFF. Switch pops to OFF position upon attitude retention failure.
TEST	- Three position center off switch spring loaded to off position (nonfunctional for simulation).
SCAS DISENGAGE	- Pushbutton located on the cyclic grip, used to manually disengage all axes simultaneously. SCAS is disengaged by the SCAS disengage switch on the cyclic stick. The SCAS is deactivated and the actuators centered. SCAS OFF panel lights and CAUTION light will come on. All axes may be re-engaged with the engage switch on the SCAS panel and all lights will go out, providing the ON/OFF switches were left in the ON position during the time the SCAS was manually disengaged.

Start Procedure:

Upon entering the aircraft, master power off and SCAS power switches OFF, all SCAS panel lights will be off. Turn master power ON, SCAS power switches OFF, all five SCAS "OFF" and master caution lights will be illuminated. Turn on SCAS switches to power the system and gyros. Engage the SCAS with the SCAS ENGAGE switch, system is then activated and SCAS "OFF" lights will go out.

SCAS Failures:

Single Channel	- PITCH, ROLL, or YAW plus CAUTION lights will come ON indicating the failed axis. Pilot will determine which channel failed by switching to channel 1 or 2

I. SCAS Control Panel (Continued)

Single Channel - for the pitch or roll axis, or may turn both channels off. If yaw axis failed, the yaw axis is turned off. When the switches are set to 1 or 2, the SCAS fail lights go out and the 1 OFF or 2 OFF light comes on depending upon which channel is selected. Likewise, when the yaw SCAS is turned off, the yaw fail light goes out. CAUTION light will remain ON, indicating SCAS failure. Yaw SCAS OFF light will illuminate.

Attitude Retention - No lights to denote failure. Indication of failure can be noted by status of attitude retention selection (solenoid held) switch (OFF position).

Notes: 1. Attitude retention is off if:

a. Pitch axis, $F_{X_{LN}} \geq 1.0$ lb

Roll axis, $F_{X_{LT}} \geq 0.5$ lb

b. Attitude retention switch is OFF.
c. FFS fails or is disengaged.
d. SCAS is disengaged.
e. Failure occurs in the attitude retention circuits. (Power to circuit or attitude gyro fails.)

2. Attitude retention is operable during single channel SCAS operation.

3. Item 1.a. does not change the status of the attitude retention switch, but momentarily deactivates the attitude retention to the SCAS. Items 1.c. through 1.e. denote a failed condition and sets the attitude retention switch to the OFF position removing attitude retention from the SCAS.

I. SCAS Control Panel (Continued)

XV-15 SCAS Pre-Flight Check List (FFS Pre-Flight Check Complete)

Airplane status - engines running, electrical and hydraulic power on, attitude gyro on and no flags, feel system engaged, all SCAS switches OFF except SCAS select switches in "BOTH".

1. SCAS status lights - Pitch "1 OFF", "2 OFF"; Roll "1 OFF", "2 OFF"; Yaw "OFF" - check ON.

2. SCAS fail lights "PITCH", "ROLL" and "YAW" - check OFF.

3. SCAS segment of the master caution panel and MASTER CAUTION light - check ON.

4. Set pitch, roll, yaw power switches to "ON".

5. Set SCAS ENGAGE switch to "ENGAGE". Pitch "1, 2 OFF"; Roll "1, 2, OFF"; Yaw "OFF" lights - check "OFF". SCAS segment of the master caution panel and MASTER CAUTION light - check "OFF".

6. Exercise cyclic stick and rudder pedals - check all SCAS lights remain "OFF".

7. Set SCAS channel select switches "PITCH" "ROLL" to "1" - check status lights Pitch "2 OFF", Roll "2 OFF", ON.

8. Set SCAS channel select switches "PITCH, ROLL" to "2" - check status lights Pitch "1 OFF", Roll "1 OFF" ON.

9. Set SCAS channel select switches "PITCH" "ROLL" to "BOTH" - check all SCAS lights "OFF".

10. Set Attitude Retention switch to "ATTD RETN" - check that switch stays ON.

11. Set and hold "TEST" switch to "STEP" - check Fail lights OFF and control (surface) motion in all axes.

12. Set and hold "TEST" switch to "FAIL" - check "PITCH" "ROLL" "YAW" Fail lights ON - check SCAS segment of master caution panel and MASTER CAUTION light ON. Check yaw control motion only. Release "TEST" switch - check for Fail and SCAS segment of master caution panel and MASTER CAUTION lights out 5 seconds after release of switch.

I. SCAS Control Panel (Continued)

XV-15 SCAS Pre-Flight Check List (FFS Pre-Flight Check Complete)

13. Press SCAS disengage button on pilot's cyclic stick--check SCAS status lights - Pitch "1 OFF", "2 OFF"; Roll "1 OFF", "2 OFF"; Yaw "OFF" all ON - check SCAS segment of master caution panel and MASTER CAUTION light ON - check attitude retention switch OFF.

14. Set SCAS ENGAGE switch to "ENGAGE".
Set Attitude Retention switch to "ATTD RETN".

15. Press SCAS Disengage button on copilot's cyclic stick - check SCAS status lights Pitch "1 OFF", "2 OFF"; Roll "1 OFF", "2 OFF"; Yaw "OFF" all ON - check SCAS segment of master caution panel and the MASTER CAUTION light ON - check Attitude Retention switch OFF.

16. Set SCAS ENGAGE switch to "ENGAGE".
Set Attitude Retention switch to "ATTD RETN".

17. Press FFS Disengage button on cyclic stick (either station) - check Attitude Retention switch OFF.

18. Engage FFS.

19. Check all FFS and SCAS lights OFF.

II. FFS Control Panel

Lights:

LONG - LAT - PEDAL

OFF	- lights out during normal operation (system engaged)
ON (RED)	- illuminates to indicate when the respective axis fails

DISENG

OFF	- lights out during normal operation (system engaged)
ON (AMBER)	- Automatically following a FFS failure (all three axis);

II. FFS Control Panel (Continued)

Lights:

ON (AMBER)	- all three lights on when system is manually disengaged by the pilot with either the disengage switch on the panel or the cyclic stick, FFS power switch on and master power on; - all three lights on when FFS power switch is set to SEC TRIM or OFF with master power on.

Note: No master caution light associated with the FFS.

Switches:

ON/SEC TRIM/OFF	- Three positions, used to apply power to the system. When in SEC TRIM, FFS is disengaged, pilot has secondary trim capability in the longitudinal axis only.
ENGAGE	- A solenoid held switch, spring loaded to disengage from the FFS disengage button on the cyclic stick or following a FFS failure. Pilot may also manually set switch to the disengage position (disengages all axes).
PEDAL TRIM	- Three position spring loaded to center. L - R indicates nose left or right. (Longitudinal and lateral trim are located on the cyclic stick.)
TEST	- Two-position toggle switch with a lever lock (nonfunctional for simulation)
FFS DISENGAGE	- Pushbutton located on the cyclic grip, used to manually disengage all axes simultaneously. Any time the FFS is disengaged, two methods of trim are available. If the FFS power switch is set

II. FFS Control Panel (Continued)

Switches:

FFS DISENGAGE	- for the SEC TRIM, secondary trim is available in longitudinal axis only. The FFS disengage button will always remove all forces regardless of the power switch selection and when the disengage button is released, the position of the controls at the time of release will be the new trim position. If the FFS disengage button on the cyclic stick is depressed and held, stick centering is available. FFS may be re-engaged by the engage switch on FFS panel if FFS was disengaged for some other reason than a failure.

Start Procedure:

Upon entering the aircraft, master power off and FFS power switch is OFF, all FFS lights will be off. Turn master power on, FFS power switch OFF, all DISENG lights will be illuminated. Turn on FFS power switch to power the system. Engage the FFS with the FFS ENGAGE switch system is then activated and DISENG lights will go out.

FFS Failures:

Primary	- LONG, LAT, or PEDAL lights will come on depending on which axis is failed. FFS is automatically disengaged for all axis and primary trim capability for all axes is lost. All three DISENG lights will be illuminated. Pilot must switch to SEC TRIM to obtain trim in longitudinal axis only. When power switch is set to SEC TRIM or OFF, FFS fail lights will go out. If pilot elects to bypass the secondary trim, he can depress the FFS disengage button on the cyclic for stick centering.

II. FFS Control Panel (Continued)

FFS Failures:

Secondary	- LONG, LAT, or PEDAL and all DISENG lights will remain the same as previous configuration but will have lost secondary trim capability.
Hydraulic	- Light status remains the same and trim status is the same as following secondary failure. If forces are applied to the controls, the FFS system will fail and auto trip. Fail/Disengage lights will appear. Forces in all failed cases will be limited to 25 pounds.

XV-15 FFS Pre-Flight Check List

Airplane status - engines running, electrical and hydraulic power ON - All FFS control panel switches assumed to be OFF, - Rudder pedals adjusted.

1. FFS "DISENG" lights, "LONG", "LATERAL" and "PEDAL" - check ON.

2. FFS Fail lights "LONG", "LATERAL" and "PEDAL" - check OFF.

3. Check cyclic stick for freedom of movement.

4. Check cyclic stick mechanical spring gradients qualitatively:

Long.	11 lb/in.
Lateral	3.4 lb/in.

5. Check rudder pedals for freedom of movement.

6. Set FFS Power Switch to "SEC TRIM". Check secondary trim operation in longitudinal axis - pilot and copilot.

7. Set FFS Power Switch to "ON". Depress disengage button and center controls.

II. FFS Control Panel (Continued)

XV-15 FFS Pre-Flight Check List

8. Set FFS engage switch to "ENGAGE" - check "DISENG" lights (3) OFF. Exercise controls and qualitatively check gradients.

Long.	2 lb/in.
Lateral	1 lb/in.
Pedal	7 lb/in.

9. Check primary trim in all three axes - pilot and copilot.

10. Set Fail Test Switch to "FAIL TEST" position. Check for FFS disengagement. Check fail lights "LONG", "LATERAL" and "PEDAL" ON. Check "DISENG" lights (3) ON.

11. Depress disengage button and center controls. "ENGAGE" FFS. Press pilot's FFS "DISENG" button. Check "DISENG" lights (3) ON. Check FFS bypass solenoid operation by pressing and holding pilot's FFS "DISENG" button while moving cyclic stick forward and aft. Upon button release, stick should lock except for mechanical spring gradient.

12. Repeat step 11 from copilot station. Depress disengage button and center controls.

13. Engage FFS, pilot or copilot, check for "DISENG" (3) and fail "LONG", "LATERAL", "PEDAL" lights OUT.

III. Rpm Governor Control Panel

Lights:

PRIMARY (A fail light)

OFF	- light out during normal operation (system engaged)
ON (RED)	- illuminates to indicate when primary governor fails. Light latches on failure and causes governor to switch to the stand-by mode. May be reset by re-engaging primary governor. If failure is not present, governor will re-engage. If failure is present, governor

III. Rpm Governor Control Panel (Continued)

ON (RED)	- will remain engaged only during the time of engagement. Fail cycle will begin after engage toggle switch is released.

PRIMARY OFF (A status light)

OFF	- light out during normal operation (system engaged) and master power off.
ON (AMBER)	- illuminates to indicate when primary governor is not engaged, master power on; - when system is manually disengaged by pilot from the governor disengage switch on collective; - following a primary governor failure.

STANDBY (A fail light)

OFF	- light out during normal operation with primary governor on; - light out during operations with standby governor on
ON (RED)	- illuminates to indicate when standby governor fails; - latches on failure and causes actuator to hydraulically lock at the present governor position - may be reset by engaging primary or standby governor. If failure is not present, governor will re-engage. If failure is present, governor will remain engaged only during the period of engagement; - during hydraulic failure (PC_2), a primary governor failure will bypass the standby and go directly to manual mode.

STANDBY ON (A status light)

OFF	- light out during normal operation with primary governor and following a standby governor failure

III. Rpm Governor Control Panel (Continued)

Lights:

ON (GREEN)	- illuminate when standby governor is active, whether engaged by the pilot or automatically following a primary governor failure.

Switches:

PRIMARY ENGAGE	- momentary on, used to activate the primary governor
STANDBY ENGAGE	- momentary on, used to activate the standby governor (non-functional for simulation)
TEST	- two position spring loaded guarded toggle (nonfunctional for simulation)
GOVERNOR DISENGAGE	- guarded pushbutton located on the collective head, used to manually disengage the rpm governor (primary and standby). PRIMARY OFF light will come on. All other panel lights will be off. Primary or standby governor may be re-engaged with either engage switch located on the RPM governor panel. Master caution lights will be on.

Start Procedure:

Upon entering the aircraft, master power off, all governor panel lights will be off. Turn master power on, PRIMARY OFF light will be on. Engage primary governor, light will go out, system (primary and standby) is then activated.

Rpm Governor Failures:

Primary	- PRIMARY, PRIMARY OFF, STANDBY ON, and CAUTION lights will come on indicating the primary governor has failed and system has switched to standby governor. Primary failure occurs if:

III. Rpm Governor Control Panel (Continued)

Rpm Governor Failures:

Primary

1. $\epsilon_{RPM} \geq \pm 3\%\ RPM_p^*$, and sign $\dot{\theta}_{ACT} \neq$ sign ϵ_{RPM}, or $|\dot{\theta}_{ACT}| < .4^\circ/SEC$

2. $\epsilon_{RPM} \geq \pm 10\%\ RPM_p$

*RPM_p is the rpm commanded by the pilot using the rpm beep switch located on the collective head. RPM_p limits are:

$$RPM_{p_{MAX}} = 601$$

$$RPM_{p_{MIN}} = 433 + 102 \cos \beta m$$

Standby

- same as primary except STANDBY ON light will go out and STANDBY light will come on indicating standby governor failure and standby governor has been switched off. RPM can then be controlled manually by the pilot using the rpm wheel located on the center console. The secondary governor is preset to 565 rpm (94%). RPM is changed in going from RPM_p to 565 rpm at a 20 RPM per second rate. The secondary governor will fail if:

$$\epsilon_{RPM} \geq \pm 10\%\ 565$$

IV. Additional Lights/Switches

RPM Warning Light:

"RPM" light on instrument panel and audio will come on indicating rpm is out of the following limits:

1. Nacelle unlocked $\Omega L/R > 625$ or $\Omega L/R < 535$
2. Nacelle locked (no audio) $\Omega L/R > 625$ or $\Omega L/R < 415$

IV. Additional Lights/Switches (Continued)

Gear Warning Light:

"GEAR" light on instrument panel will come on indicating the gear should be lowered because of the following limits:

1. Gear up $h_p < 200$ ft and $V_T < 100$ kts

"WHEELS" light will also illuminate on the center panel of the instrument panel.

Conversion Guide:

Lights will illuminate on the conversion guide located on the center of the glare shield to indicate the attitude of the aircraft during conversion. Green light indicates normal attitude, green plus amber indicates marginal and to either bring the nose of the aircraft up or down. Solid amber indicates approach to stall or increasing blade loads and to again change the attitude of the aircraft. Attitude of the aircraft can be changed with nacelle incidence or longitudinal stick. The lights are set for the following limits:

1.	α_F +4 to −2 deg	Green ON
2.	α_F +4 to +8 deg	Green ON plus upper amber
	−2 to −6 deg	Green ON plus lower amber
3.	α_F > +8 deg	Upper amber ON
	> −6 deg	Lower amber ON

Conversion guide is functional only for $V_T > 80$ knots.

RPM Increase/Decrease:

RPM can be commanded by the pilot from 80 to 100 percent with nacelles at 90 deg or from 72 to 100 percent with nacelles at 0 deg (100 percent RPM = 601 rpm). Normal operating rpm values for the XV-15 are:

1. 589 rpm in helicopter, conversion, and high RPM airplane mode

2. 517 rpm in cruise airplane mode

9	CG AND INERTIA

Inputs: Variables		Outputs:	
From Subsystem	Symbol	To Subsystem	Symbol
8a	β_m	1, 5, 6, 7	SL_{CG} WL_{CG}
	$\dot{\beta}_m$	11, 14	
		10f	WL_{CG}
10f	h_{CG}	11	$\dot{X}_{CG}$
			$\dot{Z}_{CG}$
			$\ddot{X}_{CG}$
			$\ddot{Z}_{CG}$
			$\dot{q}_{\beta_m}$
			I_{XX} I_{YY} I_{ZZ} I_{XZ}
		1, 14	h_H
		12	$\ddot{X}_{CG}$
			$\ddot{Z}_{CG}$

Inputs: Constants, Coefficients, and Data Tables

Constants: W_P, GW, SL_{SP}, SL_P, WL_{SP}, WL_P, $SL_{CG}\big|_{\beta_m=0}$, $WL_{CG}\big|_{\beta_m=0}$
l_m, $I_{XX}\big|_{\beta_m=0}$, $I_{YY}\big|_{\beta_m=0}$, $I_{ZZ}\big|_{\beta_m=0}$, $I_{XZ}\big|_{\beta_m=0}$,
L_N, I_{PYL}, λ_{PYL}

Coefficients: K_{I1}, K_{I2}, K_{I3}, K_{I4}

Data Tables: None

SUBSYSTEM NO. 9: CG AND INERTIA

Inputs: Variables

Symbol	Description	Units
β_m	Mast conversion angle (+ fwd, 0 deg = vertical or helicopter, 90 deg = horizontal or airplane)	rad
$\dot{\beta}_m$	Mast conversion rate for a tilt rotor	rad/sec
h_{CG}	Altitude of rotorcraft	ft

Inputs: Constants, Coefficients, and Data Tables

W_P	Weight of both pylons for a tilt rotor	lb
GW	Total rotorcraft gross weight	lb
SL_{SP}	Station line of engine nacelle shaft pivot point for a tilt rotor	in
SL_P	Station line of pylon center of gravity for a tilt rotor	in
WL_{SP}	Water line of engine nacelle shaft pivot point for a tilt rotor	in
WL_P	Water line of pylon center of gravity for a tilt rotor	in
$SL_{CG}\big\vert_{\beta_m=0}$	Station line of helicopter mode c.g.	in
$WL_{CG}\big\vert_{\beta_m=0}$	Water line of helicopter mode c.g.	in
l_m	Mast length for a tilt rotor	ft
$I_{XX}\big\vert_{\beta_m=0}$	Helicopter mode rolling moment of inertia, body axis	slug-ft^2
$I_{YY}\big\vert_{\beta_m=0}$	Helicopter mode pitching moment of inertia, body axis	slug-ft^2
$I_{ZZ}\big\vert_{\beta_m=0}$	Helicopter mode yawing moment of inertia, body axis	slug-ft^2

Inputs: Constants, Coefficients, and Data Tables (Concluded)

Symbol	Description	Units
$I_{XZ}\big\vert_{\beta_m=0}$	Helicopter mode product of inertia, body axis	slug-ft^2
L_N	Distance from the pylon pivot axis to the pylon c.g. for a tilt rotor	ft
I_{PYL}	Moment of inertia of the nacelle/pylon for a tilt rotor	slug-ft^2
λ_{PYL}	Angle between the fuselage water line reference and L_N at $\beta_m = 0$ for a tilt rotor	deg
K_{I1}	Roll inertia coefficient for varying inertia with mast angle for a tilt rotor	$\frac{\text{slug-ft}^2}{\text{deg}}$
K_{I2}	Pitch inertia coefficient for varying inertia with mast angle for a tilt rotor	$\frac{\text{slug-ft}^2}{\text{deg}}$
K_{I3}	Yaw inertia coefficient for varying inertia with mast angle for a tilt rotor	$\frac{\text{slug-ft}^2}{\text{deg}}$
K_{I4}	Product of inertia coefficient for varying inertia with mast angle for a tilt rotor	$\frac{\text{slug-ft}^2}{\text{deg}}$

Outputs:

SL_{CG}	Station line of c.g.	in
WL_{CG}	Water line of c.g.	in
$\dot{X}_{CG}$	Rate of longitudinal c.g. displacement as a function of mast tilt angle for a tilt rotor	in/sec

SUBSYSTEM NO. 9: CG AND INERTIA (Concluded)

Outputs: (Concluded)

Symbol	Description	Units
$\dot{Z}_{CG}$	Rate of vertical c.g. displacement as a function of mast tilt angle for a tilt rotor	in/sec
$\ddot{X}_{CG}$	Acceleration of longitudinal c.g. displacement as a function of mast tilt angle for a tilt rotor	in/sec^2
$\ddot{Z}_{CG}$	Acceleration of vertical c.g. displacement as a function of mast tilt angle for a tilt rotor	in/sec^2
$\dot{q}_{\beta_m}$	Pitch acceleration due to pylon tilt for a tilt rotor	rad/sec^2
I_{XX}	Rolling moment of inertia about c.g.	slug-ft^2
I_{YY}	Pitching moment of inertia about c.g.	slug-ft^2
I_{ZZ}	Yawing moment of inertia about c.g.	slug-ft^2
I_{XZ}	Product of inertia about c.g.	slug-ft^2
h_H	Rotor hub height from ground	ft

EQUATIONS

SUBSYSTEM NO. 9—CG AND INERTIA

A. CG Displacement as a Function of Pylon Tilt Angle

$$X_{CG} = Z\left(\sin \beta_m\right) + X\left(1 - \cos \beta_m\right)$$

$$Z_{CG} = Z\left(1 - \cos \beta_m\right) - X\left(\sin \beta_m\right)$$

Where

$$X = \left(\frac{W_P}{GW}\right)\left(SL_{SP} - SL_P\right)/12$$

$$Z = \left(\frac{W_P}{GW}\right)\left(WL_{SP} - WL_P\right)/12$$

B. CG Location

$$SL_{CG} = SL_{CG}\Big|_{\beta_m=0} + (12)\left(X_{CG}\right)$$

$$WL_{CG} = WL_{CG}\Big|_{\beta_m=0} + (12)\left(Z_{CG}\right)$$

C. Rotor Hub Height From Ground

$$h_H = h_{CG} + \left[l_m \cos \beta_m + \frac{\left(WL_{SP} - WL_{CG}\right)}{12}\right]$$

D. CG Velocity Due to Pylon Tilt Rate

$$\dot{X}_{CG} = Z\left(\dot{\beta}_m\right)\left(\cos \beta_m\right) + X\left(\dot{\beta}_m\right)\left(\sin \beta_m\right)$$

$$\dot{Z}_{CG} = Z\left(\dot{\beta}_m\right)\left(\sin \beta_m\right) - X\left(\dot{\beta}_m\right)\left(\cos \beta_m\right)$$

E. CG Acceleration

$$\ddot{X}_{CG} = Z\ddot{\beta}_m \cos \beta_m - Z\dot{\beta}_m^2 \sin \beta_m + X\ddot{\beta}_m \sin \beta_m + X\dot{\beta}_m^2 \cos \beta_m$$

$$\ddot{Z}_{CG} = Z\ddot{\beta}_m \sin \beta_m + Z\dot{\beta}_m^2 \cos \beta_m - X\ddot{\beta}_m \cos \beta_m + X\dot{\beta}_m^2 \sin \beta_m$$

F. Pitch Acceleration Due to Pylon Tilt

$$\dot{q}_{\beta_m} = \frac{\ddot{\beta}_m}{I_{YY}} \left\{2I_{PYL} + 2\left(\frac{W_p}{32.2}\right)\left(\frac{GW-W_p}{GW}\right)\left[L_N^2 + L_N\left(h_M \sin \lambda - \ell_M \cos \lambda\right)\right]\right\}$$

where

$$\lambda = \left(\frac{\lambda_{PYL}}{57.3}\right) - \beta_m$$

$$\ell_M = \left(\frac{GW}{GW-W_p}\right)\left[\frac{X_{CG}}{12} - 2\left(\frac{W_p}{GW}\right)\left(L_N \cos \lambda\right)\right]$$

$$h_M = \left(\frac{GW}{GW-W_p}\right)\left[\frac{Z_{CG}}{12} + 2\left(\frac{W_P}{GW}\right)\left(L_N \sin \lambda\right)\right]$$

G. Aircraft Inertia Change Due to Pylon Tilt

$$I_{XX} = I_{XX}\Big|_{\beta_m=0} - K_{I1}\beta_m$$

$$I_{YY} = I_{YY}\Big|_{\beta_m=0} - K_{I2}\beta_m$$

G. Aircraft Inertia Change Due to Pylon Tilt (Concluded)

$$I_{ZZ} = I_{ZZ}\Big|_{\beta_m=0} + K_{I3}\beta_m$$

$$I_{XZ} = I_{XZ}\Big|_{\beta_m=0} - K_{I4}\beta_m$$

10a	AXES TRANSFORMATION (AIRFRAME AERODYNAMIC FORCES AND MOMENTS FROM WIND TO BODY AXIS)

Inputs: Variables		Outputs:	
From Subsystem	**Symbol**	**To Subsystem**	**Symbol**
12	α_F	13, 14	$(X,Y,Z)_F$
	β_F		$(X,Z)_{iWPL}$
3	L_F		$(X,Z)_{iWPR}$
	D_F		$(X,Y,Z)_{WP}$
	Y'_F		$(X,Y,Z)_H$
	l'_F		$(X,Y,Z)_{MG}$
	M'_F		$(X,Y,Z)_{NG}$
	N'_F		$(X,Y,Z)_V(i)$
4	α_{iWL}		$(X,Y,Z)_{SD}$
	β_{iWL}		$(X,Z)_{iPYL}$
	L_{iWPL}		$(X,Y,Z)_{PYLT}$
	D_{iWPL}		
	α_{iWR}	14	$(l,M,N)_F$
	β_{iWR}		$(l,M,N)_{WP}$
	L_{iWPR}		$(l,M,N)_H$
	D_{iWPR}		
	α_{WFS}		
	L_{WP}		
	D_{WP}		

(continued on next page)

10a	AXES TRANSFORMATION (AIRFRAME AERODYNAMIC FORCES AND MOMENTS FROM WIND TO BODY AXIS) (CONTINUED)

Inputs: Variables		Outputs:	
From Subsystem	Symbol	To Subsystem	Symbol
4 (concluded)	M'_{WP}		
	Y'_{WP}		
	l'_{WP}		
	N'_{WP}		
	SD		
	D_{PYLN}		
	D_{PLAT}		
	α_{SP}		
	β_{SP}		
	α_{PLAT}		
	β_{PLAT}		
5	α_H		
	L_H		
	D_H		
	M'_H		
6	$\beta_V(i)$		
	$Y'_V(i)$		
	$D_V(i)$		
7	D_{MG}		
	D_{NG}		

(Concluded on next page)

10a	AXES TRANSFORMATION (AIRFRAME AERODYNAMIC FORCES AND MOMENTS FROM WIND TO BODY AXIS) (CONCLUDED)

Inputs: Constants, Coefficients, and Data Tables

Constants: NVSTAB

Coefficients: None

Data Tables: None

SUBSYSTEM NO. 10a--AXES TRANSFORMATION (AIRFRAME AERODYNAMIC FORCES AND MOMENTS FROM WIND TO BODY AXIS)

Inputs: Variables

Symbol	Description	Units
α_F	Fuselage angle of attack	rad
β_F	Fuselage sideslip angle	rad
L_F	Aerodynamic lift on fuselage (wind axis)	lb
D_F	Aerodynamic drag on fuselage (wind axis)	lb
Y_F'	Aerodynamic side force on fuselage (wind axis)	lb
l_F'	Aerodynamic rolling moment on fuselage (wind axis)	ft-lb
M_F'	Aerodynamic pitching moment on fuselage (wind axis)	ft-lb
N_F'	Aerodynamic yawing moment on fuselage (wind axis)	ft-lb
α_{iWL}	Angle of attack of the left wing portion immersed in the left rotor wake	rad
β_{iWL}	Sideslip angle of the left wing portion immersed in the left rotor wake	rad
L_{iWPL}	Aerodynamic lift of the left wing portion immersed in the rotor wake	lb
D_{iWPL}	Aerodynamic drag of the left wing portion immersed in the rotor wake	lb
α_{iWR}	Angle of attack of the right wing portion immersed in the right rotor wake	rad

Inputs: Variables (Continued)

Symbol	Description	Units
β_{iWR}	Sideslip angle of the right wing portion immersed in the right rotor wake	rad
L_{iWPR}	Aerodynamic lift of the right wing portion immersed in the rotor wake	lb
D_{iWPR}	Aerodynamic drag of the right wing portion immersed in the rotor wake	lb
α_{WFS}	Angle of attack of the wing portion outside the rotor wake (freestream)	rad
L_{WP}	Aerodynamic lift on the wing portion outside the rotor wake (freestream)	lb
D_{WP}	Aerodynamic drag on the wing portion outside the rotor wake (freestream)'	lb
M'_{WP}	Pitching moment of the wing-pylon in wind axis	ft-lb
Y'_{WP}	Side force moment of the wing-pylon in wind axis	lb
l'_{WP}	Rolling moment of the wing-pylon in wind axis	ft-lb
N'_{WP}	Yawing moment of the wing-pylon in wind axis	ft-lb
SD	Spinner drag	lb
D_{PYLN}	Pylon interference drag	lb
D_{PLAT}	Lateral pylon drag	lb
α_{SP}	Spinner angle of attack used for transformation from wind to body axis	rad

Inputs: Variables (Concluded)

Symbol	Description	Units
β_{SP}	Spinner sideslip angle used for transformation from wind to body axis	rad
α_{PLAT}	Pylon angle of attack used for transformation from wind to body axis	rad
β_{PLAT}	Pylon sideslip angle used for transformation from wind to body axis	rad
α_H	Horizontal stabilizer angle of attack	lb
L_H	Aerodynamic lift on the horizontal stabilizer	lb
D_H	Aerodynamic drag on the horizontal stabilizer	lb
M'_H	Aerodynamic pitching moment on the horizontal stabilizer	ft-lb
$B_V(i)$	Zero rudder sideslip angle	deg
$Y'_V c(i)$	Aerodynamic side force (lift) on the vertical fin in wind axis	lb
$D_V(i)$	Aerodynamic drag on the vertical fin (wind axis)	lb
D_{MG}	Aerodynamic drag on the main landing gear	lb
D_{NG}	Aerodynamic drag on the nose landing gear	lb

Inputs: Constants, Coefficients, and Data Tables

Symbol	Description	Units
NVSTAB	Number of vertical stabilizers	ND

Outputs:

$(X,Y,Z)_F$	Aerodynamic forces on the fuselage, body axis	lb
$(X,Z)_{iWPL}$	Aerodynamic forces on the portion of the left wing-pylon in the rotor wake, body axis	lb
$(X,Z)_{iWPR}$	Aerodynamic forces on the portion of the right wing-pylon in the rotor wake, body axis	lb
$(X,Y,Z)_{WP}$	Aerodynamic forces on the wing-pylon portion in the freestream, body axis	lb
$(X,Y,Z)_H$	Aerodynamic forces on the horizontal stabilizer, body axis	lb
$(X,Y,Z)_{MG}$	Aerodynamic forces on the main landing gear, body axis	lb
$(X,Y,Z)_{NG}$	Aerodynamic forces on the nose landing gear, body axis	lb
$(X,Y,Z)_V(i)$	Aerodynamic forces on the vertical stabilizer, body axis	lb
$(X,Y,Z)_{SD}$	Spinner drag aerodynamic forces, body axis	lb
$(X,Z)_{iPYL}$	Pylon interference drag aerodynamic forces, body axis	lb

SUBSYSTEM NO. 10a--AXES TRANSFORMATION (AIRFRAME AERODYNAMIC FORCES AND MOMENTS FROM WIND TO BODY AXIS) (CONCLUDED)

Outputs: (Concluded)

Symbol	Description	Units
$(X,Y,Z)_{PYLT}$	Lateral pylon drag model aerodynamic forces, body axis	lb
$(l,M,N)_F$	Rolling, pitching, and yawing aerodynamic moments on the fuselage about the body x-, y-, and z-axes	ft-lb
$(l,M,N)_{WP}$	Rolling, pitching, and yawing aerodynamic moments due to the wing-pylon about the body x-, y-, and z-axes	ft-lb
$(l,M,N)_H$	Rolling, pitching, and yawing aerodynamic moments due to the horizontal stabilizer about the body x-, y-, and z-axes	ft-lb

EQUATIONS

SUBSYSTEM 10a--AXES TRANSFORMATION (AIRFRAME AERODYNAMIC FORCES AND MOMENTS FROM WIND TO BODY AXIS)

A. General Form of Transformation

$$\begin{bmatrix} X_i \\ Y_i \\ Z_i \end{bmatrix}_{\substack{\text{Body}\\\text{Axis}}} = \begin{bmatrix} \cos\alpha_i \cos\beta_i & -\cos\alpha_i \sin\beta_i & -\sin\alpha_i \\ \sin\beta_i & \cos\beta_i & 0 \\ \sin\alpha_i \cos\beta_i & -\sin\alpha_i \sin\beta_i & \cos\alpha_i \end{bmatrix} \begin{bmatrix} -X_i \\ Y_i \\ -Z_i \end{bmatrix}_{\substack{\text{Wind}\\\text{Axis}}}$$

This transformation matrix is also used for the moment transformation. α_i and β_i are the individual component angles of attack and sideslip, respectively.

B. Transformation of Fuselage Forces and Moments

$$X_F = -D_F \cos\alpha_F \cos\beta_F - Y'_F \cos\alpha_F \sin\beta_F + L_F \sin\alpha_F$$

$$Y_F = -D_F \sin\beta_F + Y'_F \cos\beta_F$$

$$Z_F = -D_F \sin\alpha_F \cos\beta_F - Y'_F \sin\alpha_F \sin\beta_F - L_F \cos\alpha_F$$

$$l_F = l'_F \cos\alpha_F \cos\beta_F - M'_F \cos\alpha_F \sin\beta_F - N'_F \sin\alpha_F$$

$$M_F = l'_F \sin\beta_F + M'_F \cos\beta_F$$

$$N_F = l'_F \sin\alpha_F \cos\beta_F - M'_F \sin\alpha_F \sin\beta_F + N'_F \cos\alpha_F$$

SUBSYSTEM 10a--AXES TRANSFORMATION (AIRFRAME AERODYNAMIC FORCES AND MOMENTS FROM WIND TO BODY AXIS)

C. Transformation of Wing Forces and Moments

1. Forces Generated by Rotor Wake

$$X_{iWPK} = -D_{iWPK} \cos\alpha_{iWK} \left[\overset{\to 1}{\cos\beta_{iWK}} \right] + L_{iWPK} \sin\alpha_{iWK}$$

$$Y_{iWPK} = -D_{iWPK} \left[\overset{\to 0}{\sin\beta_{iWK}} \right]$$

$$Z_{iWPK} = -D_{iWPK} \sin\alpha_{iWK} \left[\overset{\to 1}{\cos\beta_{iWK}} \right] - L_{iWPK} \cos\alpha_{iWK}$$

(For right rotor K = R, for left rotor K = L)

2. Forces and Moments Generated by Freestream Flow

$$X_{WP} = -D_{WP} \cos\alpha_{WFS} \left[\overset{\to 1}{\cos\beta_F} \right] - Y'_{WP} \cos\alpha_{WFS} \left[\overset{\to 0}{\sin\beta_F} \right] + L_{WP} \sin\alpha_{WFS}$$

$$Y_{WP} = -D_{WP} \sin\beta_F + Y'_{WP} \left[\overset{\to 1}{\cos\beta_F} \right]$$

$$Z_{WP} = -D_{WP} \sin\alpha_{WFS} \left[\overset{\to 1}{\cos\beta_F} \right] - Y'_{WP} \sin\alpha_{WFS} \left[\overset{\to 0}{\sin\beta_F} \right] - L_{WP} \cos\alpha_{WFS}$$

NOTE: $\left[\overset{\to 1}{\cos\beta_F} \right]$ means this term is assumed to equal 1 when programmed.

$\left[\overset{\to 0}{\sin\beta_F} \right]$ means this term is assumed to equal 0 when programmed.

2. Forces and Moments Generated by Freestream Flow (Concluded)

$$l_{WP} = l'_{WP} \cos\alpha_{WFS} \left[\overset{\to 1}{\cos\beta_F} \right] - M'_{WP} \cos\alpha_{WFS} \left[\overset{\to 0}{\sin\beta_F} \right] - N'_{WP} \sin\alpha_{WFS}$$

$$M_{WP} = l'_{WP} \left[\overset{\to 0}{\sin\beta_F} \right] + M'_{WP} \left[\overset{\to 1}{\cos\beta_F} \right]$$

$$N_{WP} = l'_{WP} \sin\alpha_{WFS} \left[\overset{\to 1}{\cos\beta_F} \right] - M'_{WP} \sin\alpha_{WFS} \left[\overset{\to 0}{\sin\beta_F} \right] + N'_{WP} \cos\alpha_{WFS}$$

D. <u>Transformation of Horizontal Stabilizer Forces and Moments</u>

$$X_H = -D_H \cos\alpha_H \left[\overset{\to 1}{\cos\beta_F} \right] + L_H \sin\alpha_H$$

$$Y_H = -D_H \left[\overset{\to 0}{\sin\beta_F} \right]$$

$$Z_H = -D_H \sin\alpha_H \left[\overset{\to 1}{\cos\beta_F} \right] - L_H \cos\alpha_H$$

$$l_H = -M'_H \cos\alpha_H \left[\overset{\to 0}{\sin\beta_F} \right]$$

$$M_H = M'_H \left[\overset{\to 1}{\cos\beta_F} \right]$$

$$N_H = -M'_H \sin\alpha_H \left[\overset{\to 0}{\sin\beta_F} \right]$$

SUBSYSTEM 10a--AXES TRANSFORMATION (AIRFRAME AERODYNAMIC FORCES AND MOMENTS FROM WIND TO BODY AXIS)

E. Transformation of Vertical Stabilizer Forces

$$X_V(i) = -D_V(i)\left[\overset{\to 1}{\cos\alpha_H}\right]\cos\beta_V(i) + Y'_V(i)\left[\overset{\to 1}{\cos\alpha_H}\right]\sin\beta_V(i)$$

$$Y_V(i) = -D_V(i)\sin\beta_V(i) - Y'_V(i)\cos\beta_V(i)$$

$$Z_V(i) = -D_V(i)\left[\overset{\to 0}{\sin\alpha_H}\right]\cos\beta_V(i) + Y'_V(i)\left[\overset{\to 0}{\sin\alpha_H}\right]\sin\beta_V(i)$$

where

i = 1 to NVSTAB

NOTE: $\left[\overset{\to 1}{\cos\alpha_H}\right]$ means this term is assumed to equal 1 when programmed.

$\left[\overset{\to 0}{\sin\alpha_H}\right]$ means this term is assumed to equal 0 when programmed.

F. Transformation of Main Landing Gear Aerodynamic Forces

$$X_{MG} = -D_{MG}\cos\alpha_F\cos\beta_F$$

$$Y_{MG} = -D_{MG}\sin\beta_F$$

$$Z_{MG} = -D_{MG}\sin\alpha_F\cos\beta_F$$

SUBSYSTEM 10a--AXES TRANSFORMATION (AIRFRAME AERODYNAMIC FORCES AND MOMENTS FROM WIND TO BODY AXIS)

G. Transformation of Nose Landing Gear Aerodynamic Forces

$$X_{NG} = -D_{NG} \cos \alpha_F \cos \beta_F$$

$$Y_{NG} = -D_{NG} \sin \beta_F$$

$$Z_{NG} = -D_{NG} \sin \alpha_F \cos \beta_F$$

H. Transformation of Spinner Drag Force

$$X_{SD} = -SD \cos \alpha_{SP} \cos \beta_{SP}$$

$$Y_{SD} = -SD \sin \beta_{SP}$$

$$Z_{SD} = -SD \sin \alpha_{SP} \cos \beta_{SP}$$

I. Transformation of Pylon Interference Drag Force

$$X_{iPYL} = -D_{PYLN} \left[\cos \left(\frac{\alpha_{iWR} + \alpha_{iWL}}{2} \right) \right]$$

$$Z_{iPYL} = -D_{PYLN} \left[\sin \left(\frac{\alpha_{iWR} + \alpha_{iWL}}{2} \right) \right]$$

J. Transformation of Lateral Pylon Drag

$$X_{PYLT} = -D_{PLAT} \cos \alpha_{PLAT} \cos \beta_{PLAT}$$

$$Y_{PYLT} = -D_{PLAT} \sin \beta_{PLAT}$$

$$Z_{PYLT} = -D_{PLAT} \sin \alpha_{PLAT} \cos \beta_{PLAT}$$

10b	AXES TRANSFORMATION (ROTOR FORCES AND MOMENTS FROM WIND TO BODY AXIS)

Inputs: Variables

From Subsystem	Symbol
1	T_R
	H_R
	Y_R
	Q_R
	M_{a1R}
	l_{b1R}
	T_L
	H_L
	Y_L
	Q_L
	M_{a1L}
	l_{b1L}
8a	β_m

Outputs:

To Subsystem	Symbol
13, 14	$(X,Y,Z)_R$
	$(X,Y,Z)_L$
1	X_R
	X_L
14	$(l,M,N)_R$
	$(l,M,N)_L$

Inputs: Constants, Coefficients, and Data Tables

Constants: ϕ_m

Coefficients: None

Data Tables: None

SUBSYSTEM NO. 10b: AXES TRANSFORMATION (ROTOR FORCES AND MOMENTS FROM WIND TO BODY AXIS)

Inputs: Variables

Symbol	Description	Units
T_R	Mast axis right rotor thrust (+ up for helicopter)	lb
H_R	Mast axis H-force right rotor (+ aft for helicopter)	lb
Y_R	Mast axis Y-force right rotor (+ right for helicopter)	lb
Q_R	Mast axis right rotor torque (+ trying to slow rotor down)	ft-lb
$M_{a_{1R}}$	Mast axis longitudinal flapping restraint exerted by right rotor on airframe (+ nose up for helicopter)	ft-lb
$l_{b_{1R}}$	Mast axis lateral flapping restraint exerted by right rotor on airframe (+ outboard for helicopter)	ft-lb
T_L	Mast axis left rotor thrust (+ up for helicopter)	lb
H_L	Mast axis H-force left rotor (+ aft for helicopter)	lb
Y_L	Mast axis Y-force left rotor (+ right for helicopter)	lb
Q_L	Mast axis left rotor torque (+ trying to slow rotor down)	ft-lb
$M_{a_{1L}}$	Mast axis longitudinal flapping restraint exerted by left rotor on airframe (+ nose up for helicopter)	ft-lb
$l_{b_{1L}}$	Mast axis lateral flapping restraint exerted by left rotor on airframe (+ outboard for helicopter)	ft-lb

SUBSYSTEM NO. 10b: AXES TRANSFORMATION (ROTOR FORCES AND MOMENTS FROM WIND TO BODY AXIS) (CONCLUDED)

Inputs: Variables (Concluded)

Symbol	Description	Units
β_m	Mast conversion angle (+ fwd, 0 deg = vertical or helicopter, 90 deg = horizontal or airplane)	rad

Inputs: Constants, Coefficients, and Data Tables

ϕ_m	Lateral mast tilt	rad

Outputs:

$(X,Y,Z)_R$	Right rotor forces in body axis	lb
$(X,Y,Z)_L$	Left rotor forces in body axis	lb
$(l,M,N)_R$	Rolling, pitching, and yawing moments due to the right rotor about the body x-, y-, and z-axes	ft-lb
$(l,M,N)_L$	Rolling, pitching, and yawing moments due to the left rotor about the body x-, y-, and z-axes	ft-lb

EQUATIONS

SUBSYSTEM 10b--AXES TRANSFORMATION (ROTOR FORCES AND MOMENTS FROM WIND TO BODY AXIS)

A. Right Rotor

$$X_R = -H_R \cos\beta_m \cos\phi_m - Y_R \sin\beta_m \sin\phi_m + T_R \sin\beta_m \cos\phi_m$$

$$Y_R = H_R \sin\beta_m \sin\phi_m + Y_R \cos\phi_m \qquad + T_R \cos\beta_m \sin\phi_m$$

$$Z_R = -H_R \sin\beta_m \cos\phi_m + Y_R \cos\beta_m \sin\phi_m - T_R \cos\beta_m \cos\phi_m$$

$$l_R = l_{b1R} \cos\beta_m \cos\phi_m - M_{a1R} \sin\beta_m \sin\phi_m - Q_R \sin\beta_m \cos\phi_m$$

$$M_R = -l_{b1R} \sin\beta_m \sin\phi_m + M_{a1R} \cos\phi_m - Q_R \cos\beta_m \sin\phi_m$$

$$N_R = l_{b1R} \sin\beta_m \cos\phi_m + M_{a1R} \cos\beta_m \sin\phi_m + Q_R \cos\beta_m \cos\phi_m$$

B. Left Rotor

$$X_L = -H_L \cos\beta_m \cos\phi_m - Y_L \sin\beta_m \sin\phi_m + T_L \sin\beta_m \cos\phi_m$$

$$Y_L = -H_L \sin\beta_m \sin\phi_m - Y_L \cos\phi_m \qquad - T_L \cos\beta_m \sin\phi_m$$

$$Z_L = -H_L \sin\beta_m \cos\phi_m + Y_L \cos\beta_m \sin\phi_m - T_L \cos\beta_m \cos\phi_m$$

$$l_L = -l_{b1L} \cos\beta_m \cos\phi_m - M_{a1L} \sin\beta_m \sin\phi_m + Q_L \sin\beta_m \cos\phi_m$$

$$M_L = l_{b1L} \sin\beta_m \sin\phi_m + M_{a1L} \cos\phi_m + Q_L \cos\beta_m \sin\phi_m$$

$$N_L = -l_{b1L} \sin\beta_m \cos\phi_m + M_{a1L} \cos\beta_m \sin\phi_m - Q_L \cos\beta_m \cos\phi_m$$

10c	AXES TRANSFORMATION (EULER ANGLES)

Inputs: Variables		Outputs:	
From Subsystem	Symbol	To Subsystem	Symbol
11	p q r	16	$\dot{\theta}$
10c	ψ θ ϕ	16, 7A	$\dot{\phi}$ $\dot{\psi}$
		10c, 10d	θ ϕ
		12, 16, 7	ψ
		20, VFA	
		14	ϕ

Inputs: Constants, Coefficients, and Data Tables

None

SUBSYSTEM NO. 10c—AXES TRANSFORMATION (EULER ANGLES)

Input: Variables

Symbol	Description	Units
p	Body axis roll rate	rad/sec
q	Body axis pitch rate	rad/sec
r	Body axis yaw rate	rad/sec
θ	Euler pitch angle	rad
ϕ	Euler roll angle	rad
ψ	Euler yaw angle	rad

Outputs:

$\dot{\theta}$	Rate of change of Euler pitch angle	rad/sec
$\dot{\phi}$	Rate of change of Euler roll angle	rad/sec
$\dot{\psi}$	Rate of change of Euler yaw angle	rad/sec
θ	Euler pitch angle	rad
ϕ	Euler roll angle	rad
ψ	Euler yaw angle	rad

EQUATIONS:

$$\dot{\theta} = q \cos \phi - r \sin \phi$$

$$\dot{\phi} = p + r \tan \theta \cos \phi + q \tan \theta \sin \phi$$

$$\dot{\Psi} = \frac{r \cos \phi + q \sin \phi}{\cos \theta}$$

$$\theta = \int \dot{\theta} \, dt$$

$$\phi = \int \dot{\phi} \, dt$$

$$\Psi = \int \dot{\Psi} \, dt$$

10d	AXES TRANSFORMATION (EARTH BASED VELOCITY)

Inputs: Variables		Outputs:	
From Subsystem	Symbol	To Subsystem	Symbol
10c	ψ θ ϕ	10e	U_{EB} V_{EB} W_{EB}
12	U V W		

Inputs: Constants, Coefficients, and Data Tables

None

SUBSYSTEM NO. 10d—AXES TRANSFORMATION (EARTH BASED VELOCITIES)

Input: Variables

Symbol	Description	Units
θ	Euler pitch angle	rad
ϕ	Euler roll angle	rad
ψ	Euler yaw angle	rad
U	x-velocity (longitudinal) of the aircraft c.g. in body axis with respect to the air	ft/sec
V	y-velocity (lateral) of the aircraft c.g. in body axis with respect to the air	ft/sec
W	z-velocity (vertical) of the aircraft c.g. in body axis with respect to the air	ft/sec

Outputs:

U_{EB}	x-velocity component of the aircraft c.g. with respect to the air along earth axes	ft/sec
V_{EB}	y-velocity component of the aircraft c.g. with respect to the air along earth axes	ft/sec
W_{EB}	z-velocity component of the aircraft c.g. with respect to the air along earth axes	ft/sec

EQUATIONS:

$$U_{EB} = U \cos \Psi \cos \theta + V \cos \Psi \sin \theta \sin \phi - V \sin \Psi \cos \phi + W \cos \Psi \sin \theta \cos \phi + W \sin \Psi \sin \phi - U \text{ wind } E$$

$$V_{EB} = U \sin \Psi \cos \theta + V \cos \Psi \cos \phi + V \sin \Psi \sin \theta \sin \phi + W \sin \Psi \sin \theta \cos \phi - W \cos \Psi \sin \phi - V \text{ wind } E$$

$$W_{EB} = -U \sin \theta + V \cos \theta \sin \phi + W \cos \theta \cos \phi + W \text{ wind } E$$

10e	AXES TRANSFORMATION (GROUND VELOCITY SUMMATION)

Inputs: Variables		Outputs:	
From Subsystem	Symbol	To Subsystem	Symbol
Wind	U_W θ_W ψ_W	VFA, 10f	U_G V_G W_G
10d	U_{EB} V_{EB} W_{EB}		

Inputs: Constants, Coefficients, and Variables

None

SUBSYSTEM NO. 10e—AXES TRANSFORMATION (GROUND VELOCITY SUMMATION)

Input: Variables

Symbol	Description	Units
U_W	Wind x-velocity with respect to the ground	ft/sec
θ_W	Euler pitch angle of wind	rad
ψ_W	Grid heading of wind (+ clockwise from North)	rad
U_{EB}	x-velocity component of the aircraft c.g. with respect to the air along earth axes	ft/sec
V_{EB}	y-velocity component of the aircraft c.g. with respect to the air along earth axes	ft/sec
W_{EB}	z-velocity component of the aircraft c.g. with respect to the air along earth axes	ft/sec

Outputs:

U_G	x-velocity ground component of aircraft c.g.	ft/sec
V_G	y-velocity ground component of aircraft c.g.	ft/sec
W_G	z-velocity ground component of aircraft c.g.	ft/sec

EQUATIONS:

$$U_{WE} = U_W \ (\cos \Psi_W \cos \theta_W)$$

$$V_{WE} = U_W \ (\sin \Psi_W)$$

$$W_{WE} = U_W \ (\cos \Psi_W \sin \theta_W)$$

$$U_G = U_{EB} - U_{WE}$$

$$V_G = V_{EB} - V_{WE}$$

$$W_G = W_{EB} - W_{WE}$$

10f	AXES TRANSFORMATION (GROUND REFERENCE DISTANCES)

Inputs: Variables		Outputs:	
From Subsystem	**Symbol**	**To Subsystem**	**Symbol**
10e	U_G	Visual System	N_N
	V_G		E
	W_G		P_{AX}
			P_{AY}
9	WL_{CG}		P_{ALT}
		9, 15, 7 16, 18	h_{CG}
		15, 16, 18	P_{ALT}
		7, 16	$\dot{h}_{CG}$
		16	R_{ALT}

Inputs: Constants, Coefficients, and Data Tables

Constants: $X_o, Y_o, H_o, WL_{G2}, GRD_{ALT}$

Coefficients: None

Data Tables: None

SUBSYSTEM NO. 10f: AXES TRANSFORMATION (GROUND REFERENCE DISTANCES)

Inputs: Variables

Symbol	Description	Units
U_G	x-velocity ground component of aircraft c.g.	ft/sec
V_G	y-velocity ground component of aircraft c.g.	ft/sec
W_G	z-velocity ground component of aircraft c.g.	ft/sec
WL_{CG}	Water line of c.g.	in

Inputs: Constants, Coefficients, and Data Tables

X_o	Initial x-position of the aircraft c.g. with respect to the ground	ft
Y_o	Initial y-position of the aircraft c.g. with respect to the ground	ft
Z_o	Initial z-position of the aircraft c.g. with respect to the ground	ft
WL_{G2}	Waterline of the main landing gear	in
GRD_{ALT}	Pressure altitude on the surface of the ground (altitude above sea level)	ft

Outputs:

N_N	Distance from takeoff point in the direction of grid North (+ North)	NM
E	Distance from takeoff point in the direction of grid East (+ East)	NM

SUBSYSTEM NO. 10f: AXES TRANSFORMATION (GROUND REFERENCE DISTANCES) (CONCLUDED)

Outputs: (Concluded)

Symbol	Description	Units
P_{AX}	x-position of the aircraft c.g. with respect to the ground	NM
P_{AY}	y-position of the aircraft c.g. with respect to the ground	NM
P_{ALT}	z-position of the aircraft c.g. with respect to the ground	NM
h_{CG}	Altitude of aircraft	ft
$\dot{h}_{CG}$	Climb rate	ft/sec
R_{ALT}	Radar altitude	ft

EQUATIONS

SUBSYSTEM NO. 10f--AXES TRANSFORMATION (GROUND REFERENCE DISTANCES)

A. Ground Position

$$P_{AX} = N_N + X_O$$

$$P_{AY} = E + Y_O$$

Where

$$N_N = \frac{1}{1.6878} \int U_G \, dt$$

$$E = \frac{1}{1.6878} \int V_G \, dt$$

B. Height Above Ground (Aircraft c.g.)

$$h_{CG} = -\int W_G \, dt + H_O$$

C. Radar Altitude

$$R_{ALT} = h_{CG} - \left(\frac{WL_{CG} - WL_{G2}}{12} \right)$$

D. Pressure Altitude

$$P_{ALT} = GRD_{ALT} + h_{CG}$$

E. Rate of Climb

$$\dot{h}_{CG} = -W_G$$

11	AIRCRAFT ANGULAR ACCELERATIONS AND VELOCITIES

Inputs: Variables		Outputs:	
From Subsystem	**Symbol**	**To Subsystem**	**Symbol**
13	X_A	11	$\dot{p}$
	Y_A		$\dot{q}$
	Z_A		$\dot{r}$
14	l_A	1, 4, 5, 6	p
	M_A	10c, 11, 12	q
	N_A		r
11	p	Simulator Cab	a_{XPA}
	q		a_{YPA}
	r		a_{ZPA}
	$\dot{p}$		U_{PA}
	$\dot{q}$		V_{PA}
	$\dot{r}$		W_{PA}
9	I_{XX}	16	r
	I_{YY}		a_{YPA}
	I_{ZZ}		
	I_{XZ}		
	$\dot{X}_{CG}$		
	$\dot{Z}_{CG}$		

(Concluded on next page)

11	AIRCRAFT ANGULAR ACCELERATIONS AND VELOCITIES (CONCLUDED)

Inputs: Variables		Outputs:	
From Subsystem	Symbol	To Subsystem	Symbol
	$\ddot{X}_{CG}$		
	$\ddot{Z}_{CG}$		
	$\dot{q}_{\beta_m}$		
	SL_{CG}		
	WL_{CG}		

Inputs: Constants, Coefficients, and Data Tables

Constants: SL_{PA}, BL_{PA}, WL_{PA}, BL_{CG}, m

Coefficients: None

Data Tables: None

SUBSYSTEM NO. 11: AIRCRAFT ANGULAR ACCELERATIONS AND VELOCITIES

Inputs: Variables

Symbol	Description	Units
X_A	Total x-force on the aircraft body axis	lb
Y_A	Total y-force on the aircraft body axis	lb
Z_A	Total z-force on the aircraft body axis	lb
l_A	Total rolling moment on the aircraft in body axis	ft-lb
M_A	Total pitching moment on the aircraft in body axis	ft-lb
N_A	Total yawing moment on the aircraft in body axis	ft-lb
p	Body axis roll rate	rad/sec
q	Body axis pitch rate	rad/sec
r	Body axis yaw rate	rad/sec
$\dot{p}$	Body axis roll angular acceleration	rad/sec^2
$\dot{q}$	Body axis pitch angular acceleration	rad/sec^2
$\dot{r}$	Body axis yaw angular acceleration	rad/sec^2
I_{XX}	Rolling moment of inertia about c.g.	slug-ft^2
I_{YY}	Pitching moment of inertia about c.g.	slug-ft^2
I_{ZZ}	Yawing moment of inertia about c.g.	slug-ft^2
I_{XZ}	Product of inertia about c.g.	slug-ft^2

Inputs: Variables (Concluded)

Symbol	Description	Units
$\dot{X}_{CG}$	Rate of longitudinal displacement as a function of mast tilt angle	in/sec
$\dot{Z}_{CG}$	Rate of vertical displacement as a function of mast tilt angle	in/sec
$\ddot{X}_{CG}$	Acceleration of longitudinal displacement as a function of mast tilt angle	in/sec^2
$\ddot{Z}_{CG}$	Acceleration of vertical displacement as a function of mast tilt angle	in/sec^2
$\dot{q}_{\beta_m}$	Pitch acceleration due to pylon tilt	rad/sec^2
SL_{CG}	Station line of c.g.	in
WL_{CG}	Water line of c.g.	in

Inputs: Constants, Coefficients, and Data Tables

SL_{PA}	Station line of the pilot's station	in
BL_{PA}	Butt line of the pilot's station	in
WL_{PA}	Water line of the pilot's station	in
BL_{CG}	Butt line of c.g.	in
m'	Mass of aircraft (GW/32.2)	slugs

Outputs:

Symbol	Description	Units
$\dot{p}$	Body axis roll angular acceleration	rad/sec^2
$\dot{q}$	Body axis pitch angular acceleration	rad/sec^2
$\dot{r}$	Body axis yaw angular acceleration	rad/sec^2
p	Body axis roll rate	rad/sec
q	Body axis pitch rate	rad/sec
r	Body axis yaw rate	rad/sec
a_{XPA}	x-axis (longitudinal) acceleration at the pilot's station	ft/sec^2
a_{YPA}	y-axis (lateral) acceleration at the pilot's station	ft/sec^2
a_{ZPA}	z-axis (vertical) acceleration at the pilot's station	ft/sec^2
U_{PA}	x-velocity of the pilot's station in body axis	ft/sec
V_{PA}	y-velocity of the pilot's station in body axis	ft/sec
W_{PA}	z-velocity of the pilot's station in body axis	ft/sec

EQUATIONS

SUBSYSTEM 11--AIRCRAFT ANGULAR ACCELERATIONS AND VELOCITIES

A. Aircraft CG Angular Accelerations (Body Axes)

1. Roll Equation

$$I_{XX}\dot{p} = (I_{YY} - I_{ZZ})(q)(r) + (I_{XZ})\left(\dot{r} + p\ q\right) + (l_A)$$

2. Pitch Equation

$$I_{YY}\dot{q} = (I_{ZZ} - I_{XX})(p)(r) + (I_{XZ})(r^2 - p^2) + (M_A) - \left(\dot{q}_{\beta m}\right)(I_{YY})$$

Where $\dot{q}_{\beta m}$ is due to pylon conversion (is non-zero while the pylons accelerate to a steady state conversion rate or decelerate to zero rate)

3. Yaw Equation

$$I_{ZZ}\dot{r} = (I_{XX} - I_{YY})(p)(q) + (I_{XZ})\left(\dot{p} - r\ q\right) + (N_A)$$

4. Angular Rate Equations

$$p = \int \dot{p}\,dt$$

$$q = \int \dot{q}\,dt$$

$$r = \int \dot{r}\,dt$$

B. Pilot Station Accelerations (Body Axes)

$$a_{XPA} = \frac{X_A}{m} + \left(\dot{q} + p\ r\right)\left(Z_{PA}\right) + \left(q^2 + r^2\right)\left(X_{PA}\right)$$

$$+ \left(Y_{PA}\right)\left(p\ q - \dot{r}\right) - (2q)\left(\frac{\dot{Z}_{CG}}{12}\right) - \left(\frac{\ddot{X}_{CG}}{12}\right)$$

$$a_{YPA} = \frac{X_A}{m} + \left(\dot{p} + q\ r\right)\left(Z_{PA}\right) + \left(\dot{r} + p\ q\right)\left(X_{PA}\right)$$

$$- \left(Y_{PA}\right)\left(r^2 + p^2\right) + 2\left(\frac{p\dot{Z}_{CG}}{12} - \frac{r\dot{X}_{CG}}{12}\right)$$

$$a_{ZPA} = \frac{Z_A}{m} + \left(p\ r - \dot{q}\right)\left(X_{PA}\right) - \left(p^2 + q^2\right)\left(Z_{PA}\right)$$

$$+ \left(Y_{PA}\right)\left(\dot{p} + q\ r\right) + (2q)\left(\frac{\dot{X}_{CG}}{12}\right) - \left(\frac{\ddot{Z}_{CG}}{12}\right)$$

Where

$$X_{PA} = \frac{\left(SL_{CG} - SL_{PA}\right)}{12}$$

$$Y_{PA} = \frac{\left(BL_{PA} - BL_{CG}\right)}{12}$$

$$Z_{PA} = \frac{\left(WL_{CG} - WL_{PA}\right)}{12}$$

SUBSYSTEM 11--AIRCRAFT ANGULAR ACCELERATIONS AND VELOCITIES

C. Pilot Station Velocities (Body Axes)

$$U_{PA} = U - (q)\left(Z'_{PA}\right) - (r)\left(Y'_{PA}\right) - \left(\dot{X}_{CG}\right)$$

$$V_{PA} = V + (r)\left(X'_{PA}\right) + (p)\left(Z'_{PA}\right)$$

$$W_{PA} = W - (q)\left(X'_{PA}\right) + (p)\left(Y'_{PA}\right) - \dot{Z}_{CG}$$

Where

$$X'_{PA} = \frac{\left(SL_{CG} - SL_{PA}\right)}{12}$$

$$Y'_{PA} = \frac{\left(BL_{PA} - BL_{CG}\right)}{12}$$

$$Z'_{PA} = \frac{\left(WL_{PA} - WL_{CG}\right)}{12}$$

12	BODY AXIS LINEAR ACCELERATIONS AND VELOCITIES

Inputs: Variables		Outputs:	
From Subsystem	**Symbol**	**To Subsystem**	**Symbol**
13	X_A	1, 4, 5, 6, 10d, 12	U
	Y_A		V
	Z_A		W
12	U	7, 8a, 15	U
	V		
	W	2, 3, 4, 5, 6	V_T
			α_F
11	p		β_F
	q		
	r	5	$\dot{W}$
10c	θ		
	ϕ	1, 7, 14, 15, 18	V_T
	ψ		
		10a, 16	α_F
9	$\ddot{X}_{CG}$		β_F
	$\ddot{Z}_{CG}$		
		16	N_Z
		6	$\dot{U}$
			$\dot{V}$
			$\dot{W}$

(Concluded on next page)

12	BODY AXIS LINEAR ACCELERATIONS AND VELOCITIES (CONCLUDED)

Inputs: Constants, Coefficients, and Data Tables

Constants: GW, m, U_o, V_o, W_o, g

Coefficients: None

Data Tables: None

SUBSYSTEM NO. 12: BODY AXIS LINEAR ACCELERATIONS AND VELOCITIES

Inputs: Variables

Symbol	Description	Units
X_A	Total x-force on the aircraft body axis	lb
Y_A	Total y-force on the aircraft body axis	lb
Z_A	Total z-force on the aircraft body axis	lb
U	x-velocity (longitudinal) of the aircraft c.g. in body axis with respect to the air	ft/sec
V	y-velocity (lateral) of the aircraft c.g. in body axis with respect to the air	ft/sec
W	z-velocity (vertical) of the aircraft c.g. in body axis with respect to the air	ft/sec
p	Body axis roll rate	rad/sec
q	Body axis pitch rate	rad/sec
r	Body axis yaw rate	rad/sec
θ	Euler pitch angle	rad
ϕ	Euler roll angle	rad
ψ	Euler yaw angle	rad
$\ddot{X}_{CG}$	Acceleration of longitudinal c.g. displacement as a function of mast tilt angle	in/sec^2
$\ddot{Z}_{CG}$	Acceleration of vertical c.g. displacement as a function of mast tilt angle	in/sec^2

Inputs: Constants, Coefficients, and Data Tables

Symbol	Description	Units
GW	Total aircraft gross weight	lb
m	Mass of the aircraft (GW/32.2)	slugs
U_o	Initialization x-axis velocity	ft/sec
V_o	Initialization y-axis velocity	ft/sec
W_o	Initialization z-axis velocity	ft/sec
g	Gravitational constant (32.2 ft/sec^2)	ft/sec^2

Outputs:

U	x-velocity (longitudinal) of the aircraft c.g. in body axis with respect to the air	ft/sec
V	y-velocity (lateral) of the aircraft c.g. in body axis with respect to the air	ft/sec
W	z-velocity (vertical) of the aircraft c.g. in body axis with respect to the air	ft/sec
V_T	Total linear velocity of the aircraft c.g. with respect to the air	ft/sec
α_F	Fuselage angle of attack	rad
β_F	Fuselage sideslip angle	rad

Outputs: Concluded

Symbol	Description	Units
$\dot{U}$	Rate of change of x-velocity (longitudinal) of the c.g. in body axis with respect to the air	ft/sec
$\dot{V}$	Rate of change of y-velocity (lateral) of the c.g. in body axis with respect to the air	ft/sec
$\dot{W}$	Rate of change of z-velocity (vertical) of the c.g. in body axis with respect to the air	ft/sec
N_X	x-axis (longitudinal) acceleration at the c.g. in body axis	G's
N_Y	y-axis (lateral) acceleration at the c.g. in body axis	G's
N_Z	z-axis (vertical) acceleration at the c.g. in body axis	G's

EQUATIONS

SUBSYSTEM NO. 12--BODY AXIS LINEAR ACCELERATIONS AND VELOCITIES

A. Linear Accelerations

$$\dot{U} = -g\sin\theta + Vr - Wq + \left(\frac{X_A}{m}\right) + \left(\frac{\ddot{X}_{CG}}{12}\right)$$

$$\dot{V} = g\cos\theta\sin\phi - Ur + Wp + \left(\frac{Y_A}{m}\right)$$

$$\dot{W} = g\cos\theta\cos\phi + Uq - Vp + \left(\frac{Z_A}{m}\right) + \left(\frac{\ddot{Z}_{CG}}{12}\right)$$

Where $\ddot{X}_{CG}/12$ and $\ddot{Z}_{CG}/12$ are very minor terms resulting from pylon conversion (are non-zero while the pylons accelerate to a steady state conversion rate or decelerate to zero rate)

$$N_X = \frac{X_A}{GW}$$

$$N_Y = \frac{Y_A}{GW}$$

$$N_Z = \frac{Z_A}{GW}$$

B. Body Axis Velocities

$$U = \int \dot{U}\,dt + U_o$$

$$V = \int \dot{V}\,dt + V_o$$

SUBSYSTEM NO. 12--BODY AXIS LINEAR ACCELERATIONS AND VELOCITIES

B. Body Axis Velocities (Concluded)

$$W = \int \dot{W}\, dt + W_o$$

$$V_T = \sqrt{U^2 + V^2 + W^2}$$

C. Angle of Attack, Flight Path Angle

$$\alpha_F = \tan^{-1}\left(\frac{W}{U}\right) = \theta - \gamma$$

$$\gamma = \tan^{-1}\left(\frac{\dot{h}}{U_G}\right)$$

where

γ = angle between horizontal and flight path (positive flight path above horizon)

α = angle between flight path and body axis (positive for body axis above flight path)

θ = angle between horizontal and body axis (positive above horizon)

D. Angle of Sideslip

$$\beta_F = \tan^{-1}\left(\frac{V}{U\sqrt{1 + \frac{W^2}{U^2}}}\right)$$

E. Load Factor

$$XNZ = \cos\theta - \left(\frac{\dot{W} + \rho V - U_q}{32.2}\right)$$

13	FORCE SUMMATION

Inputs: Variables		Outputs:	
From Subsystem	**Symbol**	**To Subsystem**	**Symbol**
10a	$(X,Y,Z)_F$	12, 11	X_A
	$(X,Z)_{iWPL}$		Y_A
	$(X,Z)_{iWPR}$		Z_A
	$(X,Y,Z)_{WP}$		
	$(X,Y,Z)_H$		
	$(X,Y,Z)_{MG}$		
	$(X,Y,Z)_{NG}$		
	$(X,Y,Z)_V(i)$		
	$(X,Y,Z)_{SD}$		
	$(X,Z)_{iPYL}$		
	$(X,Y,Z)_{PYLT}$		
10b	$(X,Y,Z)_L$		
	$(X,Y,Z)_R$		
7	$(\Delta X,\Delta Y,\Delta Z)_{LG}$		
18	$(X,Z)_{JTR}$		
	$(X,Z)_{JTL}$		

(Concluded on next page)

13	FORCE SUMMATION (CONCLUDED)

Inputs: Constants, Coefficients, and Data Tables

Constants: NVSTAB

Coefficients: None

Data Tables: None

SUBSYSTEM NO. 13: FORCE SUMMATION

Inputs: Variables

Symbol	Description	Units
$(X,Y,Z)_F$	Aerodynamic forces on the fuselage, body axis	lb
$(X,Z)_{iWPL}$	Aerodynamic forces on the portion of the left wing-pylon in the rotor wake, body axis	lb
$(X,Z)_{iWPR}$	Aerodynamic forces on the portion of the right wing-pylon in the rotor wake, body axis	lb
$(X,Y,Z)_{WP}$	Aerodynamic forces on the wing-pylon portion in the freestream, body axis	lb
$(X,Y,Z)_H$	Aerodynamic forces on the horizontal stabilizer, body axis	lb
$(X,Y,Z)_{MG}$	Aerodynamic forces on the main landing gear, body axis	lb
$(X,Y,Z)_{NG}$	Aerodynamic forces on the nose landing gear, body axis	lb
$(X,Y,Z)_V(i)$	Aerodynamic forces due to the vertical stabilizer(s), body axis	lb
$(X,Y,Z)_{SD}$	Spinner drag aerodynamic forces, body axis	lb
$(X,Z)_{iPYL}$	Pylon aerodynamic interference forces, body axis	lb
$(X,Y,Z)_{PYLT}$	Lateral pylon drag model aerodynamic forces, body axis	lb
$(X,Y,Z)_L$	Left rotor forces, body axis	lb
$(X,Y,Z)_R$	Right rotor forces, body axis	lb

SUBSYSTEM NO. 13: FORCE SUMMATION (CONCLUDED)

Inputs: Variables (Concluded)

Symbol	Description	Units
$(\Delta X, \Delta Y, \Delta Z)_{LG}$	Total landing gear forces in body axis	lb
$(X,Z)_{JTR}$	Right engine jet thrust forces, body axis	lb
$(X,Z)_{JTL}$	Left engine jet thrust forces, body axis	lb

Inputs: Constants, Coefficients, and Data Tables

NVSTAB	Number of vertical stabilizers	ND

Outputs:

X_A	Total x-force on the aircraft, body axis	lb
Y_A	Total y-force on the aircraft, body axis	lb
Z_A	Total z-force on the aircraft, body axis	lb

EQUATIONS

SUBSYSTEM NO. 13--FORCE SUMMATION

A. <u>X-Force Equation</u>

$$X_A = X_F + X_{iWPR} + X_{iWPL} + X_{WP} + X_H + X_{MG} + X_{NG} + \Delta X_{LG}$$

$$+ X_L + X_R + \sum_{i=1}^{NVSTAB} X_V(i) + X_{JTR} + X_{JTL} + X_{SD} + X_{PYLT} + X_{iPYL}$$

B. <u>Y-Force Equation</u>

$$Y_A = Y_F + Y_{WP} + Y_L + Y_R + \sum_{i=1}^{NVSTAB} Y_V(i) + Y_H$$

$$+ Y_{MG} + Y_{NG} + \Delta Y_{LG} + Y_{SD} + Y_{PYLT}$$

C. <u>Z-Force Equation</u>

$$Z_A = Z_F + Z_{iWPL} + Z_{iWPR} + Z_{WP} + Z_H + Z_{NG} + Z_{MG} + \Delta Z_{LG}$$

$$+ Z_{JTR} + Z_{JTL} + Z_L + Z_R + Z_{SD} + Z_{iPYL} + Z_{PYLT}$$

14	MOMENT SUMMATION

Inputs: Variables		Outputs:	
From Subsystem	**Symbol**	**To Subsystem**	**Symbol**
9	SL_{CG}	11	l_A
	WL_{CG}		M_A
	h_H		N_A
10a	$(X,Y,Z)_F$		
	$(X,Z)_{iWPL}$		
	$(X,Z)_{iWPR}$		
	$(X,Y,Z)_{WP}$		
	$(X,Y,Z)_H$		
	$(X,Y,Z)_V(i)$		
	$(X,Y,Z)_{MG}$		
	$(X,Y,Z)_{NG}$		
	$(X,Y,Z)_{SD}$		
	$(X,Z)_{iPYL}$		
	$(X,Y,Z)_{PYLT}$		
	$(l,M,N)_F$		
	$(l,M,N)_{WP}$		
	$(l,M,N)_H$		
7	$(\Delta l,\Delta M,\Delta N)_{LG}$		
10b	$(X,Y,Z)_L$		
	$(X,Y,Z)_R$		
	$(l,M,N)_L$		
	$(l,M,N)_R$		

(Concluded on next page)

14	MOMENT SUMMATION (CONTINUED)

Inputs: Variables		Outputs:	
From Subsystem	**Symbol**	**To Subsystem**	**Symbol**
4	$(X_{iW}, Y_{iW})_R$		
	$(X_{iW}, Y_{iW})_L$		
10c	ϕ		
12	V_T		
1	T_R		
	T_L		
8a	β_m		
6	$l_{XV}(i)$		
	$l_{YV}(i)$		
	$l_{ZV}(i)$		
18	$(X,Z)_{JTR}$		
	$(X,Z)_{JTL}$		

Inputs: Constants, Coefficients, and Data Tables

Constants: $BL_{CG}, SL_F, WL_F, SL_{WP}, WL_{WP}, SL_H, WL_H,$

$SL_{MG}, WL_{MG}, SL_{NG}, WL_{NG}, SL_V(i), BL_V(i), WL_V(i),$

$SL_{SP}, BL_{SP}, WL_{SP}, l_m, R, \phi_m, NVSTAB$

(Concluded on next page)

14	MOMENT SUMMATION (CONCLUDED)

Inputs: Constants, Coefficients, and Data Tables

Coefficients: $l_{G0}, l_{G1}, l_{G2}, l_{G3}, l_{G4}$, GELLIM, GEULIM,

M_{G1}, M_{G2}, M_{G3}

Data Tables: None

SUBSYSTEM NO. 14: MOMENT SUMMATION

Inputs: Variables

Symbol	Description	Units
SL_{CG}	Station line of c.g.	in
WL_{CG}	Water line of c.g.	in
h_H	Rotor hub height above ground	ft
$(X,Y,Z)_F$	Aerodynamic forces on the fuselage, body axis	lb
$(X,Z)_{iWPL}$	Aerodynamic forces on the portion of the left wing-pylon in the rotor wake, body axis	lb
$(X,Z)_{iWPR}$	Aerodynamic forces on the portion of the right wing-pylon in the rotor wake, body axis	lb
$(X,Y,Z)_{WP}$	Aerodynamic forces on the wing-pylon portion in the freestream, body axis	lb
$(X,Y,Z)_H$	Aerodynamic forces on the horizontal stabilizer, body axis	lb
$(X,Y,Z)_V(i)$	Aerodynamic forces on the vertical stabilizer(s), body axis	lb
$(X,Y,Z)_{MG}$	Aerodynamic forces on the main landing gear, body axis	lb
$(X,Y,Z)_{NG}$	Aerodynamic forces on the nose landing gear, body axis	lb
$(X,Y,Z)_{SD}$	Spinner drag aerodynamic forces, body axis	lb

Inputs: Variables (Continued)

Symbol	Description	Units
$(X,Z)_{iPYL}$	Pylon aerodynamic interference forces, body axis	lb
$(X,Y,Z)_{PYLT}$	Lateral pylon drag model aerodynamic forces, body axis	lb
$(l,M,N)_F$	Rolling, pitching, and yawing aerodynamic moments on the fuselage about the body x-, y-, and z-axes	ft-lb
$(l,M,N)_{WP}$	Rolling, pitching, and yawing aerodynamic moments due to the wing-pylon about the body x-, y-, and z-axes	ft-lb
$(l,M,N)_H$	Rolling, pitching, and yawing aerodynamic moments due to the horizontal stabilizer about the body x-, y-, and z-axes	ft-lb
$(\Delta l,\Delta M,\Delta N)_{LG}$	Total landing gear rolling, pitching, and yawing moments in body axis	ft-lb
$(X,Y,Z)_L$	Left rotor forces, body axis	lb
$(X,Y,Z)_R$	Right rotor forces, body axis	lb
$(l,M,N)_L$	Rolling, pitching, and yawing moments due to the left rotor about the body x-, y-, and z-axes	ft-lb
$(l,M,N)_R$	Rolling, pitching, and yawing moments due to the right rotor about the body x-, y-, and z-axes	ft-lb
$(X_{iW}, Y_{iW})_R$	Moment arms for right wing-pylon z-force due to rotor wake	in
$(X_{iW}, Y_{iW})_L$	Moment arms for left wing-pylon z-force due to rotor wake	in

SUBSYSTEM NO. 14: MOMENT SUMMATION (CONTINUED)

Inputs: Variables (Concluded)

Symbol	Description	Units
ϕ	Euler roll angle	rad
V_T	Total linear velocity of the aircraft c.g. with respect to the air	ft/sec
T_R	Mast axis right rotor thrust (+ up for helicopter)	lb
T_L	Mast axis left rotor thrust (+ up for helicopter)	lb
β_m	Mast conversion angle (+ fwd, 0 deg = vertical or helicopter, 90 deg = horizontal or airplane)	deg
$l_{XV}(i)$	Stationline distance from the c.g. to the vertical stabilizer center of pressure	ft
$l_{YV}(i)$	Butt line distance from the c.g. to the vertical stabilizer center of pressure	ft
$l_{ZV}(i)$	Water line distance from the c.g. to the vertical stabilizer center of pressure	ft
$(X,Z)_{JTR}$	Right engine jet thrust forces, body axis	lb
$(X,Z)_{JTL}$	Left engine jet thrust forces, body axis	lb

SUBSYSTEM NO. 14: MOMENT SUMMATION (CONTINUED)

Inputs: Constants, Coefficients, and Data Tables

Symbol	Description	Units
BL_{CG}	Butt line of c.g.	in
SL_F	Station line of fuselage center of pressure	in
WL_F	Water line of fuselage center of pressure	in
SL_{WP}	Station line of the wing-pylon center of pressure	in
WL_{WP}	Water line of the wing-pylon center of pressure	in
SL_H	Station line of the horizontal stabilizer center of pressure	in
WL_H	Water line of the horizontal stabilizer center of pressure	in
SL_{MG}	Station line of the main landing gear	in
WL_{MG}	Water line of the main landing gear	in
SL_{NG}	Station line of the nose landing gear	in
WL_{NG}	Water line of the nose landing gear	in
$SL_V(i)$	Station line of the vertical stabilizer(s) center of pressure	in
$BL_V(i)$	Butt line of the vertical stabilizer(s) center of pressure	in
$WL_V(i)$	Water line of the vertical stabilizer(s) center of pressure	in

Inputs: Constants, Coefficients, and Data Tables (Continued)

Symbol	Description	Units
SL_{SP}	Station line of engine nacelle shaft pivot point	in
BL_{SP}	Butt line of engine nacelle shaft pivot point	in
WL_{SP}	Water line of engine nacelle shaft pivot point	in
l_m	Mast length	ft
R	Rotor radius	ft
ϕ_m	Lateral mast tilt	rad
NVSTAB	Number of vertical stabilizers	ND
l_{G0}	Ground effect rolling moment coefficient	$\frac{\text{ft-lb}}{\text{deg}}$
l_{G1}	Ground effect rolling moment coefficient	$\frac{\text{ft-lb}}{\text{deg-ft}}$
l_{G2}	Ground effect rolling moment coefficient	$\frac{\text{ft-lb}}{\text{deg-ft}^2}$
l_{G3}	Ground effect rolling moment coefficient	$\frac{\text{ft-lb}}{\text{deg-ft}^3}$
l_{G4}	Ground effect rolling moment coefficient	sec/ft
GELLIM	Lower altitude limit in the ground effect rolling moment equation	ND
GEULIM	Upper altitude limit in the ground effect rolling moment equation	ND

Inputs: Constants, Coefficients, and Data Tables (Concluded)

Symbol	Description	Units
M_{G1}	Constant in the IGE pitching moment equation	ft
M_{G2}	Constant in the IGE pitching moment equation	ND
M_{G3}	Constant in the IGE pitching moment equation	sec/ft

Outputs:

l_A	Total rolling moment on the aircraft in body axis	ft-lb
M_A	Total pitching moment on the aircraft in body axis	ft-lb
N_A	Total Yawing moment on the aircraft in body axis	ft-lb

EQUATIONS

SUBSYSTEM NO. 14--MOMENT SUMMATION

A. Pitching Moment Equation

$$M_A = (X_F)\left[\frac{WL_{CG} - WL_F}{12}\right] + Z_F\left[\frac{SL_F - SL_{CG}}{12}\right]$$

$$+(X_{iWPL} + X_{iWPR} + Y_{WP})\left[\frac{WL_{CG} - WL_W}{12}\right] - (Z_{iWPR})(X_{iWR})$$

$$-(Z_{iWPL})(X_{iWL}) + (Z_{WP})\left[\frac{SL_{WP} - SL_{CG}}{12}\right] + (X_H)\left[\frac{WL_{CG} - WL_H}{12}\right]$$

$$+(Z_H)\left[\frac{SL_H - SL_{CG}}{12}\right] + (X_{MG})\left[\frac{WL_{CG} - WL_{MG}}{12}\right] + (Z_{MG})\left[\frac{SL_{MG} - SL_{CG}}{12}\right]$$

$$+(X_{NG})\left[\frac{WL_{CG} - WL_{NG}}{12}\right] + (Z_{NG})\left[\frac{SL_{NG} - SL_{CG}}{12}\right] + \sum_{i=1}^{NVSTAB}[X_V(i)][-l_{ZV}(i)]$$

$$+(X_L + X_R)\left[\frac{WL_{CG} - WL_{SP} - (12)(l_m)(\cos\beta_m)}{12}\right]$$

$$+(Z_L + Z_R)\left[\frac{SL_{SP} - SL_{CG} - (12)(l_m)(\sin\beta_m)}{12}\right] + M_F + M_{WP}$$

(Equation concluded on next page)

SUBSYSTEM NO. 14--MOMENT SUMMATION

A. Pitching Moment Equation

$$+M_H+M_L+M_R+\Delta M_{LG}+M_{GEFF}+(X_{SD})\left[\frac{WL_{CG}-WL_{SP}-(12)(l_m)(\cos\beta_m)}{12}\right]$$

$$-(Z_{SD})\left[\frac{SL_{CG}-SL_{SP}+(12)(l_m)(\sin\beta_m)}{12}\right]-(X_{iPYL})\left[\frac{WL_{SP}-WL_{CG}}{12}\right]$$

$$+(Z_{iPYL})\left[\frac{SL_{SP}-SL_{CG}}{12}\right]+(X_{PYLT})\left[\frac{WL_{CG}-WL_{SP}}{12}\right]$$

$$+(Z_{PYLT})\left[\frac{SL_{SP}-SL_{CG}}{12}\right]+(Z_{JTR}+Z_{JTL})\left[\frac{SL_{SP}-SL_{CG}}{12}\right]$$

$$-(X_{JTR}+X_{JTL})\left[\frac{WL_{SP}-WL_{CG}}{12}\right]$$

Where the pitching moment term due to ground effect is:

$$M_{GEFF}=M_{G1}(T_R+T_L)\left[\exp^{\left(\frac{-h_H}{2R}\right)(M_{G2})}\right]\left[\exp^{(M_{G3})(V_T)}\right]$$

B. Rolling Moment Equation

$$l_A = (Y_F)\left[\frac{WL_F - WL_{CG}}{12}\right] + (Z_{iWPL})(Y_{iWL}) + (Z_{iWPR})(Y_{iWR})$$

$$+ (Y_{iWPR} + Y_{iWPL} + Y_{WP})\left[\frac{WL_{WP} - WL_{CG}}{12}\right]$$

$$+ (Y_L + Y_R)\left[\frac{WL_{SP} - WL_{CG} + (12)(l_m)(\cos\beta_m)}{12}\right] - (Z_L)\left[\frac{BL_{SP} + BL_{CG} + (12)(l_m)(\sin\phi_m)}{12}\right]$$

$$+ (Z_R)\left[\frac{BL_{SP} - BL_{CG} + (12)(l_m)(\sin\phi_m)}{12}\right] + l_F + l_{WP} + l_L + l_R + l_{GEFF}(\phi) + \Delta l_{LG}$$

$$- (Y_{MG})\left[\frac{WL_{CG} - WL_{MG}}{12}\right] - (Y_{NG})\left[\frac{WL_{CG} - WL_{NG}}{12}\right]$$

$$+ (Y_{SD})\left[\frac{WL_{SP} - WL_{CG} + (12)(l_m)(\cos\beta_m)}{12}\right] + (Y_{PYLT})\left[\frac{WL_{SP} - WL_{CG}}{12}\right]$$

$$+ \sum_{i=1}^{NVSTAB} [Y_V(i)][l_{ZV}(i)] + (Z_{JTR})\left[\frac{BL_{SP} - BL_{CG}}{12}\right] - (Z_{JTL})\left[\frac{BL_{SP} + BL_{CG}}{12}\right]$$

Where the rolling moment term due to ground effect is:

$$l_{GEFF} = \left\{(l_{G0}) + (l_{G1})\left(\frac{h_H}{2R}\right) + (l_{G2})\left(\frac{h_H}{2R}\right)^2 + (l_{G3})\left(\frac{h_H}{2R}\right)^3\right\}\left[\exp^{(l_{G4})(V_T)}\right]$$

$$\text{for } GELLIM \le \frac{h_H}{2R} \le GEULIM$$

C. Yawing Moment Equation

$$N_A = (Y_F)\left[\frac{SL_{CG} - SL_F}{12}\right] - (X_{iWPL})(Y_{iWL}) - X_{iWPR}(Y_{iWR})$$

$$+(Y_{iWPR})(X_{iWR}) + (Y_{iWPL})(X_{iWL}) + (Y_{WP})\left[\frac{SL_{CG} - SL_{WP}}{12}\right]$$

$$+(X_L)\left[\frac{BL_{SP} + BL_{CG} + (12)(l_m)(\sin\phi_m)}{12}\right] + (X_R)\left[\frac{BL_{SP} - BL_{CG} + (12)(l_m)(\sin\phi_m)}{12}\right]$$

$$+(Y_H)\left[\frac{SL_{CG} - SL_H}{12}\right] + (Y_L + Y_R)\left[\frac{SL_{CG} - SL_{SP} + (12)(l_m)(\sin\beta_m)}{12}\right]$$

$$+N_F + N_{WP} + N_L + N_R + \Delta N_{LG} + \sum_{i=1}^{NVSTAB} -\{[Y_V(i)][l_{XV}(i)] + [X_V(i)][l_{YV}(i)]\}$$

$$+(Y_{MG})\left[\frac{SL_{CG} - SL_{MG}}{12}\right] + (Y_{NG})\left[\frac{SL_{CG} - SL_{NG}}{12}\right]$$

$$+(X_{JTL})\left[\frac{BL_{SP} + BL_{CG}}{12}\right] - (X_{JTR})\left[\frac{BL_{SP} - BL_{CG}}{12}\right]$$

$$+(Y_{PYLT})\left[\frac{SL_{CG} - SL_{SP}}{12}\right] + (Y_{SD})\left[\frac{SL_{CG} - SL_{SP} + (12)(l_m)(\sin\beta_m)}{12}\right]$$

15	FLIGHT ENVIRONMENT

Inputs: Variables		Outputs:	
From Subsystem	**Symbol**	**To Subsystem**	**Symbol**
10f	h_{CG}	1, 2, 3, 4, 5, 6	ρ
	P_{ALT}		M_N
12	V_T	18	P_a
	U		T_a
		16	V_{KCAS}

Inputs: Constants, Coefficients, and Data Tables

Constants: T_o, ρ_o

Coefficients: None

Data Tables: None

SUBSYSTEM NO. 15: FLIGHT ENVIRONMENT

Inputs: Variables

Symbol	Description	Units
h_{CG}	Altitude of aircraft	ft
P_{ALT}	Pressure altitude	ft
V_T	Total linear velocity of the rotorcraft c.g. with respect to the air	ft/sec
U	x-velocity (longitudinal) of the aircraft c.g. in body axis with respect to the air	ft/sec

Inputs: Constants, Coefficients, and Data Tables

T_o	Absolute sea level standard temperature	deg K
ρ_o	Air density at sea level standard conditions	$slug/ft^3$

Outputs:

ρ	Air density	$slug/ft^3$
M_N	Mach number	ND
U_{KCAS}	Calibrated airspeed	kt
P_a	Ambient absolute pressure	lb/ft^2
T_a	Ambient absolute temperature	deg K

A. Temperature Relationships

OAT = T_a - 273.16 (outside air temperature, deg C)

$$T_a = T_o - 0.0019812(P_{ALT}) + \Delta T$$

Where

T_o = 288.16 deg K

P_{ALT} = pressure altitude

$$\theta_{TEST} = \frac{T_a}{T_o}$$

$$\delta_{STD} = \left[(T_a - \Delta T)/T_o\right]^{5.255876}$$

B. Air Density and Air Density Ratio

$$\rho = (\rho_o)(\sigma')$$

Where

$$\rho_o = 0.0023769 \text{ slugs/ft}^3$$

$$\sigma' = \left\{ \frac{\left[1.0 - (0.00000687)(P_{ALT})\right]^{5.255876}}{1 - (0.00000687)(P_{ALT}) + (\Delta T/288.16)} \right\} = \left(\frac{\delta_{STD}}{\theta_{TEST}} \right)$$

C. Velocities

$$V_S = (661.48)(\theta_T)^{1/2} \qquad \text{(in knots)}$$

$$V_S = (1116.4)(\theta_T)^{1/2} \qquad \text{(in ft/sec)}$$

$$M_N = V_T / V_S$$

$$V_{T_{KTS}} = (0.5925)\left(V_{T_{FPS}}\right)$$

$$V_T = \left(\frac{1}{\sqrt{\sigma'}}\right)(V_{EAS})$$

$$V_{KCAS} = (661.48)\left\{5\left[\left(1 + (\delta_{STD})\left\{\left[1 + \left(\frac{0.2}{\theta_{TEST}}\right)\left(\frac{V_T}{661.48}\right)^2\right]^{7/2} - 1\right\}\right)^{2/7} - 1\right]\right\}^{1/2}$$

$$U_{KCAS} = (661.48)\left\{5\left[\left(1 + (\delta_{STD})\left\{\left[1 + \left(\frac{0.2}{\theta_{TEST}}\right)\left(\frac{U}{661.48}\right)^2\right]^{7/2} - 1\right\}\right)^{2/7} - 1\right]\right\}^{1/2}$$

D. Density Altitude (ft)

$$h_D = \frac{1 - (\sigma')^{0.235}}{0.00000687535}$$

16	PILOT'S INSTRUMENT PANEL

Inputs: Variables		Outputs:	
From Subsystem	Symbol	To Subsystem	Symbol
8a	β_m	Instruments read visually by pilot in simulator cockpit	
8d	X_{FL}		
	X_{LG}		
7	LG_{TLT}		
10f	h_{CG}		
	$\dot{h}_{CG}$		
	P_{ALT}		
	R_{ALT}		
12	α_F		
	β_F		
	N_Z		
11	r		
	a_{YPA}		
15	V_{KCAS}		
10c	θ		
	ϕ		
	ψ		
	$\dot{\theta}$		
	$\dot{\phi}$		
	$\dot{\psi}$		

(Concluded on next page)

16	PILOT'S INSTRUMENT PANEL (CONCLUDED)

Inputs: Variables		Outputs:	
From Subsystem	Symbol	To Subsystem	Symbol
18	Q_{RPT}		
	Q_{LPT}		
19	Ω_R		
	Ω_L		
	Ω_{RPT}		
	Ω_{LPT}		
	Ω_{INT}		
17	$RPM_{P_{MIN}}$		

Inputs: Constants, Coefficients, and Data Tables

Constants: $AS_{CAL}, AS_o, \theta_{MAX}, \theta_{RPTI}, \theta_{INTI}, N_{RMAX}$

SUBSYSTEM NO. 16: PILOT'S INSTRUMENT PANEL

Inputs: Variables

Symbol	Description	Units
β_m	Mast conversion angle (+ fwd, 0 deg = vertical or helicopter, 90 deg = horizontal or airplane)	deg
X_{FL}	Position of flap indicator	ND
X_{LG}	Position of landing gear indicator	ND
LG_{TLT}	Landing gear touchdown light	ND
h_{CG}	Altitude of aircraft	ft
$\dot{h}_{CG}$	Climb rate	ft/sec
P_{ALT}	Pressure altitude	ft
R_{ALT}	Radar altitude	ft
α_F	Fuselage angle of attack	rad
β_F	Fuselage sideslip angle	rad
N_Z	z-axis (vertical) acceleration at the c.g. in body axis	G's
r	Body axis yaw rate	rad/sec
a_{YPA}	y-axis (lateral) acceleration at the pilot's station	ft/sec^2
V_{KCAS}	Calibrated airspeed	kt
θ	Euler pitch angle	rad
ϕ	Euler roll angle	rad
ψ	Euler yaw angle	rad

Inputs: Variables (Concluded)

Symbol	Description	Units
$\dot{\theta}$	Rate of change of Euler pitch angle	rad/sec
$\dot{\phi}$	Rate of change of Euler roll angle	rad/sec
$\dot{\psi}$	Rate of change of Euler yaw angle	rad/sec
Q_{RPT}	Right engine power turbine torque	ft-lb
Q_{LPT}	Left engine power turbine torque	ft-lb
Ω_R	Instantaneous right rotor speed	rad/sec
Ω_L	Instantaneous left rotor speed	rad/sec
Ω_{RPT}	Right engine power turbine speed	rad/sec
Ω_{LPT}	Left engine power turbine speed	rad/sec
Ω_{INT}	Interconnect drive shaft speed	rad/sec
$RPM_{P_{MIN}}$	Minimum rotor RPM limit	RPM

Inputs: Constants, Coefficients, and Data Tables

AS_{CAL}	Airspeed calibration slope correction	ND
AS_o	Airspeed calibration intercept correction	kts
Q_{MAX}	Maximum allowable rotor torque	ft-lb
θ_{RPTI}	Rotor turbine gear ratio	ND

SUBSYSTEM NO. 16: PILOT'S INSTRUMENT PANEL (CONCLUDED)

Inputs: Constants, Coefficients, and Data Tables (Concluded)

Symbol	Description	Units
θ_{INT1}	Rotor interconnect gear ratio	ND
$N_{R_{MAX}}$	Maximum rotor speed	RPM

Outputs:

Instruments read visually by pilot in simulator cockpit

EQUATIONS

SUBSYSTEM NO. 16--PILOT'S INSTRUMENT PANEL

Pilot's Controls and Switches

The simulator cab controls are conventional displacement controls and, in general, represent the layout of the XV-15 cockpit. The following are the control motions:

Controls	Symbol	Min (%)	Max (100%)	Range
F/A Cyclic	X_{LN}	Aft	Fwd	9.6 inches
Lat. Cyclic	X_{LT}	Left	Right	9.6 inches
Pedal	X_{PD}	Left	Right	5 inches
Power Lever	X_{COL}	Down	Up	10 inches
Flap Lever	X_{FL}	Up	Down	1,2,3,4 - Manual
Landing Gear	X_{LG}	Up	Down	2 position

LIST OF INSTRUMENTS IN THE CAB[1]

Instrument	Range	Units	Driver	Remarks
Wing Flaps	0-75	deg	X_{FL}	
Pylon Angle	0-100	deg	β_m	Pylon incidence $i_N = 90 - \beta_m$ 0 deg = airplane 90 deg = helicopter
Angle of Attack	± 20	deg	α_F	Fuselage angle of attack (+ nose up)
Triple Tach Left Engine	0-120	%	Ω_{LPT}	$\frac{(100)(\Omega_{LPT})}{(0.10472)(\theta_{RPT1})(N_{RMAX})}$
Right Engine	0-120	%	Ω_{RPT}	$\frac{(100)(\Omega_{RPT})}{(0.10472)(\theta_{RPT1})(N_{RMAX})}$
Rotor	0-120	%	Ω_{INT}	$\frac{(100)(\Omega_{INT})}{(0.10472)(\theta_{RPT1})(N_{RMAX})}$
Left Rotor Torque	0-120	%	Q_L	$(100)(Q_L)/(Q_{MAX})$
Right Rotor Torque	0-120	%	Q_R	$(100)(Q_R)/(Q_{MAX})$
Airspeed	0-300	Kt	U_{KIAS}	$U_{KIAS} = (U_{KCAS})(AS_{CAL}) + AS_o$
Sideslip	± 30	deg	β_F	
ADI		deg	θ, ϕ	
Directional Gyro		deg	ψ	Heading
Altimeter	0-30,000	ft	P_{ALT}	
Rate of Climb	± 3500	ft/sec	$\dot{h}_{CG}$	
Turn and Bank		deg/sec ft/sec	r a_{YPA}	
Acceleration	-2 to +4	g	N_Z	
Radar Altimeter	0-2,500	ft	R_{ALT}	

1 The list of instruments is representative of what is usually provided. Some simulations have varied substantially from this list and used head-up displays, flap-panel CRTs, and sidestick controls. Figure A16-1 presents a cockpit layout representative of early XV-15 simulations.

COCKPIT INSTRUMENT DISPLAY

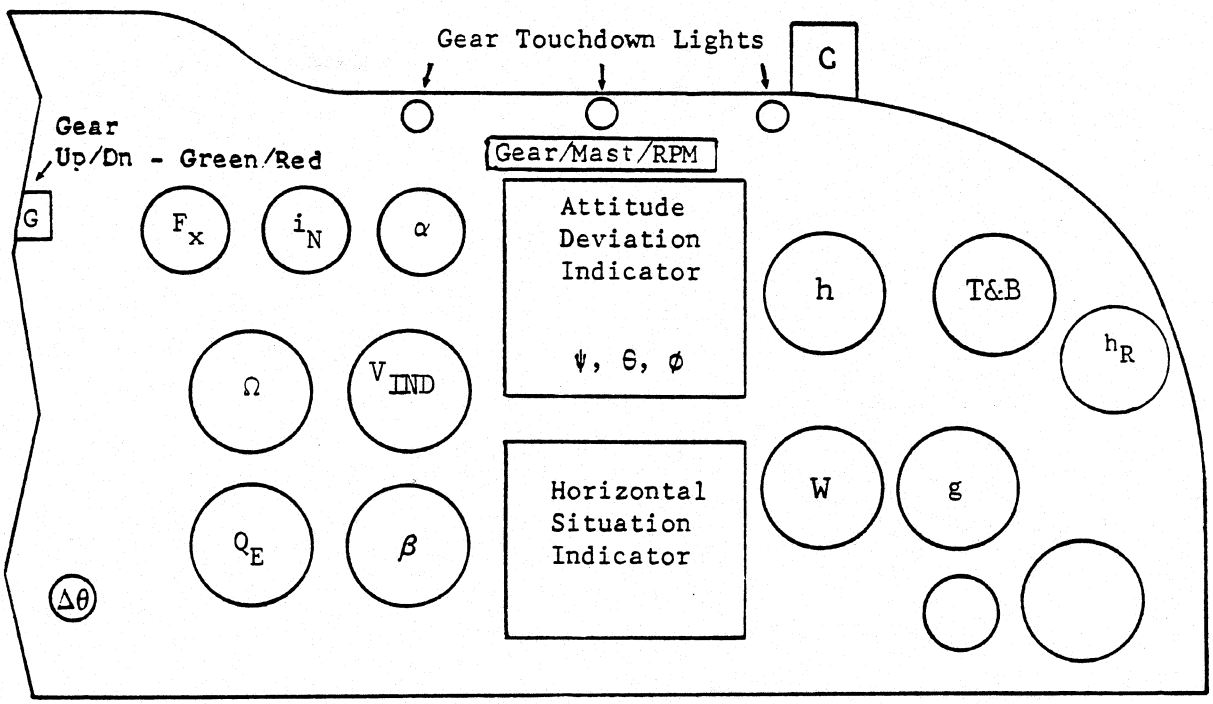

F_x Flap Position

i_N Nacelle Tilt Angle $(90-\beta_m)$

α Angle of Attack

Ω Rotor and Engines RPM

V_{IND} Airspeed (Simulator $V_{CAL}=V_{IND}$)

Q_E Engines and Cross Shaft Torque (Rotor)

β Sideslip Angle

$\Delta\theta$ Differential Collective

C Conversion Guide Indicator

h Baro Altimeter

W Vertical Velocity Indicator

T&B Turn & Bank Indicator

h_R Radar Altimeter $(h_R = h_{CG})$

g Normal Acceleration

Figure A16-1. XV-15 Pilot's Control Panel

17	ROTOR COLLECTIVE GOVERNOR

Inputs: Variables		Outputs:	
From Subsystem	**Symbol**	**To Subsystem**	**Symbol**
8d	IRPM	8a	$\theta_{oL/G}$
	MENB		$\theta_{oR/G}$
	IGB		
	IGOVENG	16	$RPM_{P_{MIN}}$
	RPM_{SEL}		
19	Ω_{INT}		
	Ω_R		
	Ω_L		
8a	β_m		

Inputs: Constants, Coefficients, and Data Tables

Constants: $\theta_{ERR\,LIM}, \theta_{FCP\,LIM}, P_{SRG}, K_{1RGA}, K_{2RGA}, K_{3RGA},$

$K_{4RGA}, RPM_{P_{MAX}}, K_{RPM}, THOGMX, THOGMN$

Coefficients: $\theta_{INT\,1}$

Data Tables: $K_{PROP} = f(\beta_m)$ Table 17-I

$K_{INTG} = f(\beta_m)$ Table 17-II

SUBSYSTEM NO. 17: ROTOR COLLECTIVE GOVERNOR

Inputs: Variables

Symbol	Description	Units
IRPM	RPM adjustment wheel (increase/ decrease)	ND
MENB	Pylon lock switch	ND
IGB	RPM governor disengage switch	ND
IGOVENG	RPM governor engage switch	ND
RPM_{SEL}	Pilot's selected operating rotor speed	RPM
Ω_{INT}	Interconnect drive shaft speed	rad/sec
Ω_R	Instantaneous right rotor speed	rad/sec
Ω_L	Instantaneous left rotor speed	rad/sec
β_m	Mast conversion angle (+ fwd, 0 deg = vertical or helicopter, 90 deg = horizontal or airplane)	deg

Inputs: Constants, Coefficients, and Data Tables

$\theta_{ERR\,LIM}$	Maximum error position limit on the governor actuator	deg
$\theta_{FCP\,LIM}$	Maximum governor flow control piston position limit	deg
P_{SRG}	Rotor collective governor actuator constant	lb/in^2
K_{1RGA}	Rotor collective governor actuator gain	ND
K_{2RGA}	Rotor collective governor actuator gain	ND

SUBSYSTEM NO. 17: ROTOR COLLECTIVE GOVERNOR (CONCLUDED)

Inputs: Constants, Coefficients, and Data Tables (Concluded)

Symbol	Description	Units
K_{3RGA}	Rotor collective governor actuator gain	ND
K_{4RGA}	Rotor collective governor actuator gain	ND
$RPM_{P_{MAX}}$	Maximum rotor RPM limit	RPM
K_{RPM}	Helicopter mode operating RPM ($\beta_m = 0$ deg)	percent
THOGMX	Governor blade angle limit (maximum)	deg
THOGMN	Governor blade angle limit (minimum)	deg
θ_{INT_1}	Rotor interconnect gear ratio	ND
K_{PROG}	Rotor collective governor proportional gain, $= f(\beta_m)$	ND
K_{INTG}	Rotor collective governor integral gain, $= f(\beta_m)$	ND

Outputs:

$\theta_{oL/G}$	Left rotor collective pitch input from the left rotor collective governor	deg
$\theta_{oR/G}$	Right rotor collective pitch input from the right rotor collective governor	deg
$RPM_{P_{MIN}}$	Minimum rotor RPM limit	RPM

EQUATIONS

SUBSYSTEM NO. 17--ROTOR COLLECTIVE GOVERNOR

NOTE: The described rotor collective governor model is based on the configuration incorporated in the Bell XV-15 and may not be appropriate for other tilt-rotor configurations (depending on mission requirements). Figure A17-1 provides a block diagram for this system.

A. RPM Error

System 1:

$$\epsilon_{RPM1} = \left[\frac{(\Omega_{INT})(9.55)}{\theta_{INT\,1}}\right] - RPM_{SEL}$$

System 2:

$$\epsilon_{RPM2} = \left[\frac{(\Omega_{INT})(9.55)}{\theta_{INT\,1}}\right] - \{XRPM - [XRPM - (K_{RPM})(RPM_{P_{MAX}})](\Delta RPM_{MAX})(\Delta t)\}$$

Where

$$XRPM = \frac{(\Omega_R)(60.0)}{2\pi}$$

and for the XV-15

$$\Delta RPM_{MAX} = 20.0 \quad RPM/sec$$

B. Electronic Command Signal

System 1:

$$\bar{\theta}_{oCMD1} = \int_{t-\Delta t}^{t} (K_{INTG})(\epsilon_{RPM1})dt + (K_{PROG})(K_{INTG})(\epsilon_{RPM1})$$

B. Electronic Command Signal (Concluded)

System 2:

$$\bar{\theta}_{oCMD2} = \int_{t-\Delta t}^{t} (K_{INTG})(\epsilon_{RPM2})dt + (K_{PROG})(K_{INTG})(\epsilon_{RPM2})$$

Where

$\bar{\theta}_{oCMD1,2}$ are limited such that

$$\theta_{oGMIN} \leq \bar{\theta}_{oCMD1,2} \leq \theta_{oGMAX}$$

C. Governor Actuator Dynamics

1. Rate and Displacement of Flow Control Valve

$$\theta_{ERROR} = \bar{\theta}_{oCMD1,2} - \theta_{oACT}$$

$$P_{RG} = P_{FCP} + P_{LOR}$$

Where limits exist such that

$$|\theta_{ERROR}| \leq \theta_{ERR\,LIM}$$

$$0 < P_{RG} < 500.0 \text{ psi}$$

$$P_{FCP} = (K_{3RGA})\left(\dot{\theta}_{oACT} - \dot{\theta}_{FCP}\right)\left(\left|\dot{\theta}_{oACT} - \dot{\theta}_{FCP}\right|\right)$$

C. Governor Actuator Dynamics (Concluded)

1. Rate and Displacement of Flow Control Valve (Concluded)

$$P_{LOR} = (K_{4RGA})(\dot{\theta}_{oACT})(|\dot{\theta}_{oACT}|)$$

$$\dot{\theta}_{FCPC} = \dot{\theta}_{oACT} - (K_{2RGA})\left(\frac{\theta_{FCP}}{|\theta_{FCP}|}\right)\left(\sqrt{|\theta_{FCP}|}\right)$$

Where

$$\text{If } |\theta_{FCP}| < \theta_{FCP_{LIM}} \text{ or if } sign(\dot{\theta}_{FCPC}) \neq sign(\theta_{FCP})$$

Then

$$\dot{\theta}_{FCP} = \dot{\theta}_{FCPC}$$

Otherwise

$$\dot{\theta}_{FCP} = 0.0$$

$$\theta_{FCP} = \int_{t-\Delta t}^{t} (\dot{\theta}_{FCP})\,dt$$

Where limits are such that

$$|\theta_{FCP}| \leq \theta_{FCP_{LIM}}$$

2. Rate and Displacement of Actuator

$$\dot{\theta}_{oACT} = (K_{IRGA})(\theta_{ERROR})\sqrt{1.0 - \left(\frac{P_{RG}}{P_{SRG}}\right)\left(\frac{\theta_{ERROR}}{|\theta_{ERROR}|}\right)}$$

$$\theta_{oACT} = \int_{t-\Delta t}^{t} \left(\dot{\theta}_{oACT}\right) dt$$

Where limits are

$$P_{SRG} \leq 499.0 \text{ psi}$$

$$THOGMN \leq \theta_{oACT} \leq THOGMX$$

D. <u>Governor Collective Pitch</u>

$$\theta_{oL/G} = \theta_{oR/G} = \theta_{oACT}$$

E. <u>Failure Logic</u>

See Figure A17-1

SYSTEM 1 (PRIMARY)

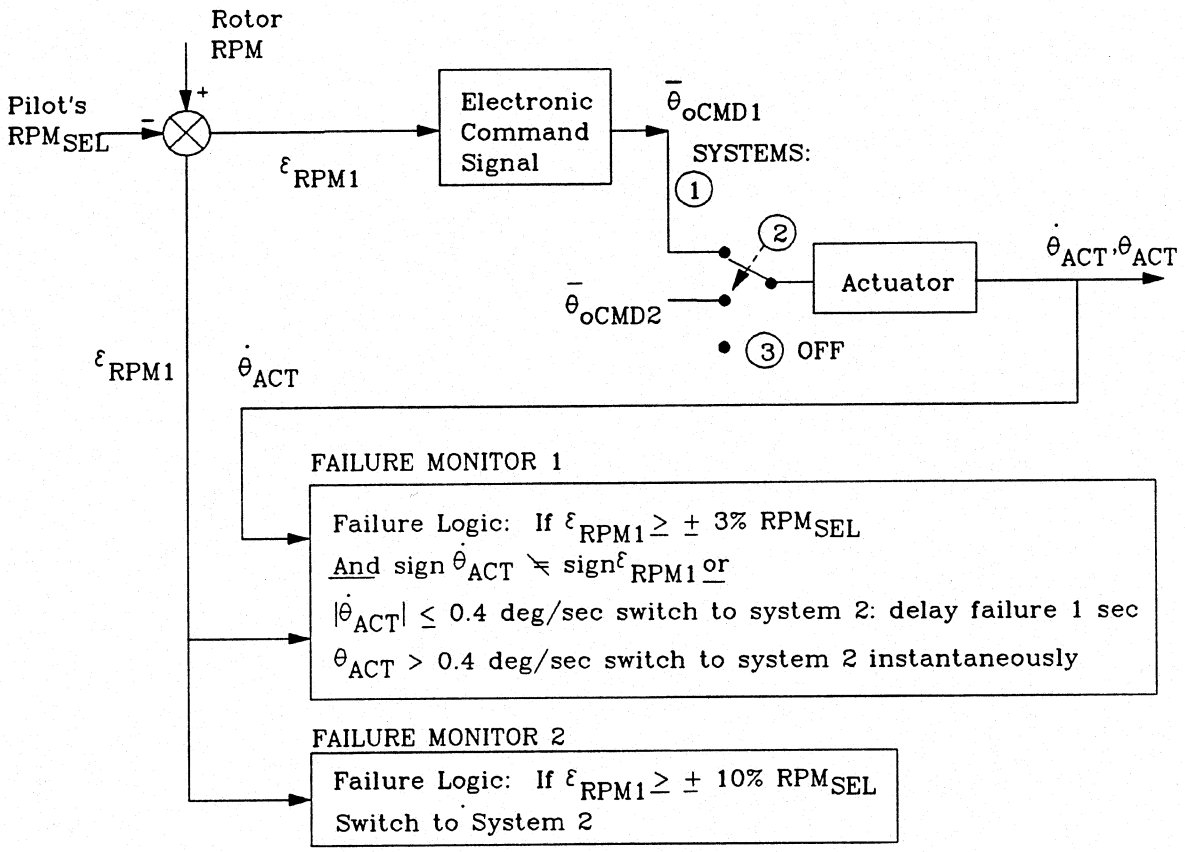

SYSTEM 2 (STANDBY)

SYNCHRONIZATION:

If on System 1: $\theta_{oCMD2} = \bar{\theta}_{oCMD1}$

If on System 2: $\theta_{oCMD2} = \theta_{oCMD2}$

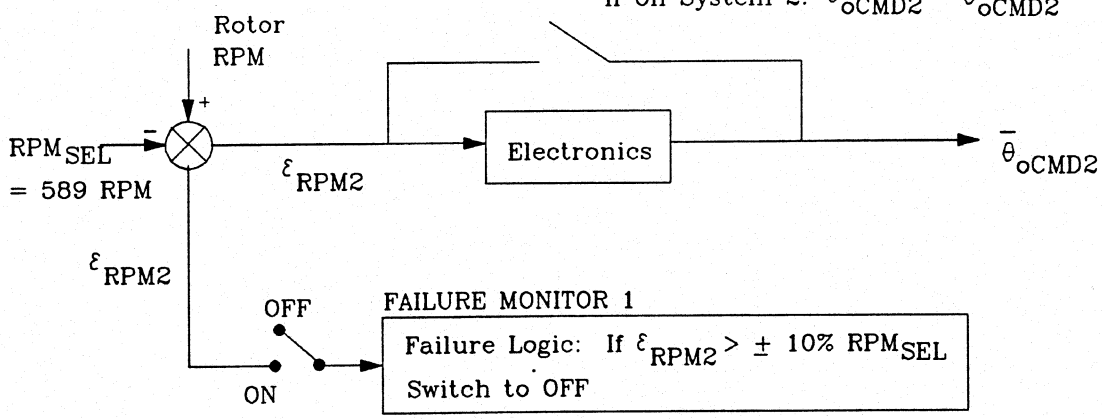

Following primary governor failure in switching to System 2, 5 sec ramp is used to get to 589 RPM from the RPM_{SEL} at failure.

Figure A17-1. XV-15 Rotor RPM Governor Failure Logic Block Diagram

NOTES ON GOVERNOR FAILURE LOGIC BLOCK DIAGRAM
(Figure A17-1)

1. Governor disengage switch on collective switches system to OFF.

2. Pilot's RPM select wheel on center console tracks actuator. Three (3) turns equals 38 deg of collective (stops at three turns).

3. With system OFF, $\theta_{oACT} = \theta_{WHEEL}$

4. RPM_{SEL} is limited as follows:

$$RPM_{SEL_{MAX}} = 601$$

$$RPM_{SEL_{MIN}} = 433 + (102)(\cos\beta_m)$$

5. RPM at failure is commanded at 20 RPM/sec to 589 RPM which becomes the new RPM_{SEL}.

6. Following a failure:

$$\dot{\theta}_{oACT}, \dot{\theta}_{FCP}, \theta_{FCP} = 0$$

Reset for standby

18	ENGINES AND FUEL CONTROLS

Inputs: Variables		Outputs:	
From Subsystem	**Symbol**	**To Subsystem**	**Symbol**
8a	X_{THR}	16, 19	Q_{RPT}
	X_{THL}		Q_{LPT}
10f	h_{CG}	13, 14	$(X,Z)_{JTR}$
12	V_T		$(X,Z)_{JTL}$
15	P_a		
	T_a		
10f	P_{ALT}		
19	Ω_{RPT}		
	Ω_{LPT}		
8a	β_m		

Inputs: Constants, Coefficients, and Data Tables

Constants: $P_o, T_o, RPME, SHP_{ACC}, \eta_{XMSN}$

Coefficients: $K_1 \rightarrow K_7, K_{11} \rightarrow K_{15}, K_{18}, \Delta\epsilon_p, \Delta\epsilon_s,$

T_D, pctmxs, pctmxp, RPM_{NII}, X_{EK}

(Concluded on next page)

18	ENGINES AND FUEL CONTROLS (CONCLUDED)

Inputs: Constants, Coefficients, and Data Tables (Concluded)

Data Tables	$RSHP = f(X_{THR})$	Table 18-I
	$K_{RAM} = \frac{RSHP}{RSHP_{V=0}} = f(V_T)$	Table 18-II
	$DSHPDT = \frac{dHP_{ROT}}{dt} = f(HP_{ENG}, P_{ALT})$	Table 18-III
	$K_{JT1} = f(V_T)$	Table 18-IV
	$K_{JT2} = f(V_T)$	Table 18-IV

SUBSYSTEM NO. 18: ENGINES AND FUEL CONTROLS

Inputs: Variables

Symbol	Description	Units
X_{THR}	Right engine throttle position at the fuel control	deg
X_{THL}	Left engine throttle position at the fuel control	deg
h_{CG}	Altitude of aircraft	ft
V_T	Total linear velocity of the aircraft c.g. with respect to air	ft/sec
P_a	Ambient absolute pressure	lb/ft^2
T_a	Ambient absolute temperature	deg K
P_{ALT}	Pressure attitude	ft
Ω_{RPT}	Right engine power turbine speed	rad/sec
Ω_{LPT}	Left engine power turbine speed	rad/sec
β_m	Mast conversion angle (+ fwd, 0 deg = vertical or helicopter, 90 deg = horizontal or airplane)	deg

Inputs: Constants, Coefficients, and Data Tables

P_o	Sea level standard atmospheric pressure	lb/in^2
T_o	Absolute sea level standard temperature	deg K
RPME	100 percent engine power turbine speed multiplier	ND

Inputs: Constants, Coefficients, and Data Tables (Continued)

Symbol	Description	Units
SHP_{ACC}	Engine accessory power loss	SHP
η_{XMSN}	Transmission efficiency	ND
K_1	Engine shaft horsepower equation coefficient	ND
K_2	Engine shaft horsepower equation coefficient	ND
K_3	Engine shaft horsepower equation coefficient	ND
K_4	Engine shaft horsepower equation coefficient	RPM
K_5	Engine shaft horsepower equation coefficient	$RPM/\sqrt{HP}$
K_6	Engine shaft horsepower equation coefficient	HP
K_7	Engine shaft horsepower equation coefficient	deg K
K_{11}	Engine throttle control coefficient	1/deg K
K_{12}	Engine throttle control coefficient	1/deg
K_{13}	Engine throttle control coefficient	$1/deg^2$
K_{14}	Engine throttle control coefficient	deg
K_{15}	Engine throttle control coefficient	1/kts
K_{18}	Engine rating (limit output)	SHP

Inputs: Constants, Coefficients, and Data Tables (Concluded)

Symbol	Description	Units
$\Delta\epsilon_p$	Commanded throttle position error threshold	ND
$\Delta\epsilon_s$	Power turbine RPM error threshold	ND
T_D	Engine throttle and power turbine response delay time	sec
pctmxs	Commanded power turbine speed at which the acceleration ceases to follow the maximum acceleration curve	percent
pctmxp	Commanded power at which the acceleration ceases to follow the maximum acceleration curve	percent
RPM_{NII}	Engine N_{II} RPM	rad/sec
X_{EK}	Right (K=1) or left (K=2) engine operating flag	ND
RSHP	Commanded (throttle) referred optimum SHP on one engine, $= f(X_{THR})$	SHP
K_{RAM}	Ram effect equation coefficient, $f(V_T)$	ND
DSHPDT	Rate of change of engine power, $= f(HP_{ENG}, P_{ALT})$	SHP/sec
K_{JT1}	Jet thrust coefficient, $= f(V_T)$	lb
K_{JT2}	Jet thrust coefficient, $= f(V_T)$	lb/SHP

SUBSYSTEM NO. 18: ENGINES AND FUEL CONTROLS (CONCLUDED)

Outputs:

Symbol	Description	Units
Q_{RPT}	Right engine power turbine torque	ft-lb
Q_{LPT}	Left engine power turbine torque	ft-lb
$(X,Z)_{JTR}$	Right engine jet thrust forces, body axis	lb
$(X,Z)_{JTL}$	Left engine jet thrust forces, body axis	lb

(Text of numbered notes is provided on the last page of the figure)

Note 1: Initialization

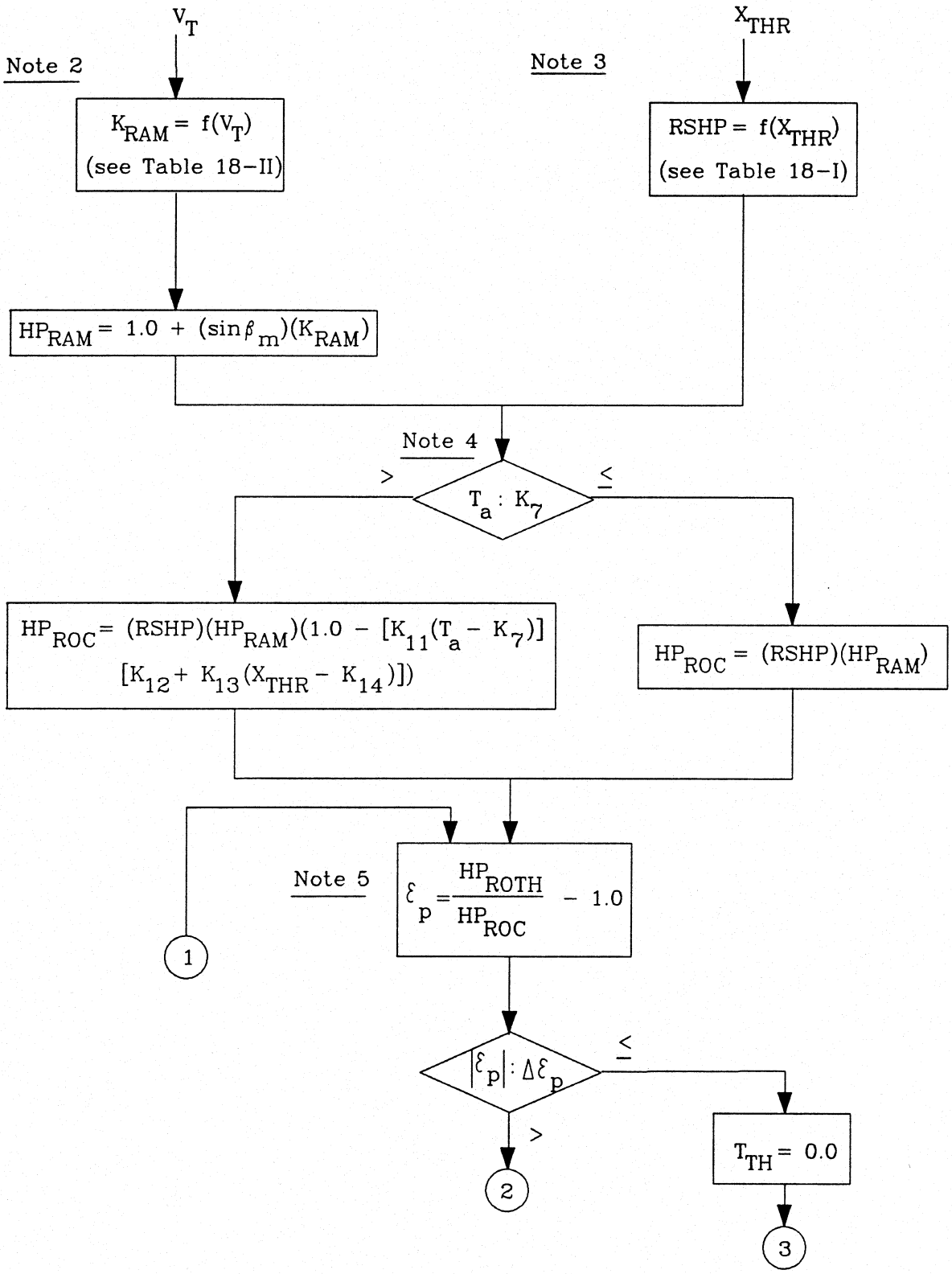

Figure A18-1. Engine Model Block Diagram

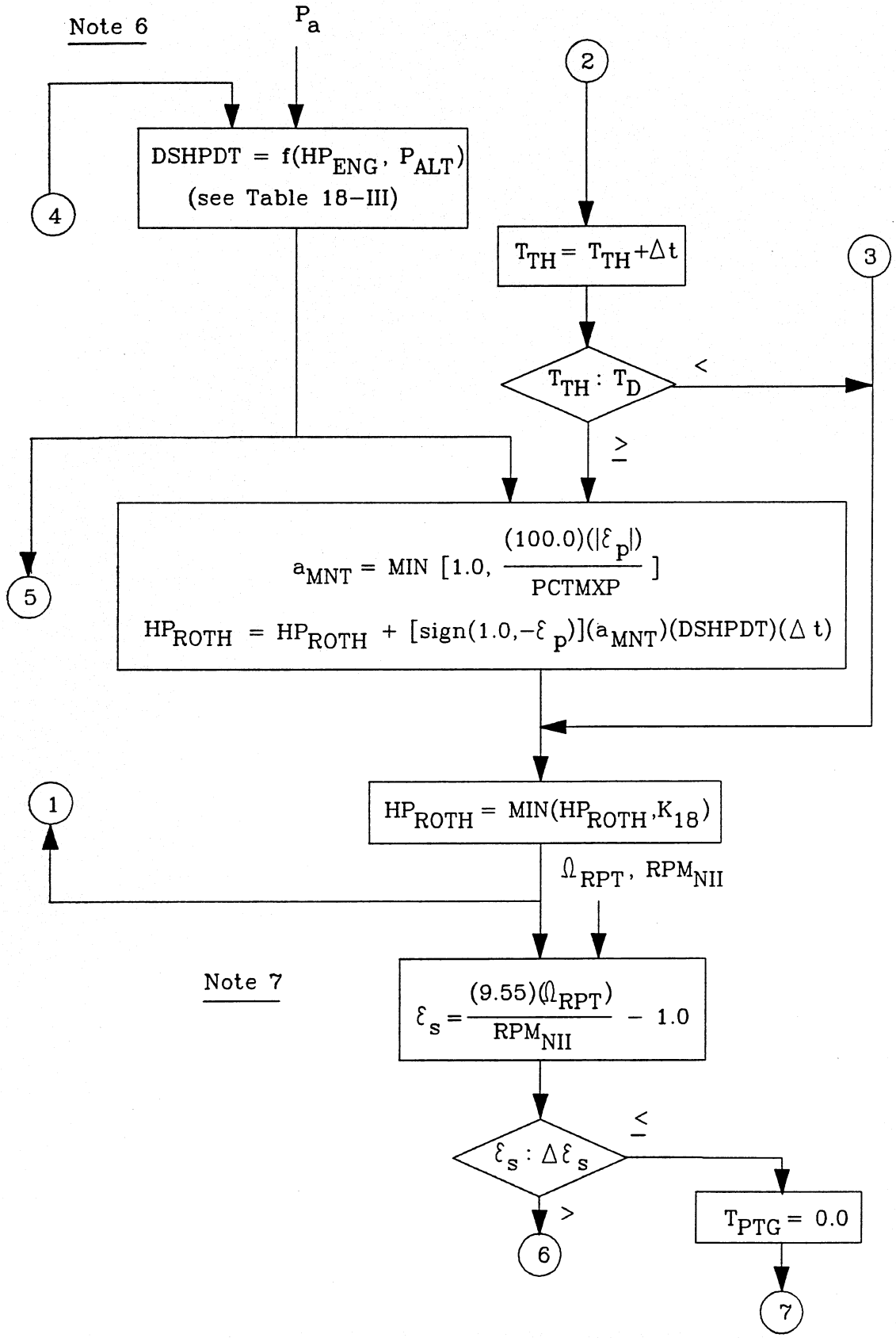

Figure A18-1 (Continued)

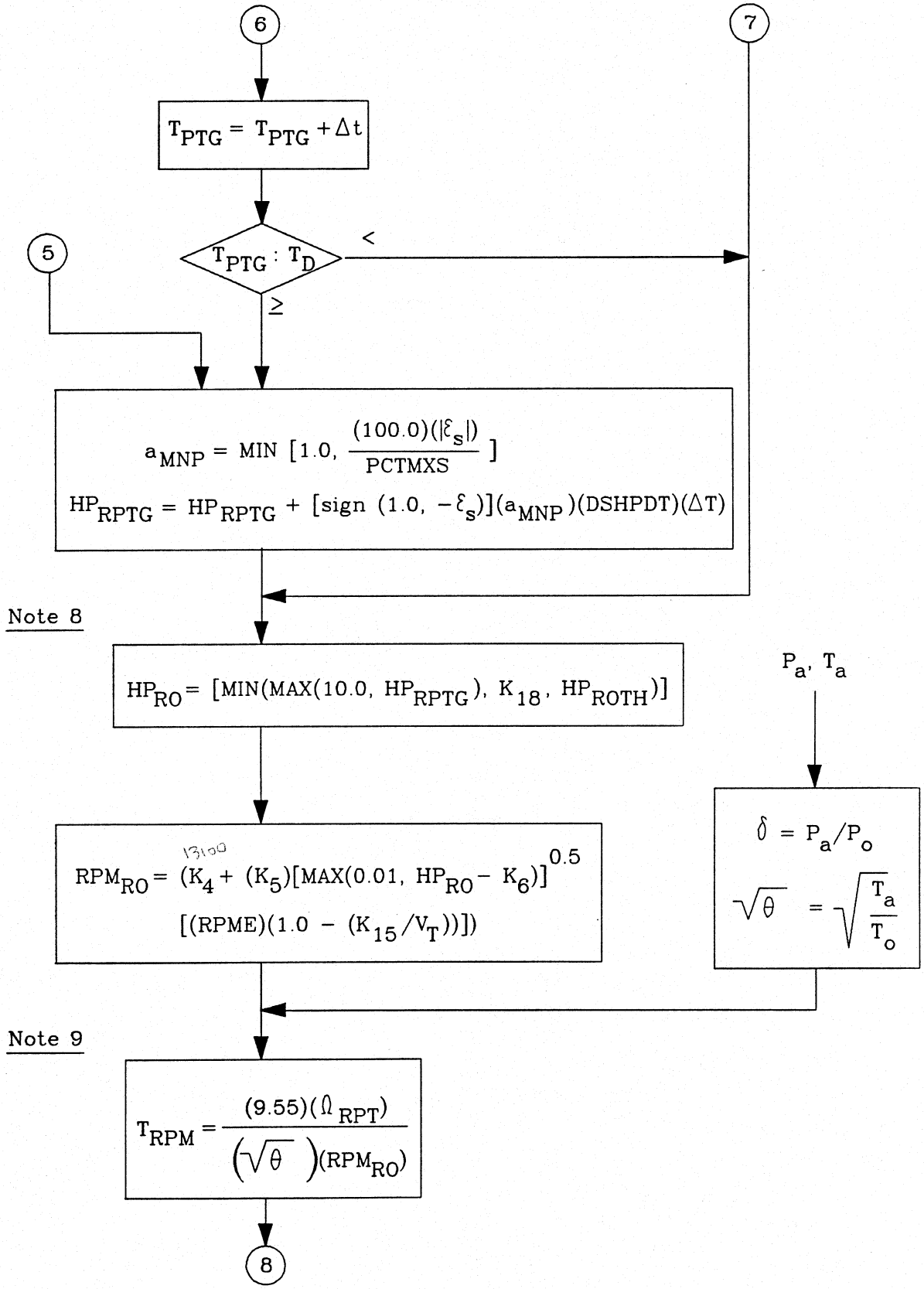

Figure A18–1 (Continued)

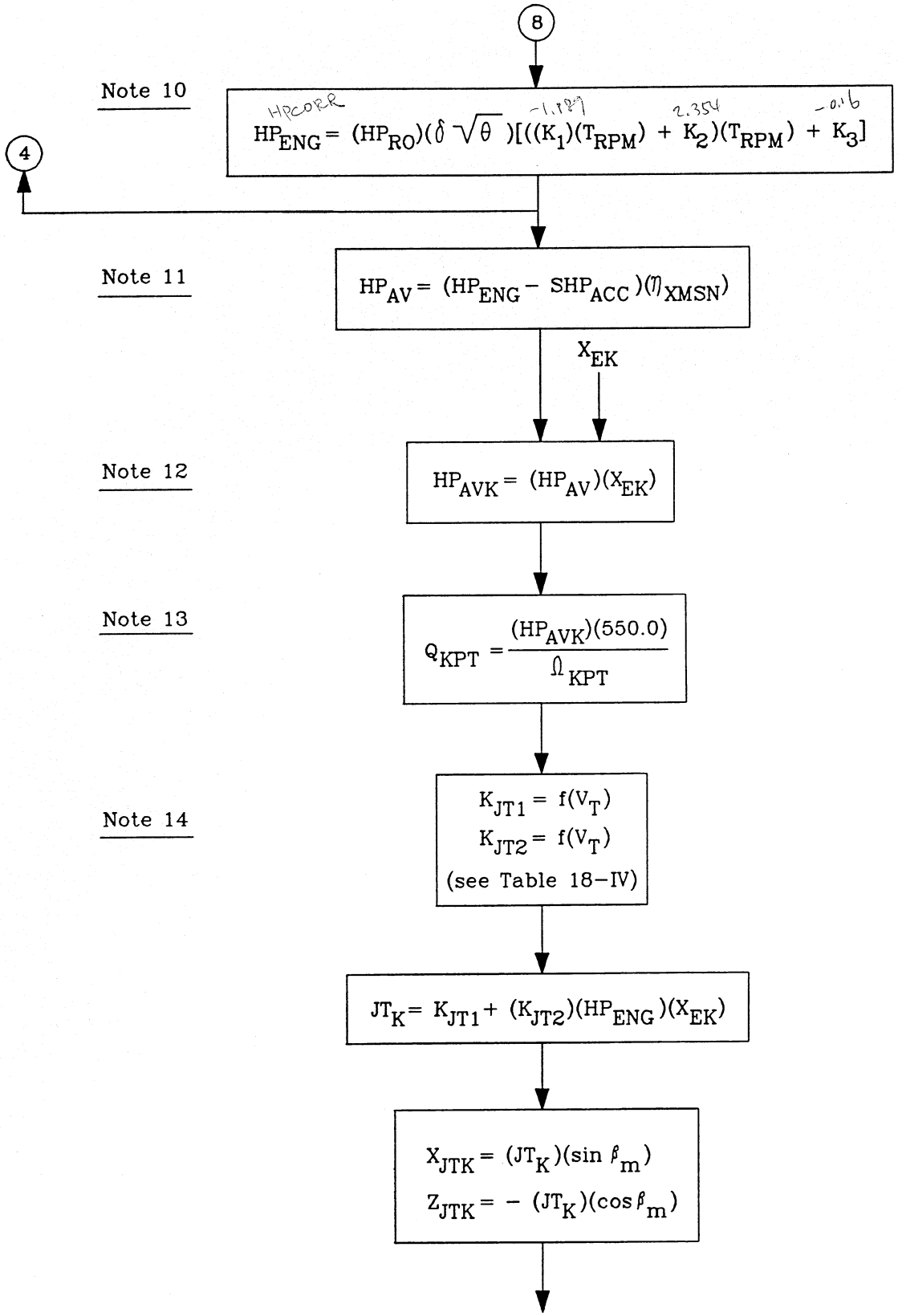

Figure A18-1 (Concluded)

NOTES FOR FIGURE A18-1

1. Upon initialization of program, set $HP_{RO} = HP_{ROC} = HP_{ROTH} = HP_{RPTG}$.

2. Engine RAM effect (data table input by user).

3. Commanded engine horsepower as a function of throttle position (data table input by user).

4. Commanded engine horsepower as modified by ambient temperature and RAM effects.

5. Engine throttle response model: the capability is included to provide a fixed time delay in the throttle response if a threshold of 0.2 percent change occurs in the throttle position. Limits are also provided in the model on the rate of the throttle response and the maximum commanded position (or power output). Δt represents the simulation cycle time.

6. The maximum engine power turbine acceleration/deceleration profile is a user input data table which is a function of pressure altitude and engine power output. Δt represents the simulation cycle time.

7. Engine power turbine NII governor model: this model regulates the engine power turbine speed using the same type of time delay and limiting features as provided in the throttle response model. (Note: for the XV-15, this model should be modified to act only as an overspeed governor if 104 percent RPM is exceeded.)

8. Optimum engine power (prior to RPM and atmospheric effect corrections).

9. Application of off-optimum RPM and atmospheric corrections to the value of optimum engine power.

10. Calculation of engine power available.

11. Calculation of available power following corrections for transmission efficiency and accessory power losses.

12. Flag check to identify if any engines are shut down. 'K' equals 'L' for the left engine and 'R' for the right engine.

NOTES FOR FIGURE A18-1 (CONCLUDED)

13. Calculation of right and left engine torques which are used in the drive system mathematical model (Subsystem 19).

14. Jet thrust calculations: jet thrust is calculated from user input data tables as a function of airspeed (for the desired engine type). The output jet thrust components in body axis are set to zero if the engine 'K' flag is set in the shut down engine position.

19	DRIVE SYSTEM DYNAMICS

Inputs: Variables		Outputs:	
From Subsystem	**Symbol**	**To Subsystem**	**Symbol**
1	Q_R	1, 16, 17	Ω_R
	Q_L		Ω_L
		16, 17	Ω_{INT}
18	Q_{RPT}		
	Q_{LPT}	16, 18	Ω_{RPT}
			Ω_{LPT}
8d	RPM_{SEL}		

Inputs: Constants, Coefficients, and Data Tables

Constants: $I_1, \theta_{RPT_1}, \theta_{INT_1}$

Coefficients: None

Data Tables: None

SUBSYSTEM NO. 19: DRIVE SYSTEM DYNAMICS

Inputs: Variables

Symbol	Description	Units
Q_R	Mast axis right rotor torque (+ trying to slow rotor down)	ft-lb
Q_L	Mast axis left rotor torque (+ trying to slow rotor down)	ft-lb
Q_{RPT}	Right engine power turbine torque	ft-lb
Q_{LPT}	Left engine power turbine torque	ft-lb
RPM_{SEL}	Pilot's commanded operating rotor speed	RPM

Inputs: Constants, Coefficients, and Data Tables

I_1	Drive system inertia	slug-ft^2
θ_{RPT_1}	Rotor turbine gear ratio	ND
θ_{INT_1}	Rotor interconnect gear ratio	ND

Outputs:

Ω_R	Instantaneous right rotor speed	rad/sec
Ω_L	Instantaneous left rotor speed	rad/sec
Ω_{INT}	Interconnect drive shaft speed	rad/sec
Ω_{RPT}	Right engine power turbine speed	rad/sec
Ω_{LPT}	Left engine power turbine speed	rad/sec

EQUATIONS

SUBSYSTEM NO. 19--DRIVE SYSTEM DYNAMICS

A. Summation of Torques at Drive Shaft and Angular Acceleration

$$F_1 = -(Q_R + Q_L) + (\theta_{RPT1})(Q_{RPT} + Q_{LPT})$$

$$\ddot{\xi} = \frac{F_1}{I_1}$$

B. Rotor Speed

$$\dot{\xi} = \dot{\xi}_{t-\Delta t} + \int_{t-\Delta t}^{t} \left(0.7\ddot{\xi} + 0.3\ddot{\xi}_{t-1}\right) dt$$

where, for simulation, PV stands for past value in the equation

$$\dot{\xi} = \dot{\xi}_{PV} + (\Delta t)\left(0.7\ddot{\xi} + 0.3\ddot{\xi}_{PV}\right)$$

$$\Omega_R = \Omega_{RO} + \dot{\xi}$$

$$\Omega_L = \Omega_R$$

where Ω_{RO}, the initial rotor reference rpm, is usually equal to

$$\Omega_{RO} = \frac{(RPM_{SEL})(2\pi)}{60.0}$$

where the pilot's selected operating rotor speed is in actuality the rotor reference RPM.

C. Power Turbine and Interconnect Shaft Angular Velocity

$$\Omega_{RPT} = (\Omega_R)(\theta_{RPT_1})$$

$$\Omega_{LPT} = \Omega_{RPT}$$

$$\Omega_{INT} = (\Omega_R)(\theta_{INT_1})$$

20	STABILITY AND CONTROL AUGMENTATION SYSTEM

Inputs: Variables		Outputs:	
From Subsystem	Symbol	To Subsystem	Symbol
8a	β_m	8a	PSCAS
			RSCAS
8d	X_{LN}		YSCAS
	X_{LT}		
	X_{PD}		
	ISCRLS		
	IQDAMP		
	IPDAMP		
	IRDAMP		
	IPCH		
	IRCH		
	IFAH		
	ISCENG		
11	p		
	q		
	r		
10c	ψ		
	θ		
	ϕ		

(Concluded on next page)

20	STABILITY AND CONTROL AUGMENTATION SYSTEM (CONCLUDED)

Inputs: Constants, Coefficients, and Data Tables

Constants: $X_{LNN}, X_{LTN}, X_{PDN}, K_{1P} \rightarrow K_{7P}, \tau_{1P} \rightarrow \tau_{6P},$

$\tau_q, K_{1Y} \rightarrow K_{3Y}, \tau_{1Y} \rightarrow \tau_{2Y}, K_{1R} \rightarrow K_{7R},$

$\tau_{1R} \rightarrow \tau_{5R}, \tau_p, PSCAS_{MX}, RSCAS_{MX}, YSCAS_{MX}$

$P_{HOLD_{MAX}}, R_{HOLD_{MAX}}$

Coefficients: None

Data Tables: None

SUBSYSTEM NO. 20: STABILITY AND CONTROL AUGMENTATION SYSTEM

Inputs: Variables

Symbol	Description	Units
β_m	Mast conversion angle (+ fwd, 0 deg = vertical or helicopter, 90 deg = horizontal or airplane)	deg
X_{LN}	Longitudinal stick position, inches from full aft	in
X_{LT}	Lateral stick position, inches from full left	in
X_{PD}	Pedal position, inches from full left	in
ISCRLS	SCAS release switch	ND
IQDAMP	Pitch SCAS ON/OFF switch	ND
IPDAMP	Roll SCAS ON/OFF switch	ND
IRDAMP	Yaw SCAS ON/OFF switch	ND
IPCH	Pitch channel switch (Channel 1, 2, both)	ND
IRCH	Roll channel switch (Channel 1, 2, both	ND
IFAH	Attitude retention ON/OFF switch	ND
ISCENG	SCAS engage switch	ND
p	Body axis roll rate	rad/sec
q	Body axis pitch rate	rad/sec
r	Body axis yaw rate	rad/sec
θ	Euler pitch angle	rad
ϕ	Euler roll angle	rad
ψ	Euler yaw angle	rad

Inputs: Constants, Coefficients, and Data Tables

Symbol	Description	Units
X_{LNN}	Longitudinal stick neutral position	in
X_{LTN}	Lateral stick neutral position	in
X_{PDN}	Pedal neutral position	in
$K_{1P} \rightarrow K_{7P}$	Pitch SCAS gains	See App. B
$\tau_{1P} \rightarrow \tau_{6P}, \tau_q$	Pitch SCAS time constants	sec
$K_{1Y} \rightarrow K_{3Y}$	Yaw SCAS gains	See App. B
$\tau_{1Y} \rightarrow \tau_{2Y}$	Yaw SCAS time constants	sec
$K_{1R} \rightarrow K_{7R}$	Roll SCAS gains	See App. B
$\tau_{1R} \rightarrow \tau_{5R}, \tau_q$	Roll SCAS time constants	sec
$PSCAS_{MX}$	Pitch (elevator) SCAS actuator limit	in
$RSCAS_{MX}$	Roll (aileron) SCAS actuator limit	in
$YSCAS_{MX}$	Yaw (rudder) SCAS actuator limit	in
$P_{HOLD_{MAX}}$	Pitch attitude hold limit	in
$R_{HOLD_{MAX}}$	Roll attitude hold limit	in

Outputs:

Symbol	Description	Units
PSCAS	Pitch (elevator) SCAS output	in
RSCAS	Roll (aileron) SCAS output	in
YSCAS	Yaw (rudder) SCAS output	in

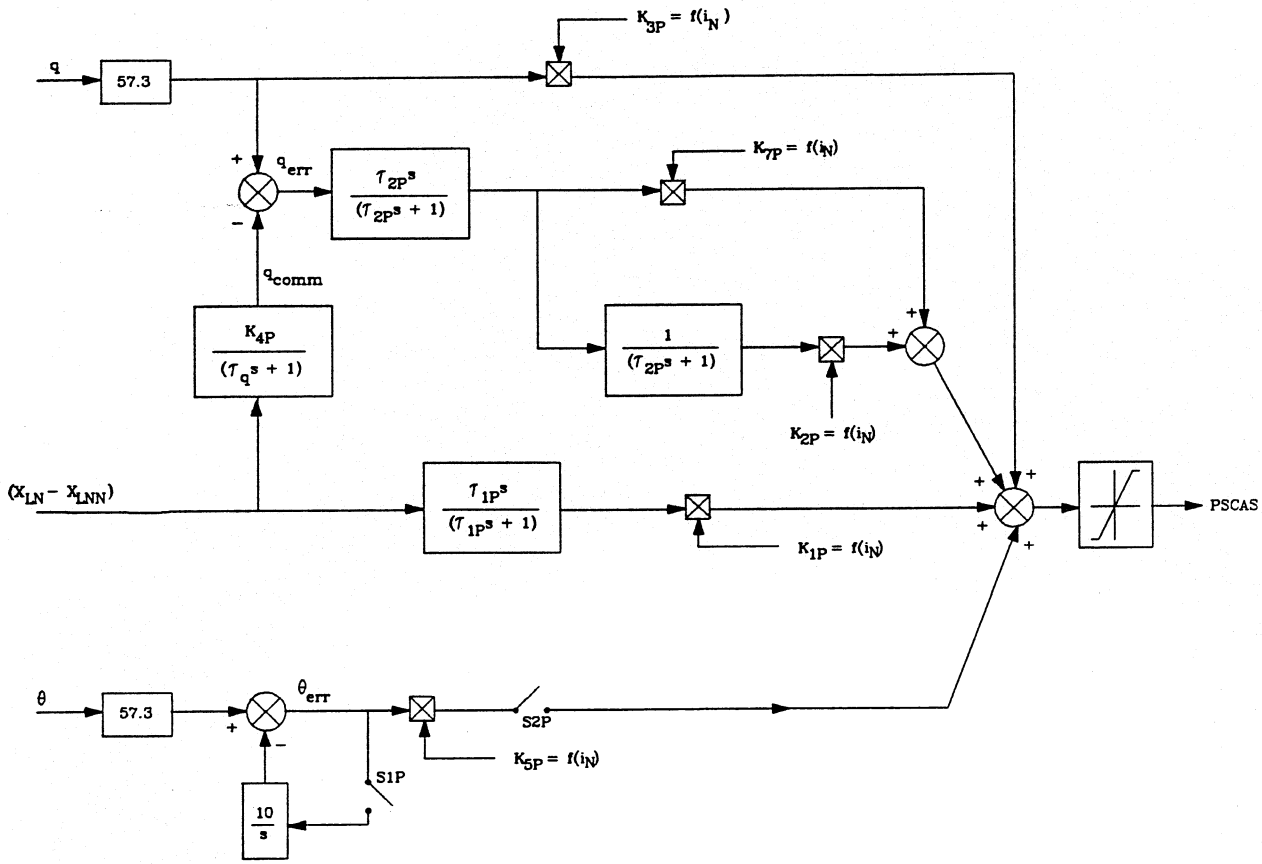

NOTES:

1. $i_N = (90 - \beta_m)$
2. Gains scheduled as $f(\beta_m)$ in form

$$K_{XP} = (K_{XP})_{\beta_m = 90} + \left[(K_{XP})_{\beta_m = 0} - (K_{XP})_{\beta_m = 90}\right](\cos\beta_m)$$

3. Limit on the output PSCAS is: $\pm$ $PSCAS_{MX}$

<u>Attitude Mode Switching</u>

Retention Mode

	OFF	ON	
		in det.	out det.
S1P	C	0	C
S2P	0	C	C

Command Mode

	OFF	ON
S1P	C	0
S2P	0	C

Figure A20-1. Modified XV-15 Pitch SCAS Block Diagram (S/N 703)

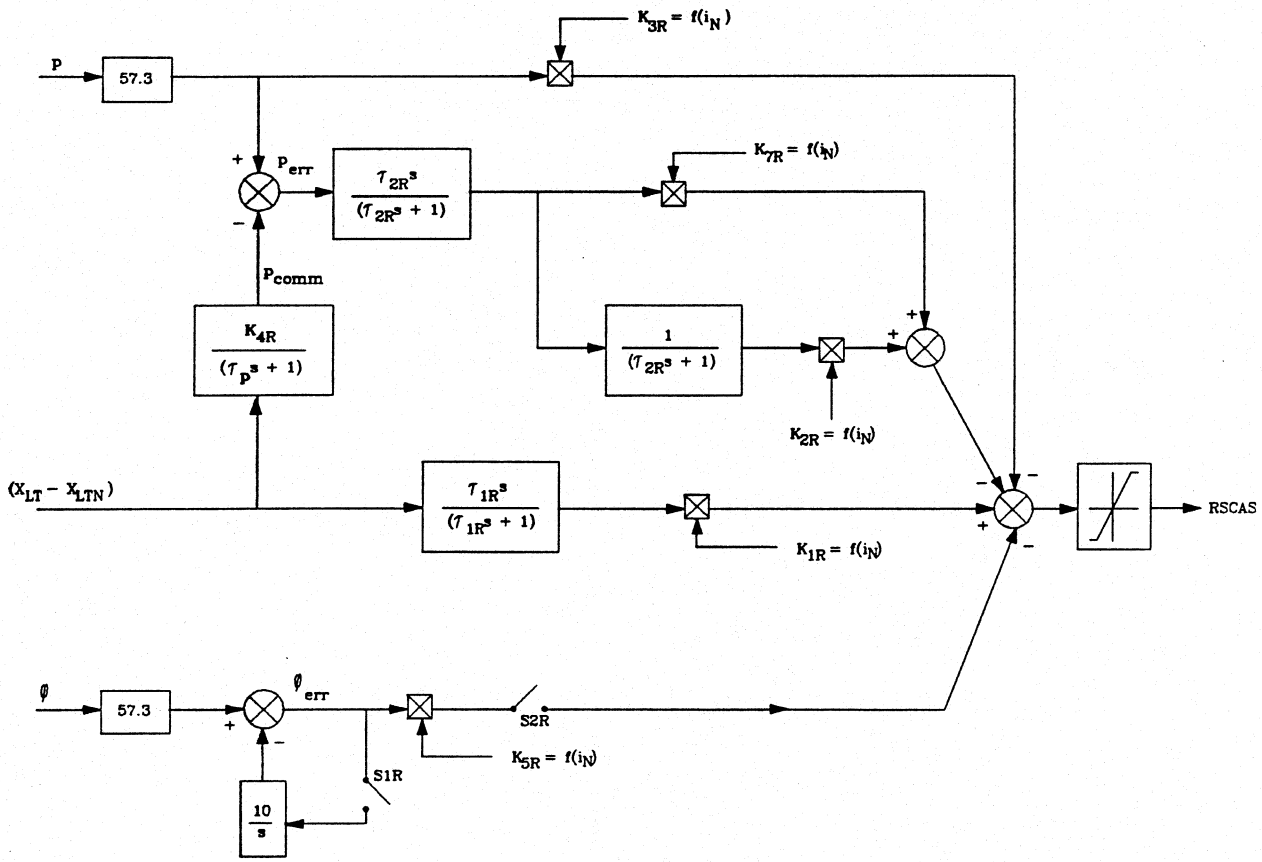

NOTES: 1. $i_N = (90 - \beta_m)$

2. Gains scheduled as $f(\beta_m)$ in form

$$K_{XR} = (K_{XR})_{\beta_m - 90} + \left[(K_{XR})_{\beta_m - 0} - (K_{XR})_{\beta_m - 90}\right](\cos\beta_m)$$

3. Limit on the output RSCAS is: $\pm$ $RSCAS_{MX}$

<u>Attitude Mode Switching</u>

Retention Mode

	OFF	ON	
		in det.	out det.
S1P	C	O	C
S2P	O	C	C

Command Mode

	OFF	ON
S1P	C	O
S2P	O	C

Figure A20-2. Modified XV-15 Roll SCAS Block Diagram (S/N 703)

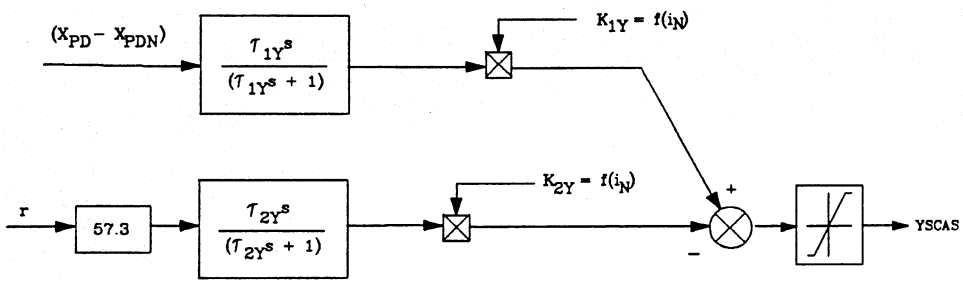

NOTES:

1. $i_N = (90 - \beta_m)$
2. Gains scheduled as $f(\beta_m)$ in form

   $$K_{XY} = (K_{XY})_{\beta_m = 90} + \left[(K_{XY})_{\beta_m = 0} - (K_{XY})_{\beta_m = 90}\right](\cos\beta_m)$$

3. Limit on the output YSCAS is: $\pm$ $YSCAS_{MX}$

Figure A20-3. Modified XV-15 Yaw SCAS Block Diagram (S/N 703)

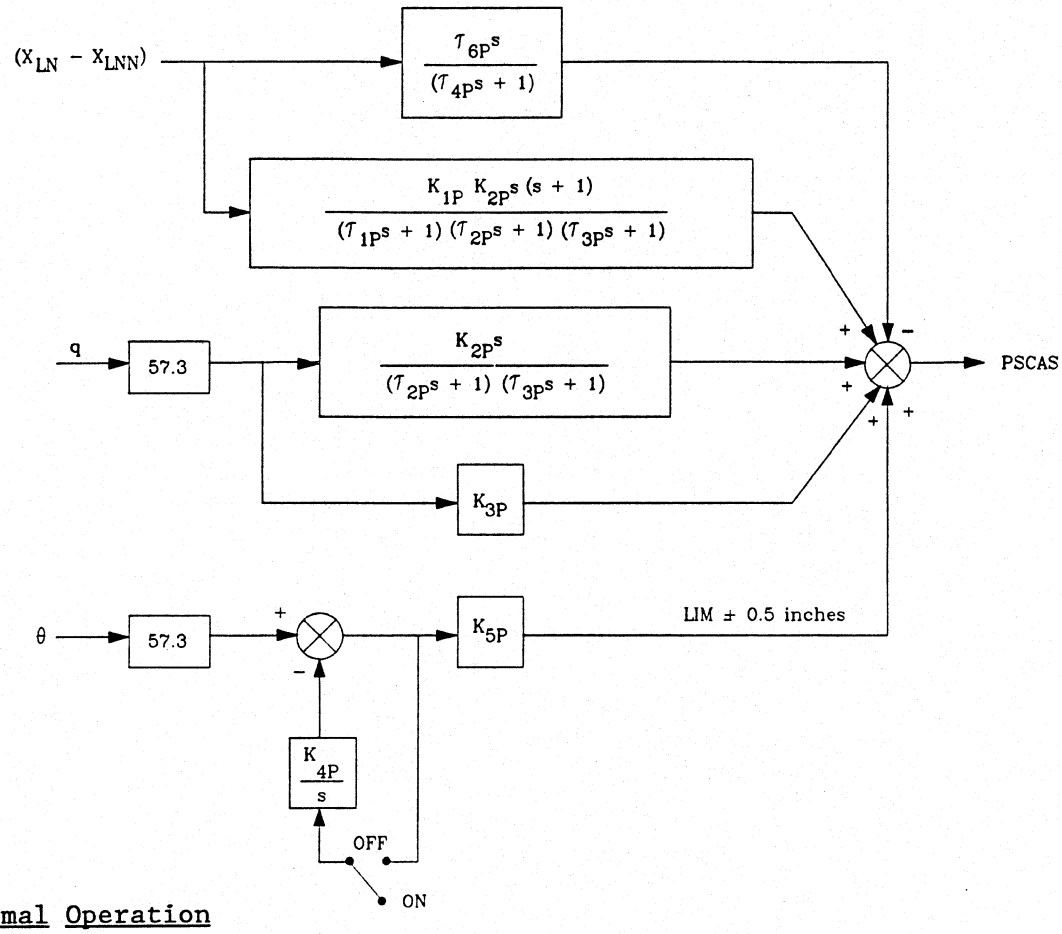

1. <u>Normal Operation</u>

   PSCAS(1) = 1/2 [sign (PSCAS)][min ($PSCAS_{MX}$, |PSCAS|)]
   PSCAS(2) = PSCAS(1)
   PSCAS = PSCAS(1) + PSCAS(2)

2. <u>Hardover</u>

   PSCAS(2) = 1/2 $PSCAS_{MX}$

3. <u>Open Feedback Loop</u>

   PSCAS(2) = 1/2 [sign (PSCAS)]($PSCAS_{MX}$)

4. <u>Attitude Hold is OFF if:</u>

   a. $|F_{XLN}| \leq 1.0$ lb or
   b. ATT RETN switch on SCAS panel is "OFF"
   c. Channel select switch is not at "BOTH"
   d. PSCAS(1) ≠ PSCAS(2) ± 20%

Figure A20-4. Bell XV-15 Pitch Axis SCAS Block Diagram (S/N 702)

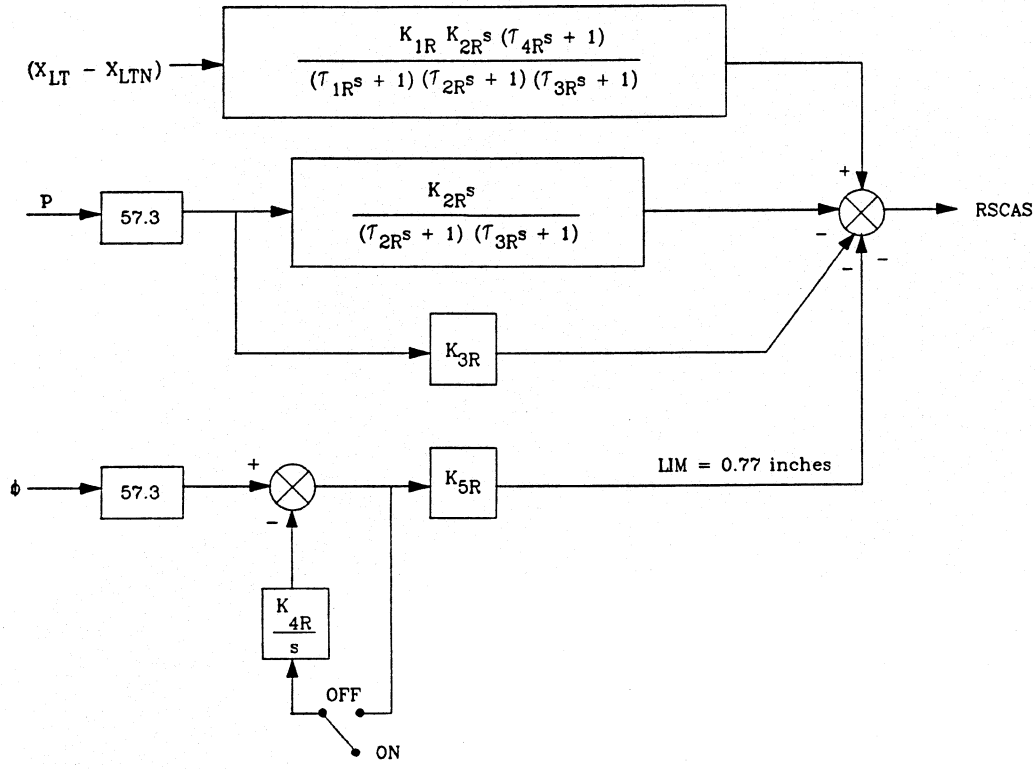

1. <u>Normal Operation</u>

   RSCAS(1) = 1/2 [sign (RSCAS)][min ($RSCAS_{MX}$) - |RSCAS|)]
   RSCAS(2) = RSCAS(1)
   RSCAS = RSCAS(1) + RSCAS(2)

2. <u>Hardover</u>

   RSCAS(2) = 1/2 $RSCAS_{MX}$

3. <u>Open Feedback Loop</u>

   RSCAS(2) = 1/2 [sign (RSCAS)]($RSCAS_{MX}$)

4. <u>Attitude Hold is OFF if:</u>

   a. $|F_{XLT}| \leq 0.5$ or
   b. ATT RETN switch on SCAS panel is "OFF"
   c. Channel select switch is not at "BOTH"
   d. RSCAS(1) ≠ RSCAS(2) ± 20%

Figure A20-5. Bell XV-15 Roll Axis SCAS Block Diagram (S/N 702)

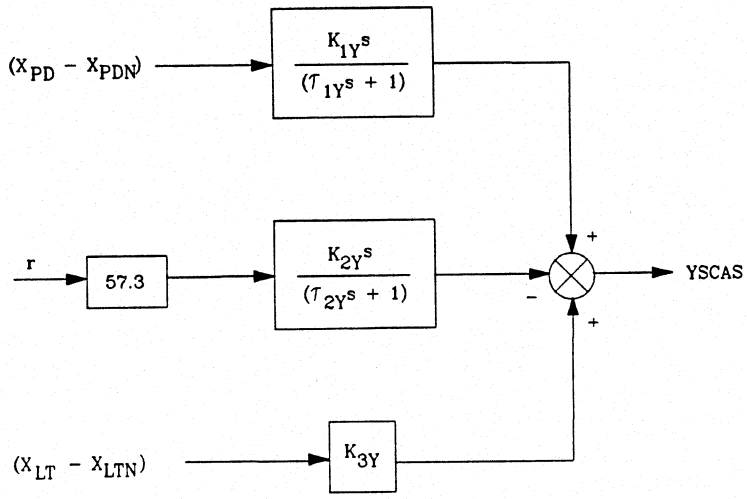

1. <u>Normal Operation</u>

   YSCAS = [sign (YSCAS)][min ($YSCAS_{MX}$, |YSCAS|)]

2. <u>Hardover</u>

   YSCAS = $YSCAS_{MX}$

3. <u>Open Feedback Loop</u>

   YSCAS = [sign (YSCAS)]($YSCAS_{MX}$)

Figure A20-6. Bell XV-15 Yaw Axis SCAS Block Diagram (S/N 702)

APPENDIX B

INPUT DATA ARRAY FOR THE XV-15 TILT-ROTOR RESEARCH AIRCRAFT

APPENDIX B

TABLE OF CONTENTS

	Page
Table I. XV-15 CG and Inertia Data	B-11
Table II. General XV-15 Design Data	B-12
Subsystem No. 1--XV-15 Rotor Aerodynamics	
Constants	B-16
Coefficients	B-17
Data Tables	
Table 1-I, Maximum Available Rotor Thrust Coefficient, $\bar{C}_T = f(\mu, \beta_m)$	B-18
Table 1-II, Sideward Flight Rotor Correction Factor, $X_{SF} = f(\lvert\bar{V}\rvert)$	B-19
Table 1-III, Side-by-Side Rotor Correction Factor, $X_{SS} = f(\lvert\bar{\mu}\rvert)$	B-20
Subsystem No. 2--XV-15 Rotor Induced Velocities	
Constants	B-21
Coefficients	B-21
Data Tables	
Table 2-Ia, Rotor Wake on Horizontal Stabilizer, $(W_i\big\|_{R/H})/W_i$, $\beta_m = 0$ deg	B-22
Table 2-Ib, Rotor Wake on Horizontal Stabilizer, $(W_i\big\|_{R/H})/W_i$, $\beta_m = 15$ deg	B-23
Table 2-Ic, Rotor Wake on Horizontal Stabilizer, $(W_i\big\|_{R/H})/W_i$, $\beta_m = 30$ deg	B-24
Table 2-Id, Rotor Wake on Horizontal Stabilizer, $(W_i\big\|_{R/H})/W_i$, $\beta_m = 60, 90$ deg	B-24
Table 2-II, Rotor Wake on Horizontal Stabilizer, K_{H_β}	B-25

TABLE OF CONTENTS (Continued)

Page

Subsystem No. 3--XV-15 Fuselage Aerodynamics

Constants B-26

Data Tables

Table 3-I, Fuselage Lift with Angle of Attack, L_α B-26

Table 3-II, Fuselage Lift with Sideslip, L_β B-28

Table 3-III, Fuselage Drag with Angle of Attack, D_α B-26

Table 3-IV, Fuselage Drag with Sideslip, D_β B-28

Table 3-V, Fuselage Pitching Moment with Angle of Attack, M_α B-26

Table 3-VI, Fuselage Pitching Moment with Sideslip, M_β B-28

Table 3-VII, Fuselage Side Force with Sideslip, Y_β B-30

Table 3-VIII, Fuselage Rolling Moment with Sideslip, l_β B-30

Table 3-IX, Fuselage Yawing Moment with Sideslip, N_β B-30

Subsystem No. 4--XV-15 Wing-Pylon Aerodynamics

Constants B-31

Coefficients B-31

Data Tables

Table 4-I, XV-15 Wing-Pylon Lift Coefficient ($C_{L_{WP}}$), Flap Setting, X_{FL1} = 0/0 ..... B-34

Table 4-II, XV-15 Wing-Pylon Lift Coefficient ($C_{L_{WP}}$), Flap Setting, X_{FL2} = 20/12.5, X_{FL3} = 40/25, X_{FL4} = 75/47 ..... B-36

Table 4-III, XV-15 Wing-Pylon Drag Coefficient ($C_{D_{WP}}$), Flap Setting, X_{FL1} = 0/0 ..... B-40

Table 4-IV, XV-15 Wing-Pylon Drag Coefficient ($C_{D_{WP}}$), Flap Setting, X_{FL2} = 20/12.5, X_{FL3} = 40/25, X_{FL4} = 75/47 ..... B-41

TABLE OF CONTENTS (Continued)

Page

Table 4-V(a), XV-15 Wing Wake Deflection on Horizontal Stabilizer ($\varepsilon_{W/HOGE}$), β_m = 90 deg B-45

Table 4-V(b), XV-15 Wing Wake Deflection on Horizontal Stabilizer ($\varepsilon_{W/HOGE}$), β_m = 60 deg B-46

Table 4-V(c), XV-15 Wing Wake Deflection on Horizontal Stabilizer ($\varepsilon_{W/HOGE}$), β_m = 30 deg B-47

Table 4-V(d), XV-15 Wing Wake Deflection on Horizontal Stabilizer ($\varepsilon_{W/HOGE}$), β_m = 15 deg B-48

Table 4-V(e), XV-15 Wing Wake Deflection on Horizontal Stabilizer ($\varepsilon_{W/HOGE}$), β_m = 0 deg B-49

Table 4-VI, XV-15 Wing-Pylon Rolling Moment, $C_{l_\beta}\Big|_{C_{L_{WP}}=M_N=0}$, 1/rad B-50

Table 4-VII, XV-15 Wing-Pylon Rolling Moment, $\dfrac{C_{l_\beta}}{C_{L_{WP}}}\Bigg|_{M_N=0}$, 1/rad B-50

Table 4-VIII, XV-15 Wing-Pylon Pitching Moment, $C_{m_{WP}}$, 1/rad B-51

Table 4-IX, Partial of Wing Coefficient of Lift with Respect to Angle of Attack $\dfrac{\partial C_{L_{WPFS}}}{\partial \alpha_{WFS}}\Bigg|_{C_{L_{WP}}=0}$ B-51

Table 4-X, Wing Coefficient of Drag at Wing Coefficient of Lift Equal to Zero, $C_{D_{oWP}}|C_{L_{WP}}=0$ B-52

Table 4-XI, XV-15 Aileron Effectiveness Correction for Flap and Mast ($K_{l_{\delta_a}}$) for $|\alpha_W| < 8$ deg B-53

Table 4-XII, XV-15 Aileron Effect on Wing Lift ($C_{l_{\delta_a}}$) B-54

Table 4-XIII and 4-IX, XV-15 Aileron Yaw Coefficient ($C_{n_{\delta_a}}$) B-54

TABLE OF CONTENTS (Continued)

Page

Table 4-XV, Pylon Interference Drag Coefficient, D_{PYINT} B-55

Table 4-XVI, Pylon Drag Factor with Sideslip, K_{PLAT} B-55

Subsystem No. 5--XV-15 Horizontal Stabilizer Aerodynamics

Constants B-56

Coefficients B-56

Data Tables

Table 5-I, XV-15 Horizontal Stabilizer Lift Coefficient, C_{LH} B-56

Table 5-II, XV-15 Horizontal Stabilizer Lift Coefficient, C_{LH} B-60

Table 5-III, XV-15 Horizontal Stabilizer Drag Coefficient, C_{DH} B-62

Table 5-IV, XV-15 Elevator/Rudder Effectiveness (τ_e/τ_r) Correction for Mach Number Effects, X_{Ke}, X_{Kr} B-64

Table 5-V(a), XV-15 Dynamic Pressure Ratio at the Horizontal Stabilizers (η_H or η_V), β_m = 0 deg, Rotors ON B-65

Table 5-V(b), XV-15 Dynamic Pressure Ratio at the Horizontal Stabilizers (η_H or η_V), β_m = 15 deg, Rotors ON B-66

Table 5-V(c), XV-15 Dynamic Pressure Ratio at the Horizontal Stabilizers (η_H or η_V), β_m = 30, 60, 90 deg, Rotors ON B-67

Table 5-VI, Dynamic Pressure Loss Factor Due to Fuselage Sideslip Angle for the Horizontal and Vertical Stabilizers, $K_{\beta HS}$ or $K_{\beta VS}$ B-68

Table 5-VII, Mach Number Effect on the Downwash Term ($\partial\varepsilon_{W/H}/\partial\alpha_W$), PCPM B-68

TABLE OF CONTENTS (Continued)

Page

Subsystem No. 6--XV-15 Vertical Fin Aerodynamic Data

Constants B-69

Coefficients B-69

Data Tables

Table 6-I, XV-15 Vertical Stabilizer Lift Coefficient (C_{YV}) B-70

Table 6-II, XV-15 Vertical Stabilizer Lift Coefficient (C_{YV}) B-73

Table 6-III, XV-15 Vertical Stabilizer Drag Coefficient (C_{DV}) B-75

Table 6-IV, XV-15 Sidewash Factor $\left(1 - \frac{\partial\sigma}{\partial\beta_F}\right)$ for Flap Setting, X_{FL1} = 0/0 ..... B-77

Table 6-V, XV-15 Sidewash Factor $\left(1 - \frac{\partial\sigma}{\partial\beta_F}\right)$ for Flap Setting, X_{FL2} = 20/12.5 ..... B-78

Table 6-VI, XV-15 Sidewash Factor $\left(1 - \frac{\partial\sigma}{\partial\beta_F}\right)$ for Flap Setting, X_{FL3} = 40/25 ..... B-79

Table 6-VII, XV-15 Sidewash Factor $\left(1 - \frac{\partial\sigma}{\partial\beta_F}\right)$ for Flap Setting, X_{FL4} = 75/47 ..... B-80

Table 6-VIII, XV-15 Rotor Sidewash Factor ($K_{\beta R}$) B-81

Subsystem No. 7A--XV-15 Landing Gear

Constants B-82

Coefficients B-82

Data Tables

Table 7A-I, Landing Gear Drag as a Percent of Gear Extension B-83

Table 7A-II, Main Landing Gear Drag as a Function of Landing Gear Position (D_{MG}) B-84

TABLE OF CONTENTS (Continued)

Page

Table 7A-III, Nose Landing Gear Drag as a Function of Landing Gear Position (D_{NG}) B-85

Figure B7A-1, Landing Gear Drag as a Function of Landing Gear Position B-86

Subsystem No. 7B--XV-15 Landing Gear

Constants B-87

Coefficients B-87

Subsystem No. 8a--XV-15 Controls

Constants B-88

Coefficients B-88

Data Tables

Table 8a-I, XV-15 F/A Cyclic Pitch to Longitudinal Gearing, $(\frac{\partial B_1}{\partial X_{LN}})$ B-89

Table 8a-II, XV-15 Differential Cyclic Pitch Gearing, $(\frac{\partial B_1}{\partial X_{PD}})$ B-90

Table 8a-III, XV-15 Differential Collective Pitch Gearing, $(\frac{\partial \theta_o}{\partial X_{LT}})$ B-91

Table 8a-IV, XV-15 Collective Pitch Gearing, $(\frac{\partial \theta_o}{\partial X_{COL}}; \theta_{oLL}$ at 0.75 R) B-92

Table 8a-V, XV-15 Commanded Pylon Conversion Rate, $\dot{\beta}_{mC}$ B-93

Table 8a-VI, XV-15 Collective Rigging Versus Throttle Rigging, X_{COL} versus $X_{THR,L}$ B-94

Table 8a-VII, XV-15 Mast Angle Versus Flapping Controller Gain, β_m versus $A_{1_{\beta_m}}$ B-95

TABLE OF CONTENTS (Continued)

Page

Table 8a-VIII, XV-15 U Velocity Versus Flapping Controller Gain, U versus $A_{1_{V_T}}$ B-95

Subsystem No. 8b--XV-15 Force Feel System Coefficients B-96

Subsystem No. 8c--XV-15 Control Force Trim System Coefficients B-97

Subsystem No. 9--XV-15 CG and Inertia
Constants B-98
Coefficients B-98

Subsystem No. 10a--XV-15 Axes Transformation (Airframe Aerodynamic Forces and Moments From Wind to Body Axis)
Constants B-99

Subsystem No. 10b--XV-15 Axes Transformation (Rotor Forces and Moments From Wind to Body Axis)
Constants: B-100

Subsystem No. 10f--XV-15 Axes Transformation (Ground Reference Difference)
Constants: B-101

Subsystem No. 11--XV-15 Angular Accelerations and Velocities
Constants B-102

Subsystem No. 12--XV-15 Body Axis Linear Acceleration and Velocities
Constants B-103

TABLE OF CONTENTS (Continued)

	Page
Subsystem No. 13--XV-15 Force Summation	B-104
Subsystem No. 14--XV-15 Moment Summation	
Constants	B-105
Coefficients	B-106
Subsystem No. 15--XV-15 Flight Environment Group	
Constants	B-107
Subsystem No. 17--XV-15 Rotor Collective Governor	
Constants	B-108
Coefficients	B-108
Data Tables	
Table 17-I, XV-15 Mast Angle Versus Rotor Collective Governor Proportional Gain, β_m versus K_{PROG}	B-109
Table 17-II, XV-15 Mast Angle Versus Rotor Collective Governor Integral Gain, β_m versus K_{INTG}	B-109
Subsystem No. 18--XV-15 Engines and Fuel Controls	
Constants	B-110
Coefficients	B-110
Data Tables	
Table 18-I, XV-15 Throttle Versus Rower Rigging, X_{THR} versus R_{SHP}	B-111
Table 18-II, XV-15 Engine RAM Effect	B-112
Table 18-III, T-53 (LTCIK-4K) Engine Acceleration Characteristics	B-112
Table 18-IV, XV-15 Jet Thrust Coefficients	B-113
Figure B18-1. T53 Engine Acceleration Characteristics	B-114

TABLE OF CONTENTS (Concluded)

	Page
Subsystem No. 19--XV-15 Drive System Constants	B-115
Subsystem No. 20--XV-15 Stability and Control Augmentation System Constants	B-116

TABLE I. XV-15 CG AND INERTIA DATA

Gross Wt.	= 13000 lbs		= 10877 lbs
	Aft CG	Fwd CG	Fwd CG
$SL_{CG}\|_{\beta_m=0}$	301.2	291.7	290.
$BL_{CG}\|_{\beta_m=0}$	0	0	0.
$WL_{CG}\|_{\beta_m=0}$	81.65	81.65	80.
$I_{XX}\|_{\beta_m=0}$	52795	52795	40940
$I_{YY}\|_{\beta_m=0}$	21360	21360	13638
$I_{ZZ}\|_{\beta_m=0}$	66335	66335	51674
$I_{XZ}\|_{\beta_m=0}$	1234	1234	1200

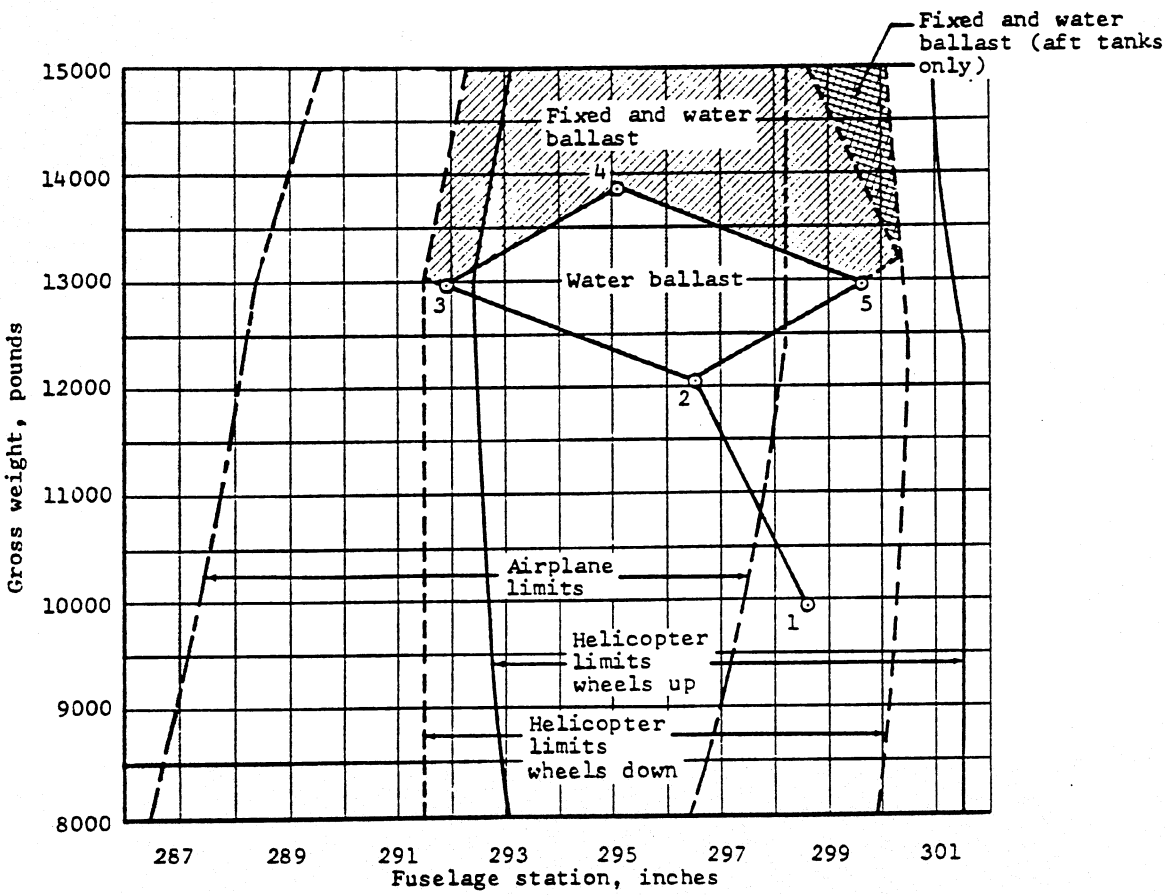

TABLE II. GENERAL XV-15 DESIGN DATA

ITEM	SYMBOL	XV-15 VALUE
Fuselage		
Center of pressure	SL_F	293.0 in
	BL_F	0.0 in
	WL_F	84.0 in
Wing-Pylon		
Center of pressure	SL_{WP}	291.7 in
	BL_{WP}	102.5 in
	WL_{WP}	95.85 in
Area	S_W	181.0 ft^2
Span	b_W	32.17 ft
Chord	c_W	5.255 ft
Sweep (quarter chord)	$[\Lambda_{c/4}]_W$	-6.5 deg
Aspect ratio	AR_W	5.7
Trailing edge	SL_{WTE}	338.19 in
Horizontal Stabilizer		
Center of pressure	SL_H	560.0 in
	BL_H	0.0 in
	WL_H	103.0 in
Area	S_H	50.25 ft^2
Span	b_H	12.83 ft
Chord	c_H	3.92 ft
Leading edge	SL_{HLE}	548.25 in
Vertical Stabilizer		
Center of pressure	SL_V	570.02 in
	BL_V	77.0 in
	WL_V	115.69 in
Number of panels	--	2
Area (per panel)	S_V	25.25 ft^2

TABLE II (Continued)

ITEM	SYMBOL	XV-15 VALUE
Vertical Stabilizer (Concluded)		
Span	b_V	7.68 ft
Chord	c_V	3.725 ft
Leading edge	SL_{VLE}	555.1 in
Rotors		
Location of shaft pivot point	SL_{SP}	300.0 in
	BL_{SP}	193.0 in
	WL_{SP}	100.0 in
Number of blades per rotor	n_b	3
Radius	R	12.5 ft
Chord	c_b	1.167 ft
Mast length	l_m	4.667 ft
Pitch-flap coupling	δ_3	-15.0 deg
Solidity	σ	0.089
Lock number	γ	3.83
Direction of rotation--inboard tip motion-helicopter/airplane		Aft/Up
Rotor RPM		
Helicopter		589 RPM
Conversion		589 RPM
Airplane		517 RPM
Blade flapping limits		± 12 deg
Flapping inertia per blade	I_b	102.5 slug-ft^2
Flapping spring rate/rotor	K_{FA}, K_{LAT}	225.0 ft-lb/deg

TABLE II (Continued)

ITEM	SYMBOL	XV-15 VALUE
Rotors (Concluded)		
Angle of outboard tilt of mast axis		
Helicopter	ϕ_m	1.0 deg*
Airplane		0.0 deg
Conversion range	β_m	-5.0 to +90.0 deg
Pylon		
Center of gravity	SL_P	291.7 in
	BL_P	193.0 in
	WL_P	118.0 in
Weight (two pylons)	W_P	4200.0 lbs
Estimated Inertia (per pylon)	I_X	100 slug-ft^2
	I_Y	500 slug-ft^2
	I_Z	450 slug-ft^2

Landing Gear (C_L gear)		Up	Down
Main gear coordinates	SL_{MG}	295.84	326.0 in
	BL_{MG}	46.01	51.25 in
	WL_{MG}#	38.0	8.25 in
Nose gear coordinates	SL_{NG}	176.76	139.0 in
	BL_{NG}	0.0	0.0 in
	WL_{NG}#	32.75	4.95 in

*The built-in dihedral of the pylon is 2.5 deg; in hover, elastic deformation reduces the dihedral to 1.0 deg.

#WL_{grd} = 11.0. WL values shown are static loaded position at design gross weight.

TABLE II (Concluded)

ITEM	SYMBOL	XV-15 VALUE
Pilot Control Limits		
Collective stick	X_{COL}	10.0 in
Longitudinal stick	X_{LN}	± 4.8 in
Lateral stick	X_{LT}	± 4.8 in
Pedal	X_{PD}	± 2.5 in
Blade pitch governor lever		7.5 in
Engine Ratings		
2 minute contingency		1760 SHP
10 minute takeoff		1550 SHP
30 minute military		1400 SHP
Normal rated		1250 SHP

Pilot Station Coordinates

		Eye Level	Seat Ref. Point
Pilot station	SL_{PA}	209.1	215.25 in
	BL_{PA}	16.5	16.5 in
	WL_{PA}	82.0	50.5 in

SUBSYSTEM NO. 1—XV-15 ROTOR AERODYNAMICS

Constants	Value
n_b	3.0
m	10
X_0/R	1.0
X_1/R	0.6
X_2/R	0.5333
X_3/R	0.4667
X_4/R	0.4
X_5/R	0.3333
X_6/R	0.2667
X_7/R	0.2
X_8/R	0.1333
X_9/R	0.0667
X_{10}/R	0.0
θ_0	0.0
θ_1	10.2
θ_2	12.3
θ_3	14.5
θ_4	17.75
θ_5	21.9
θ_6	26.15
θ_7	30.65
θ_8	34.65
θ_9	38.0
θ_{10}	40.9
R	12.5 ft
δ_3	-15.0 deg
c_b	14.0 in
I_b	102.5 slug-ft^2
l_m	4.667 ft
ϕ_m	1.0 deg

Constants	Value
BL_{CG}	0.0 in
SL_{SP}	300.0 in
BL_{SP}	193.0 in
WL_{SP}	100.0 in
K_H	225 ft-lb/deg
K_{HUB}	180,000.0 ft-lb/deg
$\bar{a}_o$	2.5 deg

Coefficients	Value
a_0	4.95
a_1	8.0
a_2	-30.0
δ_0	0.015
δ_1	-0.068
δ_2	0.81
B	0.97
α_{OL}	1.0 deg
CDMACH	0.35
CDMAX	0.11
CDALPH	0.01
CDLIM	0.85
CDFACT	0.2
CTMAXM	1.0
GECON1	1.563
GECON2	-2.912
GEWASH	-0.08
SFWASH	54.0 ft/sec

Coefficients	Value
MULO	0.1067
MUH1	0.5733
KMU1	17.807
KMU2	-0.561
KMUSF	6.0

Data Tables

Table 1-I, Maximum Available Rotor Thrust Coefficient, $\bar{C}_T = f(\mu, \beta_m)$

μ	$C_{T_{max}}/\sigma$
0.0	0.18
0.0438	0.17978
0.0876	0.17955
0.1314	0.17854
0.1751	0.17753
0.2189	0.17506
0.2627	0.17247
0.3065	0.16753
0.3503	0.15652
0.3941	0.142
0.4379	0.118
0.5	0.08

The following endurance limit tables flag the output of the program if exceeded but do not effect calculations.

	C_T/σ Endurance Limit Tables		
μ	$i_N > 75$ deg	$i_N = 60$ deg	$i_N < 30$ deg
0	0.1798	0.1798	0.1798
0.057	0.1483	0.1404	0.1326
0.114	0.1348	0.1225	0.1079
0.171	0.1236	0.1067	0.0843
0.228	0.1124	0.0899	0.0618
0.285	0.0955	0.0685	0.0449
0.342	0.0730	0.0506	0.0315
0.399	0.0562	0.0371	0.0202
0.456	0.0421	0.0247	0.0090

Table 1-II, Sideward Flight Rotor Correction Factor, $X_{SF} = f(|\bar{V}|)$

$\|\bar{V}\|$	X_{SF}
0	0
0.0455	0.16
0.091	0.62
0.136	0.91
0.182	0.70
0.227	0.55
0.273	0.39
0.319	0.21

Table 1-III, Side-by-Side Rotor Correction Factor, $X_{SS} = f(|\bar{\mu}|)$

$\lvert\bar{\mu}\rvert$	X_{SS}
0	0
0.025	0
0.050	0
0.075	-.005
0.10	-.02
0.125	-.05
0.150	-.08
0.20	-.085
0.250	-.085
0.30	-.085

SUBSYSTEM NO. 2—XV-15 ROTOR INDUCED VELOCITIES

Constants	Value
R	12.5 ft
l_m	4.667 ft
SL_H	560.0 in
SL_{SP}	300.0 in

Coefficients	Value
K_0	1.6
K_1	0.0
K_2	0.0
K_3	0.0
K_4	0.0

Data Tables

Table 2-Ia, Rotor Wake on Horizontal Stabilizer, $\frac{W_i \big|_{R/H}}{W_i}$, β_m = 0 deg

	V_T, kts							
α_F, Deg	0	20	40	60	80	100	120	≥ 140
-180	0.0	0.0	0.0	0.0	0.0	0.0	0.0	0.0
- 30	0.0	0.0	0.0	0.0	0.0	0.0	0.0	0.0
- 28	0.0	-.02	-.06	-.10	-.15	-.12	-.02	0.0
- 24	0.0	-.05	-.15	-.30	-.60	-.37	-.05	0.0
- 20	0.0	-.06	-.25	-.50	-.92	-.65	-.06	0.0
- 16	0.0	-.07	-.40	-.70	-1.10	-.85	-.07	0.0
- 12	0.0	-.07	-.46	-.85	-1.13	-.90	-.08	0.0
- 8	0.0	-.14	-.46	-.73	-1.05	-.80	-.10	0.0
- 4	0.0	-.0945	-.33	-.623	-.90	-.67	-.09	0.0
0	0.0	-.06	-.23	-.52	-.725	-.57	-.07	0.0
4	0.0	-.0314	-.113	-.392	-.55	-.45	-.03	0.0
8	0.0	-.075	-.127	-.290	-.44	-.35	-.07	0.0
12	0.0	-.06	-.10	-.250	-.38	-.27	-.06	0.0
16	0.0	-.04	-.045	-.160	-.20	-.15	-.04	0.0
20	0.0	0.0	0.0	0.0	0.0	0.0	0.0	0.0
180	0.0	0.0	0.0	0.0	0.0	0.0	0.0	0.0

Table 2-Ib, Rotor Wake on Horizontal Stabilizer, $\frac{W_i \big|_{R/H}}{W_i}$, β_m = 15 deg

	V_T, kts							
α_F, Deg	0	20	40	60	80	100	120	≥ 140
-180	0.0	0.0	0.0	0.0	0.0	0.0	0.0	0.0
- 30	0.0	0.0	0.0	0.0	0.0	0.0	0.0	0.0
- 28	0.0	-.05	-.10	-.15	-.25	-.22	-.05	0.0
- 24	0.0	-.10	-.25	-.40	-.55	-.50	-.10	0.0
- 20	0.0	-.15	-.40	-.65	-.90	-.75	-.15	0.0
- 16	0.0	-.20	-.50	-.78	-1.05	-.90	-.20	0.0
- 12	0.0	-.20	-.60	-.85	-1.08	-.95	-.20	0.0
- 8	0.0	-.16	-.55	-.80	-1.04	-.92	-.16	0.0
- 4	0.0	-.10	-.45	-.75	-.92	-.85	-.10	0.0
0	0.0	-.09	-.30	-.61	-.75	-.65	-.09	0.0
4	0.0	-.10	-.17	-.48	-.56	-.52	-.10	0.0
8	0.0	-.08	-.27	-.34	-.36	-.35	-.08	0.0
12	0.0	-.07	-.22	-.25	-.27	-.26	-.07	0.0
16	0.0	-.05	-.15	-.15	-.15	-.15	-.05	0.0
20	0.0	0.0	0.0	0.0	0.0	0.0	0.0	0.0
180	0.0	0.0	0.0	0.0	0.0	0.0	0.0	0.0

Table 2-Ic, Rotor Wake on Horizontal Stabilizer, $\frac{W_i\big|_{R/H}}{W_i}$, β_m = 30 deg

	V_T, kts							
α_F, Deg	0	20	40	60	80	100	120	> 140
-180	0.0	0.0	0.0	0.0	0.0	0.0	0.0	0.0
- 30	0.0	0.0	0.0	0.0	0.0	0.0	0.0	0.0
- 28	0.0	-.02	-.03	-.04	-.05	-.05	-.02	0.0
- 24	0.0	-.04	-.06	-.06	-.10	-.10	-.04	0.0
- 20	0.0	-.05	-.08	-.14	-.15	-.15	-.05	0.0
- 16	0.0	-.07	-.15	-.20	-.26	-.26	-.07	0.0
- 12	0.0	-.08	-.20	-.25	-.38	-.38	-.08	0.0
- 8	0.0	-.08	-.22	-.35	-.44	-.44	-.08	0.0
- 4	0.0	-.08	-.26	-.43	-.48	-.48	-.08	0.0
0	0.0	-.08	-.30	-.45	-.52	-.52	-.08	0.0
4	0.0	-.07	-.30	-.45	-.60	-.60	-.07	0.0
8	0.0	-.06	-.24	-.30	-.44	-.44	-.06	0.0
12	0.0	-.06	-.15	-.24	-.28	-.28	-.06	0.0
16	0.0	-.04	-.06	-.10	-.14	-.14	-.04	0.0
20	0.0	0.0	0.0	0.0	0.0	0.0	0.0	0.0
180	0.0	0.0	0.0	0.0	0.0	0.0	0.0	0.0

Table 2-Id, Rotor Wake on Horizontal Stabilizer, $\frac{W_i\big|_{R/H}}{W_i}$, β_m = 60, 90 deg

$$\frac{W_i\big|_{R/H}}{W_i} = 0.0$$

Table 2-II, Rotor Wake on Horizontal Stabilizer, K_{H_β}

	Mast Angle, β_m, Deg				
β_F, deg	0	15	30	60	90
0	1.0	1.0	1.0	1.0	1.0
± 4	0.9	0.99	1.1	1.0	1.0
± 8	0.625	0.96	1.3	1.0	1.0
± 12	0.30	0.89	1.4	1.0	1.0
± 16	0.05	0.70	0.8	1.0	1.0
± 20	-.17	0.15	0.45	1.0	1.0
± 24	-.28	0.0	0.225	0.5	0.5
± 28	-.17	0.0	0.07	0.25	0.25
± 32	0.0	0.0	0.0	0.0	0.0
± 180	0.0	0.0	0.0	0.0	0.0

SUBSYSTEM NO. 3—XV-15 FUSELAGE AERODYNAMICS

Constants	Value
LLANG	0.0 ft^2
DLANG	-0.5 ft^2
LBFO	-7.23 ft^2
DBFO	-1.56 ft^2
MBFO	66.5 ft^3

Data Tables

XV-15 FUSELAGE AERODYNAMICS WITH ANGLE OF ATTACK				
α_F, deg		Table 3-I L_α*	Table 3-III D_α	Table 3-V M_α
-90		0	116.0	670.0
-80	-100	-6.0	112.0	470.0
-70	-110	-14.0	108.0	270.0
-60	-120	-18.0	100.0	70.0
-50	-130	-20.0	80.0	-160.0
-40	-140	-20.0	55.0	-360.0
-36	-144	-19.0	45.0	-410.0
-32	-148	-18.0	35.0	-440.0
-28	-152	-17.0	25.0	-440.0

(Continued on next page)

*For Table 3-I only, L_α from ±100 changes sign from that shown for L_α between ±90 degrees.

XV-15 FUSELAGE AERODYNAMICS WITH ANGLE OF ATTACK				
α_F, deg		Table 3-I L_α*	Table 3-III D_α	Table 3-V M_α
-24	-156	-15.0	20.0	-430.0
-20	-160	-10.87	15.39	-380.0
-16	-164	-7.25	10.78	-370.0
-12	-168	-3.63	6.17	-295.0
-8	-172	-.01	3.0	-219.0
-4	-176	3.61	1.8	-142.5
0	±180	7.23	1.56	-66.5
4	176	10.85	1.8	9.5
8	172	14.47	2.3	85.5
12	168	18.09	3.67	123.5
16	164	21.71	5.78	142.5
20	160	25.33	7.89	133.0
24	156	28.0	10.0	95.0
28	152	32.0	15.0	95.0
32	148	36.0	20.0	133.0
36	144	40.0	25.0	114.0
40	140	43.0	30.0	95.0
50	130	45.0	50.0	20.0
60	120	40.0	70.0	-50.0
70	110	35.0	80.0	-130.0
80	100	25.0	90.0	-210.0
90		0	95.0	-300.0

*For Table 3-I only, L_α from ±100 changes sign from that shown for L_α between ±90 degrees.

XV-15 FUSELAGE AERODYNAMICS WITH SIDESLIP			
β_F, deg	Table 3-II L_β	Table 3-IV D_β	Table 3-VI M_β
0	7.23	1.56	-66.5
±2	--	--	-66.5
±4	--	--	-54.8
±6	--	--	-34
±8	--	--	-14
±10	5.00	5.0	0.
±20	0.0	10.0	70.0
±30	-15.0	20.0	140.0
±40	-40.0	40.0	210.0
±50	-90.0	60.0	210.0
±60	-120.0	80.0	140.0
±70	-125.0	100.0	70.0
±80	-130.0	120.0	0
±82	--	--	-14
±84	--	--	-34
±86	--	--	-54.8
±88	--	--	-66.5
±90	-135.0	125.0	-66.5
±92	--	--	-66.5
±94	--	--	-54.8
±96	--	--	-34
±98	--	--	-14

(Continued on next page)

XV-15 FUSELAGE AERODYNAMICS WITH SIDESLIP			
β_F, deg	Table 3-II L_β	Table 3-IV D_β	Table 3-VI M_β
±100	-130.0	120.0	0
±110	-125.0	100.0	70.0
±120	-120.0	80.0	140.0
±130	-90.0	60.0	210.0
±140	-40.0	40.0	210.0
±150	-15.0	20.0	140.0
±160	0.0	10.0	70.0
±170	5.0	5.0	0
±172	--	--	-14
±174	--	--	-34
±176	--	--	-54.8
±178	--	--	-66.5
±180	7.23	1.56	-66.5

XV-15 FUSELAGE AERODYNAMICS WITH SIDESLIP			
β_F, deg	Table 3-VII Y_β*	Table 3-VIII l_β*	Table 3-IX N_β*
0	0.0	0.0	0.0
±10	-14.5	-75.0	-202.0
±20	-29.0	-150.0	-404.0
±30	-43.5	-225.0	-600.0
±40	-50.0	-275.0	-700.0
±50	-50.0	-275.0	-700.0
±60	-43.5	-225.0	-600.0
±70	-29.0	-150.0	-404.0
±80	-14.5	-75.0	-202.0
±90	0.0	0.0	0.0
±100	14.5	75.0	202.0
±110	29.0	150.0	404.0
±120	43.5	225.0	600.0
±130	50.0	275.0	700.0
±140	50.0	275.0	700.0
±150	43.5	225.0	600.0
±160	29.0	150.0	404.0
±170	14.5	75.0	202.0
±180	0.0	0.0	0.0

*If β_F is positive, Y_β has sign of table. If β_F is negative, Y_β sign is opposite of table. $Y_{\beta_{\beta<0}} = -Y_{\beta_{\beta>0}}$, $l_{\beta_{\beta<0}} = -l_{\beta_{\beta>0}}$, $N_{\beta_{\beta<0}} = -N_{\beta_{\beta>0}}$.

SUBSYSTEM NO. 4—XV-15 WING-PYLON AERODYNAMICS

Constants	Values
l_m	4.667 ft
SL_{WP}	291.7 in
SL_{SP}	300.0 in
BL_{SP}	193.0 in
BL_{CG}	0.0 in
SL_{WTE}	338.19 in
S_W	181.0 ft^2
c_W	5.225 ft
b_W	32.17 ft
Λ_W	-6.5 deg
S_{PYL}	24.05 ft^2
ϕ_m	1.0 deg

Coefficients	Values
$C_{Y_\beta}\Big\vert_{M_N=0}$	0.0 1/rad
$\dfrac{C_{Y_p}}{C_{L_{WP}}}\Bigg\vert_{M_N=0}$	0.0 1/rad
$C_{Y_r}\Big\vert_{M_N=0}$	0.0 1/rad
$C_{l_p}\Big\vert_{C_{L_{WP}}=M_N=0}$	-0.774 1/rad
$\dfrac{C_{l_r}}{C_{L_{WP}}}\Bigg\vert_{M_N=0}$	0.27 1/rad
$\dfrac{\Delta C_{l_r}}{(\partial\alpha_{WFS}/\partial\delta_F)(\delta_F)}$	-0.0016 1/deg

Coefficients	Value
$C_{l_{\delta_a}}\Big\vert_{\substack{\delta_F = 0 \text{ deg} \\ \alpha_{WFS} < 8 \text{ deg}}}$	0.006 1/deg
$C_{n_\beta}\Big\vert_{C_{L_{WP}}=M_N=0}$	-0.0315 1/rad
$\left(\frac{C_{n_\beta}}{C^2_{L_{WPFS}}}\right)\Bigg\vert_{M_N=0}$	0.057 1/rad
$\left(\frac{C_{n_r}}{C^2_{L_{WP}}}\right)$	-0.016 1/rad
$\frac{C_{n_r}}{C_{D_{oWP}}}$	-0.32 1/rad
$\frac{C_{n_p}}{C_{L_{WP}}}\Bigg\vert_{M_N=0}$	-0.06 1/rad
$(\partial\alpha_{WFS}/\partial\delta_F)$	-0.45

Coefficients	Value
K_{np}	1.0
K_{RW}	3.0
K_{XRW}	0.26
X^*_{RWO}	0.0806
X^*_{RW1}	0.00003341 1/deg
X^*_{RW2}	0.000007386 $1/deg^2$
K_{FWO}	1.4
K_{FWDF}	-0.0035 1/deg
$(SD/q)_{\beta_m=90}$	1.0 ft^2
(SD/q)	5.5 ft^2

*Coefficients are a fit of the data below.

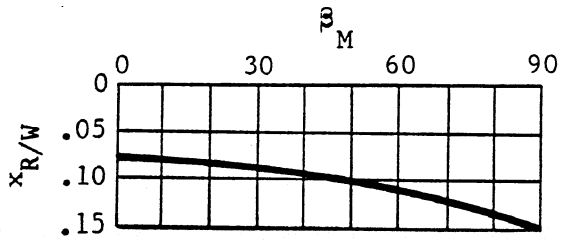

Data Tables

Table 4-I, XV-15 Wing-Pylon Lift Coefficient ($C_{L_{WP}}$), Flap Setting, X_{FL1} = 0/0

	Flap Setting, X_{FL1} = 0/0				
	Mast Angle, β_m				
	90 deg Airplane				0 deg Helicopter
	Mach Number, M_N				
α_W	0 - 0.2	0.4	0.5	0.6	0 - 0.4
-40	-.93	Not Defined	Not Defined	Not Defined	-.68
-36	-.84				-.58
-32	-.84				-.57
-28	-.89				-.62
-24	-1.00				-.72
-20	-1.15	-.84			-.88
-19.5	-1.15	-.86			-.88
-16	-.95	-.94	-.675	-.49	-.73
-15.5	-.91	-.945	-.680	-.49	-.70
-13.0	-.75	-.85	-.805	-.50	-.57
-12	-.67	-.772	-.800	-.50	-.50
-11	-.59	-.67	-.78	-.49	-.44
-8	-.33	-.37	-.4	-.41	-.22
-4	-.04	-.025	-.01	-.01	-.06
0	0.38	0.38	0.39	0.41	0.3
4	0.72	0.75	0.77	0.83	0.55
8	1.04	1.12	1.16	1.09	0.8
11	1.28	1.41	1.28	1.12	0.98

(Continued on next page)

Table 4-I, XV-15 Wing-Pylon Lift Coefficient ($C_{L_{WP}}$), Flap Setting, X_{FL1} = 0/0 (Concluded)

	Flap Setting, X_{FL1} = 0/0				
	Mast Angle, β_m				
	90 deg Airplane				0 deg Helicopter
	Mach Number, M_N				
α_W	0 - 0.2	0.4	0.5	0.6	0 - 0.4
12	1.37	1.46	1.27	1.12	1.05
13	1.42	1.45			1.09
16	1.57	1.32			1.19
17	1.57			Not	1.17
20	1.38		Not	Defined	0.98
24	1.22	Not	Defined		0.80
28	1.20	Defined			0.78
32	1.27				0.86
36	1.40				0.98
40	1.46				1.06

Table 4-II, XV-15 Wing-Pylon Lift Coefficient ($C_{L_{WP}}$), Flap Setting, X_{FL2} = 20/12.5, X_{FL3} = 40/25, X_{FL4} = 75/47

	Mach Number, M_N = 0 - 0.2					
	Flap Setting					
	X_{FL2} = 20/12.5		X_{FL3} = 40/25		X_{FL4} = 75/47	
	Mast Angle, β_m					
α_W	90 deg	0 deg	90 deg	0 deg	90 deg	0 deg
-100	0.0	0.15				
-90	0.0	0.0	0.0	0.0	0.0	0.0
-80	-0.45	-.28	-.325	-.245	-.235	-.190
-70	-.72	-.48	-.520	-.400	-.385	-.305
-60	-.79	-.60	-.610	-.480	-.450	-.333
-50	-.80	-.62	-.590	-.420	-.390	-.220
-40	-.62	-.47	-.410	-.265	-.240	-.105
-36	-.60	-.42	-.400	-.250	-.220	-.090
-32	-.60	-.40	-.425	-.260	-.240	-.095
-28	-.66	-.47	-.515	-.300	-.275	-.120
-24	-.77	-.55	-.660	-.380	-.340	-.160
-21.5	-.84	-.60	-.690	-.440	-.400	-.210
-21.0	-.85	-.61	-.680	-.440	-.400	-.210
-20	-.84	-.59	-.640	-.395	-.367	-.188
-19.2	-.81	-.54	-.580	-.360	-.310	-.140
-16	-.57	-.37	-.320	-.165	-.048	0.040
-12	-.26	-.14	0.0	0.0628	0.272	0.268
-8	0.15	0.18	0.42	0.291	0.69	0.6
-4	0.56	0.51	0.84	0.518	1.11	0.92

(Continued on next page)

Table 4-II, XV-15 Wing-Pylon Lift Coefficient ($C_{L_{WP}}$), Flap Setting, x_{FL2} = 20/12.5, X_{FL3} = 40/25, X_{FL4} = 75/47 (Continued)

	Mach Number, M_N = 0 - 0.2					
	Flap Setting					
	X_{FL2} = 20/12.5		X_{FL3} = 40/25		X_{FL4} = 75/47	
	Mast Angle, β_m					
α_W	90 deg	0 deg	90 deg	0 deg	90 deg	0 deg
0	0.92	0.79	1.18	0.749	1.44	1.15
4	1.28	1.05	1.46	0.975	1.66	1.37
8	1.54	1.28	1.70	1.205	1.88	1.59
11	1.75	1.45	1.86	1.380	2.0	1.7
12	1.81	1.51	1.92	1.433	1.99	1.67
13.6	1.88	1.54	1.94	1.500	1.87	1.55
16	1.75	1.45	1.79	1.400	1.70	1.34
18.4	1.57	1.23	1.62	1.260	1.53	1.2
20	1.46	1.10	1.51	1.200	1.46	1.14
24	1.38	1.0	1.48	1.15	1.46	1.16
28	1.4	1.0	1.54	1.20	1.54	1.29
32	1.5	1.1	1.69	1.32	1.69	1.38
36	1.6	1.2	1.76	1.41	1.78	1.44
40	1.65	1.31	1.80	1.47	1.80	1.48

Table 4-II, XV-15 Wing-Pylon Lift Coefficient ($C_{L_{WP}}$), Flap Setting, X_{FL1} = 0/0, X_{FL2} = 20/12.5, X_{FL3} = 40/25, X_{FL4} = 75/47 (Continued)

	Mast Angle, β_m = 0 deg			
	Mach Number, M_N = 0 - 0.2			
	Flap Setting			
α_W	X_{FL1} = 0/0	X_{FL2} = 20/12.5	X_{FL3} = 40/25	X_{FL4} = 75/47
-180	-0.1	-.2	-.25	-.2
-170	0.0	-.1	-.15	-.05
-160	0.2	0.1	0	0.1
-150	0.35	0.18	0.20	0.215
-140	0.4	0.29	0.32	0.25
-130	0.45	0.31	0.34	0.27
-120	0.4	0.28	0.30	0.25
-110	0.35	0.2	0.22	0.17
-100	0.2	0.15	0.12	0.08
-90	0.0	0.0	0	0.0
-80	-.25	-.28	-.245	-.19
-70	-.55	-.48	-.40	-.305
-60	-.65	-.6	-.48	-.333
-50	-.7	-.62	-.42	-.22
-40	-.68	-.47	-.265	-.105
	(Same as Tables 4-I and 4-II, between ±40 deg)			

(Continued on next page)

Table 4-II, XV-15 Wing-Pylon Lift Coefficient ($C_{L_{WP}}$), Flap Setting, X_{FL1} = 0/0, X_{FL2} = 20/12.5, X_{FL3} = 40/25, X_{FL4} = 75/47 (Concluded)

	Mast Angle, β_m = 0 deg			
	Mach Number, M_N = 0 - 0.2			
	Flap Setting			
α_W	X_{FL1} = 0/0	X_{FL2} = 20/12.5	X_{FL3} = 40/25	X_{FL4} = 75/47
40	1.06	1.31	1.47	1.48
50	1.08	1.31	1.47	1.47
60	0.9	1.2	1.36	1.36
70	0.55	0.8	1.08	1.08
80	0.3	0.3	0.70	0.7
90	0.0	0.0	0	0
100	-.2	-.5	-.4	-.5
110	-.3	-.78	-.55	-.65
120	-.35	-.9	-.65	-.75
130	-.4	-1.0	-.7	-.829
140	-.45	-.98	-.75	-.85
150	-.4	-.91	-.7	-.8
160	-.35	-.8	-.65	-.7
170	-.25	-.65	-.5	-.6
180	-.1	-.2	-.25	-.2

Table 4-III, XV-15 Wing-Pylon Drag Coefficient ($C_{D_{WP}}$), Flap Setting, X_{FL1} = 0/0

	Flap Setting, X_{FL1} = 0/0				
	Mast Angle, β_m				
	90 deg Airplane				0 deg Helicopter
	Mach Number, M_N				
α_W	0-0.2	0.4	0.5	0.6	0-0.2
-40	0.575				0.685
-36	0.505	Not			0.635
-32	0.425	Defined	Not		0.580
-28	0.327		Defined	Not	0.522
-24	0.230	0.312		Defined	0.450
-20	0.150	0.175	0.275		0.370
-16	0.089	0.089	0.135	0.240	0.295
-12	0.042	0.042	0.050	0.110	0.246
-8	0.025	0.0250	0.025	0.052	0.219
-4	0.0170	0.0170	0.0170	0.040	0.212
0	0.0204	0.0204	0.0204	0.042	0.215
4	0.0418	0.0418	0.0418	0.062	0.238
8	0.072	0.072	0.082	0.127	0.274
12	0.118	0.128	0.168	0.268	0.318
16	0.171	0.194	0.289		0.363
20	0.247	0.3050			0.436
24	0.354	0.500		Not	0.512
28	0.493		Not	Defined	0.580
32	0.600	Not	Defined		0.642
36	0.660	Defined			0.698
40	0.705				0.748

Table 4-IV, XV-15 Wing-Pylon Drag Coefficient ($C_{D_{WP}}$), Flap Setting, X_{FL2} = 20/12.5, X_{FL3} = 40/25, X_{FL4} = 75/47

	Mach Number, M_N = 0 - 0.2					
	Flap Setting					
	X_{FL2} = 20/12.5		X_{FL3} = 40/25		X_{FL4} = 75/47	
	Mast Angle, β_m					
α_W	90 deg	0 deg	90 deg	0 deg	90 deg	0 deg
-100	--	1.45	--	1.33	--	0.88
-90	--	1.57	1.18	1.44	1.145	0.90
-80	--	1.45	1.10	1.33	1.050	0.878
-70	1.0	1.15	0.93	1.12	0.89	0.822
-60	0.78	0.91	0.705	0.91	0.67	0.740
-50	0.62	0.75	0.565	0.75	0.507	0.640
-40	0.50	0.59	0.430	0.54	0.450	0.550
-36	0.40	0.53	0.335	0.468	0.400	0.525
-32	0.32	0.48	0.245	0.405	0.350	0.500
-28	0.23	0.42	0.180	0.352	0.309	0.480
-24	0.17	0.36	0.130	0.310	0.278	0.462
-20	0.11	0.33	0.090	0.282	0.260	0.450
-16	0.07	0.28	0.065	0.263	0.243	0.440
-12	0.05	0.253	0.058	0.253	0.246	0.445
-8	0.033	0.26	0.076	0.267	0.282	0.485
-4	0.044	0.26	0.106	0.307	0.330	0.536

(Continued on next page)

Table 4-IV, XV-15 Wing-Pylon Drag Coefficient ($C_{D_{WP}}$), Flap Setting, X_{FL2} = 20/12.5, X_{FL3} = 40/25, X_{FL4} = 75/47 (Continued)

	Mach Number, M_N = 0 - 0.2					
	FLap Setting					
	X_{FL2} = 20/12.5		X_{FL3} = 40/25		X_{FL4} = 75/47	
	Mast Angle, β_m					
α_W	90 deg	0 deg	90 deg	0 deg	90 deg	0 deg
0	0.072	0.3	0.141	0.345	0.372	0.580
4	0.109	0.32	0.186	0.394	0.424	0.636
8	0.157	0.37	0.243	0.453	0.492	0.706
12	0.227	0.43	0.322	0.537	0.580	0.778
16	0.29	0.48	0.404	0.589	0.667	0.814
20	0.38	0.53	0.528	0.630	0.730	0.839
24	0.51	0.63	0.630	0.690	0.790	0.880
28	0.61	0.70	0.710	0.748	0.838	0.920
32	0.70	0.75	0.764	0.800	0.883	0.955
36	0.75	0.78	0.805	0.845	0.950	0.985
40	0.79	0.83	0.865	0.888	1.025	1.015

Table 4-IV, XV-15 Wing-Pylon Drag Coefficient ($C_{D_{WP}}$), Flap Setting, X_{FL1} = 0/0, X_{FL2} = 20/12.5, X_{FL3} = 40/25, X_{FL4} = 75/47 (Continued)

	Mast Angle, β_m = 0 deg			
	Mach Number, M_N = 0 - 0.2			
	Flap Setting			
α_W	X_{FL1} = 0/0	X_{FL2} = 20/12.5	X_{FL3} = 40/25	X_{FL4} = 75/47
-180	0.3	0.4	0.45	0.5
-170	0.4	0.5	0.58	0.6
-160	0.55	0.6	0.65	0.67
-150	0.65	0.7	0.71	0.72
-140	0.75	0.75	0.77	0.77
-130	0.82	0.8	0.8	0.8
-120	0.86	0.91	0.91	0.83
-110	0.92	1.15	1.12	0.86
-100	0.95	1.45	1.33	0.88
-90	0.96	1.57	1.44	0.9
-80	0.93	1.45	1.33	0.878
-70	0.91	1.15	1.12	0.822
-60	0.86	0.91	0.91	0.74
-50	0.78	0.75	0.75	0.64
-40	0.685	0.59	0.54	0.55
	(same as Tables 4-III and 4-IV between ±40 deg)			

Table 4-IV, XV-15 Wing-Pylon Drag Coefficient ($C_{D_{WP}}$), Flap Setting, X_{FL1} = 0/0, X_{FL2} = 20/12.5, X_{FL3} = 40/25, X_{FL4} = 75/47 (Concluded)

	Mast Angle, β_m = 0 deg			
	Mach Number, M_N = 0 - 0.2			
	Flap Setting			
α_W	X_{FL1} = 0/0	X_{FL2} = 20/12.5	X_{FL3} = 40/25	X_{FL4} = 75/47
40	0.748	0.83	0.888	1.015
50	0.9	0.91	0.97	1.04
60	1.0	0.98	1.04	1.045
70	1.07	1.05	1.06	1.05
80	1.12	1.09	1.08	1.055
90	1.15	1.12	1.09	1.06
100	1.13	1.1	1.07	1.05
110	1.1	1.08	1.05	1.02
120	1.05	1.06	1.02	0.99
130	1.0	1.02	1.0	0.96
140	0.95	0.98	0.96	0.92
150	0.85	0.88	0.87	0.84
160	0.7	0.74	0.78	0.8
170	0.5	0.55	0.62	0.7
180	0.3	0.4	0.45	0.5

Table 4-V(a), XV-15 Wing Wake Deflection on Horizontal Stabilizer ($\varepsilon_{W/HOGE}$), β_m = 90 deg

	Mast Angle, β_m = 90 degrees			
	Mach Number, M_N = 0 - 0.2			
	Flap Setting			
α_W	X_{FL1} = 0/0	X_{FL2} = 20/12.5	X_{FL3} = 40/25	X_{FL4} = 75/47
-90	0	0	0	0
-16	0	0	0	0
-12	0	0.45	0.95	0.95
-8	0.06	1.25	2.54	2.54
-4	1.32	2.60	3.92	3.92
0	2.58	4.08	5.40	5.40
4	3.84	5.35	6.88	6.88
8	5.10	6.60	8.26	8.26
12	5.90	7.40	8.90	8.90
16	6.30	7.55	8.80	8.80
20	6.00	6.70	7.30	7.30
24	4.00	4.40	4.80	4.80
28	0	0	0	0
90	0	0	0	0

Table 4-V(b), XV-15 Wing Wake Deflection on Horizontal Stabilizer ($\varepsilon_{W/HOGE}$), β_m = 60 deg

	Mast Angle, β_m = 60 degrees			
	Mach Number, M_N = 0 - 0.2			
	Flap Setting			
α_W	X_{FL1} = 0/0	X_{FL2} = 20/12.5	X_{FL3} = 40/25	X_{FL4} = 75/47
-90	0	0	0	0
-16	0	0	0	0
-12	0	0	0	0
-8	0	0.9	1.78	1.78
-4	1.2	2.25	3.38	3.38
0	2.6	3.80	4.98	4.98
4	4.0	5.30	6.58	6.58
8	5.2	6.80	8.18	8.18
12	6.4	7.80	9.2	9.2
16	6.8	8.20	9.5	9.5
20	6.3	7.40	8.4	8.4
24	4.1	4.80	5.5	5.5
28	0	0	0	0
90	0	0	0	0

Table 4-V(c), XV-15 Wing Wake Deflection on Horizontal Stabilizer ($\varepsilon_{W/HOGE}$), β_m = 30 deg

	Mast Angle, β_m = 30 degrees			
	Mach Number, M_N = 0 - 0.2			
	Flap Setting			
α_W	X_{FL1} = 0/0	X_{FL2} = 20/12.5	X_{FL3} = 40/25	X_{FL4} = 75/47
-90	0	0	0	0
-16	0	0	0	0
-12	0	0	0	0
-8	0	0.7	1.3	1.3
-4	1.18	2.1	2.9	2.9
0	2.70	3.6	4.5	4.5
4	4.22	5.2	6.1	6.1
8	5.74	6.7	7.7	7.7
12	7.0	7.9	8.9	8.9
16	7.3	8.2	9.1	9.1
20	6.7	7.4	8.1	8.1
24	4.1	4.8	5.5	5.5
28	0	0	0	0
90	0	0	0	0

Table 4-V(d), XV-15 Wing Wake Deflection on Horizontal Stabilizer ($\varepsilon_{W/HOGE}$), β_m = 15 deg

	Mast Angle, β_m = 15 degrees			
	Mach Number, M_N = 0 - 0.2			
	Flap Setting			
α_W	X_{FL1} = 0/0	X_{FL2} = 20/12.5	X_{FL3} = 40/25	X_{FL4} = 75/47
-90	0	0	0	0
-16	0	0	0	0
-12	0	0.4	0.7	0.7
-8	0	1.2	2.4	2.4
-4	1.26	2.7	4.1	4.1
0	2.80	4.3	5.8	5.8
4	4.34	6.0	7.5	7.5
8	5.88	7.1	9.2	9.2
12	7.1	8.7	10.4	10.4
16	7.3	8.9	10.8	10.8
20	6.7	8.2	9.8	9.8
24	4.1	5.3	6.4	6.4
28	0	0	0	0
90	0	0	0	0

Table 4-V(e), XV-15 Wing Wake Deflection on Horizontal Stabilizer ($\varepsilon_{W/HOGE}$), β_m = 0 deg

	Mast Angle, β_m = 0 degrees			
	Mach Number, M_N = 0 - 0.2			
	Flap Setting			
α_W	X_{FL1} = 0/0	X_{FL2} = 20/12.5	X_{FL3} = 40/25	X_{FL4} = 75/47
-90	0	0	0	0
-16	0	0	0	0
-12	0	0.8	1.47	1.47
-8	0.09	1.6	3.03	3.03
-4	1.62	3.1	4.59	4.59
0	3.15	4.7	6.15	6.15
4	4.68	6.2	7.71	7.71
8	6.21	7.8	9.27	9.27
12	7.1	8.5	9.8	9.8
16	7.5	8.6	9.7	9.7
20	7.0	7.5	8.0	8.0
24	4.8	4.9	5.0	5.0
28	0	0	0	0
90	0	0	0	0

Table 4-VI, XV-15 Wing-Pylon Rolling Moment, $C_{l_\beta}\Big|_{C_{L_{WP}}=M_N=0}$, 1/rad

	Flap Setting	
β_m, deg	X_{FL1} = 0/0	X_{FL2} = 20/12.5, X_{FL3} = 40/25, X_{FL4} = 75/47
0	-.012	-.136
30	0.089	0.064
60	0.078	0.034
90	0.039	-.051

Table 4-VII, XV-15 Wing-Pylon Rolling Moment, $\frac{C_{l_\beta}}{C_{L_{WP}}}\Big|_{M_N=0}$, 1/rad

	Flap Setting	
β_m, deg	X_{FL1} = 0/0	X_{FL2} = 20/12.5, X_{FL3} = 40/25, X_{FL4} = 75/47
0	0.09	0.09
30	0	-.01
60	-.02	0
90	-.05	0

Table 4-VIII, XV-15 Wing-Pylon Pitching Moment, $C_{m_{WP}}$, 1/rad

	Flap Setting			
β_m, deg	X_{FL1} = 0/0	X_{FL2} = 20/12.5	X_{FL3} = 40/25	X_{FL4} = 75/47
0	0.025	-.05	-.110	-.115
15	0.070	-.01	-.090	-.110
30	0.080	0.0	-.060	-.080
60	0.050	-.05	-.110	-.130
90	-.025	-.11	-.170	-.190

Table 4-IX, Partial of Wing Coefficient of Lift with Respect to Angle of Attack, $\left.\frac{\partial C_{L_{WPFS}}}{\partial \alpha_{WFS}}\right|_{C_{L_{WP}}=0}$

	Mach Number, $M_N < 0.2$			
		Flap Setting		
β_m, deg	X_{FL1} = 0/0	X_{FL2} = 20/12.5	X_{FL3} = 40/25	X_{FL4} = 75/47
0	0.057	0.0575	0.057	0.0563
90	0.0799	0.08	0.08	0.08

$$\left.\frac{\partial C_{L_{WPFS}}}{\partial \alpha_{WFS}}\right|_{C_{L_{WP}}=0} = \frac{C_{L_1} - C_{L_2}}{\alpha_1 - \alpha_2}$$

Table 4-IX, Partial of Wing Coefficient of Lift with Respect to Angle of Attack, $\left.\frac{\partial C_{L_{WPFS}}}{\partial \alpha_{WFS}}\right|_{C_{L_{WP}}=0}$ (Concluded)

	Flap Setting, X_{FL1}			
	Mach Number, M_N			
β_m, deg	$M_N = 0.2$	$M_N = 0.4$	$M_N = 0.5$	$M_N = 0.6$
90	0.0799	0.0837	0.0915	0.0988

Table 4-X, Wing Coefficient of Drag at Wing Coefficient of Lift Equal to Zero, $C_{D_{oWP}}|C_{L_{WP}}=0$

	Mach Number, $M_N < 0.2$			
	Flap Setting			
β_m, deg	$X_{FL1} = 0/0$	$X_{FL2} = 20/12.5$	$X_{FL3} = 40/25$	$X_{FL4} = 75/47$
0	0.2126	0.2512	0.256	0.442
90	0.0177	0.0419	0.058	0.243

$$C_{D_{oWP}}\Big|_{C_L=0} = C_{D_{\alpha_{W_{C_L}}}} = C_{D_1} - \frac{(C_{D_1} - C_{D_2})(\alpha_1 - \alpha_W)}{(\alpha_1 - \alpha_2)}$$

$$\alpha_{W_{C_L=0}} = \alpha_1 - \frac{(\alpha_1 - \alpha_2)C_{L_1}}{(C_{L_1} - C_{L_2})}$$

Table 4-X, Wing Coefficient of Drag at Wing Coefficient of Lift Equal to Zero, $C_{D_{oWP}}|C_{L_{WP}}=0$ (Concluded)

	Flap Setting, X_{FL1}			
	Mach Number, M_N			
β_m, deg	M_N = 0.2	M_N = 0.4	M_N = 0.5	M_N = 0.6
90	0.0177	0.0178	0.0179	0.0405

Table 4-XI, XV-15 Aileron Effectiveness Correction for Flap and Mast ($K_{l_{\delta_a}}$) for $|\alpha_W| \leq 8$ deg

Flap Setting	Mast Angle, β_m	$K_{l_{\delta_a}}$*
X_{FL1} = 0/0	0 deg	0.68
	90 deg	1.00
X_{FL2} = 20/12.5	0 deg	0.67
	90 deg	0.88
X_{FL3} = 40/25	0 deg	0.66
	90 deg	0.73
X_{FL4} = 75/47	0 deg	0.45
	90 deg	0.34

For $8 < \alpha_W \leq 25$ deg, interpolate straight line between values in table and zero; for $\alpha_W > 25$ deg, $K_{l_{\delta_a}} = 0.0$

*Straight line variation with mast angle.

Table 4-XII, XV-15 Aileron Effect on Wing Lift ($C_{L_{\delta_a}}$)

Flap Setting	Mast Angle, β_m	$C_{L_{\delta_a}}$, 1/deg
X_{FL1} = 0/0	All	0.00316
X_{FL2} = 20/12.5	All	0.00396
X_{FL3} = 40/25	All	0.00476
X_{FL4} = 75/47	All	0.0

Table 4-XIII and 4-XIV, XV-15 Aileron Yaw Coefficient ($C_{n_{\delta_a}}$)

$$C_{n_{\delta_a}} = K_{no_{\delta_a}} + (K_{n_{\delta_a}})(C_{L_{WPFS}})(C_{l_{\delta_a}}) \quad , \text{ where:}$$

Flap Setting	Mast Angle, β_m	4-XIII $K_{no_{\delta_a}}$	4-XIV $K_{n_{\delta_a}}$
X_{FL1} = 0/0	0 deg	0.00046	-.61
	30 deg	0.00092	-.62
	90 deg	0.00143	-.415
X_{FL2} = 20/12.5	0 deg	0.00046	-.405
	30 deg	0.001005	-.20
	90 deg	0.00123	-.30
X_{FL3} = 40/25	0 deg	0.00046	-.24
	30 deg	0.00109	-.09
	90 deg	0.00103	-.24
X_{FL4} = 75/47	0 deg	-.00003	-.405
	30 deg	0.00035	-.087
	90 deg	0.00029	-.275

Table 4-XV, Pylon Interference Drag Coefficient, D_{PYINT}

Mast Angle, β_m	D_{PYINT}
-5.0	13.5
0.0	13.5
15.0	13.5
30.0	13.5
45.0	13.5
50.0	13.4
55.0	13.25
60.0	13.0
65.0	12.0
70.0	10.5
75.0	8.0
80.0	5.7
85.0	3.4
90.0	1.0

Table 4-XVI, Pylon Drag Factor with Sideslip, K_{PLAT}

$\overline{\alpha}_{PYL}$	K_{PLAT}
0.0	0.0
10.0	0.04
20.0	0.1
30.0	0.5
40.0	0.95
45.0	1.0
90.0	1.0

SUBSYSTEM NO. 5—XV-15 HORIZONTAL STABILIZER AERODYNAMICS

Constants	Values
SL_H	560.0 in
WL_H	103.0 in
S_H	50.25 ft^2
c_H	3.92 ft
i_H	0.0 deg

Coefficients	Values
τ_e	0.518
$C_{LH\beta}$	-0.00422
K_{HNU}	0.8
D_{WB}	1.0
C_{MHO}	0.0
C_{MHA}	0.0 1/deg
D_{Ke}	0.24

Table 5-I, XV-15 Horizontal Stabilizer Lift Coefficient, C_{LH}

	Mach Number, M_N = 0 - 0.2						
	Elevator Angle, δ_e						
α_H, deg	0 deg	-10 deg	-15 deg	-20 deg	10 deg	15 deg	20 deg
-180	0	-.40	-.60	-.80	0.40	0.60	0.80
-170	0.70	0.30	0.10	-.10	1.10	1.30	1.50
-160	0.60	0.28	0.08	-.10	0.95	1.13	1.30
-150	0.84	0.39	0.16	-.04	1.20	1.35	1.45
-140	0.98	0.48	0.20	0	1.38	1.49	1.60
-130	0.99	0.50	0.22	0.03	1.36	1.43	1.54
-120	0.86	0.46	0.20	0.04	1.15	1.23	1.30

(Continued on next page)

Table 5-I, XV-15 Horizontal Stabilizer Lift Coefficient, C_{LH} (Continued)

	Mach Number, M_N = 0 - 0.2						
	Elevator Angle, δ_e						
α_H, deg	0 deg	-10 deg	-15 deg	-20 deg	10 deg	15 deg	20 deg
-110	0.66	0.38	0.16	0.04	0.90	0.96	1.00
-100	0.40	0.24	0.10	0.04	0.50	0.56	0.60
-90	0	0	0	0	0	0	0
-80	-.425	-.560	-.580	-.600	-.360	-.285	-.220
-70	-.720	-.865	-.890	-.920	-.600	-.490	-.380
-60	-.900	-1.060	-1.090	-1.120	-.770	-.640	-.510
-50	-1.002	-1.175	-1.205	-1.240	-.890	-.745	-.600
-40	-1.050	-1.240	-1.260	-1.300	-.960	-.800	-.640
-36	-1.04	-1.24	-1.26	-1.3	-.92	-.775	-.63
-32	-1.03	-1.23	-1.255	-1.29	-.89	-.735	-.60
-28	-1.010	-1.210	-1.240	-1.280	-.840	-.680	-.560
-24	-.980	-1.185	-1.220	-1.260	-.780	-.615	-.500
-20	-.930	-1.160	-1.198	-1.235	-.690	-.500	-.420
-18.4	-.920	-1.200	-1.210	-1.240	-.660	-.540	-.480
-17.5	-.930	-1.260	-1.250	-1.250	-.710	-.565	-.450
-16.8	-.990	-1.310	-1.290	-1.310	-.740	-.550	-.420
-16.0	-1.12	-1.40	-1.330	-1.330	-.710	-.510	-.380
-15.6	-1.10	-1.44	-1.380	-1.350	-.700	-.480	-.350
-14.2	-1.0082	-1.40	-1.55	-1.450	-.610	-.400	-.270
-12.5	-.8875	-1.31	-1.49	-1.60	-.480	-.280	-.150
-12	-.852	-1.26025	-1.464375	-1.60318	-.44375	-.239625	-.10082

(Continued on next page)

Table 5-I, XV-15 Horizontal Stabilizer Lift Coefficient, C_{LH} (Continued)

	Mach Number, M_N = 0 - 0.2						
	Elevator Angle, δ_e						
α_H, deg	0 deg	-10 deg	-15 deg	-20 deg	10 deg	15 deg	20 deg
8	0.568	0.15975	-.044375	-.18318	0.97625	1.180375	1.31918
12.0	0.852	0.44375	0.239625	0.10082	1.250	1.420	1.500
12.2	0.8662	0.45795	0.253825	0.11502	1.270	1.430	1.480
13.0	0.923	0.51475	0.310625	0.17182	1.30	1.370	1.450
15.0	1.0	0.650	0.450	0.290	1.200	1.270	1.360
16.0	0.98	0.690	0.475	0.320	1.160	1.240	1.320
16.8	0.94	0.700	0.490	0.340	1.150	1.200	1.320
18.0	0.89	0.680	0.500	0.370	1.130	1.220	1.340
20	0.88	0.600	0.465	0.380	1.180	1.280	1.380
24	0.935	0.660	0.455	0.330	1.300	1.380	1.440
28	1.00	0.730	0.500	0.380	1.370	1.440	1.500
32	1.05	0.780	0.540	0.400	1.430	1.490	1.540
36	1.08	0.820	0.560	0.410	1.470	1.535	1.570
40	1.10	0.840	0.570	0.410	1.510	1.560	1.590
50	1.09	0.83	0.56	0.36	1.50	1.56	1.59
60	0.88	0.63	0.45	0.29	1.15	1.22	1.26
70	0.62	0.42	0.30	0.20	0.78	0.80	0.83
80	0.34	0.21	0.16	0.10	0.40	0.41	0.42
90	0	0	0	0	0	0	0
100	-.40	-.50	-.56	-.60	-.24	-.10	-.04

(Continued on next page)

Table 5-I, XV-15 Horizontal Stabilizer Lift Coefficient, C_{LH} (Concluded)

	Mach Number, M_N = 0 - 0.2						
	Elevator Angle, δ_e						
α_H, deg	0 deg	-10 deg	-15 deg	-20 deg	10 deg	15 deg	20 deg
110	-.66	-.90	-.96	-1.00	-.38	-.16	-.04
120	-.86	-1.15	-1.23	-1.30	-.46	-.20	-.04
130	-.99	-1.36	-1.43	-1.45	-.50	-.22	-.03
140	-.98	-1.38	-1.49	-1.60	-.48	-.20	0
150	-.84	-1.20	-1.35	-1.45	-.39	-.16	0.04
160	-.60	-.95	-1.13	-1.30	-.28	-.08	0.10
170	-.70	-1.10	-1.30	-1.50	-.30	-.10	0.10
180	0	-.40	-.60	-.80	0.40	0.60	0.80

Table 5-II, XV-15 Horizontal Stabilizer Lift Coefficient, C_{LH}

	Elevator Angle, δ_e = 0 deg			
	Mach Number, M_N			
α_H, deg	0 - 0.2	0.4	0.5	0.6
-40.0	Use values from Table 5-I for δ_e=0 deg from -180 to 180 deg	-1.1	Not Defined	Not Defined
-36.0		-1.09		
-32.0		-1.04		
-28.0		-1.0		
-24.0		-.9		
-20.0		-.93	-.8	-.79
-18.0		-.97	-.85	-.8
-16.0		-1.02	-.91	-.87
-14.0		-.98	-.94	-.9
-12.0		-.93	-.88	-.86
-10.0		-.775	-.78	-.75
-8.0		-.62	-.656	-.63
-6.0		-.465	-.492	-.528
-4.0		-.31	-.328	-.352
-2.0		-.155	-.164	-.176
0.0		0.0	0.0	0.0
2.0		0.155	0.164	0.176
4.0		0.31	0.328	0.352
6.0		0.465	0.492	0.528
8.0		0.62	0.656	0.63
10.0		0.775	0.78	0.75
12.0		0.93	0.88	0.86

(Continued on next page)

Table 5-II, XV-15 Horizontal Stabilizer Lift Coefficient, C_{LH} (Concluded)

	Elevator Angle, δ_e = 0 deg			
	Mach Number, M_N			
α_H, deg	0 - 0.2	0.4	0.5	0.6
14.0	Use	0.98	0.94	0.9
16.0	values	1.02	0.91	0.87
18.0	from	0.97	0.85	0.8
20.0	Table 5-I	0.93	0.8	0.79
24.0	for	0.9	Not	Not
28.0	δ_e=0 deg	1.0	Defined	Defined
32.0	from	1.04		
36.0	-180 to	1.09		
40.0	180 deg	1.1		

Table 5-III, XV-15 Horizontal Stabilizer Drag Coefficient, C_{DH}

	Elevator Angle, δ_e = 0 deg			
	Mach Number, M_N			
α_H, deg	0 - 0.2	0.4	0.5	0.6
-180	0.01			
-170	0.02			
-160	0.20			
-150	0.40			
-140	0.55			
-130	0.67			
-120	0.78			
-110	0.85			
-100	0.89			
-90	0.92	Not		
-80	0.91	Defined	Not	
-70	0.87		Defined	Not
-60	0.81			Defined
-50	0.72			
-40	0.60			
-36	0.54			
-32	0.47			
-28	0.39			
-24	0.30			
-20	0.20			
-16	0.115	0.135		
-12	0.068	0.068	0.088	
-8	0.035	0.035	0.035	0.045
-4	0.015	0.015	0.015	0.015

(Continued on the next page)

Table 5-III, XV-15 Horizontal Stabilizer Drag Coefficient, C_{DH} (Concluded)

	Elevator Angle, δ_e = 0 deg			
	Mach Number, M_N			
α_H, deg	0 - 0.2	0.4	0.5	0.6
0	0.00875	0.00875	0.00875	0.00875
4	0.015	0.015	0.015	0.015
8	0.035	0.035	0.045	0.065
12	0.068	0.075	0.105	Not Defined
16	0.115	0.145	Not Defined	
20	0.20	Not Defined		
24	0.34			
28	0.48			
32	0.61			
36	0.72			
40	0.80			
50	0.93			
60	1.05			
70	1.14			
80	1.18			
90	1.20			
100	1.19			
110	1.14			
120	1.06			
130	0.96			
140	0.80			
150	0.60			
160	0.36			
170	0.02			
180	0.01			

Table 5-IV, XV-15 Elevator/Rudder Effectiveness (τ_e/τ_r) Correction for Mach Number Effects, X_{Ke}, X_{Kr}

Mach Number, M_N	X_{Ke} or X_{Kr}
0.0	1.0
0.2	1.0
0.4	0.965
0.5	0.95
0.6	0.93
0.7	0.90

Table 5-V(a), XV-15 Dynamic Pressure Ratio at the Horizontal and Vertical Stabilizers (η_H or η_V), β_m = 0 deg, Rotors ON

	Mast Angle, β_m = 0 deg					
	Velocity, V_T, kts					
α_F, deg	0	20	40	60	80	≥ 100
-180	1.0	1.0	1.0	1.0	1.0	1.0
-40	1.0	1.0	1.0	1.0	1.0	1.0
-30	1.0	1.17	1.08	1.0	0.92	0.935
-28	1.0	1.20	1.12	1.0	0.92	0.935
-24	1.0	1.40	1.21	1.0	0.92	0.935
-20	1.0	1.70	1.43	1.05	0.93	0.935
-16	1.0	1.90	1.67	1.18	0.96	0.935
-12	1.0	2.08	1.80	1.37	1.0	0.935
-8	1.0	2.20	1.88	1.54	1.25	0.935
-4	1.0	2.20	1.80	1.52	1.23	0.935
0	1.0	2.07	1.70	1.35	1.05	0.935
4	1.0	1.90	1.60	1.10	1.0	0.935
8	1.0	1.70	1.46	1.00	0.93	0.935
12	1.0	1.55	1.30	0.90	0.86	0.86
16	1.0	1.37	1.05	0.82	0.80	0.80
20	1.0	1.20	0.93	0.80	0.80	0.72
30	1.0	1.0	1.0	1.0	1.0	1.0
180	1.0	1.0	1.0	1.0	1.0	1.0

Table 5-V(b), XV-15 Dynamic Pressure Ratio at the Horizontal and Vertical Stabilizers (η_H or η_V), β_m = 15 deg, Rotors ON

	Mast Angle, β_m = 15 deg					
	Velocity, V_T, kts					
α_F, deg	0	20	40	60	80	≥ 100
-180	1.0	1.0	1.0	1.0	1.0	1.0
-40	1.0	1.0	1.0	1.0	1.0	1.0
-30	1.0	1.24	1.1	0.97	0.92	0.935
-28	1.0	1.37	1.14	0.98	0.90	0.935
-24	1.0	1.54	1.24	0.99	0.88	0.935
-20	1.0	1.80	1.35	1.0	0.87	0.935
-16	1.0	2.0	1.52	1.03	0.87	0.935
-12	1.0	2.2	1.63	1.08	0.92	0.935
-8	1.0	2.38	2.04	1.15	0.97	0.935
-4	1.0	2.44	2.24	1.25	1.0	0.935
0	1.0	2.42	2.25	1.3	1.05	0.935
4	1.0	2.36	2.0	1.23	1.06	0.935
8	1.0	2.23	1.8	1.15	1.05	0.935
12	1.0	2.0	1.6	1.06	1.03	0.935
16	1.0	1.8	1.4	1.0	0.97	0.935
20	1.0	1.6	1.2	0.92	0.9	0.80
30	1.0	1.0	1.0	1.0	1.0	1.0
180	1.0	1.0	1.0	1.0	1.0	1.0

Table 5-V(c), XV-15 Dynamic pressure Ratio at the Horizontal and Vertical Stabilizers (η_H or η_V), β_m = 30, 60, 90 deg, Rotors ON

	Velocity, V_T, > 100 kts		
	Mast Angle, β_m, deg		
α_F, deg	30	60	90
-180	1.0	1.0	1.0
-40	1.0	1.0	1.0
-30	1.0	1.0	1.0
-28	1.0	1.0	1.0
-24	1.0	1.0	1.0
-20	1.0	1.0	1.0
-16	1.0	1.0	1.0
-12	1.0	1.05	1.0
-8	1.0	1.05	1.0
-4	1.0	1.05	1.0
0	1.0	1.05	1.0
4	1.0	1.05	1.0
8	1.0	1.05	1.0
12	1.0	1.05	1.0
16	1.0	1.05	1.0
20	0.8	0.8	0.8
30	1.0	1.0	1.0
180	1.0	1.0	1.0

Table 5-VI, Dynamic Pressure Loss Factor Due to Fuselage Sideslip Angle for the Horizontal and Vertical Stabilizers, $K_{\beta HS}$ or $K_{\beta VS}$

Sideslip Angle (β_F), deg	$K_{\beta HS}$ or $K_{\beta VS}$
0	1.0
±5	0.996
±10	0.985
±15	0.966
±20	0.94
±30	0.866
±45	0.707
±60	0.5

Table 5-VII, Mach Number Effect on the Downwash Term ($\partial\varepsilon_{W/H}/\partial\alpha_W$), PCPM

Mach Number, M_N	PCPM
0.0	0.0799
0.2	0.0799
0.4	0.0856
0.5	0.0905
0.6	0.0994

SUBSYSTEM NO. 6—XV-15 VERTICAL FIN AERODYNAMIC DATA

Constants	Values
NVSTAB	2
SL_{V1}	570.02 in
WL_{V1}	-115.69 in
BL_{V1}	77.0 in
SL_{V2}	570.02 in
WL_{V2}	115.69 in
BL_{V2}	77.0 in
S_{V1}	20.25 ft^2
S_{V2}	20.25 ft^2
i_{V1}	0.0 deg
i_{V2}	0.0 deg
BL_{CG}	0.0 in
SL_{SP}	300.0 in
BL_{SP}	193.0 in
l_m	4.667 ft
R	12.5 ft
b_W	32.17 ft

Coefficients	Values
τ_r	0.27
$\partial\sigma/\partial\hat{p}$	-0.1
$\partial\sigma/\partial\hat{r}$	0.0
K_{VNU}	1.0
a_V	3.02522 1/rad
D_{Kr}	0.24

Data Tables

Table 6-I, XV-15 Vertical Stabilizer Lift Coefficient (C_{YV})

	Mach Number, M_N = 0 - 0.2				
	Rudder Angle, δ_r				
β_V, deg	0 deg	15 deg	20 deg	-15 deg	-20 deg
-180	0	0.20	0.33	-.20	-.33
-170	0.53	0.73	0.86	0.33	0.20
-160	0.60	0.70	0.80	0.50	0.40
-150	0.72	0.82	0.92	0.62	0.52
-140	0.79	0.89	0.98	0.70	0.60
-130	0.77	0.86	0.97	0.69	0.60
-120	0.64	0.73	0.81	0.57	0.49
-110	0.47	0.55	0.60	0.44	0.37
-100	0.24	0.30	0.31	0.23	0.20
-90	0	0	0	0	0
-80	-.40	-.33	-.28	-.41	-.42
-70	-.64	-.57	-.52	-.67	-.70
-60	-.84	-.77	-.72	-.90	-.91
-50	-.99	-.92	-.88	-1.05	-1.07
-40	-1.0	-.96	-.92	-1.07	-1.11
-32	-.93	-.86	-.74	-1.06	-1.08
-28	-.94	-.77	-.68	-1.08	-1.1
-26	-.98	-.76	-.71	-1.1	-1.12
-24	-1.03	-.77	-.72	-1.12	-1.16
-22	-1.05	-.77	-.71	-1.17	-1.22

(Continued on next page)

Table 6-I, XV-15 Vertical Stabilizer Lift Coefficient (C_{YV}) (Continued)

	Mach Number, M_N = 0 - 0.2				
	Rudder Angle, δ_r				
β_V, deg	0 deg	15 deg	20 deg	-15 deg	-20 deg
-20	-1.05	-.73	-.67	-1.25	-1.3
-18	-.96	-.655	-.5616	-1.265	-1.3584
-16	-.86	-.555	-.4616	-1.165	-1.2584
-12	-.635	-.330	-.2366	-.94	-1.0334
-8	-.425	-.12	-.0266	-.73	-.8234
8	0.425	0.73	0.8234	0.12	0.0266
12	0.635	0.94	1.0334	0.33	0.2366
16	0.86	1.165	1.2584	0.555	0.4616
18	0.96	1.265	1.3584	0.655	0.5616
20	1.05	1.25	1.3	0.73	0.67
22	1.05	1.17	1.22	0.77	0.71
24	1.03	1.12	1.16	0.77	0.72
26	0.98	1.1	1.12	0.76	0.71
28	0.94	1.08	1.1	0.77	0.68
32	0.93	1.06	1.08	0.86	0.74
40	1.0	1.07	1.11	0.96	0.92
50	0.99	1.05	1.07	0.92	0.88
60	0.84	0.90	0.91	0.77	0.72
70	0.64	0.67	0.70	0.57	0.52
80	0.40	0.41	0.42	0.33	0.28
90	0	0	0	0	0

(Continued on next page)

Table 6-I, XV-15 Vertical Stabilizer Lift Coefficient (C_{YV}) (Concluded)

	Mach Number, M_N = 0 - 0.2				
	Rudder Angle, δ_r				
β_V, deg	0 deg	15 deg	20 deg	-15 deg	-20 deg
100	-.24	-.23	-.20	-.30	-.31
110	-.47	-.44	-.37	-.55	-.60
120	-.64	-.57	-.49	-.73	-.81
130	-.77	-.69	-.60	-.86	-.97
140	-.79	-.70	-.60	-.89	-.98
150	-.72	-.62	-.52	-.82	-.92
160	-.60	-.50	-.40	-.70	-.80
170	-.53	-.33	-.20	-.73	-.86
180	0	0.20	0.33	-.20	-.33

Table 6-II, XV-15 Vertical Stabilizer Lift Coefficient (C_{YV})

	Rudder Angle, δ_r = 0 deg			
	Mach Number, M_N			
β_V, deg	0 - 0.2	0.4	0.5	0.6
-40.0	Use values from Table 6-I for δ_r=0 deg from -180 to 180 deg	-1.0	Not defined	Not defined
-36.0		-.99		
-32.0		-.97		
-28.0		-.9		
-24.0		-.83		
-20.0		-.84	-.7	-.35
-18.0		-.85	-.73	-.375
-16.0		-.83	-.75	-.4
-14.0		-.775	-.73	-.425
-12.0		-.696	-.7	-.45
-10.0		-.58	-.61	-.47
-8.0		-.464	-.488	-.45
-6.0		-.348	-.366	-.396
-4.0		-.232	-.244	-.264
-2.0		-.116	-.122	-.132
0.0		0.0	0.0	0.0
2.0		0.116	0.122	0.132
4.0		0.232	0.244	0.264
6.0		0.348	0.366	0.396
8.0		0.464	0.488	0.45
10.0		0.58	0.61	0.47
12.0		0.696	0.7	0.45

(Continued on next page)

Table 6-II, XV-15 Vertical Stabilizer Lift Coefficient (C_{YV}) (Concluded)

	Rudder Angle, δ_r = 0 deg			
	Mach Number, M_N			
β_V, deg	0 - 0.2	0.4	0.5	0.6
14.0	Use	0.775	0.73	0.425
16.0	values	0.83	0.75	0.4
18.0	from	0.85	0.73	0.375
20.0	Table 6-I	0.84	0.7	0.35
24.0	for	0.83		
28.0	δ_r=0 deg	0.9	Not	Not
32.0	from	0.97	defined	defined
36.0	-180 to	0.99		
40.0	180 deg	1.0		

Table 6-III, XV-15 Vertical Stabilizer Drag Coefficient (C_{DV})

	Rudder Angle, δ_r = 0 deg			
	Mach Number, M_N			
β_V, deg	0 - 0.2	0.4	0.5	0.6
-180	0.0071			
-170	0.03			
-160	0.60			
-150	0.88			
-140	1.13			
-130	1.30			
-120	1.43			
-110	1.51			
-100	1.58	Not		
-90	1.60	Defined	Not	Not
-80	1.58		Defined	Defined
-70	1.52			
-60	1.45			
-50	1.34			
-40	1.20			
-32	1.1			
-28	0.87			
-24	0.58			
-20	0.324			
-16	0.160	0.33		
-12	0.080	0.15	0.20	0.32
-8	0.024	0.044	0.07	0.12
-4	0.014	0.014	0.015	0.02

(Continued on next page)

Table 6-III, XV-15 Vertical Stabilizer Drag Coefficient (C_{DV}) (Concluded)

	Rudder Angle, δ_r = 0 deg			
	Mach Number, M_N			
β_V, deg	0 - 0.2	0.4	0.5	0.6
0	0.0071	0.0071	0.0071	0.0071
4	0.014	0.014	0.015	0.02
8	0.024	0.044	0.07	0.12
12	0.08	0.15	0.20	0.32
16	0.16	0.33		
20	0.324			
24	0.58			
28	0.87			
32	1.1			
40	1.2			
50	1.34			
60	1.45			
70	1.52			
80	1.58		Not	Not
90	1.60	Not	Defined	Defined
100	1.58	Defined		
110	1.51			
120	1.43			
130	1.30			
140	1.13			
150	0.88			
160	0.60			
170	0.03			
180	0.0071			

Table 6-IV, XV-15 Sidewash Factor $\left(1 - \frac{\partial\sigma}{\partial\beta_F}\right)$ for Flap Setting, $X_{FL1} = 0/0$

		Flap Setting, deg, $X_{FL1} = 0/0$					
		Sideslip Angle, $\lvert\beta_F\rvert$, deg					
β_m, deg	α_F, deg	0 & 4	8	12	16	20 - 50	> 50
0	≤-10.0	1.0	1.0	1.0	1.0	1.0	1.0
	-3.0	1.1	1.05	1.015	0.985	1.01	1.0
	0	1.038	1.044	0.965	0.933	1.0	1.0
	7.0	0.863	0.810	0.772	0.787	0.958	1.0
	13.0	0.524	0.517	0.474	0.491	0.673	1.0
	≥ 28.0	1.0	1.0	1.0	1.0	1.0	1.0
30	≤-10.0	1.0	1.0	1.0	1.0	1.0	1.0
	-3.0	1.13	1.072	0.97	1.025	1.0	1.0
	0	1.248	1.093	0.977	1.015	1.056	1.0
	7.0	0.995	0.961	0.865	0.845	0.953	1.0
	13.0	0.677	0.595	0.523	0.526	0.681	1.0
	≥ 28.0	1.0	1.0	1.0	1.0	1.0	1.0
60	≤-10.0	1.0	1.0	1.0	1.0	1.0	1.0
	-3.0	1.15	1.05	1.0	1.06	1.1	1.0
	0	1.21	1.08	0.975	1.02	1.025	1.0
	7.0	0.945	0.975	0.9	0.88	0.92	1.0
	13.0	0.69	0.645	0.585	0.59	0.7	1.0
	≥ 28.0	1.0	1.0	1.0	1.0	1.0	1.0
90	≤-10.0	1.0	1.0	1.0	1.0	1.0	1.0
	-3.0	1.09	1.10	1.18	1.15	1.04	1.0
	0	1.0	1.0	1.0	1.0	1.0	1.0
	7.0	0.834	0.865	0.866	0.842	0.924	1.0
	13.0	0.659	0.676	0.622	0.642	0.680	1.0
	≥ 28.0	1.0	1.0	1.0	1.0	1.0	1.0

Table 6-V, XV-15 Sidewash Factor $\left(1 - \frac{\partial\sigma}{\partial\beta_F}\right)$ for Flap Setting, X_{FL2} = 20/12.5

		Flap Setting, deg, X_{FL2} = 20/12.5					
		Sideslip Angle, $\lvert\beta_F\rvert$, deg					
β_m, deg	α_F, deg	0 & 4	8	12	16	20 - 50	> 50
0	≤-10.0	1.0	1.0	1.0	1.0	1.0	1.0
	-3.0	1.2	1.15	1.10	1.05	1.04	1.0
	0	1.12	1.10	1.05	0.98	1.0	1.0
	7.0	0.89	0.87	0.80	0.80	0.90	1.0
	13.0	0.55	0.55	0.45	0.57	0.68	1.0
	≥ 28.0	1.0	1.10	1.0	1.0	1.0	1.0
30	≤-10.0	1.0	1.0	1.0	1.0	1.0	1.0
	-3.0	1.10	1.06	1.02	1.075	1.03	1.0
	0	1.17	1.10	1.02	1.06	1.055	1.0
	7.0	1.01	0.95	0.92	0.86	0.92	1.0
	13.0	0.775	0.70	0.575	0.50	0.684	1.0
	≥ 28.0	1.0	1.0	1.0	1.0	1.0	1.0
60	≤-10.0	1.0	1.0	1.0	1.0	1.0	1.0
	-3.0	1.05	1.04	1.05	1.08	1.08	1.0
	0	1.10	1.075	0.98	1.04	1.05	1.0
	7.0	0.98	0.98	1.00	0.92	0.91	1.0
	13.0	0.80	0.75	0.70	0.60	0.73	1.0
	≥ 28.0	1.0	1.0	1.0	1.0	1.0	1.0
90	≤-10.0	1.0	1.0	1.0	1.0	1.0	1.0
	-3.0	1.08	1.11	1.17	1.12	1.04	1.0
	0	0.99	1.08	1.05	1.02	1.04	1.0
	7.0	0.90	0.95	0.95	0.91	0.98	1.0
	13.0	0.75	0.71	0.72	0.67	0.70	1.0
	≥ 28.0	1.0	1.0	1.0	1.0	1.0	1.0

Table 6-VI, XV-15 Sidewash Factor $\left(1 - \frac{\partial\sigma}{\partial\beta_F}\right)$ for Flap Setting, X_{FL3} = 40/25

		Flap Setting, deg, X_{FL3} = 40/25					
		Sideslip Angle, $\lvert\beta_F\rvert$, deg					
β_m, deg	α_F, deg	0 & 4	8	12	16	20 - 50	> 50
0	<-10.0	1.0	1.0	1.0	1.0	1.0	1.0
	-3.0	1.315	1.26	1.185	1.1	1.059	1.0
	0	1.228	1.208	1.12	1.045	1.0	1.0
	7.0	0.89	0.91	0.86	0.809	0.86	1.0
	13.0	0.535	0.59	0.396	0.443	0.678	1.0
	≥ 28.0	1.0	1.0	1.0	1.0	1.0	1.0
30	<-10.0	1.0	1.0	1.0	1.0	1.0	1.0
	-3.0	1.065	1.027	1.055	1.14	1.055	1.0
	0	1.1	1.115	1.058	1.12	1.065	1.0
	7.0	1.025	0.935	0.972	0.882	0.86	1.0
	13.0	0.884	0.82	0.629	0.456	0.689	1.0
	≥ 28.0	1.0	1.0	1.0	1.0	1.0	1.0
60	<-10.0	1.0	1.0	1.0	1.0	1.0	1.0
	-3.0	1.02	1.03	1.08	1.117	1.04	1.0
	0	0.945	1.07	0.998	1.05	1.09	1.0
	7.0	1.03	0.985	1.015	0.95	0.908	1.0
	13.0	0.915	0.9	0.8	0.61	0.745	1.0
	≥ 28.0	1.0	1.0	1.0	1.0	1.0	1.0
90	<-10.0	1.0	1.0	1.0	1.0	1.0	1.0
	-3.0	1.07	1.121	1.16	1.072	1.04	1.0
	0	0.984	1.15	1.09	1.05	1.064	1.0
	7.0	0.982	1.035	1.03	0.993	1.015	1.0
	13.0	0.842	0.74	0.77	0.695	0.725	1.0
	≥ 28.0	1.0	1.0	1.0	1.0	1.0	1.0

Table 6-VII, XV-15 Sidewash Factor $\left(1 - \frac{\partial\sigma}{\partial\beta_F}\right)$ for Flap Setting, X_{FL4} = 75/47

		Flap Setting, deg, X_{FL4} = 75/47					
		Sideslip Angle, $\lvert\beta_F\rvert$, deg					
β_m, deg	α_F, deg	0 & 4	8	12	16	20 - 50	> 50
0	<-10.0	1.0	1.0	1.0	1.0	1.0	1.0
	-3.0	1.8	1.22	1.155	1.105	1.048	1.0
	0	1.128	1.185	1.125	1.045	1.01	1.0
	7.0	0.846	0.99	0.948	0.92	0.862	1.0
	13.0	0.535	0.65	0.44	0.51	0.65	1.0
	≥ 28.0	1.0	1.0	1.0	1.0	1.0	1.0
30	<-10.0	1.0	1.0	1.0	1.0	1.0	1.0
	-3.0	1.05	1.072	1.14	1.135	1.08	1.0
	0	0.979	1.01	1.105	1.1	1.035	1.0
	7.0	0.82	0.862	0.998	0.986	0.932	1.0
	13.0	0.65	0.72	0.7	0.52	0.78	1.0
	≥ 28.0	1.0	1.0	1.0	1.0	1.0	1.0
60	<-10.0	1.0	1.0	1.0	1.0	1.0	1.0
	-3.0	1.025	1.085	1.15	1.115	1.075	1.0
	0	0.915	1.005	1.1	1.1	1.04	1.0
	7.0	0.855	0.90	1.015	0.955	0.995	1.0
	13.0	0.73	0.8	0.8	0.61	0.82	1.0
	≥ 28.0	1.0	1.0	1.0	1.0	1.0	1.0
90	<-10.0	1.0	1.0	1.0	1.0	1.0	1.0
	-3.0	1.058	1.15	1.145	1.075	1.04	1.0
	0	1.0	1.12	1.12	1.05	1.088	1.0
	7.0	0.905	1.005	1.03	0.99	1.028	1.0
	13.0	0.782	0.76	0.72	0.66	0.71	1.0
	≥ 28.0	1.0	1.0	1.0	1.0	1.0	1.0

Table 6-VIII, XV-15 Rotor Sidewash Factor ($K_{\beta R}$)

	Sideslip Angle, β_F, deg						
Velocity, V_T, kts	0	±5	±10	±15	±20	±25	±30
0	1.0	1.0	1.0	1.0	1.0	1.0	1.0
20	1.0	1.0	1.0	1.0	1.0	1.0	1.0
40	-.5	0.25	0.80	1.25	1.5	1.0	1.0
60	0.2	0.40	0.80	1.1	1.4	1.0	1.0
80	0.5	0.60	0.80	1.0	1.2	1.0	1.0
100	0.75	0.80	0.80	1.0	1.0	1.0	1.0
120	1.0	1.0	1.0	1.0	1.0	1.0	1.0
350	1.0	1.0	1.0	1.0	1.0	1.0	1.0

SUBSYSTEM NO. 7A—XV-15 LANDING GEAR

Constants	Value
BL_{CG}	0.0 in
SL_{G1}	139.0 in
$SL_{G2,3}$	326.0 in
WL_{G1}	4.95 in
$WL_{G2,3}$	8.25 in
BL_{G1}	0.0 in
$BL_{G2,3}$	51.25 in
$\delta_{B_{n_{MIN}}}$	0.1 rad
K_{B_n}	-10 ft/sec^2-rad
A_{MAX}	-5 ft/sec^2
g	32.2 ft/sec^2
T_{DN} (VAX version)	7.0 sec
T_{UP} (VAX version)	10.0 sec

Coefficients	Value
DPOD	1.15 ft^2
G_{A_1}	100.0 lb-sec/ft
$G_{A_{2,3}}$	775.0 lb-sec/ft
G_{B_n}	0.0 lb-sec/ft^3
G_{C_1}	175.0 lb/ft^4
$G_{C_{2,3}}$	325.0 lb/ft^4
μ_{S_n}	0.03
μ_{G_n}	0.5
μ_{RF}	0.015

Data Tables

Table 7A-I, Landing Gear Drag as a Percent of Gear Extension

NOTE: The VAX/VMS version of the mathematical model uses data in this data table format and not the format of Tables 7A-II and 7A-III (only aerodynamics of the landing gear are simulated in the VAX/VMS version).

Percent (%) Gear Extension	Nose Gear Drag, ft^2	Main Gear Drag, ft^2
0.0	0.0	0.0
10.0	0.28	1.04
20.0	0.48	1.38
30.0	0.5	1.5
40.0	0.62	1.9
50.0	0.74	2.26
60.0	0.82	2.54
70.0	0.9	2.76
80.0	0.96	2.92
90.0	1.0	2.98
100.0	1.0	3.0

Table 7A-II, Main Landing Gear Drag as a Function of Landing Gear Position (D_{MG})

Cycle Time, sec	Main Gear Drag During Extension ($D_{o_{MGD}}$), ft^2	Main Gear Drag During Retraction ($D_{o_{MGU}}$), ft^2
0.0	0.0	3.0
0.5	0.9	3.0
1.0	1.25	3.0
1.5	1.4	2.95
2.0	1.5	2.9
2.5	1.8	2.83
3.0	2.2	2.75
3.5	2.4	2.65
4.0	2.6	2.55
4.5	2.73	2.4
5.0	2.85	2.3
5.5	2.95	2.13
6.0	3.0	1.9
6.5	3.0	1.7
7.0	3.0	1.5
7.5	3.0	1.5
8.0	3.0	1.4
8.5	3.0	1.25
9.0	3.0	1.05
9.5	3.0	0.75
10.0	3.0	0.0

Table 7A-III, Nose Landing Gear Drag as a Function of Landing Gear Position (D_{NG})

Cycle Time, sec	Nose Gear Drag During Extension ($D_{o_{NGD}}$), ft^2	Nose Gear Drag During Retraction ($D_{o_{NGU}}$), ft^2
0.0	0.0	1.0
0.5	0.25	1.0
1.0	0.4	1.0
1.5	0.5	1.0
2.0	0.5	0.98
2.5	0.6	0.95
3.0	0.7	0.9
3.5	0.75	0.85
4.0	0.8	0.8
4.5	0.85	0.77
5.0	0.9	0.73
5.5	0.95	0.7
6.0	0.98	0.65
6.5	1.0	0.6
7.0	1.0	0.5
7.5	1.0	0.5
8.0	1.0	0.5
8.5	1.0	0.4
9.0	1.0	0.3
9.5	1.0	0.2
10.0	1.0	0.0

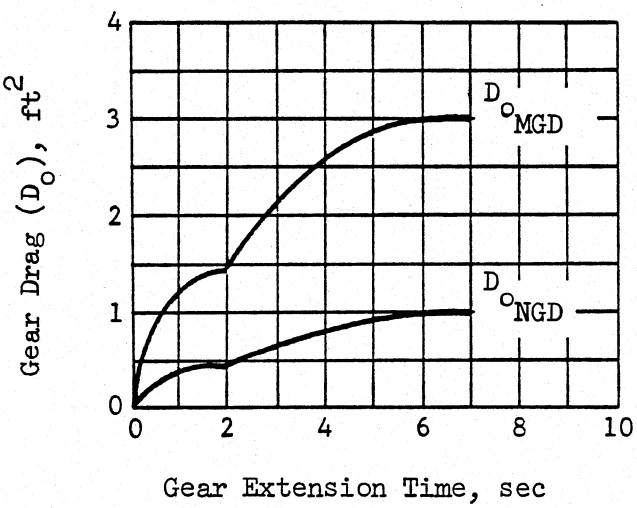

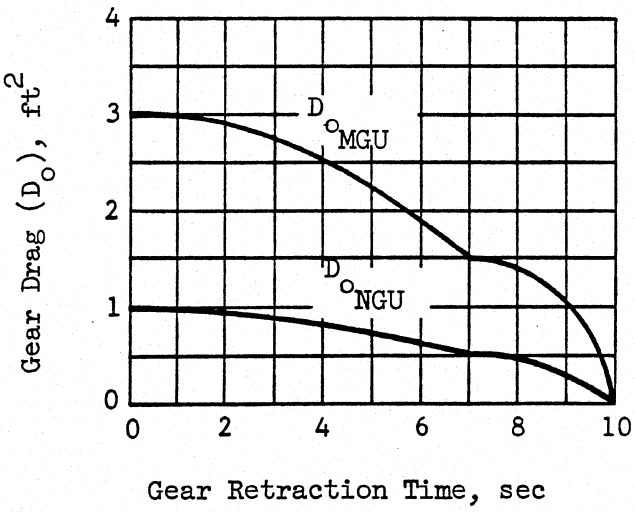

Figure B7A-1. Landing Gear Drag as a Function of Landing Gear Position

SUBSYSTEM NO. 7B—XV-15 LANDING GEAR

Constants	Value
BL_{CG}	0.0 in
SL_{G1}	139.0 in
$SL_{G2,3}$	326.0 in
WL_{G1}	4.95 in
$WL_{G2,3}$	8.25 in
BL_{G1}	0.0 in
$BL_{G2,3}$	51.25 in
Z_{TIRE_n}	0.1 ft

Coefficients	Values
G_{1_1}	7800
$G_{1_{2,3}}$	24000
G_{2_1}	15.32
$G_{2_{2,3}}$	14.877
μ_o	0.015
μ_1	0.014
μ_{S_1}	0.075
$\mu_{S_{2,3}}$	0.15
DPOD	1.15 ft^2

Data Tables

See Subsystem 7A, Tables 7A-II and 7A-III

SUBSYSTEM NO. 8a—XV-15 CONTROLS

Constants	Value
COLRATE	0.2 deg/sec
$\Delta\theta_{oLIM}$	± 0.5 deg
PBMMAX	90.0 deg
PBMMIN	-5.0 deg
δ_{B1}	1.5 deg
X_{LNN}	4.8 in
X_{LTN}	4.8 in
X_{PDN}	2.5 in

Coefficients	Value
$\partial\delta_e/\delta X_{LN}$	4.167 deg/in
$\partial\delta_r/\partial X_{PD}$	8.0 deg/in
$\partial\delta_a/\partial X_{LT}$	3.93 deg/in
$\partial\delta_F/\partial t$	4.0 deg/sec
w_n	2.0 rad/sec
ζ_D	0.7

Data Tables

Table 8a-I, XV-15 F/A Cyclic Pitch to Longitudinal Stick Gearing, $\left(\frac{\partial B_1}{\partial X_{LN}}\right)$

Mast Angle, β_m, deg	$\frac{\partial B_1}{\partial X_{LN}}$, deg/in
0	2.1
10	2.09
20	1.98
30	1.81
40	1.60
50	1.35
60	1.04
70	0.71
80	0.362
90	0

NOTES: 1. $X_{LN} = \pm 4.8$ in (from center position)

2. $B_1 = 10.0625$ deg at $\beta_m = 0$ deg

Table 8a-II, XV-15 Differential Cyclic Pitch Gearing, $\left(\frac{\partial B_1}{\partial X_{PD}}\right)$

	$\frac{\partial B_1}{\partial X_{PD}}$, deg/in		
	U, KCAS		
Mast Angle, β_m, deg	0 - 60	80	> 100
0	1.6	1.04	0.40
10	1.58	1.025	0.394
20	1.51	0.975	0.375
30	1.39	0.90	0.345
40	1.225	0.795	0.305
50	1.035	0.67	0.257
60	0.803	0.52	0.200
70	0.55	0.325	0.137
80	0.28	0.18	0.069
90	0	0	0

NOTES: 1. $X_{PD} = \pm 2.5$ in (from center position)

2. $\Delta B_1 = \pm 4.0$ deg at 0 - 60 KCAS

$\Delta B_1 = \pm 2.6$ deg at 80 KCAS

$\Delta B_1 = \pm 1.0$ deg at 100 KCAS

Table 8a-III, XV-15 Differential Collective Pitch Gearing, $\left(\frac{\partial \theta_o}{\partial X_{LT}}\right)$

Mast Angle, β_m, deg	$\frac{\partial \theta_o}{\partial X_{LT}}$, deg/in
0	0.625
10	0.606
20	0.575
30	0.541
40	0.50
50	0.438
60	0.365
70	0.293
80	0.209
90	0.121

NOTES: 1. $X_{LT} = \pm 4.8$ in (from center position)

2. $\Delta\theta_o = \pm 3$ deg at $\beta_m = 0$ deg

Table 8a-IV, XV-15 Collective Pitch Gearing,
$\left(\frac{\partial \theta_o}{\partial X_{COL}};\ \theta_{oLL} \text{ at } 0.75\ R\right)$

Mast Angle, β_m, deg	$\frac{\partial \theta_o}{\partial X_{COL}}$, deg/in	θ_{oLL} at 0.75 R, deg
0	1.6	-2.3
10	1.5	-1.0
20	1.35	1.0
30	1.13	4.0
40	0.92	7.0
50	0.71	10.2
60	0.52	13.5
70	0.34	16.7
80	0.15	19.5
90	0	21.3

Table 8a-V, XV-15 Commanded Pylon Conversion Rate, $\dot{\beta}_{mC}$

Mast Angle, β_m, deg	Conversion Rate, $\dot{\beta}_{mC}$, deg/sec	
	Present Low Rate	Original High Rate Rigging
-5	2.73(1)	3.0(1)
0	2.73(1)	3.0(1)
2	2.73(1)	3.0(1)
2.5	7.83(2)	15.0(2)
10	7.83	14.25
20	7.83	13.3
30	7.83	12.45
40	7.83	11.7
50	7.83	11.4
60	7.83	11.4
70	7.83	11.63
80	7.83	12.5
87	7.83(2)	14.0(2)
87.5	1.96(1)	2.8(1)
90	1.96(1)	2.8(1)

NOTES: 1. When conversion starts at mast angle of -5, 0, or 90; $\dot{\beta}$ = 2.73 or 1.96. When conversion stops at mast angle of -5, 0, or 90; $\dot{\beta}_m = 0$.

2. Δt from quarter rate to maximum rate; Δt = 0.05 sec.

Table 8a-VI, XV-15 Collective Rigging Versus Throttle Rigging, X_{COL} versus $X_{THR,L}$

Collective Rigging, X_{COL}, in	Throttle Rigging, $X_{THR,L}$, deg
0	42.25
0.5	47.5
1.0	51.5
1.5	56.0
2.0	58.25
2.5	61.0
3.0	63.25
3.5	66.0
4.0	68.25
4.5	70.5
5.0	73.0
5.5	75.5
6.0	78.0
6.5	80.5
7.0	83.25
7.5	86.0
8.0	90.0
8.5	94.0
9.0	98.0
9.5	102.0
10.0	105.0

Table 8a-VII, XV-15 Mast Angle Versus Flapping Controller Gain, β_m versus $A_{1_{B_m}}$

Mast Angle, β_m, deg	Flapping Controller Gain, $A_{1_{B_m}}$
0	1.0
15	1.0
30	1.0
45	0.92
60	0.707
75	0.384
90	0

Table 8a-VIII, XV-15 U Velocity Versus Flapping Controller Gain, U versus $A_{1_{V_T}}$

U Velocity, U, KCAS	Flapping Controller Gain, $A_{1_{V_T}}$
0	0
20	0
40	-4
60	-4
80	-4
100	-4
400	-4

SUBSYSTEM NO. 8b—XV-15 FORCE FEEL SYSTEM

Coefficients	Values
G_{LNO}	3.5 lb/in
G_{LN1}	0.108 lb/in/psf
K_{LN}	11.25 lb/in
ζ_{LN}	0.85
H_{LN}	2.85 lb
G_{LT_0}	1.0 lb/in
G_{LT_1}	0.023 lb/in/psf
K_{LT}	3.5 lb/in
ζ_{LT}	0.85
H_{LT}	3.75 lb
G_{PDO}	5.0 lb/in
G_{PD1}	0.167 lb/in/psf
ζ_{PD}	0.85
H_{PD}	8.8 lb
H_{RUD}	0.37 ft^2/in
$F_{ACT_{RUD_{LIM}}}$	45.0 lb
$\dot{X}_{LNTO}$	1.0 in/sec
$\dot{X}_{LNT1}$	-0.00262 in/sec/psf
$\dot{X}_{LTTO}$	1.0 in/sec
$\dot{X}_{LTT1}$	-0.00262 in/sec/psf
$\dot{X}_{PDTO}$	0.5 in/sec
$\dot{X}_{PDT1}$	-0.00131 in/sec/psf
$\dot{X}_{LNTO}$ (FSS OFF)	0.25 in/sec

SUBSYSTEM NO. 8c—XV-15 CONTROL FORCE TRIM SYSTEM

Coefficients	Values
$\dot{X}_{LNTO}$	1.0 in/sec
$\dot{X}_{LNT1}$	-0.00262 in/sec/psf
$\dot{X}_{LTTO}$	1.0 in/sec
$\dot{X}_{LTT1}$	-0.00262 in/sec/psf
$\dot{X}_{PDTO}$	0.5 in/sec
$\dot{X}_{PDT1}$	-0.00131 in/sec/psf

SUBSYSTEM NO. 9—XV-15 CG AND INERTIA

Constants	Values
W_p	4200.0 lb
GW	13000.0 lb
SL_{SP}	300.0 in
SL_P	291.7 in
WL_{SP}	100.0 in
WL_P	118.0 in
$SL_{CG}\big\vert_{\beta_m = 0}$	300.0 in
$WL_{CG}\big\vert_{\beta_m = 0}$	81.65 in
l_m	4.667 ft
$I_{XX}\big\vert_{\beta_m = 0}$	52795.0 slug-ft^2
$I_{YY}\big\vert_{\beta_m = 0}$	21360.0 slug-ft^2
$I_{ZZ}\big\vert_{\beta_m = 0}$	66335.0 slug-ft^2
$I_{XZ}\big\vert_{\beta_m = 0}$	1234.0 slug-ft^2
L_N	1.65 ft
I_{PYL}	500.0 slug-ft^2
λ_{PYL}	66.0 deg

Coefficients	Values
K_{I1}	20.5 slug-ft^2/deg
K_{I2}	11.24 slug-ft^2/deg
K_{I3}	9.26 slug-ft^2/deg
K_{I4}	1.76 slug-ft^2/deg

SUBSYSTEM NO. 10a—XV-15 AXES TRANSFORMATION (AIRFRAME AERODYNAMIC FORCES AND MOMENTS FROM WIND TO BODY AXIS)

Constants	Values
NVSTAB	2

SUBSYSTEM NO. 10b—XV-15 AXES TRANSFORMATION (ROTOR FORCES AND MOMENTS FROM WIND TO BODY AXIS)

Constants	Values
ϕ_m	1.0 deg

SUBSYSTEM NO. 10f—XV-15 AXES TRANSFORMATION (GROUND REFERENCE DIFFERENCE)

Constants	Values
X_o	user specified, ft
Y_o	user specified, ft
H_o	user specified, ft
WL_{G2}	8.25 in
GRD_{ALT}	user specified, ft

SUBSYSTEM NO. 11—XV-15 ANGULAR ACCELERATIONS AND VELOCITIES

Constants	Values
SL_{PA}	215.25 in
BL_{PA}	16.5 in
WL_{PA}	82.0 in
BL_{CG}	0.0 in
m	403.7 slugs

SUBSYSTEM NO. 12—XV-15 BODY AXIS LINEAR ACCELERATION AND VELOCITIES

Constants	Value
GW	13000.0 lbs2
m	403.7 slugs
U_o	user specified, ft
V_o	user specified, ft
W_o	user specified, ft
g	32.2 ft/sec^2

SUBSYSTEM NO. 13—XV-15 FORCE SUMMATION

Constants	Values
NVSTAB	2

SUBSYSTEM NO. 14—XV-15 MOMENT SUMMATION

Constants	Values
BL_{CG}	0.0 in
SL_F	293.0 in
WL_F	84.0 in
SL_{WP}	291.7 in
WL_{WP}	95.85 in
SL_H	560.0 in
WL_H	103.0 in
SL_{MG}	324.0 in
WL_{MG}	7.4 in
SL_{NG}	139.0 in
WL_{NG}	4.95 in
$SL_V(i)$	570.02 in
$BL_V(1)$	-77.0 in
$BL_V(2)$	77.0 in
$WL_V(i)$	115.69 in
SL_{SP}	300.0 in
BL_{SP}	193.0 in
WL_{SP}	100.0 in
l_m	4.667 ft
R	12.5 ft
ϕ_m	1.0 deg
NVSTAB	2

SUBSYSTEM NO. 14—XV-15 MOMENT SUMMATION (Concluded)

Coefficients	Values
l_{G0}	-7506.0 ft-lb/deg
l_{G1}	23366.0 ft-lb/deg
l_{G2}	-20134.0 ft-lb/deg
l_{G3}	5290.0 ft-lb/deg
l_{G4}	-0.1 sec/ft
GELLIM	1.6386
GEULIM	0.5
M_{G1}	-0.9 ft
M_{G2}	-2.6
M_{G3}	-0.08 sec/ft

SUBSYSTEM NO. 15—XV-15 FLIGHT ENVIRONMENT GROUP

Constants	Values
T_o	288.15 deg K
ρ_o	0.0023769 slug-ft^3

SUBSYSTEM NO. 17—XV-15 ROTOR COLLECTIVE GOVERNOR

Constants	Values
$\theta_{ERR_{LIM}}$	0.84 deg
$\theta_{FCP_{LIM}}$	5.0 deg
P_{SRG}	500.0 lb/in^2
K_{1RGA}	9.5
K_{2RGA}	0.487
K_{3RGA}	492.1
K_{4RGA}	6.2
$RPM_{P_{MAX}}$	601.0 RPM
K_{RPM}	0.98 (98 percent)
THOGMX	33.5 deg
THOGMN	-5.0 deg

Coefficients	Values
θ_{INT_1}	11.3

Data Tables

Table 17-I, XV-15 Mast Angle Versus Rotor Collective Governor Proportional Gain, β_m versus K_{PROG}

Mast Angle, β_m, deg	Rotor Collective Governor Integral Gain, K_{PROG}
0.0	0.5
15.0	0.41666
30.0	0.3333
45.0	0.25
60.0	0.1666
75.0	0.08333
90.0	0.0

Table 17-II, XV-15 Mast Angle Versus Rotor Collective Governor Integral Gain, β_m versus K_{INTG}

Mast Angle, β_m, deg	Rotor Collective Governor Integral Gain, K_{INTG}
0.0	0.1
15.0	0.1
30.0	0.1
45.0	0.1
60.0	0.1
75.0	0.1
90.0	0.1

SUBSYSTEM NO. 18—XV-15 ENGINES AND FUEL CONTROLS

Constants	Values
P_o	2116.22 lb/ft^2
T_o	288.15 deg K
RPME	1.0
SHP_{ACC}	10.0 SHP
η_{XMSN}	0.93

Coefficients	Values
K_1	-0.94
K_2	1.94
K_3	0.0
K_4	13100.0 RPM
K_5	235.0 RPM/SHP
K_6	475.0 SHP
K_7	288.16 deg K
K_{11}	0.0032 1/deg K
K_{12}	0.875 1/deg K
K_{13}	0.00125 1/deg K
K_{14}	0.0 deg K
K_{15}	0.0 1/kts
K_{18}	1400.0 SHP
$\Delta\varepsilon_p$	0.002
$\Delta\varepsilon_s$	0.002
T_D	0.0 sec
pctmxs	6.0 percent
pctmxp	6.0 percent
RPM_{NII}	22200 rad/sec
$X_{E1,2}$	1.0 engine operating 0.0 engine not operating

Data Tables

Table 18-I, XV-15 Throttle Versus Power Rigging, X_{THR} versus R_{SHP}

Throttle, X_{THR}	Power Rigging, R_{SHP}	
	S/N 703	S/N 702
42	105	127
45	120	140
50	160	183
55	235	263
60	320	355
65	430	473
70	560	613
75	718	783
80	890	968
85	1070	1160
90	1250	1355
95	1390	1505
100	1520	1645
105	1622	1755

Table 18-II, XV-15 Engine RAM Effect

Velocity, V_T, kt	Engine Ram Effect, K_{RAM}
0	0.00
50	0.003
100	0.017
150	0.04
200	0.07
250	0.118
300	0.193

Table 18-III, T-53 (LTCIK-4K) Engine Acceleration Characteristics

$(SHP/\delta\sqrt{\theta})_{AVG}$	$(\Delta SHP/\delta\sqrt{\theta})/\Delta t$
127.0	100.0
350.0	600.0
500.0	945.0
560.0	1040.0
630.0	1120.0
720.0	1170.0
850.0	1200.0
950.0	1185.0
1050.0	1150.0
1300.0	1000.0
1500.0	835.0
1750.0	550.0

Table 18-IV, XV-15 Jet Thrust Coefficients

Velocity, V_T, kts	Jet Thrust Coefficient, K_{JT1}, lb	Jet Thrust Coefficient, K_{JT2}, lb/SHP
0	16	0.084
100	-17	0.063
200	-57	0.045
300	-100	0.030

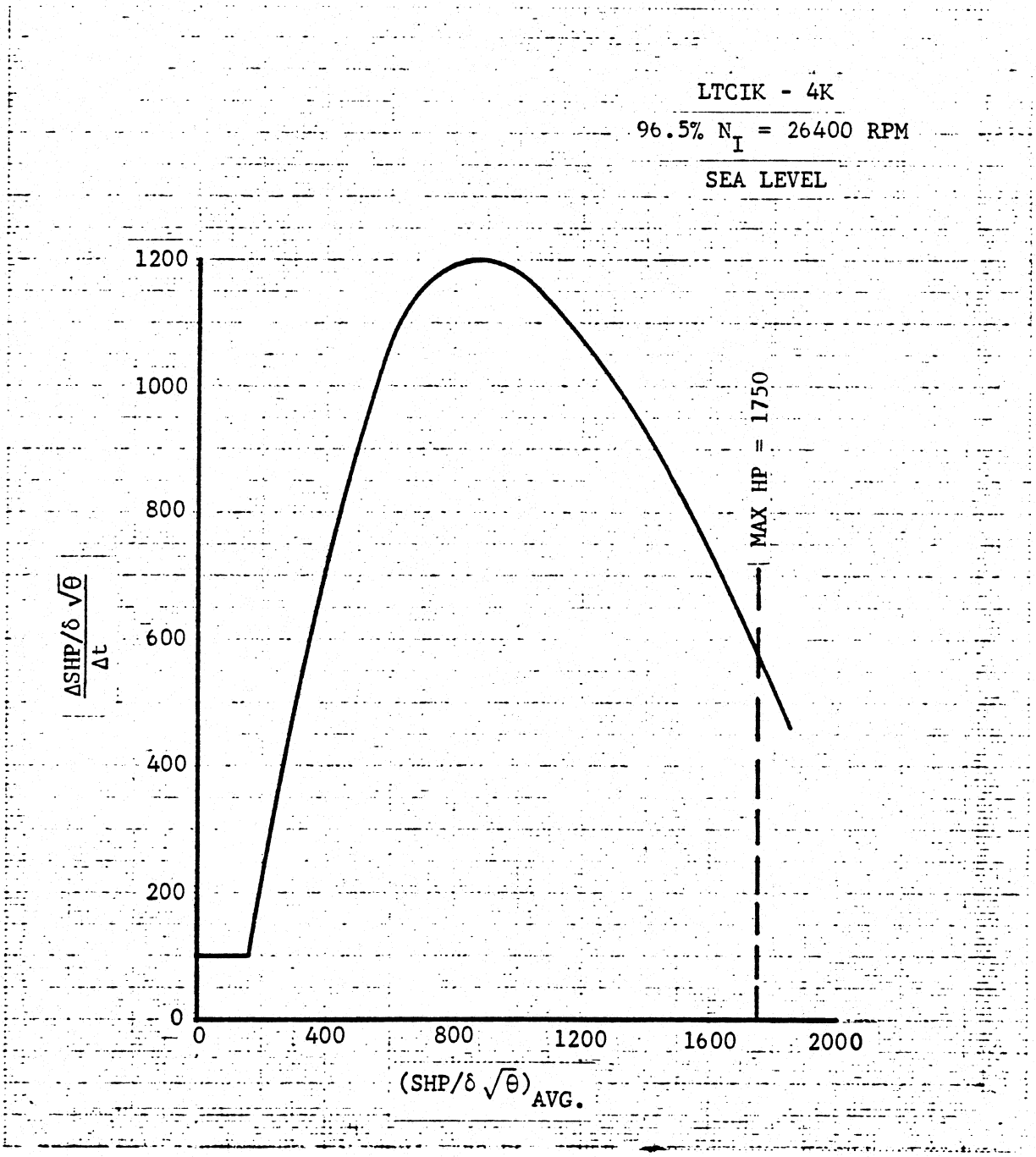

Figure B18-1. T53 Engine Acceleration Characteristics

SUBSYSTEM NO. 19—XV-15 DRIVE SYSTEM

Constants	Values
I_1	824 slug-ft^2
θ_{RPT_1}	35.133
θ_{INT_1}	11.3

Constants	Values
Ames Research Center Modified Pitch SCAS	
τ_{1P}	0.3 sec
τ_{2P}	3.0 sec
τ_q	0.3 sec
K_{1P}, $\beta_m = 0$	0.6 in/in
K_{1P}, $\beta_m = 90$	-1.0 in/in
K_{2P}, $\beta_m = 0$	0.921 in/deg/sec
K_{2P}, $\beta_m = 90$	0.386 in/deg/sec
K_{3P}, $\beta_m = 0$	0.107 in/deg/sec
K_{3P}, $\beta_m = 90$	0.0 in/deg/sec
K_{4P}, $\beta_m = 0$	-7.5 deg/sec/in
K_{4P}, $\beta_m = 90$	-7.5 deg/sec/in
K_{5P}, $\beta_m = 0$	0.2 in/deg
K_{5P}, $\beta_m = 90$	0.2 in/deg
K_{7P}, $\beta_m = 0$	0.092 in/deg/sec
K_{7P}, $\beta_m = 90$	0.059 in/deg/sec
$PSCAS_{MX}$	± 1.078 in

SUBSYSTEM NO. 20—XV-15 STABILITY AND CONTROL AUGMENTATION SYSTEM (Continued)

Constants	Values
Ames Research Center Modified Roll SCAS	
τ_{1R}	0.3 sec
τ_{2R}	3.0 sec
τ_p	0.3 sec
K_{1R}, $\beta_m = 0$	1.0 in/in
K_{1R}, $\beta_m = 90$	1.0 in/in
K_{2R}, $\beta_m = 0$	0.535 in/deg/sec
K_{2R}, $\beta_m = 90$	0.803 in/deg/sec
K_{3R}, $\beta_m = 0$	0.064 in/deg/sec
K_{3R}, $\beta_m = 90$	0.057 in/deg/sec
K_{4R}, $\beta_m = 0$	10.0 deg/sec/in
K_{4R}, $\beta_m = 90$	10.0 deg/sec/in
K_{5R}, $\beta_m = 0$	0.2 in/deg
K_{5R}, $\beta_m = 90$	0.2 in/deg
K_{7R}, $\beta_m = 0$	0.15 in/deg/sec
K_{7R}, $\beta_m = 90$	0.15 in/deg/sec
$RSCAS_{MX}$	± 1.617 in

SUBSYSTEM NO. 20—XV-15 STABILITY AND CONTROL AUGMENTATION SYSTEM (Continued)

Constants	Values
Ames Research Center Modified Yaw SCAS	
τ_{1Y}	2.7 sec
τ_{2Y}	2.7 sec
K_{1Y}, $\beta_m = 0$	2.94 in/in
K_{1Y}, $\beta_m = 90$	0.0 in/in
K_{2Y}, $\beta_m = 0$	0.16 in/deg/sec
K_{2Y}, $\beta_m = 90$	0.08 in/deg/sec
$YSCAS_{MX}$	± 0.4 in

SUBSYSTEM NO. 20—XV-15 STABILITY AND CONTROL AUGMENTATION SYSTEM (Continued)

Constants	Values
Bell Helicopter Textron Pitch SCAS	
τ_{1P}	0.5 sec
τ_{2P}	3.15 sec
τ_{3P}	3.15 sec
τ_{4P}	3.15 sec
τ_{5P}	3.15 sec
τ_{6P}	1.0 sec
K_{1P}, $\beta_m = 0$	7.5 deg/sec/in
K_{1P}, $\beta_m = 90$	4.5 deg/sec/in
K_{2P}, $\beta_m = 0$	0.47 in/deg/sec
K_{2P}, $\beta_m = 90$	1.105 in/deg/sec
K_{3P}, $\beta_m = 0$	0.1 in/deg/sec
K_{3P}, $\beta_m = 90$	0.06 in/deg/sec
K_{4P}, $\beta_m = 0$	10.0 deg/sec/in
K_{4P}, $\beta_m = 90$	10.0 deg/sec/in
K_{5P}, $\beta_m = 0$	0.2 in/deg/sec
K_{5P}, $\beta_m = 90$	0.1 in/deg/sec
K_{6P}, $\beta_m = 0$	0.0 in/deg/sec
K_{6P}, $\beta_m = 90$	0.6 in/deg/sec
$PSCAS_{MX}$	± 1.0 in
$P_{HOLD_{MAX}}$	0.5 in

Constants	Values
Bell Helicopter Textron Roll SCAS	
τ_{1R}	0.5 sec
τ_{2R}	3.0 sec
τ_{3R}	3.0 sec
τ_{4R}	3.0 sec
τ_{5R}	3.0 sec
K_{1R}, $\beta_m = 0$	30.0 deg/sec/in
K_{1R}, $\beta_m = 90$	30.0 deg/sec/in
K_{2R}, $\beta_m = 0$	0.8 in/deg/sec
K_{2R}, $\beta_m = 90$	0.8 in/deg/sec
K_{3R}, $\beta_m = 0$	0.3 in/deg/sec
K_{3R}, $\beta_m = 90$	0.3 in/deg/sec
K_{4R}, $\beta_m = 0$	10.0 deg/sec/in
K_{4R}, $\beta_m = 90$	10.0 deg/sec/in
K_{5R}, $\beta_m = 0$	0.15 in/deg
K_{5R}, $\beta_m = 90$	0.15 in/deg
$RSCAS_{MX}$	± 1.54 in
$R_{HOLD_{MAX}}$	0.77 in

SUBSYSTEM NO. 20—XV-15 STABILITY AND CONTROL AUGMENTATION SYSTEM (Concluded)

Constants	Values
Bell Helicopter Textron Yaw SCAS	
τ_{1Y}	2.7 sec
τ_{2Y}	2.7 sec
K_{1Y}, $\beta_m = 0$	12.0 in/in
K_{1Y}, $\beta_m = 90$	0.0 in/in
K_{2Y}, $\beta_m = 0$	0.6 in/deg/sec
K_{2Y}, $\beta_m = 90$	0.3 in/deg/sec
K_{3Y}, $\beta_m = 0$	0.0 in/in
K_{3Y}, $\beta_m = 90$	0.0 in/in
$YSCAS_{MX}$	± 0.8 in

APPENDIX C

SIGMA 8/VMS
GENERIC TILT ROTOR MATHEMATICAL MODEL
INPUT DATA REQUIREMENTS

NOTE:

This section was not revised for Rev. A, because the Sigma 8 version of the computer program was not systematically updated to be compatible with the Rev. A mathematical model when this document was completed.

TABLE OF SUBSYSTEMS

SUBSYSTEM NO. 1—ROTOR GROUP

Sigma 8 Name	Equation Name	Description	Value	Units
NUMB	n_b	Number of rotor blades	3	-ND-
RBLADE	R	Radius of rotor disc	12.5	ft
CHORDB	c_b	Blade chord	1.167	ft
XMASTL	l_m	Mast length	4.667	ft
DELTA3	δ_3	Pitch flap coupling	-0.261799	rad
XIB	I_b	Blade flapping inertia	102.5	slug-ft^2
XKFA,XKLT	K_H	Flapping hub spring rate	225.0	ft-lb/deg
SLSP	SL_{SP}	S.L. of shaft pivot point	300.0	in
BLSPR	BL_{SP}	B.L. of shaft pivot point	193.0	in
WLSP	WL_{SP}	W.L. of shaft pivot point	100.0	in
BTIPLS	B	Blade tip loss factor	0.97	-ND-
DELBPD(1)	δ_o	Const in CDF equation	0.015	-ND-
DELBPD(2)	δ_1	Const in CDF equation	-0.068	1/rad
DELBPD(3)	δ_2	Const in CDF equation	0.81	1/rad^2
SLP	SL_p	S.L. of pylon c.g.	291.7	in
WLP	WL_p	W.L. of pylon c.g.	118.0	in
WAITP	W_p	Weight of two pylons	3986.0	lbs
BETMIC	β_m	Mast tilt angle	0.0	deg
PHIM	ϕ_M	Mast dihedral angle	1.0	deg
ISTN	m	Number of blade segments	10	-ND-
XBTD(1)	X_{m-9}	Blade station/R	1.0	-ND-
XBTD(2)	X_{m-8}	Blade station/R	0.6	-ND-
XBTD(3)	X_{m-7}	Blade station/R	0.5333	-ND-
XBTD(4)	X_{m-6}	Blade station/R	0.4667	-ND-
XBTD(5)	X_{m-5}	Blade station/R	0.4	-ND-
XBTD(6)	X_{m-4}	Blade station/R	0.3333	-ND-
XBTD(7)	X_{m-3}	Blade station/R	0.2667	-ND-
XBTD(8)	X_{m-2}	Blade station/R	0.2	-ND-
XBTD(9)	X_{m-1}	Blade station/R	0.1333	-ND-

SUBSYSTEM NO. 1—ROTOR GROUP (Continued)

Sigma 8 Name	Equation Name	Description	Value	Units
XBTD(10)	X_m	Blade station/R	0.0667	-ND-
XBTD(11)	X_{m+1}	Blade station/R	0.0	-ND-
THTBT(1)	θ_{m-9}	Blade twist	0.0	deg
THTBT(2)	θ_{m-8}	Blade twist	10.2	deg
THTBT(3)	θ_{m-7}	Blade twist	12.3	deg
THTBT(4)	θ_{m-6}	Blade twist	14.5	deg
THTBT(5)	θ_{m-5}	Blade twist	17.75	deg
THTBT(6)	θ_{m-4}	Blade twist	21.9	deg
THTBT(7)	θ_{m-3}	Blade twist	26.15	deg
THTBT(8)	θ_{m-2}	Blade twist	30.65	deg
THTBT(9)	θ_{m-1}	Blade twist	34.65	deg
THTBT(10)	θ_m	Blade twist	38.0	deg
THTBT(11)	θ_{m+1}	Blade twist	40.9	deg
[illegible]0	K_0	Const-wing velocity equ	1.6	-ND-
XK1	K_1	Const-wing velocity equ	0.0	-ND-
XK2	K_2	Const-wing velocity equ	0.0	-ND-
XK3	K_3	Const-wing velocity equ	0.0	-ND-
XK4	K_4	Const-wing velocity equ	0.0	-ND-
SLWTE	SL_{WTE}	Sta line wing trail edge	338.1	in
RKRW	K_{RW}	Skew angle vel dist fact	3.0	-ND-
NHI	ℓ	No. of aero segments	8	-ND-
ALFOL	α_{0_L}	Const-blade zero lift	1.0	deg
AOBAR	$\bar{a}_o$	Precone angle	0.0436325	rad
HUBK	K_{HUB}	Coning hub spring	180000.0	ft-lb/deg
ABLO	a_o	Const-slope of lift curve	4.95	-ND-
ABL1	a_1	Const-slope of lift curve	8.0	-ND-
ABL2	a_2	Const-slope of lift curve	30.0	-ND-
CDALPH	CDALPH	Drag coef slope w/alpha	0.01	-ND-
CDLIM	CDLIM	Onset-profile drag rise	0.85	-ND-
CDMACH	CDMACH	Lower limit-mach effect	0.35	-ND-
[illegible]FACT	CDFACT	Drag coefficient factor	0.2	-ND-

SUBSYSTEM NO. 1—ROTOR GROUP (Concluded)

Sigma 8 Name	Equation Name	Description	Value	Units
CDMAX	CDMAX	Max drag coefficient	0.11	-ND-
GEWASH	GEWASH	A/S washout IGE	-0.08	sec/ft
GECON1	GECON1	Const in IGE equation	1.5629	-ND-
GECON2	GECON2	Const in IGE equation	-2.9119	-ND-
SFWASH	SFWASH	A/S washout for rotor X_{SF} effect	54.0	fps
XKR1	KMU1	Induced vel dist equ	17.807	-ND-
XKR2	KMU2	Induced vel dist equ	-0.561	-ND-
XMULL	MUL0	Induced vel dist equ	0.1067	-ND-
XMUUL	MUH1	Induced vel dist equ	0.5733	-ND-
SDQAXL	SDBM90	Spinner drag, $\beta_m = 90$	1.0	ft^2
SDQRDL	SDBM	Spinner drag equ const	5.5	ft^2

SUBSYSTEM NO. 1—ROTOR GROUP TABLES

Sigma 8 Name	Equation Name	Description
TCT	C_T^-	Maximum available rotor thrust coefficient, = $f(\mu)$, Size (9)
CTINS	CTEL	Maximum available rotor thrust coefficient, = $f(\mu, \beta_m)$, Size (9 x 3)
XSS	X_{SS}	Side-by-side rotor effect, = $f(\bar{u})$, Size (10)
XSF	X_{SF}	Sidewash effect, = $f(\lvert\bar{v}\rvert)$, Size (8)

SUBSYSTEM NO. 2—ROTOR INDUCED VELOCITIES GROUP TABLES

Sigma 8 Name	Equation Name	Description
WKH	$\frac{W_i \mid R/H}{W_{i_{L,R}}}$	Ratio of the induced z-axis rotor wake velocity on the horizontal stabilizer to the mean induced velocity at the rotor (for both right and left rotor), $= f(\alpha_F, V_T, \beta_m)$, Size (16 x 8 x 3), (non-dimensional)
XKHB	K_{H_β}	Rotor wake on the horizontal stabilizer (constant), $= f(\beta_F, \beta_m)$, Size (10 x 5), (non-dimensional)

SUBSYSTEM NO. 3—FUSELAGE GROUP

Sigma 8 Name	Equation Name	Description	Value	Units
SLF	SL_F	Sta line fuse center of press	293.0	in
[illegible]F	WL_F	Water line fuse center of press	84.0	in
TLC	LBFO	Lift (zero sideslip)	-7.23	ft^2
TDC	DBFO	Drag (zero sideslip)	-1.56	ft^2
TMC	MBFO	Pitch moment (zero sideslip)	66.5	ft^3
XFUSL	LLANG	Extra fuselage lift	0.0	ft^2
XFUSD	DLANG	Extra fuselage drag	-0.5	ft^2
XDPOD	DPOD	Drag/q land gear pod	1.15	ft^2

SUBSYSTEM NO. 3—FUSELAGE GROUP TABLES

Sigma 8 Name	Equation Name	Description
TLA	L_α	Fuselage lift/q vs angle of attack, $= f(\alpha)$, Size (61)
TDA	D_α	Fuselage drag/q vs angle of attack, $= f(\alpha)$, Size (61)
TMA	M_α	Fuselage pitching moment/q vs angle of attack, $= f(\alpha)$, Size (61)

SUBSYSTEM NO. 3—FUSELAGE GROUP TABLES (Concluded)

Sigma 8 Name	Equation Name	Description
TLB	L_β	Fuselage lift/q vs sideslip, = f(β), Size (37)
TDB	D_β	Fuselage drag/q vs sideslip, = f(β), Size (37)
TMB	M_β	Fuselage pitching moment/q vs sideslip, = f(β), Size (37)
TYB	Y_β	Fuselage side force/q vs sideslip, = f(β), Size (37)
TLLB	l_β	Fuselage rolling moment/q vs sideslip, = f(β), Size (37)
TNB	N_β	Fuselage yawing moment/q vs sideslip, = f(β), Size (37)

SUBSYSTEM NO. 4—WING/PYLON GROUP

Sigma 8 Name	Equation Name	Description	Value	Units
SLW	SL_W	Sta line wing center of press	291.17	in
WLW	WL_W	Water line wing center of press	95.85	in
AREA	S_W	Wing area	181.0	ft^2
SPAN	b_W	Wing span	32.17	ft
CHORD	c_W	Wing chord	5.225	ft
CSWEP	$(\Lambda_{c/4})_W$	Wing sweep angle at C/4	-6.5	deg
ARW	AR_W	Wing aspect ratio	5.7	-ND-
CYBM	$C_{Y_\beta}\Big\vert_{M_N=0}$	Const used in Y force equ	0.0	1/rad
CYPM	$\dfrac{C_{Y_p}}{C_{L_{WP}}}\Bigg\vert_{M_N=0}$	Const used in Y force equ	0.0	1/rad
CYRM	$C_{Y_r}\Big\vert_{M_N=0}$	Const used in Y force equ	0.0	1/rad
CLPM	$C_{l_p}\Big\vert_{\substack{C_L=0\\M_N=0}}$	Const in roll moment equ	-0.774	1/rad

SYSTEM NO. 4—WING/PYLON GROUP (Continued)

Sigma 8 Name	Equation Name	Description	Value	Units
CLRM	$\left.\frac{C_{l_r}}{C_{L_{WP}}}\right\|_{M_N=0}$	Const in roll moment equ	0.27	1/rad
CLRAF	$\frac{\Delta C_{l_r}}{(\partial\alpha/\partial\delta_F)}(\delta_F)$	Const in roll moment equ	-0.0016	1/deg
CLDA	$C_{l_{\delta_a}}\Big\|_{\alpha_W^{F_1} < 8\text{ deg}}$	Const in roll moment equ	0.006	1/deg
CNBO	$C_{n_\beta}\Big\|_{M_N=0}^{C_L=0}$	Const in yaw moment equ	-0.0315	1/rad
[illegible]M	$\left.\left(\frac{C_{n_\beta}}{C_{L_{WP}}^2}\right)\right\|_{M_N=0}$	Const in yaw moment equ	0.057	1/rad
CNRL	$\left(\frac{C_{n_r}}{C_{L_{WP}}^2}\right)$	Const in yaw moment equ	-0.016	1/rad
CNRD	$\left(\frac{C_{n_r}}{C_{D_{o_{WP}}}}\right)$	Const in yaw moment equ	-0.32	1/rad
CNPL	$\left.\frac{C_{n_p}}{C_{L_{WP}}}\right\|_{M_N=0}$	Const in yaw moment equ	-0.06	1/rad
FKNP	K_{np}	Const in yaw moment equ	1.0	-ND-
XKFWB	KFWO	Const download with flaps	1.4	-ND-
XKFWS	KFWDF	Slope download with flaps	-0.0035	1/deg
CXRW	KXRW	Const rotor flow on wings	0.26	-ND-
XRWO	XRWO	Const rotor flow on wings	0.0806	-ND-

SUBSYSTEM NO. 4—WING/PYLON GROUP (Concluded)

Sigma 8 Name	Equation Name	Description	Value	Units
XRW1	XRW1	Const rotor flow on wings	0.33410E-04	1/deg
XRW2	XRW2	Const rotor flow on wings	0.73860E-05	$1/deg^2$
DQP90	CPYLN1	Const in pylon drag equation	1.0	ft^2
DQP0	CPYLN2	Const in pylon drag equation	13.5	ft^2

SUBSYSTEM NO. 4—WING/PYLON GROUP TABLES

Sigma 8 Name	Equation Name	Description
CMOWP	$C_{M_{o_{WP}}}$	Wing-pylon pitching moment coefficient, = $f(\beta_m, F_X)$ Size (5 x 4), (non-dimensional)
CLWP1	$C_{L_{WP}}$	Wing-pylon lift coefficient for F_X = 0 deg, = $f(\alpha'_{F/W}/\alpha_W, \beta_m, M_N)$, Size (28 x 2 x 4), (non-dimensional)
CLWP2	$C_{L_{WP}}$	Wing-pylon lift coefficient for F_X = 20 deg, = $f(\alpha'_{F/W}/\alpha_W, \beta_m)$, Size (55 x 2), (non-dimensional)
CLWP3	$C_{L_{WP}}$	Wing-pylon lift coefficient for F_X = 40 deg, = $f(\alpha'_{F/W}/\alpha_W, \beta_m)$, Size (32 x 2), (non-dimensional)
CLWP4	$C_{L_{WP}}$	Wing-pylon lift coefficient for F_X = 75 deg, = $f(\alpha'_{F/W}/\alpha_W, \beta_m)$, Size (32 x 2), (non-dimensional)
CDWP1	$C_{D_{WP}}$	Wing-pylon drag coefficient for F_X = 0 deg, = $f(\alpha'_{F/W}/\alpha_W, \beta_m, M_N)$, Size (21 x 2 x 4), (non-dimensional)
CDWP2	$C_{D_{WP}}$	Wing-pylon drag coefficient for F_X = 20 deg, = $f(\alpha'_{F/W}/\alpha_W, \beta_m)$, Size (49 x 2), (non-dimensional)
CDWP3	$C_{D_{WP}}$	Wing-pylon drag coefficient for F_X = 40 deg = $f(\alpha'_{F/W}/\alpha_W, \beta_m)$, Size (26 x 2), (non-dimensional)
CDWP4	$C_{D_{WP}}$	Wing-pylon drag coefficient for F_X = 75 deg, = $f(\alpha'_{F/W}/\alpha_W, \beta_m)$, Size (26 x 2), (non-dimensional)
EWH	$\epsilon_{W/H}$	Wing wake deflection at the horizontal stabilizer, = $f(\alpha_W, F_X, \beta_m)$, Size (12 x 4 x 5), (non-dimensional)
CLB	$C_{l_\beta}\Big\vert_{\substack{C_L=0 \\ M_N=0}}$	Wing-pylon rolling moment coefficient, = $f(\beta_m, F_X)$ Size (4 x 4), (1/rad)

SUBSYSTEM NO. 4—WING/PYLON GROUP TABLES (Concluded)

Sigma 8 Name	Equation Name	Description
CLBL	$\left.\frac{C_{l_\beta}}{C_{L_{WP}}}\right\|_{M_N=0}$	Aerodynamic coefficient in the wing rolling moment equation, = $f(\beta_m, F_X)$, Size (4 x 4), (1/rad)
FKLDA	$K_{l_{\delta_a}}$	Aileron effectiveness in roll, = $f(\alpha_w, \beta_m, F_X)$, Size (2 x 2 x 4)
FKNOA	$K_{no_{\delta_a}}$	Yawing moment equation coefficient, = $f(\beta_m, F_X)$, Size (3 x 4), (1/deg)
FKNDA	$K_{n_{\delta_a}}$	Yawing moment equation coefficient, = $f(\beta_m, F_X)$, Size (3 x 4), (non-dimensional)
CDO	$C_{D_{o_{WP}}}\Big\|_{C_{L_{WP}}=0}$	Wing coefficient of drag at wing coefficient of lift equal to zero, = $f(M_N, \beta_m, F_X)$, Size (4 x 2 x 4)
CLDAI	$C_{l_{\delta_A}}$	Wing lift coefficient due to aileron deflection, = $f(F_X)$, Size (4)
LA1	$\left.\frac{\partial C_{L_{WP}}}{\partial \alpha_W}\right\|_{C_{L_{WP}}=0}$	Partial of wing coefficient of lift with respect to angle of attack, = $f(M_N, \beta_m)$, Size (4 x 2)

SUBSYSTEM NO. 5—HORIZONTAL STABILIZER GROUP

Sigma 8 Name	Equation Name	Description	Value	Units
SLH	SL_H	Sta line center of pressure	560.0	in
WLH	WL_H	Water line center of pressure	103.0	in
SH	S_H	Area	50.25	ft^2
CLHB	$C_{L_{H\beta}}$	Const in lift equation	-0.00422	1/deg
XIH	i_H	Horizontal stab incidence	0.0	deg
HTEL,HTED	τ_e	Elevator effectiveness	0.518	-ND-
XKHNU	KHNU	Q-loss multiplier	1.0	-ND-

SUBSYSTEM NO. 5—HORIZONTAL STABILIZER GROUP TABLES

Sigma 8 Name	Equation Name	Description
CLH	C_{L_H}	Horizontal stabilizer lift coefficient, = $f(\alpha_H, \delta_e)$, Size (56 x 7), (non-dimensional)
CLHM	C_{L_H}	Horizontal stabilizer lift coefficient, = $f(\alpha_H, M_N)$, Size (17 x 4), (non-dimensional)
CDH	C_{D_H}	Horizontal stabilizer drag coefficient, = $f(\alpha_M, M_N)$, Size (49 x 4), (non-dimensional)
HKE	K_e	Elev/rudder effectiveness, = $f(M_N)$, Size (4), (non-dimensional)
ETAH	η_H	Dynamic pressure ratio at the horizontal tail, = $f(\alpha_F, V_T, \beta_m)$, Size (18 x 6 x 5), (non-dimensional)

SUBSYSTEM NO. 6—VERTICAL STABILIZER GROUP

Sigma 8 Name	Equation Name	Description	Value	Units
SLV	SL_V	Sta line center of pressure	570.02	in
WLV	WL_V	Water line center of pressure	115.69	in
BLV	BL_V	Buttline center of pressure	77.0	in
SF	S_V	Area	50.5	ft^2
DSIGP	$\partial\sigma/\partial\hat{p}$	Const in sideslip angle equ	-0.1	-ND-
DSIGR	$\partial\sigma/\partial\hat{r}$	Const in sideslip angle equ	0.0	-ND-
HTRL,HTRD	τ_r	Rudder effectiveness	0.27	-ND-
BETWK1	BETWK1	Sideslip wake off fin	5.0	deg
BETWK2	BETWK2	Sideslip opp wake on fin	28.0	deg
BETWK3	BETWK3	Sideslip opp wake off fin	60.0	deg
XKVNU	KVNU	Q-loss multiplier	1.0	-ND-

SUBSYSTEM NO. 6—VERTICAL STABILIZER GROUP TABLES

Sigma 8 Name	Equation Name	Description
CYV1	C_{Y_V}	Vertical fin side force (lift) coefficient, $= f(\beta_V, \delta_r)$, Size (50 x 5), (non-dimensional)
CYV2	C_{Y_V}	Vertical fin side force (lift coefficient, $= f(\beta_V, M_N)$, Size (19 x 4), (non-dimensional)
CDV	C_{D_V}	Vertical fin drag coefficient, $= f(\beta_V, M_N)$, Size (47 x 4), (non-dimensional)
DSIG1	$\left(1 - \frac{\partial\sigma}{\partial\beta_F}\right)$	Vertical stabilizer sidewash factor for $F_X = 0$ deg, $= f(\beta_F, \alpha_F, \beta_m)$, Size (6 x 6 x 4), (non-dimensional)
DSIG2	$\left(1 - \frac{\partial\sigma}{\partial\beta_F}\right)$	Vertical stabilizer sidewash factor for $F_X = 20$ deg, $= f(\beta_F, \alpha_F, \beta_m)$, Size (6 x 6 x 4), (non-dimensional)
DSIG3	$\left(1 - \frac{\partial\sigma}{\partial\beta_F}\right)$	Vertical stabilizer sidewash factor for $F_X = 40$ deg, $= f(\beta_F, \alpha_F, \beta_m)$, Size (6 x 6 x 4), (non-dimensional)
DSIG4	$\left(1 - \frac{\partial\sigma}{\partial\beta_F}\right)$	Vertical stabilizer sidewash factor for $F_X = 75$ deg, $= f(\beta_F, \alpha_F, \beta_m)$, Size (6 x 6 x 4), (non-dimensional)
XKB	K_β	Rotor sidewash factor on dynamic pressure, $= f(V_T, \beta_v)$ Size (8 x 7), (non-dimensional)

SUBSYSTEM NO. 7A—LANDING GEAR GROUP

Sigma 8 Name	Equation Name	Description	Value	Units
SLNG	SL_{G1}	Station line nose gear	139.0	in
WLNG	WL_{G1}	Water line nose gear	4.95	in
BLNG	BL_{G1}	Butt line nose gear	0.0	in
SLMG	$SL_{G2,3}$	Station line main gear	324.0	in
WLMG	$WL_{G2,3}$	Water line main gear	7.4	in
BLMG	$BL_{G2,3}$	Butt line main gear	51.25	in
DBMIN	$\delta_{B_{n_{MIN}}}$	Brake threshold deflection	5.73	deg
BRK	K_{B_n}	Brake sensitivity	-0.1745	ft/sec^2-deg

SUBSYSTEM NO. 7A—LANDING GEAR GROUP (Concluded)

Sigma 8 Name	Equation Name	Description	Value	Units
AMAX	A_{MAX}	Maximum braking deceleration	-5.0	ft/sec^2
GA1	G_{A_1}	Nose gear linear damping term	100.0	lb-sec/ft
GA2,GA3	$G_{A_{2,3}}$	Main gear linear damping term	775.0	lb-sec/ft
GB1,GB2,GB3	G_{B_n}	Landing gear nonlinear damping term	0.0	$lb\text{-}sec/ft^3$
GC1	G_{C_1}	Nose gear nonlinear stiffness term	175.0	lb/ft^4
GC2,GC3	$G_{C_{2,3}}$	Main gear nonlinear stiffness term	325.0	lb/ft^4
US1,US2,US3	μ_{S_n}	Landing gear side force slope	0.03	-ND-
UG	μ_{G_n}	Landing gear maximum side force coefficient	0.5	-ND-
UR	μ_{RF}	Coefficient of rolling friction	0.015	-ND-

SUBSYSTEM NO. 7A—LANDING GEAR GROUP TABLES

Sigma 8 Name	Equation Name	Description
DOMGD	$D_{o_{MGD}}$	Drag of main landing gear during extension, = f(t), Size (21), (ft^2)
DOMGU	$D_{o_{MGU}}$	Drag of main landing gear during retraction, = f(t), Size (21), (ft^2)
DONGD	$D_{o_{NGD}}$	Drag of nose landing gear during extension, = f(t) Size (21), (ft^2)
DONGU	$D_{o_{NGU}}$	Drag of nose landing gear during retraction, = f(t) Size (21), (ft^2)

SYSTEM NO. 8—CONTROL SYSTEM GROUP

Sigma 8 Name	Equation Name	Description	Value	Units
XLNN	X_{LNN}	Long cyclic neutral	4.8	in
XLTN	X_{LTN}	Lat cyc neutral position	4.8	in
XPDN	X_{PDN}	Pedals neutral position	2.5	in
DEXLN	$\partial\delta_e/\partial X_{LN}$	D(elevator)/D(XLN)	4.16	deg/in
DAXLT	$\partial\delta_a/\partial X_{LT}$	D(aileron)/D(XLT)	3.93	deg/in
DRXPD	$\partial\delta_r/\partial X_{PD}$	D(rudder)/D(XPD)	8.0	deg/in
DB1	DB1	B1 rigging offset constant	1.5	deg
LTRNJ	X_{LT}	Lateral control range	9.6	in
LNRNJ	X_{LN}	Longitudinal control range	9.6	in
PDRNJ	X_{PD}	Pedal control range	5.0	in
COLRNJ	X_{COL}	Power lever control range	10.0	in
BETMAX	PBMMAX	Max fwd mast tilt	90.0	deg
BETMIN	PBMMIN	Max aft mast tilt	-5.0	deg
RTLOW	$\dot{\beta}_m$	Pylon conversion rate--low	1.5	deg/sec
RTHIGH	$\dot{\beta}_m$	Pylon conversion rate--high	7.5	deg/sec
GLNO	G_{LNO}	Longitudinal force feel system gradient	3.5	lb/in
GLN1	G_{LN1}	Longitudinal force feel system gradient	0.108	lb/in/psf
AKLN	K_{LN}	Longitudinal force feel system constant (system off)	11.25	lb/in
ZENFFS	ζ_{LN}	Longitudinal force feel system viscous damping coefficient	0.85	-ND-
HLN	H_{LN}	Longitudinal force feel system hysteresis force	2.85	lb
GLTO	G_{LTO}	Lateral force feel system gradient	1.0	lb/in
GLT1	G_{LT1}	Lateral force feel system gradient	0.023	lb/in/psf
AKLT	K_{LT}	Lateral force feel system constant (system off)	3.5	lb/in
ZETFFS	ζ_{LT}	Lateral force feel system viscous damping coefficient	0.85	-ND-

SUBSYSTEM NO. 8—CONTROL SYSTEM GROUP (Concluded)

Sigma 8 Name	Equation Name	Description	Value	Units
HLT	H_{LT}	Lateral force feel system hysteresis force	3.75	lb
GPDO	G_{PDO}	Pedal force feel system gradient	5.0	lb/in
GPD1	G_{PD1}	Pedal force feel system hysteresis	0.167	lb/in/psf
ZEDFFS	ζ_{PD}	Pedal force feel system viscous damping coefficient	0.85	-ND-
HPD	H_{PD}	Pedal force feel system hysteresis force	8.8	lb
HRUD	H_{RUD}	Rudder force feel constant	0.37	ft^2/in
FARUDL	$F_{ACT_{RUD_{LIM}}}$	Rudder force feel actuator limit	45.0	lb
XDLNTO	$\dot{X}_{LNTO}$	Longitudinal trim rate force feel system constant	1.0	in/sec
XDLNT1	$\dot{X}_{LNT1}$	Longitudinal trim rate force feel system constant	-0.00262	in/sec/psf
XDLTTO	$\dot{X}_{LTTO}$	Lateral trim rate force feel system constant	1.0	in/sec
XDLTT1	$\dot{X}_{LTT1}$	Lateral trim rate force feel system constant	-0.00262	in/sec/psf
XDLPDO	$\dot{X}_{PDTO}$	Pedal trim rate force feel system constant	0.5	in/sec
XDLPD1	$\dot{X}_{PDT1}$	Pedal trim rate force feel system constant	-0.00131	in/sec/psf

SUBSYSTEM NO. 8—CONTROL SYSTEM GROUP TABLES

Sigma 8 Name	Equation Name	Description
C1	$\partial B_1/\partial X_{LN}$	Cyclic/longitudinal stick gradient vs β_m, Size (10)
C2	$\partial B_1/\partial X_{PD}$	Differential cyclic pitch control gearing ratio, $= f(\beta_m, V_T)$, Size (10 x 3), (deg/in)
C3	$\partial \theta_o/\partial X_{LT}$	Diff coll/lat stick gradient vs β_m, Size (10)

SUBSYSTEM NO. 8—CONTROL SYSTEM GROUP TABLES (Concluded)

Sigma 8 Name	Equation Name	Description
C4	$\partial\theta_o/\partial X_{COL}$	Blade pitch/power lever gradient vs β_m, Size (10)
C5	$\theta_{o_{LL}}$	Min blade pitch at 0.75R vs β_m, Size (10)
THP	$X_{THR,L}$	Throttle vs power lever, Size (21)
AIB	$A_{1_{\beta_m}}$	Lateral flap controller vs β_m, Size (7)
AIV	$A_{1_{V_T}}$	Lateral flap controller vs A/S, Size (7)

SUBSYSTEM NO. 11—AIRCRAFT ACCELERATIONS AND VELOCITIES GROUP

Sigma 8 Name	Equation Name	Description	Value	Units
SLPA	SL_{PA}	Station line of the pilot	215.25	in
[illegible]PA	BL_{PA}	Butt line of the pilot	16.5	in
[illegible]PA	WL_{PA}	Water line of the pilot	82.0	in

SUBSYSTEM NO. 14—IGE MOMENT GROUP

Sigma 8 Name	Equation Name	Description	Value	Units
XLG0	L_{G0}	Const-IGE roll moment equ	-7506.0	ft-lb/deg
XLG1	L_{G1}	Const-IGE roll moment equ	23366.0	ft-lb/deg
XLG2	L_{G2}	Const-IGE roll moment equ	-20134.0	ft-lb/deg
XLG3	L_{G3}	Const-IGE roll moment equ	5290.0	ft-lb/deg
XLG4	L_{G4}	Const-IGE roll moment equ	-0.1	sec/ft
XH2	GEULIM	IGE up limit--roll moment equ	1.6386	-ND-
XH1	GELLIM	IGE low limit--roll moment equ	0.5	-ND-
GEM1	M_{G1}	Const-IGE pitch moment equ	-0.9	ft
GEM2	M_{G2}	Const-IGE pitch moment equ	-2.6	-ND-
[illegible]M3	M_{G3}	Const-IGE pitch moment equ	-0.08	sec/ft

SUBSYSTEM NOS. 17, 18, AND 19—POWER MANAGEMENT GROUP

Sigma 8 Name	Equation Name	Description	Value	Units
THINT1	θ_{INT_1}	Rotor-interconn gear ratio	11.3	-ND-
TD	t_D	Rotor governor delay time	0.0	sec
PCTMXS	pctmxs	Max % HP/sec power turb gov	6.0	%/sec
PCTMXP	pctmxp	Max % HP/sec throttle	6.0	%/sec
XI1	I_1	Drive system inertia	824.0	slug-ft^2
THRPT1	θ_{RPT_1}	Rotor-turbine gear ratio	35.133	-ND-
EK1	K_1	Const in drive syst equs	-0.94	-ND-
EK2	K_2	Const in drive syst equs	1.94	-ND-
EK3	K_3	Const in drive syst equs	0.0	-ND-
EK4	K_4	Const in drive syst equs	13100.0	RPM
EK5	K_5	Const in drive syst equs	235.0	RPM/$\sqrt{SHP}$
EK6	K_6	Const in drive syst equs	475.0	HP
EK7	K_7	Const in drive syst equs	288.16	deg K
EK11	K_{11}	Const in drive syst equs	0.0032	1/deg K
EK12	K_{12}	Const in drive syst equs	0.875	1/deg K
EL13	K_{13}	Const in drive syst equs	0.00125	1/deg K
EK14	K_{14}	Const in drive syst equs	0.0	deg K
THTMX	THOGMN	Minimum pitch-governor	-5.0	deg
THTMU	THOGMX	Maximum pitch-governor	33.5	deg
PRGK	K_{PRG}	Coll. governor proportional gain at β_m=90	0.1	-ND-
TK1G1	K_{1G}	Coll. governor integral gain at β_m=90	0.05	-ND-

SUBSYSTEM NO. 18—POWER PLANT GROUP TABLES

Sigma 8 Name	Equation Name	Description
RSPN	RSHP	Shaft horsepower vs throttle, = f(X_{THR}), Size (14)
TJET1	K_{JT_1}	Constant jet thrust equ, = f(V_T), Size (4), (1b)

SUBSYSTEM NO. 18—POWER PLANT GROUP TABLES (Concluded)

Sigma 8 Name	Equation Name	Description
TJET2	K_{JT_2}	Slope-jet thrust equ, = $f(V_T)$, Size (4), (lb/SHP)
DHPR	$\frac{dHP_{ROT}}{dt_{TH}}$	Engine acceleration characteristics, = f(SHP), Size (19)
RSHP	$\frac{RSHP}{RSHP_{V=0}}$	Ram effect, = $f(V_T)$, Size (7)

SUBSYSTEM NO. 20—SCAS GROUP

Sigma 8 Name	Equation Name	Description	Value	Units
Bell Roll SCAS				
ST1RF	τ_{1R}	Roll time constant	0.5	sec
ST2RF	τ_{2R}	Roll time constant	3.0	sec
ST3RF	τ_{3R}	Roll time constant	3.0	sec
ST4RF	τ_{4R}	Roll time constant	3.0	sec
ST5RF	τ_{5R}	Roll time constant	3.0	sec
SK1R0F	$K_{1R,\beta_m} = 0$	Roll gain	30.0	deg/sec/in
SK1R90F	$K_{1R,\beta_m} = 90$	Roll gain	30.0	deg/sec/in
SK2R0F	$K_{2R,\beta_m} = 0$	Roll gain	0.8	in/deg/sec
SK2R90F	$K_{2R,\beta_m} = 90$	Roll gain	0.8	in/deg/sec
SK3R0F	$K_{3R,\beta_m} = 0$	Roll gain	0.3	in/deg/sec
SK3R90F	$K_{3R,\beta_m} = 90$	Roll gain	0.3	in/deg/sec
SK4R0F	$K_{4R,\beta_m} = 0$	Roll gain	10.0	deg/sec/in
SK4R90F	$K_{4R,\beta_m} = 90$	Roll gain	10.0	deg/sec/in
SK5R0F	$K_{5R,\beta_m} = 0$	Roll gain	0.15	in/deg
SK5R90F	$K_{5R,\beta_m} = 90$	Roll gain	0.15	in/deg

SUBSYSTEM NO. 20—SCAS GROUP (Continued)

Sigma 8 Name	Equation Name	Description	Value	Units
Bell Pitch SCAS				
ST1PF	τ_{1P}	Pitch time constant	0.5	sec
ST2PF	τ_{2P}	Pitch time constant	3.15	sec
ST3PF	τ_{3P}	Pitch time constant	3.15	sec
ST4PF	τ_{4P}	Pitch time constant	3.15	sec
ST5PF	τ_{5P}	Pitch time constant	3.15	sec
ST6PF	τ_{6P}	Pitch time constant	1.0	sec
SK1POF	$K_{1P,\beta_m} = 0$	Pitch gain at $\beta_m = 0$	7.5	deg/sec/in
SK1P90F	$K_{1P,\beta_m} = 90$	Pitch gain at $\beta_m = 90$	4.5	deg/sec/in
SK2POF	$K_{2P,\beta_m} = 0$	Pitch gain at $\beta_m = 0$	0.47	in/deg/sec
SK2P90F	$K_{2P,\beta_m} = 90$	Pitch gain at $\beta_m = 90$	1.105	in/deg/sec
SK3POF	$K_{3P,\beta_m} = 0$	Pitch gain at $\beta_m = 0$	0.1	in/deg/sec
SK3P90F	$K_{3P,\beta_m} = 90$	Pitch gain at $\beta_m = 90$	0.06	in/deg/sec
SK4POF	$K_{4P,\beta_m} = 0$	Pitch gain at $\beta_m = 0$	10.0	deg/sec/in
SK4P90F	$K_{4P,\beta_m} = 90$	Pitch gain at $\beta_m = 90$	10.0	deg/sec/in
SK5POF	$K_{5P,\beta_m} = 0$	Pitch gain at $\beta_m = 0$	0.2	in/deg/sec
SK5P90F	$K_{5P,\beta_m} = 90$	Pitch gain at $\beta_m = 90$	0.1	in/deg/sec
SK6POF	$K_{6P,\beta_m} = 0$	Pitch gain at $\beta_m = 0$	0.0	in/deg/sec
SK6P90F	$K_{6P,\beta_m} = 90$	Pitch gain at $\beta_m = 90$	0.6	in/deg/sec
Bell Yaw SCAS				
ST1YF	τ_{1Y}	Yaw time constant	2.7	sec
ST2YF	τ_{2Y}	Yaw time constant	2.7	sec
SK1YOF	$K_{1Y,\beta_m} = 0$	Yaw gain at $\beta_m = 0$	12.0	in/in
SK1Y90F	$K_{1Y,\beta_m} = 90$	Yaw gain at $\beta_m = 90$	0.0	in/in
SK2YOF	$K_{2Y,\beta_m} = 0$	Yaw gain at $\beta_m = 0$	0.6	in/deg/sec
SK2Y90F	$K_{2Y,\beta_m} = 90$	Yaw gain at $\beta_m = 90$	0.3	in/deg/sec
SK3YOF	$K_{3Y,\beta_m} = 0$	Yaw gain at $\beta_m = 0$	0.0	in/in
SK3Y90F	$K_{3Y,\beta_m} = 90$	Yaw gain at $\beta_m = 90$	0.0	in/in

SUBSYSTEM NO. 20—SCAS GROUP (Continued)

Sigma 8 Name	Equation Name	Description	Value	Units
Modified Roll SCAS				
ST1RN	τ_{1R}	Roll time constant	0.4	sec
ST2RN	τ_{2R}	Roll time constant	3.0	sec
STPRN	τ_P	Roll time constant	0.4	sec
SK1RON	$K_{1R,\beta_m} = 0$	Roll gain at $\beta_m = 0$	1.0	in/in
SK1R90N	$K_{1R,\beta_m} = 90$	Roll gain at $\beta_m = 90$	0.5	in/in
SK2RON	$K_{2R,\beta_m} = 0$	Roll gain at $\beta_m = 0$	1.03	in/deg/sec
SK2R90N	$K_{2R,\beta_m} = 90$	Roll gain at $\beta_m = 90$	1.03	in/deg/sec
SK3RON	$K_{3R,\beta_m} = 0$	Roll gain at $\beta_m = 0$	0.064	in/deg/sec
SK3R90N	$K_{3R,\beta_m} = 90$	Roll gain at $\beta_m = 90$	0.064	in/deg/sec
SK4RON	$K_{4R,\beta_m} = 0$	Roll gain at $\beta_m = 0$	10.0	deg/sec/in
SK4R90N	$K_{4R,\beta_m} = 90$	Roll gain at $\beta_m = 90$	10.0	deg/sec/in
SK5RON	$K_{5R,\beta_m} = 0$	Roll gain at $\beta_m = 0$	TBD	in/deg
SK5R90N	$K_{5R,\beta_m} = 90$	Roll gain at $\beta_m = 90$	TBD	in/deg
SK6RON	$K_{6R,\beta_m} = 0$	Roll gain at $\beta_m = 0$	TBD	deg/in
SK6R90N	$K_{6R,\beta_m} = 90$	Roll gain at $\beta_m = 90$	TBD	deg/in
SK7RON	$K_{7R,\beta_m} = 0$	Roll gain at $\beta_m = 0$	0.135	in/deg/sec
SK7R90N	$K_{7R,\beta_m} = 90$	Roll gain at $\beta_m = 90$	0.135	in/deg/sec
Modified Pitch SCAS				
ST1PN	τ_{1P}	Pitch time constant	0.3	sec
ST2PN	τ_{2P}	Pitch time constant	3.15	sec
STQPN	τ_q	Pitch time constant	0.4	sec
SK1PON	$K_{1P,\beta_m} = 0$	Pitch gain at $\beta_m = 0$	0.6	in/in
SK1P90N	$K_{1P,\beta_m} = 90$	Pitch gain at $\beta_m = 90$	-1.0	in/in
SK2PON	$K_{2P,\beta_m} = 0$	Pitch gain at $\beta_m = 0$	1.04	in/deg/sec
SK2P90N	$K_{2P,\beta_m} = 90$	Pitch gain at $\beta_m = 90$	0.48	in/deg/sec
SK3PON	$K_{3P,\beta_m} = 0$	Pitch gain at $\beta_m = 0$	0.107	in/deg/sec
SK3P90N	$K_{3P,\beta_m} = 90$	Pitch gain at $\beta_m = 90$	0.107	in/deg/sec

SUBSYSTEM NO. 20—SCAS GROUP (Concluded)

Sigma 8 Name	Equation Name	Description	Value	Units
Modified Pitch SCAS (Concluded)				
SK4PON	$K_{4P,\beta_m} = 0$	Pitch gain at $\beta_m = 0$	-7.5	deg/sec/in
SK4P90N	$K_{4P,\beta_m} = 90$	Pitch gain at $\beta_m = 90$	-7.5	in/deg/sec
SK5PON	$K_{5P,\beta_m} = 0$	Pitch gain at $\beta_m = 0$	TBD	in/deg
SK5P90N	$K_{5P,\beta_m} = 90$	Pitch gain at $\beta_m = 90$	TBD	in/deg
SK6PON	$K_{6P,\beta_m} = 0$	Pitch gain at $\beta_m = 0$	TBD	deg/in
SK6P90N	$K_{6P,\beta_m} = 90$	Pitch gain at $\beta_m = 90$	TBD	deg/in
SK7PON	$K_{7P,\beta_m} = 0$	Pitch gain at $\beta_m = 0$	0.133	in/deg/sec
SK7P90N	$K_{7P,\beta_m} = 90$	Pitch gain at $\beta_m = 90$	0.1	in/deg/sec
Modified Yaw SCAS				
ST1YN	τ_{1Y}	Yaw time constant	2.7	sec
ST2YN	τ_{2Y}	Yaw time constant	2.7	sec
SK1YON	$K_{1Y,\beta_m} = 0$	Yaw gain at $\beta_m = 0$	2.94	in/in
SK1Y90N	$K_{1Y,\beta_m} = 90$	Yaw gain at $\beta_m = 90$	0.0	in/in
SK2YON	$K_{2Y,\beta_m} = 0$	Yaw gain at $\beta_m = 0$	0.125	in/deg/sec
SK2Y90N	$K_{2Y,\beta_m} = 90$	Yaw gain at $\beta_m = 90$	0.026	in/deg/sec

FLIGHT CONFIGURATION GROUP

***** Most of the following variables are user input variables *****

Sigma 8 Name	Equation Name	Description	Value	Units
WAITIC	GW	A/C gross weight	13000.0	lb
SLCGBO	$SL_{CG}\|_{\beta_m=0}$	A/C c.g. S.L. at $\beta_m = 0$	300.0	in
BLCG	BL_{CG}	A/C c.g. B.L. at $\beta_m = 0$	0.0	in
WLCGBO	$WL_{CG}\|_{\beta_m=0}$	A/C c.g. W.L. at $\beta_m = 0$	81.65	in

FLIGHT CONFIGURATION GROUP (Concluded)

Sigma 8 Name	Equation Name	Description	Value	Units
XIXXBO	$I_{XX}\|_{\beta_m=0}$	A/C roll inertia at $\beta_m = 0$	48668.0	slug-ft^2
XIYYBO	$I_{YY}\|_{\beta_m=0}$	A/C pitch inertia at $\beta_m = 0$	17907.0	slug-ft^2
XIZZBO	$I_{ZZ}\|_{\beta_m=0}$	A/C yaw inertia at $\beta_m = 0$	60254.0	slug-ft^2
XIXZBO	$I_{XZ}\|_{\beta_m=0}$	A/C cross inertia at $\beta_m = 0$	1234.0	slug-ft^2
XKI1	K_{I1}	Constant in IXX equation	20.5	1/deg
XKI2	K_{I2}	Constant in IYY equation	11.24	1/deg
XKI3	K_{I3}	Constant in IZZ equation	9.26	1/deg
XKI4	K_{I4}	Constant in IXZ equation	1.76	1/deg
DCXTRM	X_{LN}	Longitudinal stick position	4.8	in
DWXTRM	X_{LT}	Lateral stick position	4.8	in
DPXTRM	X_{PD}	Pedal position input	2.5	in
COLSTK	X_{COL}	Collective stick position	6.96	in
[illegible]MIC	β_m	Initial mast angle	0.0	deg
RPMPIC	$\Omega_{R,L}$	Center rotor RPM	589.0	RPM
VEQIC	U	Velocity along X-gnd axis	200.0	kts
VEQIC	V	Velocity along Y-gnd axis	0.0	kts
VEQIC	W	Velocity along Z-gnd axis	0.0	kts
PHIIC	ϕ	Euler roll angle	0.0	deg
THETIC	θ	Euler pitch angle	-3.0	deg
PSIIC	ψ	Euler yaw angle	0.0	deg
PBIC	p	A/C roll rate (X-body)	0.0	deg/sec
QBIC	q	A/C pitch rate (Y-body)	0.0	deg/sec
RBIC	r	A/C yaw rate (Z-body)	0.0	deg/sec
HIC	h	A/C position ground axis Z	5000.0	ft
VNW	U_W	Velocity of air mass	0.0	ft/sec
VEW	V_W	Velocity of air mass	0.0	ft/sec
VDW	W_W	Velocity of air mass	0.0	ft/sec
GAMVIC	--	Rate of descent (+ down)	0.0	ft/min
XIFLAP	X_{FL}	Flaps switch setting	1	-ND-
[illegible]ELC	X_{LG}	Landing gear selector SW.	0	-ND-
MARR	--	1=SCAS ON, 0=SCAS OFF	1	-ND-
NSYS	--	Governor engaged	1	-ND-

APPENDIX D

COMPREHENSIVE LIST OF SYMBOLS

GENERIC TILT-ROTOR SIMULATION MATHEMATICAL MODEL

LIST OF SYMBOLS

A_{MAX}	Maximum braking deceleration (ft/sec^2)
AR_W	Wing aspect ratio (non-dimensional)
AS_{CAL}	Airspeed calibration slope correction (non-dimensional)
AS_o	Airspeed calibration intercept correction (kts)
ASAS	Roll (aileron) SCAS input (in)
$A_{1_{B_m}}$	Lateral flapping controller coefficient, = $f(\beta_m)$ (non-dimensional)
A_{1L}	Left rotor lateral cyclic input (rad)
A_{1R}	Right rotor lateral cyclic input (rad)
$A_{1_{V_T}}$	Lateral flapping controller coefficient, = f(U) (deg)
a_0	Blade lift coefficient (1/rad)
$\bar{a}_o$	Precone angle (deg)
a_V	Lift curve slope of the vertical tail (1/rad)
a_{XPA}	x-axis (longitudinal) acceleration at the pilot's station (ft/sec^2)
a_{YPA}	y-axis (lateral) acceleration at the pilot's station (ft/sec^2)

a_{ZPA}	z-axis (vertical) acceleration at the pilot's station (ft/sec^2)
a_1	Blade lift coefficient ($1/\mu$)
a_{1L}	Left rotor longitudinal flapping (+ backward for helicopter) (rad)
a_{1R}	Right rotor longitudinal flapping (+ backward for helicopter) (rad)
$\dot{a}_{1L}$	Left rotor longitudinal flapping rate (rad/sec)
$\dot{a}_{1R}$	Right rotor longitudinal flapping rate (rad/sec)
a_2	Blade lift coefficient ($1/\mu^2$)
B	Blade tip loss factor (non-dimensional)
$B_{FT_{XLN}}$	Longitudinal control force trim switch constant (non-dimensional)
$B_{FT_{XLT}}$	Lateral control force trim switch constant (non-dimensional)
$B_{FT_{XPD}}$	Pedal control force trim switch constant (non-dimensional)
$B_V(i)$	Zero rudder sideslip angle (deg)
BL_{CG}	Butt line of c.g. (in)
BL_{Gn}	Butt line of landing gear [where n = 1 (nose), 2 (right), 3 (left), landing gear] (in)
BL_{PA}	Butt line of the pilot's station (in)

BL_{SP}	Butt line of engine nacelle shaft pivot point (in)
BL_V	Butt line of the vertical stabilizer center of pressure (in)
$BL_V(i)$	Butt line of the vertical stabilizer(s) center of pressure (in)
B_{1L}	Left rotor forward cyclic input (rad)
B_{1R}	Right rotor forward cyclic input (rad)
$\partial B_1/\partial X_{LN}$	Longitudinal cyclic pitch control gearing ratio, = $f(\beta_m)$ (deg/in)
$\partial B_1/\partial X_{PD}$	Differential cyclic pitch control gearing ratio, = $f(\beta_m, V_T)$ (deg/in)
b_{1L}	Left rotor lateral flapping (+ outboard for helicopter) (rad)
b_{1R}	Right rotor lateral flapping (+ outboard for helicopter) (rad)
$\dot{b}_{1L}$	Left rotor lateral flapping rate (rad/sec)
$\dot{b}_{1R}$	Right rotor lateral flapping rate (rad/sec)
b_W	Wing span (ft)
CDALPH	Rotor drag equation coefficient (slope with alpha) (non-dimensional)
CDFACT	Rotor drag equation coefficient (non-dimensional)
C_{DH}	Horizontal stabilizer drag coefficient, = $f(\alpha_H, M_N)$ (non-dimensional)

CDLIM	Onset of profile drag rise (non-dimensional)
CDMACH	Coefficient for lower limit of rotor mach effects (non-dimensional)
CDMAX	Maximum rotor drag coefficient (non-dimensional)
$C_{D_{0_{WP}}}\Big\vert_{C_{L_{WP}}=0}$	Wing coefficient of drag at wing coefficient of lift equal to zero, $=f\ (M_N,\ \beta_m,\ F_X)$ (non-dimensional)
C_{DV}	Vertical fin drag coefficient, $= f(\beta_V,\ \delta_r,\ M_N)$ (non-dimensional)
$C_{D_{WP}}$	Wing-pylon drag coefficient, $= f(\alpha_W,\ \beta_m,\ F_X,\ M_N)$ (non-dimensional)
C_{LH}	Horizontal stabilizer lift coefficient, $= f(\alpha_H,\ \delta_e,\ M_N)$ (non-dimensional)
$C_{LH\beta}$	Horizontal stabilizer lift coefficient as a function of sideslip angle (1/deg)
$C_{L_{WP}}$	Wing-pylon lift coefficient, $= f(\alpha_W,\ \beta_m,\ F_X,\ M_N)$ (non-dimensional)
$C_{L_{\alpha_a}}$	Aerodynamic coefficient for the wing lift coefficient reduction due to aileron deflection, $= f(\delta_F)$ (1/deg)
$\dfrac{\partial C_{L_{WP}}}{\partial \alpha_W}\Big\vert_{C_{L_{WP}}=0}$	Partial of wing coefficient of lift with respect to angle of attack, $= f(M_N,\ \beta_m)$ (non-dimensional)
$C_{l_p}\Big\vert_{\substack{C_L=0\\ M_N=0}}$	Aerodynamic coefficient in the wing rolling moment equation (1/rad)
$\dfrac{C_{l_r}}{C_{L_{WP}}}\Big\vert_{M_N=0}$	Aerodynamic coefficient in the wing rolling moment equation (1/rad)

$\dfrac{\Delta C_{l_r}}{(\partial\alpha_{WFS}/\partial\delta_F)(\delta_F)}$	Aerodynamic coefficient in the wing rolling moment equation (1/deg)
$C_{l_\beta}\Big\vert_{C_{L_{WP}}=M_N=0}$	Aerodynamic coefficient in the wing rolling moment equation, = $f(\delta_F, \beta_F, \beta_m)$ (1/rad)
$\dfrac{C_{l_\beta}}{C_{L_{WP}}}\Bigg\vert_{M_N=0}$	Aerodynamic coefficient in the wing rolling moment equation, = $f(\delta_F, \beta_F, \beta_m)$ (1/rad)
$C_{l_{\delta_a}}$	Aerodynamic rolling moment coefficient due to wing aileron deflection (1/deg)
$C_{l_{\delta_a}}\Big\vert_{\substack{\delta_F = 0 \text{ deg} \\ \alpha_{WFS} < 8 \text{ deg}}}$	Aerodynamic coefficient in the wing rolling moment equation (1/deg)
C_{MHO}	Horizontal stabilizer pitching moment coefficient at zero angle of attack (non-dimensional)
C_{MHA}	Horizontal stabilizer pitching moment coefficient variation with angle of attack (1/deg)
$C_{m_{WP}}$	Wing-pylon pitching moment coefficient, = $f(\delta_F, \beta_m)$ (non-dimensional)
$\dfrac{C_{n_p}}{C_{L_{WP}}}\Bigg\vert_{M_N=0}$	Aerodynamic coefficient in the wing yawing moment equation (1/rad)
$\dfrac{C_{n_r}}{C_{D_{oWP}}}$	Aerodynamic coefficient in the wing yawing moment equation (1/rad)
$\dfrac{C_{n_r}}{C^2_{L_{WP}}}$	Aerodynamic coefficient in the wing yawing moment equation (1/rad)

$C_{n_\beta}\Big\vert_{C_{L_{WP}}=M_N=0}$	Aerodynamic coefficient in the wing yawing moment equation (1/rad)
$\dfrac{C_{n_\beta}}{C^2_{L_{WP}}}\Bigg\vert_{M_N=0}$	Aerodynamic coefficient in the wing yawing moment equation (1/rad)
COLRATE	Differential collective trim rate constant (deg/sec)
C_{RFL}	Left rotor force coefficient (non-dimensional)
C_{RFR}	Right rotor force coefficient (non-dimensional)
C_T^-	Maximum available rotor thrust coefficient, = $f(\mu, \beta_m)$ (non-dimensional)
CTMAXM	Rotor CT maximum multiplier coefficient (non-dimensional)
$\dfrac{C_{Y_p}}{C_{L_{WP}}}\Bigg\vert_{M_N=0}$	Aerodynamic coefficient in the wing side force equation (1/rad)
$C_{Y_r}\Big\vert_{M_N=0}$	Aerodynamic coefficient in the wing side force equation (1/rad)
C_{YV}	Vertical fin side force (lift) coefficient, = $f(\beta_V, \delta_r, M_N)$ (non-dimensional)
$C_{Y_\beta}\Big\vert_{M_N=0}$	Aerodynamic coefficient in the wing side force equation (1/rad)
c_b	Blade chord (in)
c_H	Horizontal stabilizer chord (ft)
c_W	Wing chord (ft)

DBFO	Fuselage drag at α = 0 deg, β = 0 deg (ft^2)
DB1	B1 Offset rigging constant (deg)
D_F	Aerodynamic drag on fuselage (wind axis) (lb)
D_H	Aerodynamic drag on the horizontal stabilizer (lbs)
D_{iWPL}	Aerodynamic drag of the left wing portion immersed in the rotor wake (lb)
D_{iWPR}	Aerodynamic drag of the right wing portion immersed in the rotor wake (lb)
D_{Ke}	Elevator effectiveness reduction factor for large elevator angles (non-dimensional)
D_{Kr}	Rudder effectiveness reduction factor for large rudder angles (non-dimensional)
DLANG	Extra fuselage drag (ft^2)
D_{MG}	Aerodynamic drag on the main landing gear (lb)
D_{NG}	Aerodynamic drag on the nose landing gear (lb)
$D_{o_{MG}}$	Drag of the main landing gear (VAX version), = $f(LG_{PCT})$ (ft^2)
$D_{o_{MGD}}$	Drag of the main landing gear during extension (Sigma 8 version), = f(t) (ft^2)
$D_{o_{NG}}$	Drag of the nose landing gear (VAX version), = $f(LG_{PCT})$ (ft^2)

$D_{o_{NGD}}$	Drag of the nose landing gear during extension, = f(t) (ft^2)
$D_{o_{MGU}}$	Drag of the main landing gear during retraction (Sigma 8 version), = f(t) (ft^2)
$D_{o_{NGU}}$	Drag of the nose landing gear during retraction (Sigma 8 version), = f(t) (ft^2)
D_{PLAT}	Lateral pylon drag (lb)
DPOD	Fuselage landing gear pod drag (ft^2)
D_{PYINT}	Pylon interference drag, = $f(\beta_m)$ (lb)
D_{PYLN}	Pylon interference drag (lb)
$D_V(i)$	Aerodynamic drag on the vertical fin (wind axis) (lbs)
D_{WB}	Coefficient in the wing/body damping equation (non-dimensional)
D_{WP}	Aerodynamic drag on the wing portion outside the rotor wake (freestream) (lb)
D_α	Fuselage drag variation with angle of attack, = $f(\alpha)$ (ft^2)
D_β	Fuselage drag variation with sideslip angle, = $f(\beta)$ (ft^2)
DSHPDT	Rate of change of engine power, = $f(HP_{ENG}, P_{ALT})$ (SHP/sec)
E	Distance from takeoff point in the direction of grid East (+ East) (nautical miles)

$F_{ACT_{RUD_{LIM}}}$	Rudder force feel actuator limit (lb)
F_{B_n}	Brake force (+ aft) (lb)
F_{D_n}	Gear drag force in the plane of the landing surface due to friction (+ aft) (lb)
F_{LN}	Longitudinal stick force from the pilot (+ fwd) (lb)
F_{LT}	Lateral stick force from the pilot (+ right) (lb)
F_{N_n}	Gear normal force (+ down) (lb)
F_{PD}	Pedal force from the pilot (+ right) (lb)
F_{S_n}	Gear side force in the plane of the landing surface (+ to the right) (lb)
Λ_{A_n}	Landing gear linear damping term (lb-sec/ft)
G_{B_n}	Landing gear nonlinear damping term (lb-sec/ft^3)
G_{C_n}	Landing gear nonlinear stiffness term (lb/ft^4)
GEARDN	Landing gear extension time (sec)
GEARUP	Landing gear retraction time (sec)
GECON1	Constant in the rotor ground effect equation (ft/sec)
GECON2	Constant in the rotor ground effect equation (ft/sec)
GELLIM	Lower altitude limit in the ground effect rolling moment equation (non-dimensional)

GEULIM	Upper altitude limit in the ground effect rolling moment equation (non-dimensional)
GEWASH	Airspeed washout for rotor ground effects (ft/sec)
G_{LN0}	Longitudinal force feel system gradient (lb/in)
G_{LN1}	Longitudinal force feel system gradient (lb/in/PSF)
G_{LT0}	Lateral force feel system gradient (lb/in)
G_{LT1}	Lateral force feel system gradient (lb/in/PSF)
G_{PD0}	Pedal force feel system gradient (lb/in)
G_{PD1}	Pedal force feel system gradient (lb/in/PSF)
GW	Total aircraft gross weight (lb)
G_{XLN}	Longitudinal force feel system gradient (system on) (lb/in)
G_{XLT}	Lateral force feel system gradient (system on) (lb/in)
G_{XPD}	Pedal force feel system gradient (system on) (lb/in)
GRD_{ALT}	Pressure altitude on the surface of the ground (altitude above sea level) (ft)
$G_{1_n-4_n}$	Landing gear ground dynamic coefficients (gear oleo force) (non-dimensional)
g	Gravitational constant (ft/sec^2)
H_L	Mast axis H-force left rotor (+ aft for helicopter) (lb)

H_{LN}	Longitudinal force feel system hysteresis force (lb)
H_{LT}	Lateral force feel system hysteresis force (lb)
H_{PD}	Pedal force feel system hysteresis force (lb)
H_R	Mast axis H-force right rotor (+ aft for helicopter) (lb)
H_{RUD}	Rudder force feel constant (ft^2/in)
H_{XLN}	Longitudinal force feel system hysteresis force (lb)
H_{XLT}	Lateral force feel system hysteresis force (lb)
H_{XPD}	Pedal force feel system hysteresis force (lb)
h_{CG}	Altitude of aircraft (ft)
$\dot{h}_{CG}$	Climb rate (ft/sec)
h_H	Rotor hub height above ground (ft)
h_M	Waterline distance from the pylon pivot axis to the non-tilting c.g. position (ft)
h_p	Pressure altitude (ft)
IAN	Yaw trim switch (non-dimensional)
IDIFF	Differential collective switch position (non-dimensional)
IFAH	Attitude retention ON/OFF switch (non-dimensional)
IFFENG	Force feel system engage switch (non-dimensional)

IFFON	Force feel system ON/OFF switch (non-dimensional)
IGB	RPM governor disengage switch (non-dimensional)
IGOVENG	RPM governor engage switch (non-dimensional)
IMB	Force feel system release switch (non-dimensional)
INACB	Nacelle beep switch position (non-dimensional)
IPCH	Pitch channel switch (Channel 1, 2, both) (non-dimensional)
IPDAMP	Roll SCAS ON/OFF switch (non-dimensional)
I_{PYL}	Moment of inertia of the nacelle/pylon (slug-ft^2)
IQDAMP	Pitch SCAS ON/OFF switch (non-dimensional)
IRCH	Roll channel switch (Channel 1, 2, both) (non-dimensional)
IRDAMP	Yaw SCAS ON/OFF switch (non-dimensional)
IRPM	RPM adjustment wheel (increase/decrease) (non-dimensional)
ISCENG	SCAS engage switch (non-dimensional)
ISCRLS	SCAS release switch (non-dimensional)
I_b	Blade flapping inertia (slug-ft)
I_{XX}	Rolling moment of inertia about c.g. (slug-ft^2)

$I_{XX}\Big\vert_{\beta_m=0}$	Helicopter rolling moment of inertia, body axis (slug-ft^2)
I_{XZ}	Product of inertia about c.g. (slug-ft^2)
$I_{XZ}\Big\vert_{\beta_m=0}$	Helicopter product of inertia, body axis (slug-ft^2)
I_{YY}	Pitching moment of inertia about c.g. (slug-ft^2)
$I_{YY}\Big\vert_{\beta_m=0}$	Helicopter pitching moment of inertia, body axis (slug/ft^2)
I_{ZZ}	Yawing moment of inertia about c.g. (slug-ft^2)
$I_{ZZ}\Big\vert_{\beta_m=0}$	Helicopter yawing moment of inertia, body axis (slug-ft^2)
I_1	Drive system inertia (slug-ft^2)
i_H	Horizontal stabilizer incidence (deg)
$i_V(i)$	Incidence of vertical stabilizer (deg)
JT_L	Left engine jet thrust (lb)
JT_R	Right engine jet thrust (lb)
K_{B_n}	Brake sensitivity (ft/sec^2-deg)
K_e	Elevator effectiveness factor, = $f(\delta_e, M_N)$ (non-dimensional)
K_{FWO}	Constant in the rotor downwash/wing equation for flap effects (non-dimensional)

K_{FWDF}	Slope in the rotor downwash/wing equation for flap effects (1/deg)
K_{HNU}	Horizontal stabilizer dynamic pressure loss multiplier (non-dimensional)
K_H	Flapping spring rate (ft-lb/deg)
K_{HUB}	Coning hubspring (ft-lb/deg)
K_{H_β}	Rotor wake on the horizontal stabilizer (constant) $= f(\beta_m, \beta_F)$ (non-dimensional)
K_{INTG}	Rotor collective governor integral gain, $= f(\beta_m)$ (non-dimensional)
K_{I1}	Roll inertia coefficient for varying inertia with mast angle (slug-ft^2/deg)
K_{I2}	Pitch inertia coefficient for varying inertia with mast angle (slug-ft^2/deg)
K_{I3}	Yaw inertia coefficient for varying inertia with mast angle (slug-ft^2/deg)
K_{I4}	Product of inertia coefficient for varying inertia with mast angle (slug-ft^2/deg)
K_{JT1}	Jet thrust coefficient, $= f(V_T)$ (lb)
K_{JT2}	Jet thrust coefficient, $= f(V_T)$ (lb/SHP)
K_{LN}	Longitudinal force feel system constant (system off) (lb/in)
K_{LT}	Lateral force feel system constant (system off) (lb/in)

KMU1	Induced velocity distribution equation coefficient (non-dimensional)
KMU2	Induced velocity distribution equation coefficient (non-dimensional)
KMUSF	Induced velocity distribution equation coefficient for sideward flight (non-dimensional)
$K_{l_{\delta_a}}$	Aileron effectiveness correction factor, = $f(\alpha_{WFS}, \beta_m, \delta_F)$
K_{np}	Wing yawing moment equation constant (non-dimensional)
$K_{n_{\delta_a}}$	Yawing moment (aileron) coefficient, = $f(\delta_F, \beta_m)$ (non-dimensional)
$K_{no_{\delta_a}}$	Yawing moment (aileron) coefficient, = $f(\delta_F, \beta_m)$ (1/deg)
K_{PLAT}	Pylon lateral drag coefficient, = $f(\overline{\alpha}_{PYL})$ (non-dimensional)
K_{PROG}	Rotor collective governor proportional gain, = $f(\beta_m)$ (non-dimensional)
K_r	Rudder effectiveness factor (non-dimensional)
K_{RPM}	Helicopter mode operating rpm (β_m = 0 deg) (percent)
K_{RW}	Rotor skew angle velocity distribution factor (non-dimensional)
K_{VNU}	Vertical stabilizer dynamic pressure loss multiplier (non-dimensional)
K_{XRW}	Constant in the rotor downwash/wing equation (non-dimensional)

$K_{\beta HS}$	Sideslip factor on dynamic pressure ratio at the constant, = $f(\beta_F)$ (non-dimensional)
$K_{\beta R}$	Rotor sidewash factor on dynamic pressure, = $f(\beta_F, V_T)$ (non-dimensional)
$K_{\beta VS}$	Sideslip factor on dynamic pressure ratio at the vertical stabilizer, = $f(\beta_F)$ (non-dimensional)
$K_0 \ldots K_4$	Constants in the rotor/wing wake equation (non-dimensional)
K_1	Engine shaft horsepower equation coefficient (non-dimensional)
K_2	Engine shaft horsepower equation coefficient (non-dimensional)
K_3	Engine shaft horsepower equation coefficient (non-dimensional)
K_4	Engine shaft horsepower equation coefficient (RPM)
K_5	Engine shaft horsepower equation coefficient (RPM/$\sqrt{HP}$)
K_6	Engine shaft horsepower equation coefficient (HP)
K_7	Engine shaft horsepower equation coefficient (deg K)
K_{11}	Engine throttle control coefficient (1/deg K)
K_{12}	Engine throttle control coefficient (1/deg)
K_{13}	Engine throttle control coefficient (1/deg^2)
K_{14}	Engine throttle control coefficient (deg)

K_{15}	Engine throttle control coefficient (1/kt)
K_{18}	Engine rating (limit output) (SHP)
$K_{1P} \rightarrow K_{7P}$	Pitch SCAS gains (see Appendix B)
$K_{1R} \rightarrow K_{7R}$	Roll SCAS gains (see Appendix B)
$K_{1Y} \rightarrow K_{3Y}$	Yaw SCAS gains (see Appendix B)
K_{1RGA}	Rotor collective governor actuator gain (non-dimensional)
K_{2RGA}	Rotor collective governor actuator gain (non-dimensional)
K_{3RGA}	Rotor collective governor actuator gain (non-dimensional)
K_{4RGA}	Rotor collective governor actuator gain (non-dimensional)
LBFO	Fuselage lift at $\alpha = 0$ deg, $\beta = 0$ deg (ft^2)
L_F	Aerodynamic lift on fuselage (wind axis) (lb)
LG_{TLT}	Landing gear touchdown light (non-dimensional)
L_H	Aerodynamic lift on the horizontal stabilizer (lb)
L_{iWPL}	Aerodynamic lift of the left wing portion immersed in the rotor wake (lb)
L_{iWPR}	Aerodynamic lift of the right wing portion immersed in the rotor wake (lb)
LLANG	Extra fuselage lift (ft^2)

L_{LG}	Landing gear position indicator (non-dimensional)
L_N	Distance from the pylon pivot axis to the pylon c.g. (ft)
L_{WP}	Aerodynamic lift on the wing portion outside the rotor wake (freestream) (lb)
L_α	Fuselage lift variation with angle of attack, = $f(\alpha)$ (ft^2)
L_β	Fuselage lift variation with sideslip angle, = $f(\beta)$ (ft^2)
l_A	Total rolling moment on the aircraft in body axis (ft-lb)
$l_{b_{1L}}$	Mast axis lateral flapping restraint exerted by left rotor on airframe (+ outboard for helicopter) (ft-lb)
$l_{b_{1R}}$	Mast axis lateral flapping restraint exerted by right rotor on airframe (+ outboard for helicopter) (ft-lb)
l_F'	Aerodynamic rolling moment on fuselage (wind axis) (ft-lb)
l_{G0}	Ground effect rolling moment coefficient (ft-lb/deg)
l_{G1}	Ground effect rolling moment coefficient (ft-lb/deg-ft)
l_{G2}	Ground effect rolling moment coefficient (ft-lb/deg-ft^2)
l_{G3}	Ground effect rolling moment coefficient (ft-lb/deg-ft^3)
l_{G4}	Ground effect rolling moment coefficient (sec/ft)
l_m	Mast length (ft)

$(l,M,N)_F$	Rolling, pitching, and yawing aerodynamic moments on the fuselage about the body x-, y-, and z-axes (ft-lb)
$(l,M,N)_H$	Rolling, pitching, and yawing aerodynamic moments due to the horizontal stabilizer about the body x-, y-, and z-axes (ft-lb)
$(l,M,N)_L$	Rolling, pitching, and yawing moments due to the left rotor about the body x-, y-, and z-axes (ft-lb)
$(l,M,N)_R$	Rolling, pitching, and yawing moments due to the right rotor about the body x-, y-, and z-axes (ft-lb)
$(l,M,N)_{WP}$	Rolling, pitching, and yawing aerodynamic moments due to the wing-pylon about the body x-, y-, and z-axes (ft-lb)
l'_{WP}	Rolling moment of the wing-pylon in wind axis (ft-lb)
$(\Delta l,\Delta M,\Delta N)_{LG}$	Total landing gear rolling, pitching, and yawing moments in body axis (ft-lb)
$l_{XV}(i)$	Station line distance from the c.g. to the vertical stabilizer center of pressure (ft)
$l_{YV}(i)$	Butt line distance from the c.g. to the vertical stabilizer center of pressure (ft)
$l_{ZV}(i)$	Water line distance from the c.g. to the vertical stabilizer center of pressure (ft)
l_β	Fuselage rolling moment variation with sideslip angle, $= f(\beta)$ (ft^3)
ℓ_M	Stationline distance from the pylon pivot axis to the non-tilting c.g. position (ft)
M_A	Total pitching moment on the aircraft in body axis (ft-lb)

$M_{a_{1L}}$	Mast axis longitudinal flapping restraint exerted by left rotor on airframe (+ nose up for helicopter) (ft-lb)
$M_{a_{1R}}$	Mast axis longitudinal flapping restraint exerted by right rotor on airframe (+ nose up for helicopter) (ft-lb)
MBFO	Fuselage pitching moment at $\alpha = 0$ deg, $\beta = 0$ deg (ft^3)
MENB	Pylon lock switch (non-dimensional)
$M_F^{\prime}$	Aerodynamic pitching moment on fuselage (wind axis) (ft-lb)
M_{G1}	Constant in the IGE pitching moment equation (ft)
M_{G2}	Constant in the IGE pitching moment equation (non-dimensional)
N_{G3}	Constant in the IGE pitching moment equation (sec/ft)
$M_H^{\prime}$	Aerodynamic pitching moment on the horizontal stabilizer (ft-lb)
M_N	Mach number (non-dimensional)
$M_{WP}^{\prime}$	Pitching moment of the wing-pylon in wind axis (ft-lb)
MUHO	Induced velocity distribution equation coefficient (non-dimensional)
MUH1	Induced velocity distribution equation coefficient (non-dimensional)
M_α	Fuselage pitching moment variation with angle of attack, $= f(\alpha)$ (ft^3)

M_β	Fuselage pitching moment variation with sideslip angle, $= f(\beta)$ (ft^2)
m	Number of rotor segments (non-dimensional)
m	Aircraft mass (GW/32/2) (slug)
N_A	Total yawing moment on the aircraft in body axis (ft-lb)
N_F'	Aerodynamic yawing moment on fuselage (wind axis) (ft-lb)
N_N	Distance from takeoff point in the direction of grid North (+ North) (nautical miles)
$N_{R_{MAX}}$	Maximum rotor speed (RPM)
N_{WP}'	Yawing moment of the wing-pylon in wind axis (ft-lb)
N_X	x-axis (longitudinal) acceleration at the c.g. in body axis (g's)
N_Y	y-axis (lateral) acceleration at the c.g. in body axis (g's)
N_Z	z-axis (vertical) acceleration at the c.g. in body axis (g's)
N_β	Fuselage yawing moment variation with sideslip angle, $= f(\beta)$ (ft^3)
NVSTAB	Number of vertical stabilizers (non-dimensional)
n_b	Number of rotor blades (non-dimensional)
P_{AX}	x-position of the aircraft c.g. with respect to the ground (nautical miles)

P_{AY}	y-position of the aircraft c.g. with respect to the ground (nautical miles)
P_{AZ}	z-position of the aircraft c.g. with respect to the ground (nautical miles)
P_{ALT}	Pressure altitude
PCPM	Mach number effect on the $(\partial\varepsilon_{W/H}/\partial\alpha_W)$, $f(M_N)$ (non-dimensional)
PBMMAX	Maximum forward pylon position (deg)
PBMMIN	Maximum aft pylon position (deg)
PSCAS	Pitch (elevator) SCAS output (in)
$PSCAS_{MX}$	Pitch (elevator) SCAS actuator limit (in)
$P_{HOLD_{MAX}}$	Pitch attitude hold limit (in)
P_a	Ambient absolute pressure (lb/ft^2)
P_o	Sea level standard atmospheric pressure (lb/in^2)
P_{SRG}	Rotor collective governor actuator constant (lb/in^2)
p	Body axis roll rate (rad/sec)
pctmxp	Commanded power at which the acceleration ceases to follow the maximum acceleration curve (percent)
pctmxs	Commanded power turbine speed at which the acceleration ceases to follow the maximum acceleration curve (percent)
$\dot{p}$	Body axis roll angular acceleration (rad/sec^2)

Q_L	Mast axis left rotor torque (+ trying to slow rotor down) (ft-lb)
Q_{LPT}	Left engine power turbine torque (ft-lb)
Q_{MAX}	Maximum allowable rotor torque (ft-lb)
Q_R	Mast axis right rotor torque (+ trying to slow rotor down) (ft-lb)
Q_{RPT}	Right engine power turbine torque (ft-lb)
q	Body axis pitch rate (rad/sec)
$\dot{q}$	Body axis pitch angular acceleration (rad/sec^2)
q_F	Fuselage dynamic pressure (lb/ft^2)
$\dot{q}_{\beta_m}$	Pitch acceleration due to pylon tilt (rad/sec^2)
R	Rotor radius (ft)
R_{ALT}	Radar altitude (ft)
$R_{HOLD_{MAX}}$	Roll attitude hold limit (in)
RPME	100 percent engine power turbine speed multiplier (nondimensional)
RPM_{NII}	Engine N_{II} RPM (rad/sec)
$RPM_{P_{MAX}}$	Maximum rotor RPM limit (RPM)
$RPM_{P_{MIN}}$	Minimum rotor RPM limit (RPM)
RPM_{SEL}	Pilot's selected operating rotor speed (RPM)

RSCAS	Roll (aileron) SCAS output (in)
$RSCAS_{MX}$	Roll (aileron) SCAS actuator limit (in)
RSHP	Commanded (throttle) referred optimum SHP on one engine, $= f(X_{THR})$ (SHP)
K_{RAM}	Ram effect equation coefficient, $= f(V_T)$ (non-dimensional)
R_{WL}	Left rotor wake contraction ratio (non-dimensional)
R_{WR}	Right rotor wake contraction ratio (non-dimensional)
r	Body axis yaw rate (rad/sec)
$\dot{r}$	Body axis yaw angular acceleration (rad/sec^2)
SD	Spinner drag (lb)
(SD/q)	Constant in the variable drag portion of the spinner drag equation (function of mast angle) (ft^2)
$(SD/q)_{\beta_m=90}$	Constant for drag of the spinner at 90 deg mast angle (ft^2)
SFWASH	Airspeed washout for side-by-side rotor effect (ft/sec)
S_H	Horizontal stabilizer area (ft^2)
SHP_{ACC}	Engine accessory power loss (SHP)
SL_{CG}	Station line of c.g. (in)
$SL_{CG}\Big\vert_{\beta_m=0}$	Station line of helicopter c.g. (in)

SL_F	Station line of fuselage center of pressure (in)
SL_{Gn}	Station line of landing gear [where n = 1 (nose), 2 (right), 3 (left) landing gear] (in)
SL_H	Station line of the horizontal stabilizer center of pressure (in)
SL_{MG}	Station line of the main landing gear (in)
SL_{NG}	Station line of the nose landing gear (in)
SL_P	Station line of pylon center of gravity (in)
SL_{PA}	Station line of the pilot's station (in)
SL_{SP}	Station line of engine nacelle shaft pivot point (in)
$SL_V(i)$	Station line of the vertical stabilizer(s) center of pressure (in)
SL_{WP}	Station line of the wing-pylon center of pressure (in)
SL_{WTE}	Station line of the wing trailing edge (in)
S_{PYL}	Projected lateral pylon area (ft^2)
$S_V(i)$	Vertical stabilizer total area (ft^2)
S_W	Wing area (ft^2)
T_a	Ambient absolute temperature (deg K)
T_{DN}	Time for landing gear to extend (VAX version) (sec)
THOGMN	Governor blade angle limit (minimum) (deg)

THOGMX	Governor blade angle limit (maximum) (deg)
T_L	Mast axis left rotor thrust (+ up for helicopter) (lb)
T_o	Absolute sea level standard temperature (deg K)
T_R	Mast axis right rotor thrust (+ up for helicopter) (lb)
T_{UP}	Time for landing gear to retract (VAX version) (sec)
T_D	Engine throttle and power turbine response delay time (sec)
U	x-velocity (longitudinal) of the aircraft c.g. in body axis with respect to the air (ft/sec)
U_{EB}	x-velocity of the aircraft c.g. with respect to the air along earth axes (ft/sec)
U_G	x-velocity ground component of aircraft c.g. (ft/sec)
$U_i \Big\vert^{B}_{R/H}$	Induced x-velocity at horizontal stabilizer in body axis due to the rotor (ft/sec)
$U_i \Big\vert^{B}_{R/V}$	Induced x-velocity at the vertical fin in body axis due to the rotor (ft/sec)
$U_i \Big\vert^{B}_{R/WL}$	Induced x-velocity at the left wing in body axis due to the rotor (ft/sec)
$U_i \Big\vert^{B}_{R/WR}$	Induced x-velocity at the right wing in body axis due to the rotor (ft/sec)
U_{KCAS}	Calibrated airspeed (kt)
U_o	Initialization x-axis velocity (ft/sec)

U_{PA}	x-velocity of the pilot's station in body axis (ft/sec)
U_W	Wind x-velocity with respect to the ground (ft/sec)
$\dot{U}$	Rate of change of x-velocity (longitudinal) of the rotorcraft c.g. in body axis with respect to the air (ft/sec^2)
V	y-velocity (lateral) of the aircraft c.g. in the body axis with respect to the air (ft/sec)
$\bar{V}$	Ratio of the total velocity of the hub to the rotor tip speed (non-dimensional)
V_{EB}	y-velocity of the aircraft c.g. with respect to the air along earth axes (ft/sec)
V_G	y-velocity ground component of aircraft c.g. (ft/sec)
V_o	Initialization y-axis velocity (ft/sec)
V_{PA}	y-velocity of the pilot's station in body axis (ft/sec)
V_T	Total linear velocity of the aircraft c.g. with respect to the air (ft/sec)
$\dot{V}$	Rate of change of y-velocity (lateral) of the rotorcraft c.g. in body axis with respect to the air (ft/sec^2)
W	z-velocity (vertical) of the aircraft c.g. in body axis with respect to the air (ft/sec)
$\dot{W}$	Rate of change of z-velocity (vertical) of the aircraft c.g. in body axis with respect to the air (ft/sec)
W_{EB}	z-velocity component of the aircraft c.g. with respect to the air along earth axes (ft/sec)

W_G	z-velocity ground component of aircraft c.g. (ft/sec)
$W_i\Big\vert^{B}_{R/H}$	Induced z-velocity at horizontal stabilizer in body axis due to the rotor (ft/sec)
$W_i\Big\vert^{B}_{R/V}$	Induced z-velocity at the vertical fin in body axis due to the rotor (ft/sec)
$W_i\Big\vert^{B}_{R/WL}$	Induced z-velocity at the left wing in body axis due to the rotor (ft/sec)
$W_i\Big\vert^{B}_{R/WR}$	Induced z-velocity at the right wing in body axis due to the rotor (ft/sec)
$W_i\Big\vert_{R/WL}$	Induced velocity at the left wing in mast axis due to the rotor (ft/sec)
$W_i\Big\vert_{R/WR}$	Induced velocity at the right wing in mast axis due to the rotor (ft/sec)
$\dfrac{W_i\Big\vert_{R/H}}{W_i}$	Ratio of the induced z-axis rotor wake velocity on the horizontal stabilizer to the mean induced velocity at the rotor (for both right and left rotor) = $f(\alpha_F, \beta_m, V_T)$ (non-dimensional)
W_{iL}	Mast axis uniform component of induced velocity at left rotor (+ downward for helicopter (ft/sec)
W_{iR}	Mast axis uniform component of induced velocity at right rotor (+ down for helicopter) (ft/sec)
W_o	Initialization z-axis velocity (ft/sec)
WL_{CG}	Water line of c.g. (in)
$WL_{CG}\Big\vert_{\beta_m=0}$	Water line of helicopter c.g. (in)
WL_F	Water line of the fuselage center of pressure (in)

WL_{Gn}	Water line of landing gear [where n = 1 (nose), 2 (right), 3 (left) landing gear] (in)
WL_H	Water line of the horizontal stabilizer center of pressure (in)
WL_{MG}	Water line of the main landing gear (in)
WL_{NG}	Water line in the nose landing gear (in)
WL_P	Water line of pylon center of gravity (in)
WL_{PA}	Water line of the pilot's station (in)
WL_{SP}	Water line of engine nacelle shaft pivot point (in)
$WL_V(i)$	Water line of the vertical stabilizer(s) center of pressure (in)
WL_{WP}	Water line of the wing-pylon center of pressure (in)
W_P	Weight of both pylons (lb)
W_{PA}	z-velocity of the pilot's station in body axis (ft/sec)
$(X,Y,Z)_F$	Aerodynamic forces on the fuselage, body axis (lb)
$(X,Y,Z)_H$	Aerodynamic forces on the horizontal stabilizer, body axis (lb)
$(X,Z)_{iPYL}$	Pylon interference drag forces in body axis (lb)
$(X,Y,Z)_L$	Left rotor forces in body axis (lb)
$(X,Y,Z)_{MG}$	Aerodynamic forces on the main landing gear, body axis (lb)

$(X,Y,Z)_{NG}$	Aerodynamic forces on the nose landing gear, body axis (lb)
$(X,Y,Z)_{PYLT}$	Lateral pylon drag model aerodynamic forces, body axis (lb)
$(X,Y,Z)_{R}$	Right rotor forces in body axis (lb)
$(X,Y,Z)_{SD}$	Spinner drag aerodynamic forces in body axis (lb)
$(X,Y,Z)_{V}(i)$	Aerodynamic forces on the vertical stabilizer(s), body axis (lb)
$(X,Y,Z)_{WP}$	Aerodynamic forces on the wing-pylon portion in the freestream, body axis (lb)
$(X,Z)_{iWPL}$	Aerodynamic forces on the portion of the left wing-pylon in the rotor wake, body axis (lb)
$(X,Y)_{iWPR}$	Aerodynamic forces on the portion of the right wing-pylon in the rotor wake, body axis (lb)
$(X,Z)_{JTL}$	Left engine jet thrust forces, body axis (lb)
$(X,Z)_{JTR}$	Right engine jet thrust forces, body axis (lb)
X_A	Total x-force on the aircraft body axis (lbs)
X_{CG}	Longitudinal c.g. displacement as a function of mast tilt angle (in)
$\dot{X}_{CG}$	Rate of longitudinal c.g. displacement as a function of mast tilt angle (in/sec)
$\ddot{X}_{CG}$	Acceleration of longitudinal c.g. displacement as a function of mast tilt angle (in/sec^2)

X_{COL}	Collective stick position, inches from full down (in)
X_{EK}	Right (K = 1) or left (K = 2) engine operating flag (nondimensional)
X_{Ke}	Elevator effectiveness factor, = $f(M_N)$ (non-dimensional)
X_{FL}	Position of flap indicator (non-dimensional)
$(X_{iW}, Y_{iW})_L$	Moment arms for left wing-pylon z-force due to rotor wake (in)
$(X_{iW}, Y_{iW})_R$	Moment arms for right wing-pylon z-force due to rotor wake (in)
X_{Kr}	Rudder effectiveness factor, = $f(M_N)$ (non-dimensional)
X_L	Left rotor x-force (body axis) (lb)
X_{LG}	Position of landing gear indicator (non-dimensional)
X_{LN}	Longitudinal stick position, inches from full aft (in)
X_{LNN}	Longitudinal stick neutral position (in)
X_{LNT}	Longitudinal stick force feel trim position (in)
$\dot{X}_{LNT0}$	Longitudinal trim rate force feel system constant (in/sec)
$\dot{X}_{LNT1}$	Longitudinal trim rate force feel system constant (in/sec/PSF)
$\dot{X}_{LTT0}$	Lateral trim rate force feel system constant (in/sec)
$\dot{X}_{LTT1}$	Lateral trim rate force feel system constant (in/sec/PSF)

X_{LT}	Lateral stick position, inches from full left (in)
X_{LTN}	Lateral stick neutral position (in)
X_{LTT}	Lateral stick force feel trim position (in)
X_m	Blade station/R (non-dimensional)
X_o	Initial x-position of the aircraft c.g. with respect to the ground (ft)
X_{PD}	Pedal position, inches from full left (in)
X_{PDN}	Pedal neutral position (in)
X_{PDT}	Pedal force feel trim position (in)
$\dot{X}_{PDT0}$	Pedal trim rate force feel system constant (in/sec)
$\dot{X}_{PDT1}$	Pedal trim rate force feel system constant (in/sec/PSF)
X_R	Right rotor x-force (body axis) (lb)
X_{RW0}	Constant in the rotor downwash/wing equation (non-dimensional)
X_{RW1}	Constant in the rotor downwash/wing equation (1/deg)
X_{RW2}	Constant in the rotor downwash/wing equation (1/deg^2)
X_{SF}	Sideward flight rotor correction factor, = $f(\lvert\bar{V}\rvert)$ (non-dimensional)
X_{SS}	Side-by-side rotor effect correction factor, = $f(\bar{u})$ (non-dimensional)

X_{THL}	Left engine throttle position at the fuel control (deg)
X_{THR}	Right engine throttle position at the fuel control (deg)
$(\Delta X, \Delta Y, \Delta Z)_{LG}$	Total landing gear forces in body axis (lb)
X_{β_m}	Position of mast tilt actuator (percent)
Y_A	Body axis total y-force on the aircraft (lb)
$Y_F^{\prime}$	Aerodynamic side force on fuselage (wind axis) (lb)
Y_L	Mast axis Y-force left rotor (+ right for helicopter) (lb)
Y_o	Initial y-position of the aircraft c.g. with respect to the ground (ft)
Y_R	Mast axis Y-force right rotor (+ right for helicopter) (lb)
YSCAS	Yaw (rudder) SCAS output (in)
$YSCAS_{MX}$	Yaw (rudder) SCAS actuator limit (in)
$Y_V^{\prime}(i)$	Aerodynamic side force (lift) on the vertical fin in wind axis (lb)
$Y_{WP}^{\prime}$	Side force moment of the wing-pylon in wind axis (ft-lb)
Y_β	Fuselage side force variation with sideslip angle, $= f(\beta)$ (ft^2)
Z_A	Total body axis z-force on the aircraft (lb)
Z_{CG}	Vertical c.g. displacement as a function of mast tilt angle (in)

Z_o	Initial z-position of the aircraft c.g. with respect to the ground (ft)
$\dot{Z}_{CG}$	Rate of vertical c.g. displacement as a function of mast tilt angle (in/sec)
$\ddot{Z}_{CG}$	Acceleration of vertical c.g. displacement as a function of mast tilt angle (in/sec^2)
Z_n	Landing gear stroke (ft)
Z_n'	Landing gear oleo stroke (ft)
$\dot{Z}_n$	Landing gear stroke rate (ft/sec)
Z_{TIRE_n}	Maximum tire deflection (ft)
$\partial\alpha_{WFS}/\partial\delta_F$	Partial of wing angle of attack with respect to partial of flap deflection (non-dimensional)
α_F	Fuselage angle of attack (rad)
α_H	Horizontal stabilizer angle of attack (deg)
α_{iWL}	Angle of attack of the wing portion immersed in the left rotor wake (deg)
α_{iWR}	Angle of attack of the wing portion immersed in the right rotor wake (deg)
α_{OL}	Blade zero lift coefficient (deg)
α_{PLAT}	Pylon angle of attack used for transformation from wind to body axis (rad)
α_{SP}	Spinner angle of attack used for transformation from wind to body axis (rad)

α_{WFS}	Angle of attack of the wing portion outside the rotor wake (freestream) (rad)
$\dot{\alpha}_F$	Rate of change of fuselage angle of attack (rad/sec)
β_F	Fuselage sideslip angle (rad)
β_{iWL}	Sideslip angle of the wing portion immersed in the left rotor wake (deg)
β_{iWR}	Sideslip angle of the wing portion immersed in the right rotor wake (deg)
β_m	Mast conversion angle (+ forward, 0 deg = vertical or helicopter, 90 deg = horizontal or airplane) (rad)
$\dot{\beta}_m$	Mast conversion rate (deg/sec)
$\dot{\beta}_{mC}$	Commanded mast conversion rate, = $f(\beta_m)$ (deg/sec)
β_{PLAT}	Pylon sideslip angle used for transformation from wind to body axis (rad)
β_{SP}	Spinner sideslip angle used for transformation from wind to body axis (rad)
β_V	Rudder sideslip angle (rad)
ΔS_{t_n}	Oleo stroke (- for compression) (ft)
$\Delta \dot{S}_{t_n}$	Oleo stroke rate (- for compression) (ft/sec)
δ_a	Aileron mean deflection angle (+ right aileron up) (deg)
$\partial \delta_a / \partial X_{LT}$	Aileron to lateral stick position gearing ratio (deg/in)
$\partial \delta_F / \partial t$	Rate of change of flaps with time (deg/sec)

δ_{B_n}	Brake pedal deflection (deg)
δ_{B1}	B1 offset rigging constant (deg)
$\delta_{B_{n_{MIN}}}$	Brake threshold deflection (deg)
δ_e	Elevator mean deflection angle (+ trailing edge down) (deg)
$\partial\delta_e/\partial X_{LN}$	Elevator to longitudinal stick position gearing ratio (deg/in)
δ_F	Flap position indicator (non-dimensional)
δ_{NW}	Nose wheel steering angle (rad)
δ_r	Rudder mean deflection angle (+ trailing edge right) (deg)
$\partial\delta_r/\partial X_{PD}$	Rudder to pedal position gearing ratio (deg/in)
δ_0	Blade drag coefficient (non-dimensional)
δ_1	Blade drag coefficient (1/rad)
δ_2	Blade drag coefficient ($1/rad^2$)
δ_3	Pitch flap coupling (deg)
$\varepsilon_{W/H}$	Wing wake deflection at the horizontal stabilizer, $= f(\alpha_{WFS}, \beta_m, \delta_F, M_N)$
$\Delta\varepsilon_p$	Commanded throttle position error threshold (nondimensional)
$\Delta\varepsilon_s$	Power turbine RPM error threshold (nondimensional)

ζ_d	Lateral flapping controller damping parameter (non-dimensional)
ζ_{LN}	Longitudinal force feel system viscous damping coefficient (non-dimensional)
ζ_{LT}	Lateral force feel system viscous damping coefficient (non-dimensional)
ζ_{PD}	Pedal force feel system viscous damping coefficient (non-dimensional)
ζ_{XLN}	Longitudinal force feel viscous damping coefficient (non-dimensional)
ζ_{XLT}	Lateral force feel viscous damping coefficient (non-dimensional)
ζ_{XPD}	Pedal force feel viscous damping coefficient (non-dimensional)
η_H	Dynamic pressure ratio at the horizontal tail, $= f(\alpha_F, \beta_m, V_T)$ (non-dimensional)
η_{XMSN}	Transmission efficiency (nondimensional)
η_V	Dynamic pressure ratio at the vertical tail (non-dimensional)
θ	Euler pitch angle (rad)
$\dot{\theta}$	Rate of change of Euler pitch angle (rad/sec)
$\theta_{ERR_{LIM}}$	Maximum error position limit on the governor actuator (deg)
$\theta_{FCP_{LIM}}$	Maximum governor flow control piston position limit (deg)

θ_{INT_1}	Rotor interconnect gear ratio (non-dimensional)
θ_m	Blade twist (deg)
$\partial\theta_o/\partial X_{COL}$	Collective pitch control gearing ratio, = $f(\beta_m)$ (deg/in)
$\partial\theta_o/\partial X_{LT}$	Differential collective pitch control gearing ratio, = $f(\beta_m)$ (deg/in)
$\Delta\theta_{oLIM}$	Differential collective trim limit (deg)
θ_{oL}	Left rotor root collective pitch (rad)
θ_{oLL}	Root collective pitch lower limit, = $f(\beta_m)$ (deg)
$\theta_{oL/G}$	Left rotor collective pitch input from the left rotor collective governor (deg)
$\theta_{oR/G}$	Right rotor collective pitch input from the right rotor collective governor (deg)
θ_{oR}	Right rotor root collective pitch (rad)
θ_{RPT_1}	Rotor turbine gear ratio (non-dimensional)
θ_W	Euler pitch angle of wind (rad)
$(\Lambda_{c/4})_W$	Wing quarter chord sweep angle (deg)
Λ_w	Wing quarter chord sweep angle (deg)
λ_L	Inflow ratio, left rotor (non-dimensional)
λ_{PYL}	Angle between the fuselage waterline reference and L_N at $\beta_m = 0$ (deg)

λ_R	Inflow ratio, right rotor (non-dimensional)
ρ	Air density (slug/ft^3)
ρ_o	Air density at sea level standard conditions (slug/ft^3)
$\partial\sigma/\partial\hat{p}$	Roll rate correction coefficient to fin sideslip angle (non-dimensional)
$\partial\sigma/\partial\hat{r}$	Yaw rate correction coefficient to fin sideslip angle (non-dimensional)
$\left(1 - \frac{\partial\sigma}{\partial\beta_F}\right)$	Vertical stabilizer sidewash factor, = $f(\beta_F, \beta_m, \delta_F, \alpha_F)$ (non-dimensional)
τ_e	Elevator effectiveness ($\partial\alpha_H/\partial\delta_e$) (non-dimensional)
τ_p	Roll SCAS time constant (sec)
τ_q	Pitch SCAS time constant (sec)
τ_r	Rudder effectiveness ($\partial\beta_V/\partial\delta_r$) (non-dimensional)
$\tau_{1P} \rightarrow \tau_{6P}$	Pitch SCAS time constants (sec)
$\tau_{1R} \rightarrow \tau_{5R}$	Roll SCAS time constants (sec)
$\tau_{1Y} \rightarrow \tau_{2Y}$	Yaw SCAS time constants (sec)
ϕ	Euler roll angle (rad)
$\dot{\phi}$	Rate of change of Euler roll angle (rad/sec)
ϕ_m	Lateral mast tilt (deg)
ψ	Euler yaw angle (rad)

$\dot{\psi}$	Rate of change of Euler yaw angle (rad/sec)
ψ_W	Grid heading of wind (+ clockwise from North) (rad)
$\bar{\mu}$	Rotor hub advance ratio (non-dimensional)
μ_{G_n}	Landing gear maximum side force coefficient (non-dimensional)
μ_L	Tip speed (advance) ratio, left rotor (non-dimensional)
μ_R	Tip speed (advance) ratio, right rotor (non-dimensional)
μ_{RF}	Coefficient of rolling friction (non-dimensional)
μ_{S_n}	Landing gear side force slope (non-dimensional)
$(\mu_{o,1,s_n})$	Landing gear ground dynamic coefficients (gear rolling friction and side force) (non-dimensional)
Ω_{INT}	Interconnect drive shaft speed (rad/sec)
Ω_L	Instantaneous left rotor speed (rad/sec)
Ω_{LPT}	Left engine power turbine speed (rad/sec)
Ω_L'	Total left rotor speed (corrected for aircraft angular rate) (rad/sec)
Ω_R	Instantaneous right rotor speed (rad/sec)
Ω_{RPT}	Right engine power turbine speed (rad/sec)

Ω_R'	Total right rotor speed (corrected for aircraft angular rate) (rad/sec)
ω_n	Lateral flapping controller natural frequency (rad/sec)

1. Report No.	2. Government Accession No.	3. Recipient's Catalog No.
NASA CR-166536		

4. Title and Subtitle	5. Report Date
A MATHEMATICAL MODEL FOR REAL TIME FLIGHT SIMULATION OF A GENERIC TILT-ROTOR AIRCRAFT	October 1983*
	6. Performing Organization Code
7. Author(s)	8. Performing Organization Report No.
S. W. Ferguson	STI TR-1195-2
	10. Work Unit No.
9. Performing Organization Name and Address	
Systems Technology, Inc. 2672 Bayshore-Frontage Road, Suite 505 Mountain View, California 94043	11. Contract or Grant No. NAS2-11317
	13. Type of Report and Period Covered Final
12. Sponsoring Agency Name and Address	
NASA Ames Research Center Moffett Field, California 94035	14. Sponsoring Agency Code

15. Supplementary Notes

*March 1988 (Rev. A), September 1988 (Rev. A Final)

16. Abstract

This report documents a mathematical model for real time flight simulation of a generic tilt-rotor aircraft. The mathematical model equations describe the kinematic, dynamic, and aerodynamic characteristics of a rotor as well as the airframe and flight control system. The model is intended for use in support of tilt-rotor aircraft design, pilot training, and flight testing. The generic tilt-rotor mathematical model is based on a model originally developed by Bell Helicopter Textron in support of the XV-15 tilt-rotor research aircraft. Real time and non-real time versions of the generic tilt-rotor mathematical model are available. The real time version of this model has been implemented by Computer Sciences Corporation on the NASA Ames Research Center Sigma 8 simulation computer. A non-real time version of the model has been implemented by Systems Technology, Inc., on a VAX 11/780 computer as program GTRSIM. Documentation on the GTRSIM version is provided in NASA CR-166535 which is entitled, "Generic Tilt-Rotor Simulation (GTRSIM) User's and Programmer's Guide." Validation documentation for the generic tilt-rotor mathematical model is provided in NASA CR-166537 which is entitled "Development and Validation of the Generic Tilt-Rotor Simulation (GTRSIM) Program."

17. Key Words (Suggested by Author(s))		18. Distribution Statement
Tilt-Rotor	Rotorcraft Simulation	Unclassified - Unlimited
XV-15	Simulation Validation	
GTRSIM	Simulation	

19. Security Classif. (of this report)	20. Security Classif. (of this page)	21. No. of Pages	22. Price*
UNCLASSIFIED	UNCLASSIFIED	533	

*For sale by the National Technical Information Service, Springfield, Virginia 22161